# SYNTHESIS AND STRUCTURAL STUDIES OF BENZIMIDAZOLE BASED SALTS AND THEIR METAL COMPLEXES

**Ph.D. THESIS**

*by*

**RADHA RAMAN MAURYA**

**DEPARTMENT OF CHEMISTRY**
**INDIAN INSTITUTE OF TECHNOLOGY ROORKEE**
**ROORKEE-247 667 (INDIA)**
**JULY, 2014**

# SYNTHESIS AND STRUCTURAL STUDIES OF BENZIMIDAZOLE BASED SALTS AND THEIR METAL COMPLEXES

**A THESIS**

*Submitted in partial fulfilment of the requirements for the award of the degree*

*of*

**DOCTOR OF PHILOSOPHY**

*in*

**CHEMISTRY**

*by*

**RADHA RAMAN MAURYA**

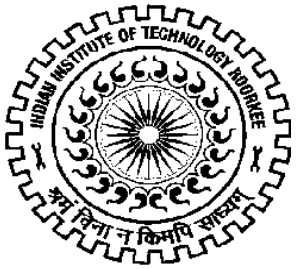


**DEPARTMENT OF CHEMISTRY**
**INDIAN INSTITUTE OF TECHNOLOGY ROORKEE**
**ROORKEE-247 667 (INDIA)**
**JULY, 2014**

# INDIAN INSTITUTE OF TECHNOLOGY ROORKEE
# ROORKEE

## CANDIDATE'S DECLARATION

I hereby certify that the work which is being presented in the thesis entitled "**SYNTHESIS AND STRUCTURAL STUDIES OF BENZIMIDAZOLE BASED SALTS AND THEIR METAL COMPLEXES"** in partial fulfilment of the requirements for the award of the Degree of Doctor of Philosophy and submitted in the Department of Chemistry of the Indian Institute of Technology Roorkee, Roorkee is an authentic record of my own work carried out during a period from January, 2009 to July, 2014 under the supervision of Dr. U. P. Singh, Professor, Department of Chemistry, Indian Institute of Technology Roorkee, Roorkee.

The matter presented in this thesis has not been submitted by me for the award of any other degree of this or any other Institute.

**(RADHA RAMAN MAURYA)**

This is to certify that the above statement made by the candidate is correct to the best of my knowledge.

(Udai P. Singh)
Supervisor

Dated: July, 2014

The Ph.D. Viva-Voce examination of **Mr. Radha Raman Maurya**, Research Scholar, has been held on …… .

Signature of Supervisor Chairman, SRC Signature of External Examiner

Head of the Deptt./Chairman, ODC

## ABSTRACT

the development of molecules of pharmaceutical or biological interest. The various benzimidazole derivatives have miscellaneous therapeutic applications viz., antiulcers, antihypertensives, antivirals, antifungals, anticancers and antihistaminics and s

Benzimidazoles are typical nitrogen-containing heterocyclic and aromatic compounds in which six-membered benzene molecules are fused with five-membered imidazole moiety. The benzimidazole is a very useful structural motif for ome important drugs are omeprazole, pimobendam, mebendazole etc. The well-known benzimidazole compound in nature is *N*-ribosyl-dimethylbenzimidazole, which serves as an axial ligand for cobalt in vitamin $B_{12}$. The benzimidazole and its derivatives have been widely used as a versatile ligand in the coordination as well as in supramolecular chemistry. It has a strong tendency to coordinate with the metal centers, which can lead to materials with potential applications in various fields. They are also used for the preparation of co-crystals and salts with other moieties and it has been found that their properties and reactivity's are often better than the sum of the properties of each individual component. Benzimidazole is commercially available and the usual synthesis involves the condensation of *o*-phenylenediamine with formic acid, or with the equivalent trimethyl orthoformate. This method is very useful for the preparation of derivatives of benzimidazoles by altering the carboxylic acid. It is important to mention that benzimidazole and its derivatives promote intra and inter-molecular interactions, such as hydrogen bonding and π- stacking, which results in the formation of molecular aggregates.

The different positional isomer of pyridine dicarboxylic acid are also well known for the formation of supramolecules because of their capability of forming robust dimeric and catemeric synthons through O-H···O type hydrogen bonds. It has also a very strong tendency to coordinate with the metal ions either by pyridyl nitrogen or through carboxylic group.

For the sake of convenience, the work embodied in the thesis is presented in the following chapters.

The **first** chapter of the thesis is the general introduction and presents an up to date survey of literature related to (i) the co-crystallization of benzimidazole ligands

with organic as well as inorganic acids (ii) their chelation with metal complexes and (iii) their different application in various fields viz., fluorescence properties, biological activities etc. The different type of co-crystal, salts and metal complexes related to the present research have been post in the context of the cited work.

Some salts of pyridine dicraboxylic acid (various positional isomers) with different benzimidazole bases have been synthesized and characterized by different physico-chemical methods are described in the **second** chapter of the thesis. The reaction of pyridine-2,3-dicarboxylic acid (2,3-$PDCAH_2$), pyridine-2,4-dicarboxylic acid (2,4-$PDCAH_2$), pyridine-2,5-dicarboxylic acid (2,5-$PDCAH_2$), pyridine-2,6-dicarboxylic acid (2,6-$PDCAH_2$), pyridine-3,4-dicarboxylic acid (3,4-$PDCAH_2$) and pyridine-3,5-dicarboxylic acid (3,5-$PDCAH_2$) with different benzimidazole bases e.g., 1,4-bis(1H-benzimidazol-2-yl)butane ($H_2BBBu$) and tris(1H-benzimidazol-2-yl)methyl)amine ($H_3NTB$) resulted into the formation of salts viz., $[(H_4BBBu)^{2+}.(2,3\text{-}PDCA)^{2-}]$, $[(H_4BBBu)^{2+}.(2,4\text{-}PDCA)^{2-}]$, $[(H_4BBBu)^{2+}.(2,5\text{-}PDCA)^{2-}]$, $[(H_4BBBu)^{2+}.(2,6\text{-}PDCA)^{2-}.H_2O]$, $[(H_4BBBu)^{2+}.2(3,4\text{-}PDCAH)^{-}.2H_2O]$, $[(H_4BBBu)^{2+}.(3,5\text{-}PDCA)^{2-}.3H_2O]$, $[(H_5NTB)^{2+}.2(2,3\text{-}PDCAH)^{-}.DMF]$, $[(H_4NTB)^{+}.(2,4\text{-}PDCAH)^{-}.2CH_3OH.H_2O]$, $[(H_5NTB)^{2+}.(2,5\text{-}PDCA)^{2-}.DMF]$, $[(H_4NTB)^{+}.(2,6\text{-}PDCAH)^{-}.C_2H_5OH.CH_3OH.H_2O]$, $[(H_5NTB)^{2+}.(3,4\text{-}PDCA)^{2-}.DMF]$, $[(H_6NTB)^{3+}.(3,5\text{-}PDCA)^{2-}.(3,5\text{-}PDCAH)^{-}.DMF]$. During salt formation either one or both the proton has been transferred from the carboxylic acid to the nitrogen of the benzimidazole based ligand bearing lone pair of electron. An attempt has also been made to incorporate metal in the above prepared salts. These complexes are $(H_3BBPr)^{+}[Zn(2,3\text{-}PDCAH)_3]^{-}$, $(H_3BBBu)^{+}[Zn(2,3\text{-}PDCAH)_3]^{-}$, $(H_3BBHex)^{+}[Zn(2,3\text{-}PDCAH)_3]^{-}$, $(H_4BBPr)^{2+}[Ni(2,6\text{-}PDCA)_2]^{2-}.7H_2O$, $(H_4BBBu)^{2+}[Ni(2,6\text{-}PDCA)_2]^{2-}$ and $(H_4BBHex)^{2+}[Ni(2,6\text{-}PDCA)_2]^{2-}.CH_3OH$. All the compounds consist of a protonated cationic benzimidazole based ligand and an anionic metal complexes core. These salts and metal complexes have been characterized by different methods including elemental analysis, IR and single crystal X-ray crystallography. Due to the presence of nitrogen-rich benzimidazole bases, each salt and metal complexes contain infinite two or three dimensional structures held together by primary N-H···O, N-H···N, O-H···N, O-H···O hydrogen bonds and secondary C-H···O, C-H···π interactions.

The **third** chapter of the thesis deals with the preparation of some salts and co-crystal of different benzimidazole ligands such as N,N,N',N'-tetrakis(1H-benzimidazol-2yl)methyl)ethane-1,2-diamine ($H_4EDTB$) and N,N,N′,N′-tetrakis(1H-benzimidazol-

2ylmethyl)propane-1,3-diamine ($H_4$PDTB) with various inorganic and organic acids viz. $HClO_4$, HCl, $HNO_3$, $H_3PO_4$, HBr, HF, $CF_3COOH$ and $CH_3COOH$. The reaction of acids with different benzimidazoles in aqueous methanol/DMSO resulted into the formation of salts and co-crystal, viz., $[(H_8EDTB)^{4+}.4(ClO_4)^-.H_2O]$, $[(H_8EDTB)^{4+}.4(Br)^-.4DMSO]$, $[2(H_7EDTB)^{3+}.3(SiF_6)^{2-}.14H_2O]$, $[(H_8EDTB)^{4+}.4(H_2PO_4)^-.2H_3PO_4]$, $[H_4EDTB.2CH_3COOH]$, $[(H_8PDTB)^{4+}.4(ClO_4)^-.H_2O]$, $[(H_8PDTB)^{4+}.4(Cl)^-.2H_2O]$, $[(H_8PDTB)^{4+}.2(H_2PO_4)^-.(H_7P_3O_{12})^{2-}.3H_3PO_4]$, $[(H_8PDTB)^{4+}.4(NO_3)^-]$, $[2(H_5PDTB)^+.2(CF_3COO)^-.5H_2O]$ and $[(H_8PDTB)^{4+}.3(ClO_4)^-.(H_2PO_4)^-]$. These salts and co-crystal have been characterized by different methods including elemental analysis, IR spectroscopy, UV-Visible spectroscopy, and single crystal X-ray crystallography. During salt formation the proton has been transferred from the acid to the nitrogen of the benzimidazole based ligand bearing lone pair of electron, while in the case of co-crystal no proton has been relocated. The selectivity of these ligands has also been checked through anion selectivity test and shows that these ligands are superiorly selective for perchlorate anion. The colorimetric test of these ligands shows that the methanolic solution of the ligands ($H_4$EDTB and $H_4$PDTB) are orange-red in color but after addition of the acids the color changes to light blue to dark blue. These salts and co-crystal have also been used for photoluminescence studies.

The **fourth** chapter of the thesis deals with the synthesis of mono and dinuclear zinc (II) and cadmium (II) complexes with N,N,N',N'-tetrakis(1H-benzimidazol-2yl)methyl)ethane-1,2-diamine ($H_4$EDTB) and N,N,N′,N′-tetrakis(1H-benzimidazol-2ylmethyl)propane-1,3-diamine ($H_4$PDTB). The reaction of $Zn(NO_3)_2.6H_2O$, $Cd(NO_3)_2.4H_2O$ and $Zn(ClO_4)_2.6H_2O$ with $H_4$EDTB and $H_4$EDTB resulted in the formation of $[Zn(H_4EDTB)](NO_3)_2.CH_3OH$, $[Cd(H_4EDTB)NO_3]NO_3.CH_3OH.2H_2O$, $[Zn(H_4EDTB)](ClO_4)_2$, $[Zn(H_4PDTB)](NO_3)_2.DMF$, $[Cd_2(H_4PDTB)(\eta^1\text{-}NO_3)_2(\eta^2\text{-}NO_3)_2.H_2O].2H_2O$ and $[Zn_2(H_4PDTB)(H_2O)_2.(DMF)_2](ClO_4)_4.2H_2O$. These complexes have been characterized by different methods including elemental analysis, IR spectroscopy and single crystal X-ray crystallography. These complexes showed penta- to hepta-coordination number depending on the presence of different types of counter ions and the difference in the ligands. Both the zinc complexes are six coordinated derived from zinc nitrate either with $H_4$EDTB or $H_4$PDTB and the two counter nitrate anion are present in the lattice. The cadmium nitrate with $H_4$EDTB forms a seven coordinated mononuclear system whereas with $H_4$PDTB forms a dinuclear system with

different coordination number. The photoluminescence properties of these metal complexes have also been studied with absorption and emission spectra and revealed that they shows luminescence due to the complexation resulting in the enhancement in rigidity of the molecule.

The starting materials, reagents, synthetic procedures, experimental details and various spectroscopic measurements are described in the **fifth** chapter of the thesis. Methods for the preparation of different type of ligands, organic salts, co-crystal and metal complexes have also been reported in this chapter.

## ACKNOWLEDGEMENT

*I humbly and politely bow my head to thyness, the Lord Shiva and Goddess Saraswati the "Goddess of Wisdom" Who bestowed upon me an opportunity to do this work and gave me an ample vision and strength to understand and grasp very minutely the happening on this earth. It's the gracious blessing of God that made to realize the truth and follow me to precede the right path for acquiring few pebbles of knowledge from its seashore.*

*In the beginning, I would like to convey my deepest gratitude to my supervisor* ***Prof. Udai P. Singh,*** *Department of Chemistry, IIT Roorkee for his management, professionalism, and continued hopefulness, which make him an outstanding advisor. I am highly thankful for his time, attempt, and editing skills. His constant support, the trust he placed in my abilities, encouragement and judicious interventions made this thesis to come into picture. I humbly acknowledge a life time's gratitude to him. No words articulate to acknowledge the didactic guidance rendered by him.*

*I am highly grateful to* ***Prof. Anil Kumar****,* ***Prof. V. K. Gupta*** *and* ***Prof. Kamaluddin,*** *the present and the former Heads of the Department of Chemistry, Indian Institute of Technology-Roorkee for providing the necessary environment of research in the department and in our lab.*

*I voice my appreciation to* ***Dr. Nem Singh*** *Department of Chemistry, IIT Delhi, for their potential and moral support.*

*This arduous task would not become so simple if my senior* ***Dr. Sujata Kashyap*** *has not supported me morally and mentally. I will be highly thankful for her useful suggestions. With great pleasure I would like to thank my lab mates,* ***Dr. Nidhi Goel, Dr. Sandeep Singh****,* ***Dr. Kapil Tomar****,* ***Shikha, Neetu, Deependra and Pankaj*** *for their support, co-operation and encouragement. I would also express my wholehearted thanks to my friends* ***Varun, Sudhir, Manohar, Anand, Sandeep, Anoop, Jitendra sir, Navneet, Chetan, Shailendra, Sunandu, Deep and Prasad.***

*I am also very much thankful to* ***Reeta aunty****,* ***Ravi*** *and* ***Akhand*** *for providing me homely atmosphere.*

*I wish to acknowledge* ***Mr. Abdul Haq.*** *and* ***Mr. V. P. Saxena*** *for their technical assistance. I am grateful to* ***Mr. Hem Singh, Mr. Tilak Ram, Mr. Ramesh*** *and* ***Mr. Madan Pal*** *for their co-operation for completion my work. I also thanks to all members of Institute Instrumentation Center and Chemistry Department for their kind co-operation and help throughout my research work.*

*The financial assistance by University Grant Commission (UGC), New Delhi in the form of Junior and Senior Research Fellowship during for this investigation is thankfully acknowledged.*

*I deeply appreciated the cooperation of* ***Dr. Rajesh Singh*** *their encouragement and moral support during research work.*

*At last but not the least, I wish to extend my genuine gratefulness to my father,* ***Shri Ghan Shyam Dass Maurya*** *and mother* ***Smt. Shyam Wati****, brothers, bhabhi, sisters and brother-in-laws for their unconditional love, encouragement and blessing, affection and support, without whom this work would never be accomplished. These pages wouldn't be sufficient to mention the enormous efforts made by my parents to educate me and to take care of my entire requirements.*

*The youngest members of my family* ***Kunnu*** *and* ***Laddu*** *have always been the stress buster throughout my Ph.D. work.*

*At the end, I am extremely grateful to those people, whose names have been unknowingly left, thank you very much for your prayers. It had really helped me a lot. I apologize and believe that they will be always with me as they were during the times of need.*

**(Radha Raman Maurya)**

## LIST OF PUBLICATIONS / CONFERENCES / SYMPOSIUM:

**Publications:**

1. **Udai P. Singh, Radha Raman Maurya, Sujata Kashyap,** "Effect of anions on supramolecular architecture of benzimidazole based ionic salts", *Struct. Chem*., **25**, 733 (2014).
2. **Udai P. Singh, Radha Raman Maurya, Sujata Kashyap, "**Anion directed supramolecular architecture of benzimidazole-based receptor", *J. Mol. Struct.*, (Communicated*)* (2014).
3. Udai P. Singh, **Radha Raman Maurya**, **Sujata Kashyap** "Synthesis and characterization of Zn(II) and Cd(II) complexes with benzimidaole derived ligand", *Transition Met. Chem*., (Communicated*)* (2014).

**Conferences / Symposium:**

1. **Radha Raman Maurya**, Udai P. Singh, 7th RSC-CRSI Symposium in Chemistry, Banaras Hindu University, Varansi , January 31, (2013).
2. **Radha Raman Maurya**, Udai P. Singh, "Structural assemblies in salts of tris(2- benzimidazolylmethyl)amine (ntb) with different pyridine dicarboxylic acids", P-81, 15th CRSI, National Symposium in Chemistry, Banaras Hindu University, Varansi, February 1-3, (2013).
3. **Radha Raman Maurya,** Udai P. Singh, "Synthesis and structural characterization of various binary salts of pyridine dicarboxylic acids", P-106, 1th ICRACS-2013, International conference on recent advance in chemical sciences, Arya P.G. College, Panipat Haryana, February 24-26, (2013).
4. **Radha Raman Maurya,** Sujata Kashyap and Udai P. Singh " Synthesis and crystal structures of zinc and cadmium complexes with N,N,N',N'-tetrakis(1H,benzimidazol-2ylmethyl)alkylene diamine ligand", P-185, 42nd National Seminar on Crystallography and International Workshop on Application of X-ray Diffraction for Drug Discovery, Jawahar Lal Nehru University (JNU), New Delhi, November 21-23, (2013).
5. Actively participate in Symposium on Modern Trends in Inorganic Chemistry-XV (MTIC-XV), Indian Institute of Technology Roorkee, December 13-16, (2013).

# CONTENTS

# *Chapter 1*

# *General Introduction*

Benzimidazoles are typical nitrogen-containing heterocyclic, aromatic compounds which share a fundamental structural characteristic of six-membered benzene molecules fused with five-membered imidazole moiety (Fig. 1.1).

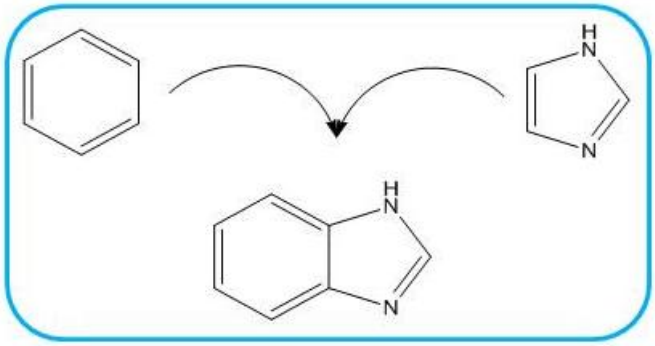

**Fig. 1.1** The benzimidazole skeleton by the fusion of benzene and imidazole

The basic ‘6+5’ heterocyclic structure is shared by another class of chemical compounds e.g. purines (Fig. 1.2). Among the members of this group, several are very well known and important biomolecules, two of the four nucleic acid bases (adenine and guanine), uric acid, and caffeine [1].

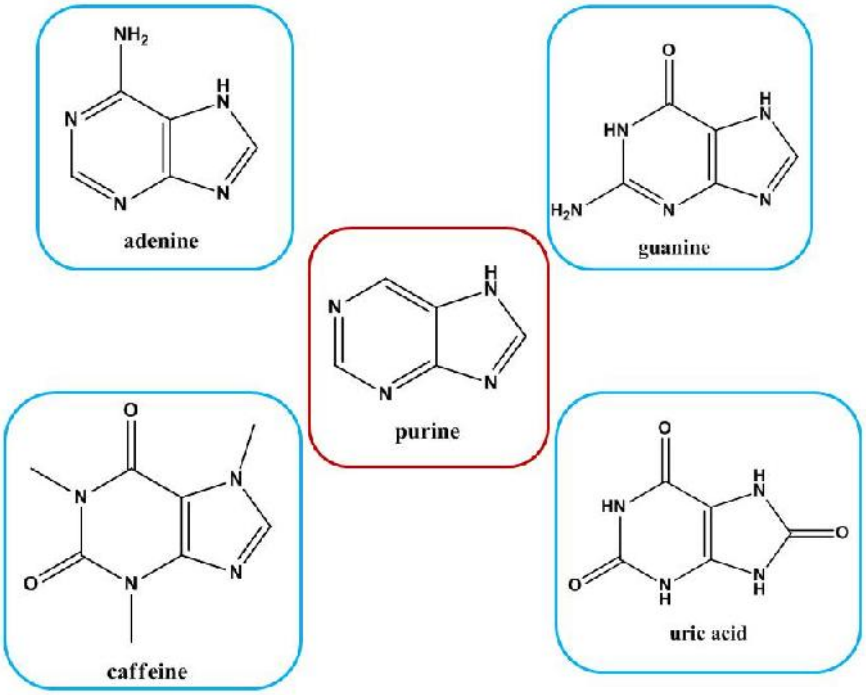


**Fig. 1.2** Purines, including some of the most well-known biomolecules

This important group of substances has found practical applications in a number of fields. From the fundamental structural similarity to the benzimidazole, different type of benzimidazole derivatives are known as biologically active small

molecules, such as vitamin $B_{12}$, a variety of antimicrobial, antiparasitic and even antitumor agents (Fig.1.3-1.4) [2-4].

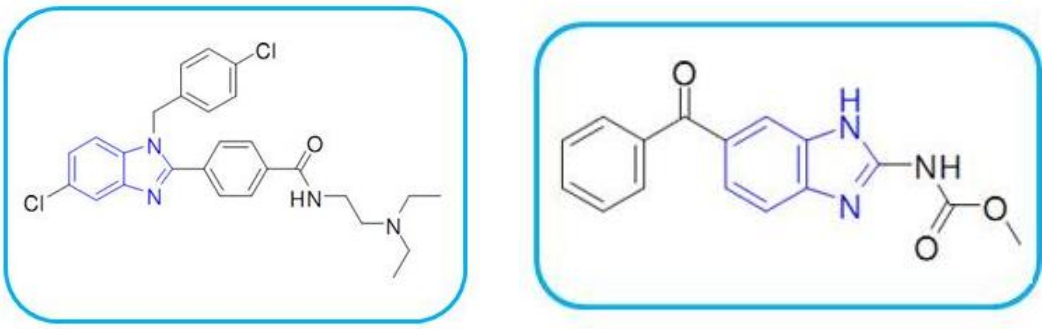


**(a)** **(b)**

**Fig. 1.3 (a)** Examples of antibacterial **(b)** Antimicrobial agents containing benzimidazole moiety (colored blue)

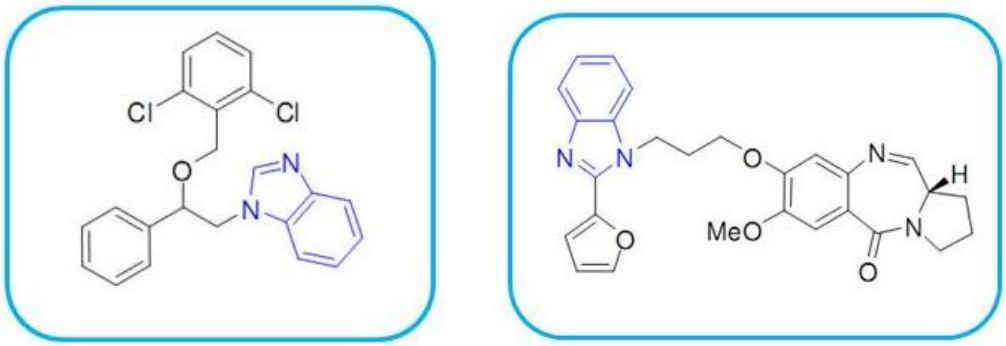


**(a)** **(b)**

**Fig 1.4 (a)** Antiparasitic **(b)** Antitumor agents containing the benzimidazole moiety

Benzimidazoles are also known as benziminazoles or 1,3-benzodiazoles [5-6]. They possess both acidic and basic characteristics and the NH group present in benzimidazoles has a relatively strong acidic character as well as weakly basic in nature. Another important characteristic of benzimidazoles is that they have a strong capacity to form salts. Benzimidazoles with unsubstituted NH groups exhibit fast prototropic tautomerism, which leads to equilibrium mixtures of asymmetrically substituted benzimidazoles.

Historically, the first benzimidazole was prepared in 1872 by Hoebrecker, who obtained 2,5 (or 2,6) dimethylbenzimidazole by the reduction of 2-nitro-4-

methylacetanilide [7]. Alternatively, benzimidazoles have also been prepared from 2-nitroanilides, in a two-step process. In the first step, the nitro group is reduced using one of the many possible reagents (such as zinc, iron, tin (II) chloride, hydrogen, or Raney nickel). The second step involves the ring closure of the 2-aminoanilide derivative with either a carboxylic acid or an aldehyde [8-9]. However, this procedure sometimes requires multistep reactions to prepare the starting anilides, resulting in compromised yields and purity. In recent years, some innovative and improved pathways for the synthesis of benzimidazoles have been developed.

Literature revealed that the benzimidazole as well as its derivative has various applications in different field e. g., anion sensing, catalysis, gas adsorption, biological activity etc. and some of them has been illustrated in the following sections.

Shao et al. [10] reported two novel and neutral benzimidazole derivatives as anion receptors bearing a 1,10-phenanthroline fluorophore, N,N′-di-(2′-benzimidazolyl-methylene)-1, 10-phenanthroline-2,9-diamide (**1**) and N,N′-di-[2′-(benzimidazolyl-2′-)ethyl-]-1,10-phenanthroline-2,9-diamide (**2**), which exhibits a turn-on and turn-off fluorescence responses to various anions and investigated their fluorescent response toward anions in DMSO solution (Fig. 1.5). They found two different fluorescent responses in presence of anions in the process of anions binding: a quenching of the fluorescence emission for $F^-$ and $AcO^-$ and an enhancement of the fluorescence emission for $Cl^-$, $Br^-$ and $I^-$.

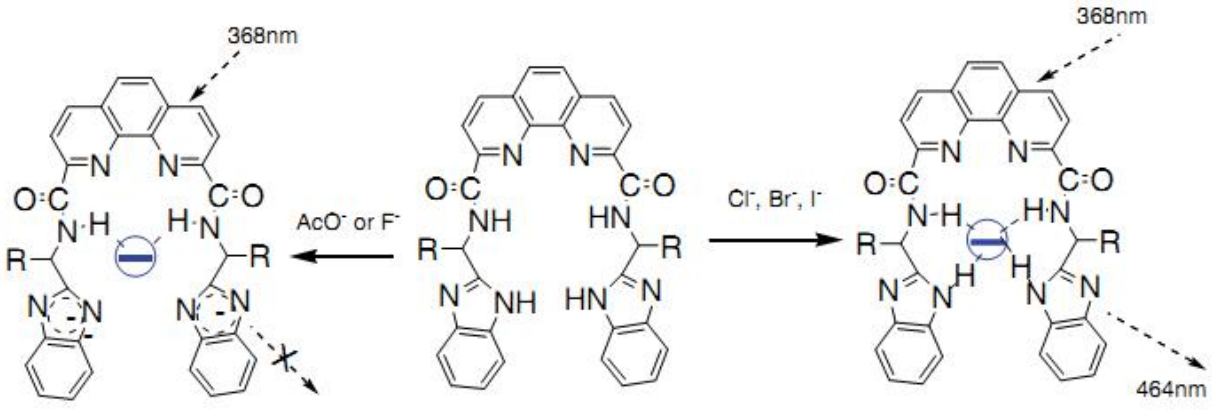


**Fig. 1.5** The proposed binding mode in solution

Hranjec et al. [11] synthesized 2-(1H-benzimidazol-2-yl)-3-(4-N,N′-dimethylamino-phenyl)-acrylonitrile hydrochloride monohydrate (**4**) by the reaction of 2-cyanomethyl-benzimidazole and 4-N,N´-dimethyl-amino-benzaldehyde (Scheme 1.1)

and characterized by $^{1}H$ and $^{13}C$ NMR, UV-Vis and fluorescence spectroscopy, IR, MS and confirmed by single crystal structure (Fig. 1.6). They found that the structure of **4** is almost planar with the dihedral angle of 6.99(6)° between benzimidazole and phenyl rings.

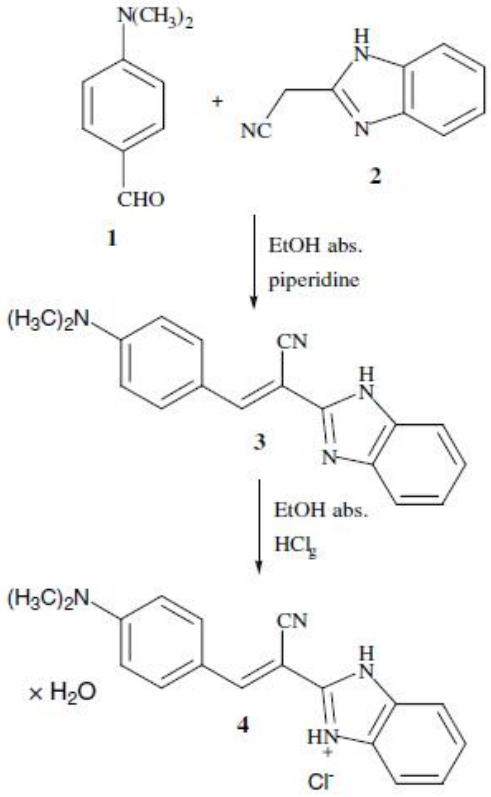


**Scheme 1.1** Reaction scheme for preparation of 2-(1H-benzimidazol-2-yl)-3-(4-N,N-dimethylamino-phenyl)-acrylonitrile hydrochloride monohydrate (**4**)

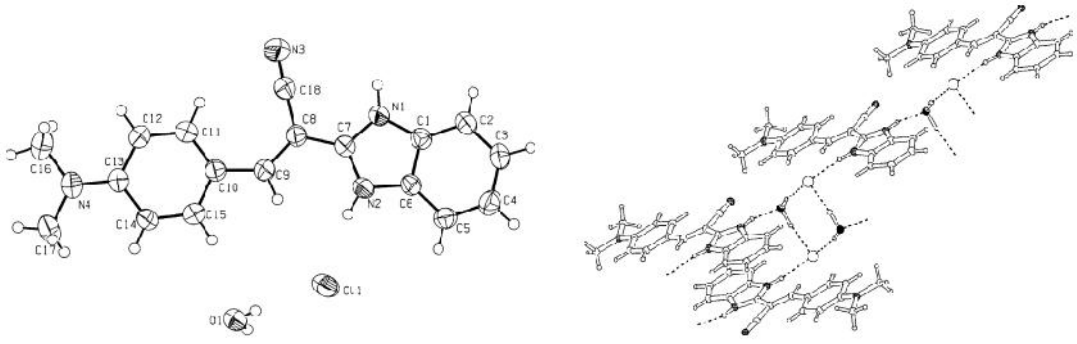

**(a)** **(b)**

**Fig 1.6 (a)** Crystal structure of **4**. **(b)** Different non-covalent interactions in **4**

Li et al. [12] reported a new simple bis(benzimidazole) dication which can act as a template for threading through dibenzo-24-crown-8 (Scheme 1.2 and Fig. 1.7). They described the effect of the solvent and counter ion on the magnitude of the binding interaction and on the hydrogen bonding array in the solid state.

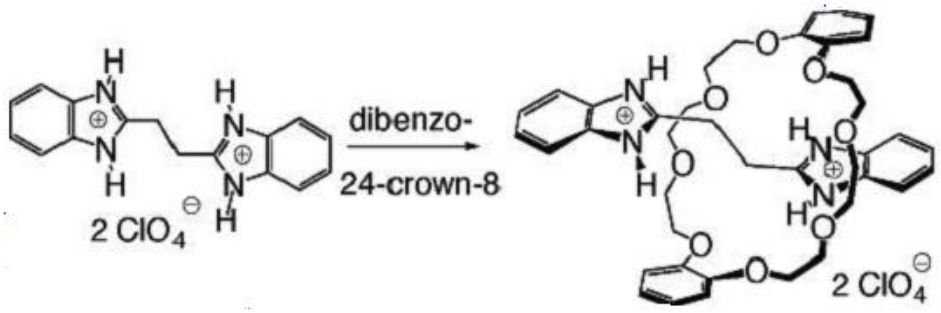


**Scheme 1.2**

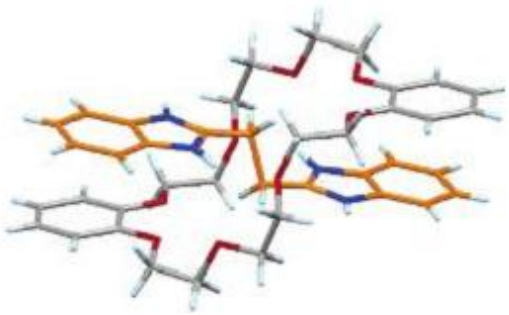

**Fig 1.7** Crystal structure of bis(benzimidazole) dication

Rachocki et al. [13] search the factors which determine the hydrogen bond motif and the structure of the crystals in a new proton conductor from the family of benzimidazole compounds of dicarboxylic acids. They solved the molecular structure of benzimidazole-sebacic acid salt by X-ray diffractions and confirmed by $^{1}H$ and $^{13}C$ NMR experiments combined with DFT calculations (Fig. 1.8). They found an undulated layer-type structure with banana-shaped acid molecules linked by O−H···O bonds into rectangular-type wavy chains and flat base molecules attached to the carboxylic groups by N−H···O bonds in the salt. They also compared the architecture of benzimidazole salts with weak dicarboxylic acids of shorter carbon chains and mentioned the role of the acid chain length in the formation of structural and hydrogen bond motifs.

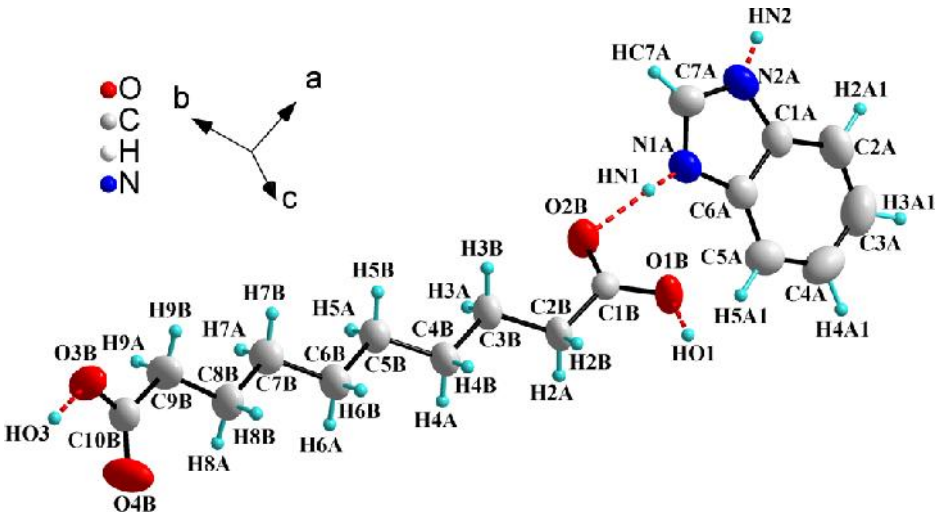


**Fig 1.8** Crystal structure of benzimidazole salt with sebacic acid

Jin et al. [14] prepared organic salts of $L_1$-$L_4$ with 5-nitrosalicylic acid, 5-sulfosalicylic acid and phthalic acid and characterized them though single crystal X-ray diffraction (Scheme 1.3). They demonstrated that the strength and directionality of the N-H···O, O-H···O, and N-H···N hydrogen bonds (ionic or neutral) between carboxylic acids and ditopic imidazoles were mainly responsible for the formation of binary organic salts.

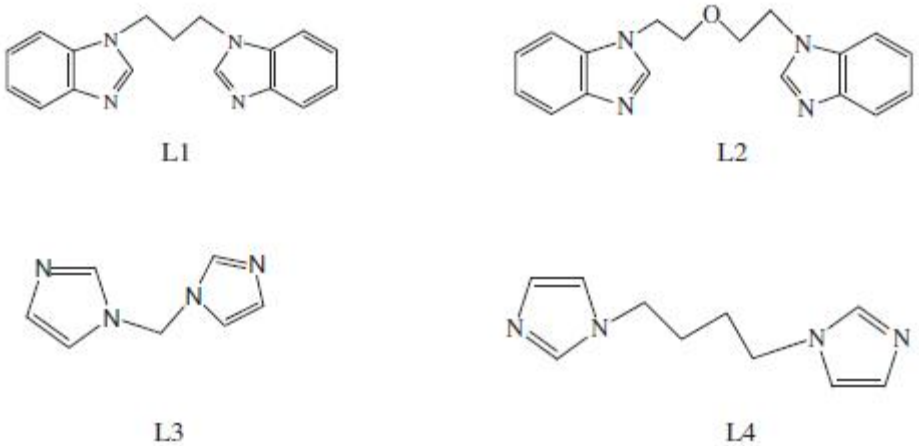

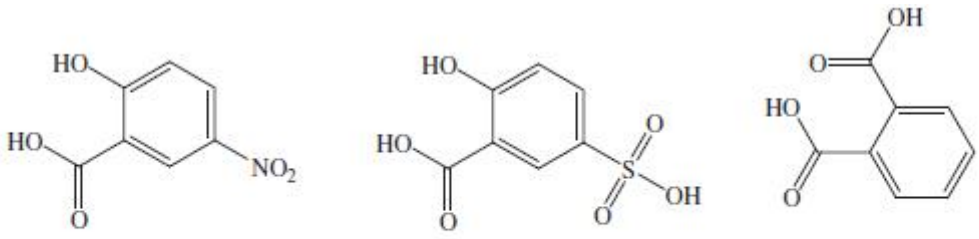


5-Nitro salicylic acid  5-Sulfosalicylic Acid  Phthalic acid

**Scheme 1.3**

Jin et al. [15] further prepared eight crystalline organic acid–base adducts derived from alkane bridged bis(N-benzimidazole) with organic acids (2,4,6-trinitrophenol, *p*-nitrobenzoic acid, *m*-nitrobenzoic acid, 3,5-dinitrobenzoic acid, 5-sulfosalicylic acid and oxalic acid) and characterized by X-ray diffraction analysis, IR, melting point and elemental analysis. They found that out of the eight compounds five were organic salts (**1**, **4**, **6**, **7** and **8**) and the other three (**2**, **3**, and **5**) were co-crystals and involves an extensive intermolecular classical hydrogen bonds as well as other non-covalent interactions (Fig. 1.9).

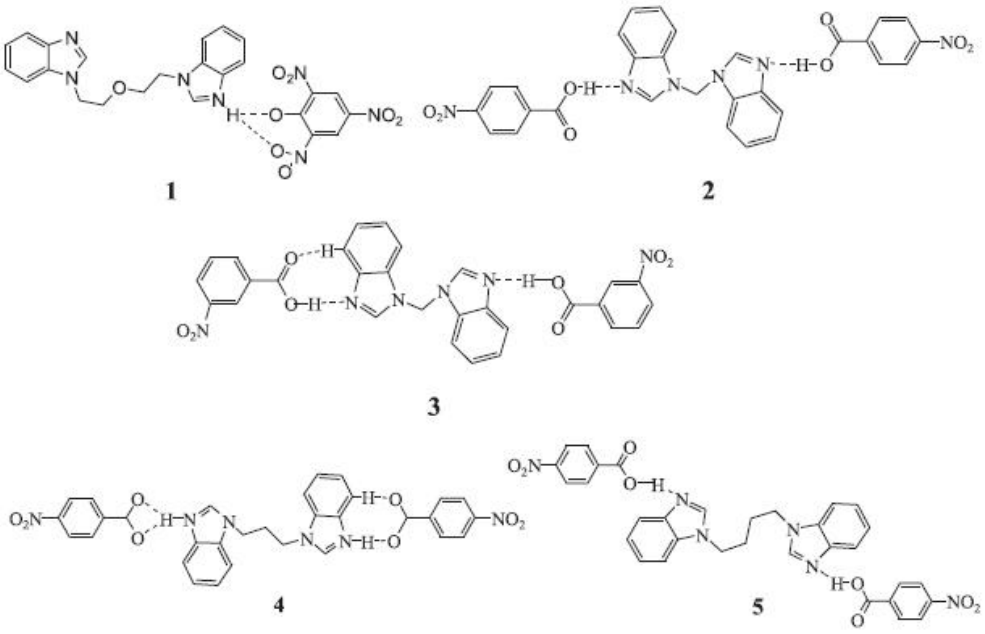

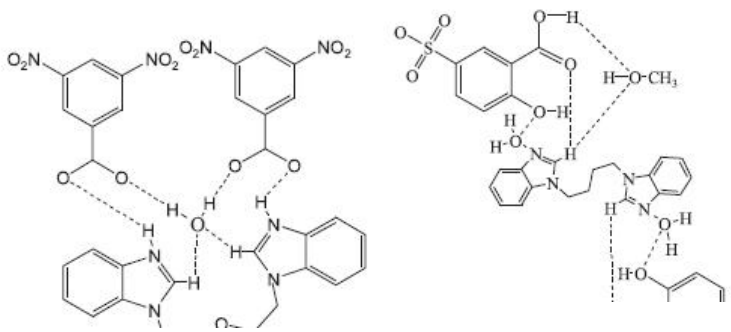

**Fig 1.9** Schematic presentation of organic salts (**1**, **4**, **6**, **7** and **8**) and co-crystals (**2**, **3** and **5**)

The other literature related to the formation of co-crystals and salts are described in the related chapters (Chapter 2 and 3).

Wang et al. [16] prepared $\{[Cd(H_2C4BIm)Cl_2].(H_2C4BIm)\}_n$ (**1**) and $[Cd(HC4BIm)(NCS)]_n$ (**2**) by the reaction of Cd(II) salt with 2,2'-(1,4-butanediyl)bis(1H-benzimidazole) ($H_2C4BIm$ = 2,2′-(1,4-butanediyl)bis(1H-benzimidazole). They got two coordination polymers, by changing the coordinated anions in hydrothermal condition and found that the ligand serves as a bidentate bridging ligand in complex **1** and acts as a tridentate ligand in complex **2**, respectively (Fig. 1.10). In addition, they also studied the fluorescence properties for both the complexes and found that complex **1** exhibits blue fluorescence property (Fig. 1.11).

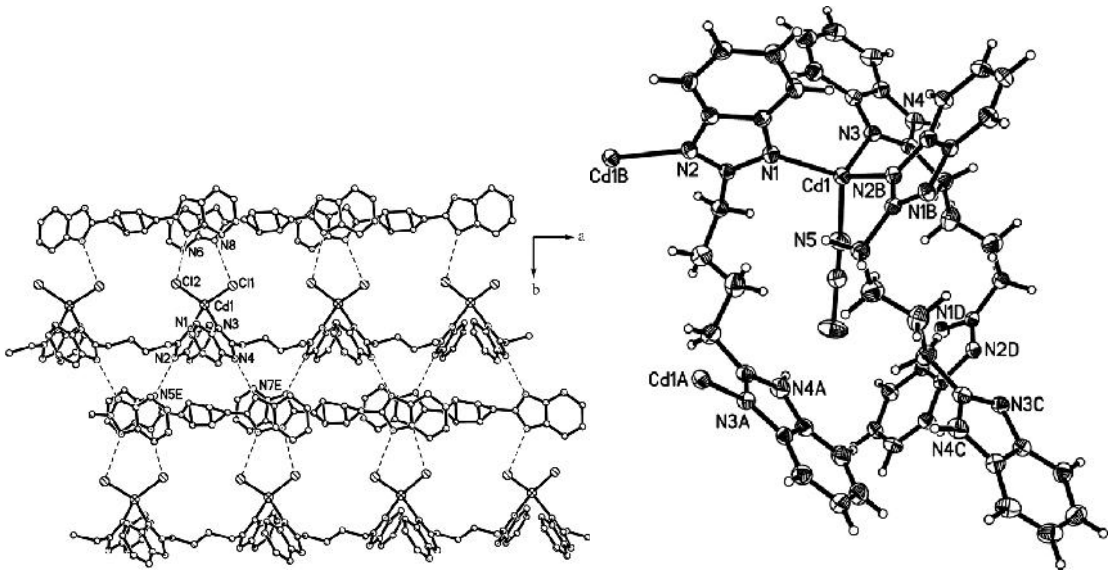


**Fig. 1.10 (a)** 2D Sheet formed by the hydrogen bonding in complex **1**. **(b)** The coordination environment of Cd(II) atom in complex **2**

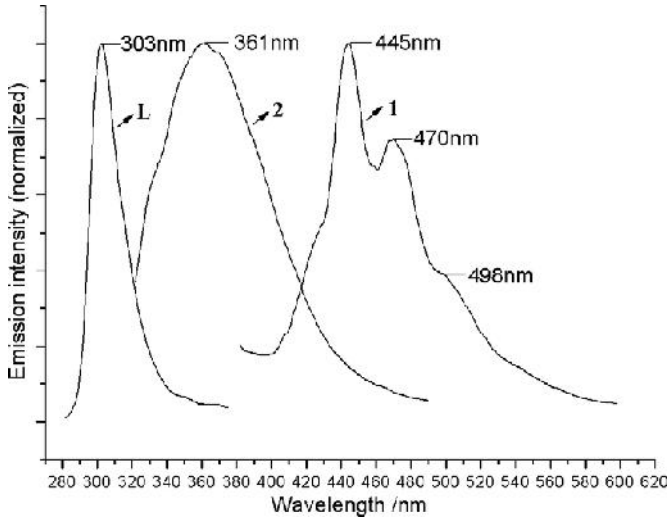


**Fig. 1.11** Normalized fluorescence emission spectrum of complexes **1, 2** and the $H_2C4BIm$ ligand in the solid state at room temperature

Esparza-Ruiz et al. [17] studied the structural and spectroscopic characterization of coordination compounds of four aromatic amines derived from benzimidazole viz., 2-aminobenzimidazole (L1), 1-(S-methylcarbodithioate)-2-aminobenzimidazole (L2), 2-(2-aminophenyl)-1H-benzimidazole (L3) and 6,6-dimethyl-5H-benzimidazolyl[1,2-c]quinazoline (L4) (Scheme 1.4) and synthesized their metal complexes $[Co(L1)_2(CH_3COO)_2]$ (**1**), $[Ni(L1)_2(CH_3COO)_2]$ (**2**), $[Co(L2)_2Cl_2]$ (**3**), $[Co(L2)_2Br_2]$

(**4**), $[Co(L2)_2Cl_2]$ (**5**), $[Zn(L2)_2Br_2]$ (**6**) $[Co(L3)Cl_2]$ (**7**), $[Zn(L3)Cl_2]$ (**8**), $[Ni(L3)_2(H_2O)_2](NO_3)_2]$ (**9**) and $[Zn(L4)_2Cl_2]$ (**10**). They found that ligand (L1) and (L2) behave as monodentate ligands, whereas (L3) coordinates in a bidentate fashion with the metal ions, where the aniline group was assisted by the imidazolic nitrogen and gives a six membered ring. They found an interesting fact that the reaction of L3 with $ZnCl_2$ in acetone produces a tetracoordinated zinc (II) compound $[Zn(L4)_2Cl_2]$ (**10**) with two tetracyclic ligands (Fig. 1.12), where a condensation reaction occurs between L3 and the acetone which results in a new ligand (L4).

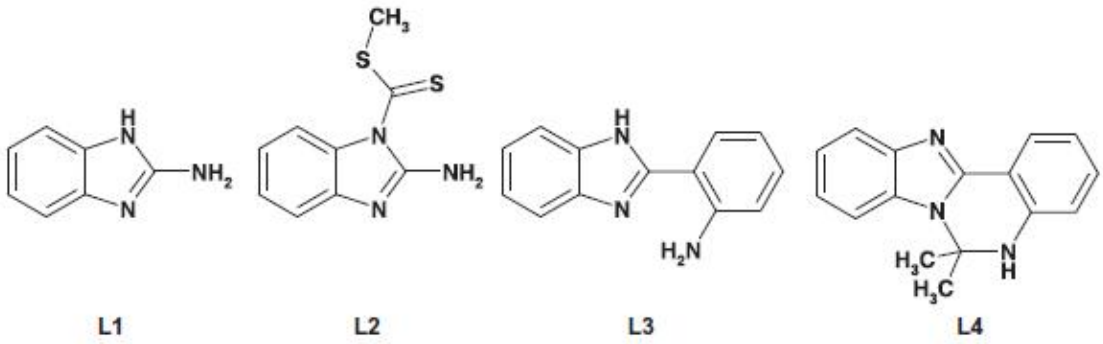


**Scheme 1.4**

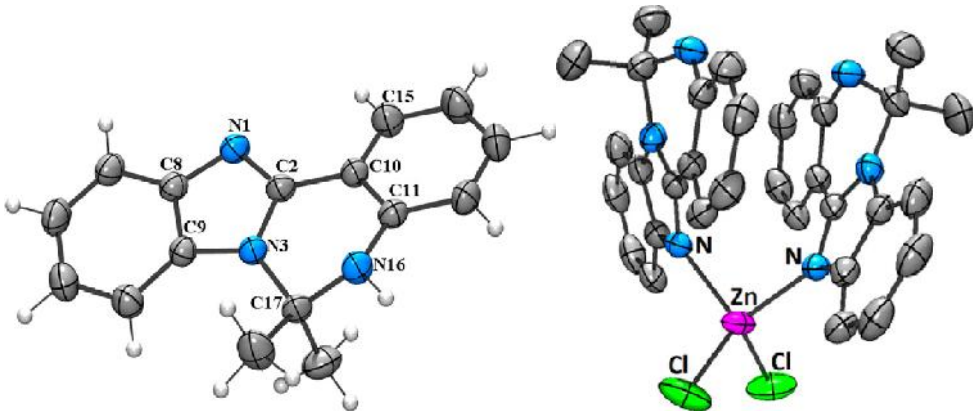


**(a)** **(b)**

**Fig. 1.12 (a)** Crystal structure of L4 and **(b)** $[Zn(L4)_2Cl_2]$ (**10**)

Liu et al. [18] designed two novel zinc (II) complexes containing bis-benzimidazole derivatives viz., $Zn(bpbp)Cl_2$ **(1)** and $[Zn(bpbp)_2](ClO_4)_2 \cdot C_2H_5OH \cdot H_2O$ **(2)** (bpbp = 2,6-bis(1-phenyl-1H-benzo[*d*]imidazol-2-yl)pyridine) (Fig. 1.13-1.14) and -evaluated their *in vitro* anticancer activities.

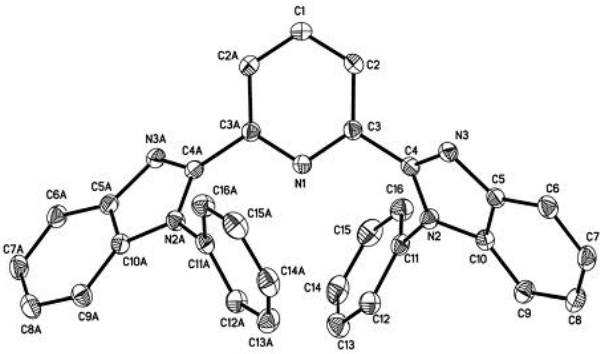

**Fig 1.13** Crystal structures of ligand bpbp

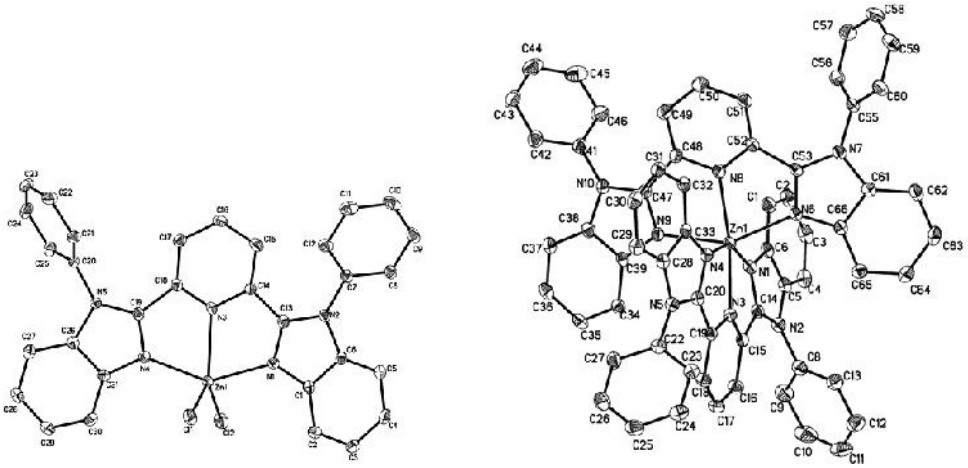

**(a)** **(b)**

**Fig 1.14 (a)** Crystal structures of $Zn(bpbp)Cl_2$ **(1)** and **(b)** $Zn(bpbp)_2](ClO_4)_2 \cdot C_2H_5OH \cdot H_2O$ **(2)**

Dey et al. [19] prepared metal–organic gels (MOGs) by the reaction of L1 (L1 = pyridine-3,5-bis(1-methyl-benzimidazole-2-yl) (Scheme 1.5) with $CuCl_2$, $CuBr_2$ or $CdBr_2$ in alcoholic solutions and found that they exhibit self sustainability with greater firmness, confirmed by rheological studies. They further obtained crystalline complexes of coordination polymers of L1 with $CdBr_2$, $HgCl_2$, $HgBr_2$, $HgI_2$, $CdI_2$ and $CuCl_2$ and found that in these structures, the N-atoms of pyridine and benzimidazole coordinate to the metal centers with M4L4 metallamacrocycles. They found that MOGs were formed by intertwined gel fibers which provide stability to the gel structures through coordination, hydrogen bonding and π···π interactions as studied by microscopic analysis, such as POM, SEM and TEM studies. They observed that MOGs

exhibit thixotropic behavior as well as chemo-responsive behavior and the xerogel materials of the MOGs exhibits $N_2$ gas sorption property.

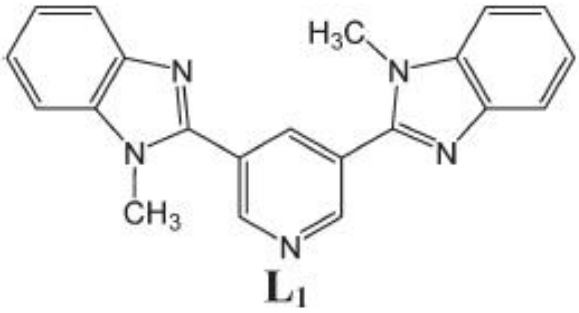


**L1**

**Scheme 1.5** The chemical drawings of L1

Meng et al. [20] synthesized coordination complexes $\{[Cd_2(dcpp)(beb)_2(H_2O)]\cdot H_2O\}_n$ (**1**), $[Cd_2(dcpp)(bmb)(H_2O)_2]_n$ (**2**), $\{[Cd_2(dcpp)(2,2'\text{-bipy})\text{-}(H_2O)_2]\cdot 2H_2O\}_n$ (**3**) and $\{[Cd_2(dcpp)(4,4'\text{-bipy})_{0.5}(H_2O)_3]\cdot H_2O\}_n$ (**4**) by utilizing a butterfly-shaped multidentate carboxylic acid $H_4$dcpp = 4,5-di(4′-carboxylphenyl)phthalic acid and N-donor ligands beb = 1,4-bis(2-ethylbenzimidazol-1-ylmethyl)benzene, bmb = 1,4-bis(2-methylbenzimidazol-1-ylmethyl) benzene, 2,2′-bipy = 2,2′-bipyridine, 4,4′-bipy = 4,4′-bipyridine (Fig. 1.15). They indicate that complexes **1−4** were potential semi-conductive materials on the basis of optical energy gaps of these complexes and moreover, these complexes could also be applied to catalyze the reaction of photocatalytic degradation of methylene orange (MO) under high-pressure mercury lamp irradiation.

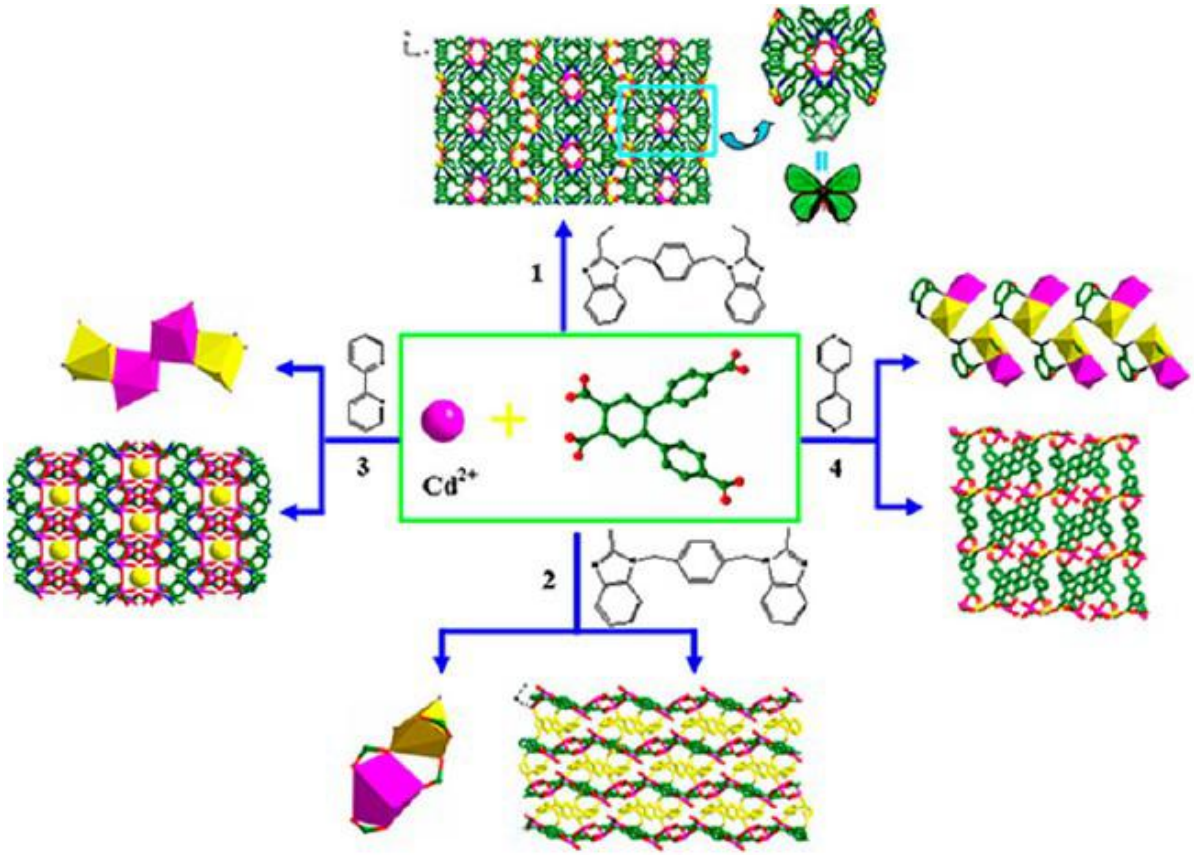


**Fig. 1.15** Schematic presentation of structures of complexes **1-4**

Tarulli et al. [21] synthesized new distorted tetrahedral cadmium complex $[Cd(tsac)_2(bzim)_2].CH_3OH$ (tsac = anion of thiosaccharine, bzim = benzimidazole) and characterized by single crystal X-ray diffraction and FTIR spectrum. They found that the Cd(II) cation is at the centre of a distorted tetrahedral environment, coordinated by two thiosaccharinato anions through their sulphur atoms and two neutral benzimidazole molecules (Fig. 1.16). They also observed that the ligand–Cd–ligand angles are in the range from 95.08(4) to 122.89(4)$^o$ and the complex was stabilized by electrostatic interactions between the Cd(II) ion and the thiosaccharinate N-atoms.

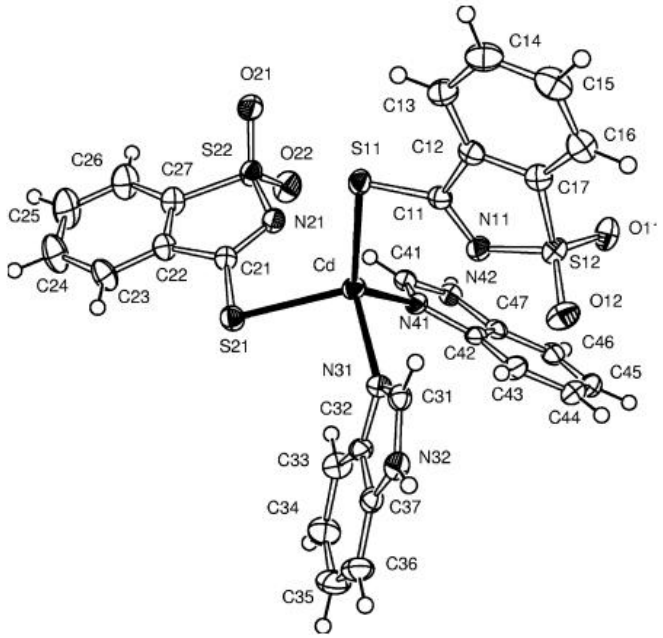


**Fig 1.16** Crystal structure of $[Cd(tsac)_2(bimz)_2]$

Sokol et al. [22] synthesized 2-(1-vinyl)imidazol-2-yl)benzimidazole (L) and 2-(1-ethyl)imidazol-2-yl)benzimidazole (L'), $[Cu(L)Cl_2]$ (**1**) and $[Zn(L')Cl_2]$ (**2**) and studied the effect of complexation on the conformation, degree of bond conjugation and molecular interactions in the crystal structure. They found that the ligand act as a N,N´-bidentate chelating ligand with zinc and copper metal and copper formed a distorted square complex whereas zinc complex had a distorted tetrahedron geometry (Fig. 1.17).

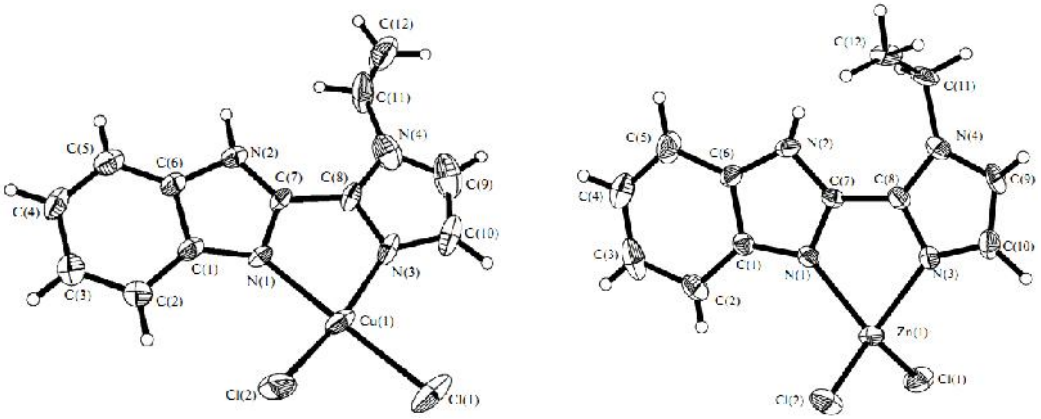


**(a)** **(b)**

**Fig 1.17 (a)** Crystal structure of complex **1** and **(b) 2**

Liu et al. [23] reported seven new metal complexes $[Zn(L_1)_2]_n$ (**1**), $[Co(L_2)(L_A)]_n$ (**2**), $[Zn(L_2)(L_B)]_n$ (**3**), $[Cu(L_2)(SO_4)]_2$ (**4**), $[Co_2(L_1)_2Cl_4]$ (**5**), $[Co(L_2)(L_C)_2]$ (**6**) and $[Zn(L_2)(NO_3)_2]$ (**7**) ($L_1$ = 2,2´-bis(benzimidazol-l-yl)ethylether,

$L_2$ = 1,2-bis[2´-(benzimidazol-1-yl)ethoxy] ethane, $L_A$ = succinate, $L_B$ = terephthalate and $L_C$ = 4-aminobenzoate) based on dibenzimidazolyl bidentate ligands and structurally characterized by X-ray diffraction analyses (Scheme 1.6). They also studied the fluorescence emission spectra and quantum yields of ligands and metal complexes. They found that the ligand $L_1$ showed weak double emission bands centered at 305 and 335 nm, corresponding to intraligand transitions [24], whereas complexes **1-7** also exhibits a double emission bands in the region of 285-320 nm and 330-340 nm, but they are stronger than that of $L_1$, which would originate from the metal perturbed intraligand processes [25] (Fig. 1.18).

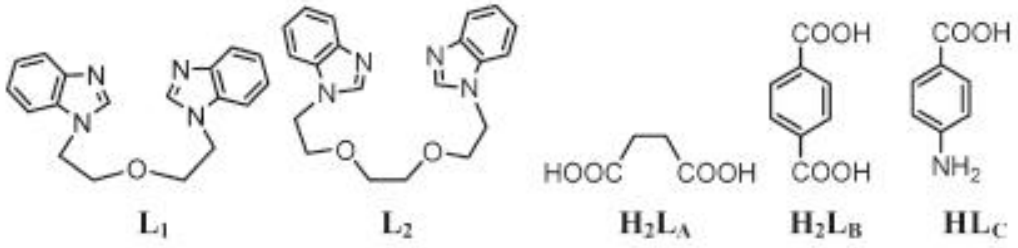


**Scheme 1.6** Schematic presentation of $L_1$, $L_2$, $H_2L_A$, $H_2L_B$ and $H_2L_C$

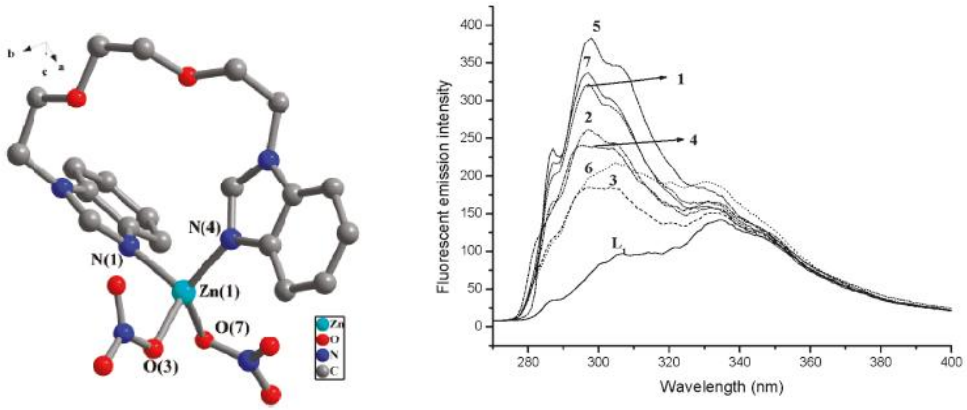


**(a)** **(b)**

**Fig 1.18 (a)** Perspective view of **7**. **(b)** Emission spectra of $\mathbf{L_1}$ and **1-7** at room temperature in $CH_3CN$ solution

Li et al. [26] constructed seven coordination polymers namely, $[Cd_2(ODPT)(L1)(H_2O)_2].H_2O$ (**1**), $[Cd_2(ODPT)(L2)(H_2O)_2]$ (**2**), $[Zn_2(BPTC)(L3)].(H_2O)_3$ (**3**), [Cd(*m*-BDC)(L4)] (**4**), [CdL5] (**5**), $[CdL6].H_2O$ (**6**) and $[ZnL6].H_2O$ (**7**) ($H_4$ODPT=4,4´-oxidiphthalic acid, $H_4$BPTC = 3,3´,4,4´-benzophenone tetracarboxylate ligand, $H_2$*m*-BDC= 1,4-benzenedicarboxylate acid, L1=1,4-di(1H-

benzo[d]imidazol-2-yl)butane, L2=bis((1H-benzo[d]imidazol-2-yl)methyl)amine, L3=1,4-bis(1-(pyridin-4-ylmethyl)-1H-benzo[d]imidazol-2-yl)butane, L4=bis((1-(pyridin-4-ylmethyl)-1H-benzo[d]imidazol-2-yl)-methyl)amine, $H_2L5$=4,4´-(2,2´-(butane-1,4-diyl)bis(1H-benzo[d]imidazole-2,1-diyl))bis(methylene)dibenzoic acid and $H_2L6$= 2,2´-(2,2´-azanediylbis(methylene)bis(1H-benzo[d]imidazole-2,1-diyl))diacetic acid) under hydrothermal conditions. They characterized them by elemental analyses, IR spectra, and thermogravimetric (TG) analyses and further determined their structures by single crystal X-ray diffraction analyses (Fig. 1.19).

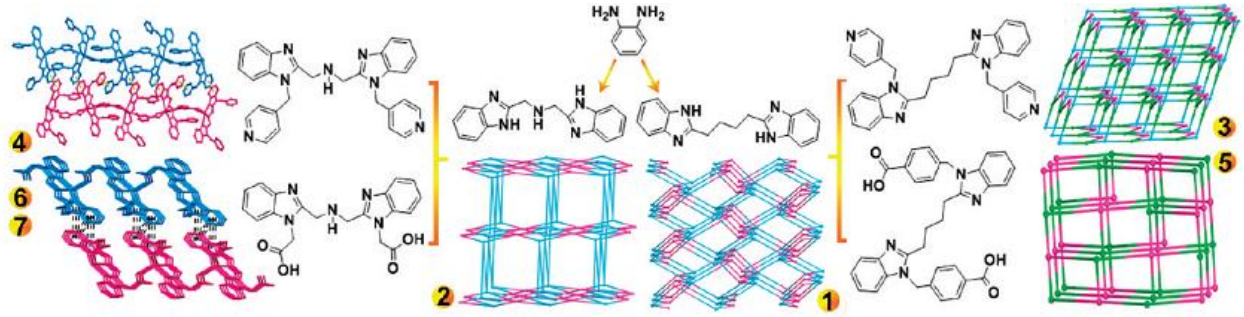


**Fig. 1.19** View of all Seven Compounds

Guo et al. [27] synthesized five metal complexes $[Co(p\text{-bdc})(beb)_{0.5}]_n$ (**1**) $\{[Co(p\text{-bdc})(bmb)]\cdot H_2O\}_n$ (**2**) $\{[Co(p\text{-bdc})(bmp)]\cdot H_2O\}_n$ (**3**) $\{[Zn(p\text{-bdc})(bmp)]\cdot H_2O\}_n$ (**4**) and $[Zn_2(p\text{-bdc})_2(bmp)(H_2O)_2]_n$ (**5**) under hydrothermal conditions ($p$-$H_2$bdc = 1,4-benzenedicarboxylic acid, beb = 1,4-bis(2-ethylbenzimidazol-1-ylmethyl)benzene, bmb = 1,4-bis(2-methylbenzimidazol-1-ylmethyl)benzene and bmp = 1,5-bis(2-methyl-benzimidazol) pentane) and characterized by X-ray diffraction and thermal analysis (Fig. 1.20). They observed on the basis of structural analysis that the steric hindrance resulting from changing of ligands can tune the final interpenetrating networks directly.

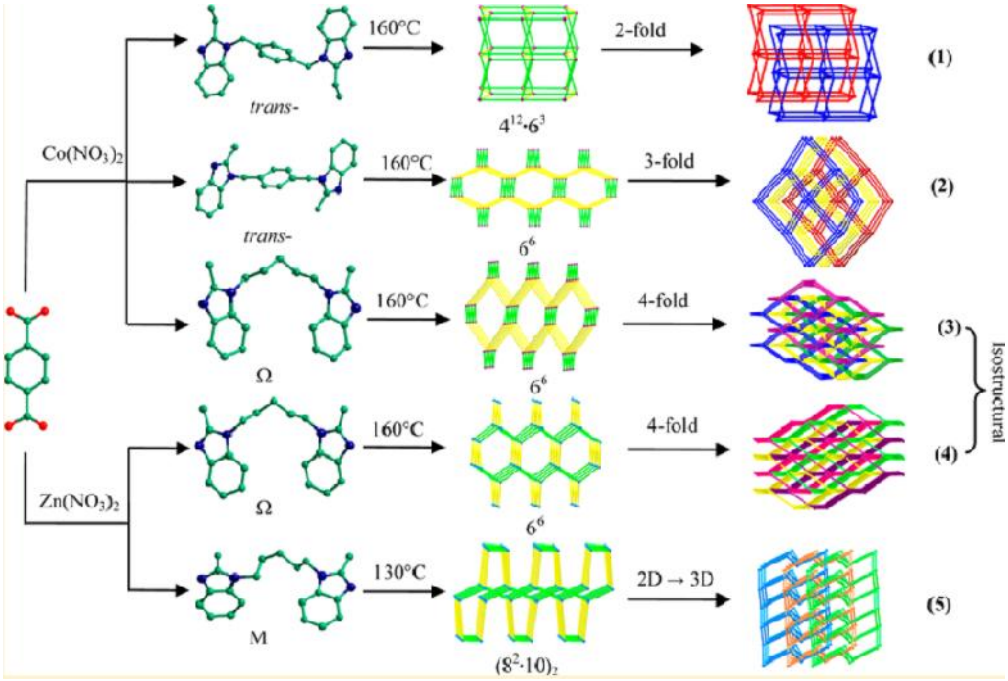


**Fig. 1.20** Schematic representation of coordination environments of Co(II) and Zn(II)

Liu et al. [28] constructed two novel metal-organic frameworks $[Ni_7(H_2O)_6L_2(O)_2](Cl)_2(NO_3)_2.6(H_2O).(Emim)_2$ (**1**) and $[Ni_2(H_2O)_2L].7(H_2O)$ (**2**) using ionothermal and hydrothermal synthesis, respectively (Scheme 1.7). By inspection of the structures of **1** and **2**, they believed that the different reaction conditions play an important role in forming the final structures and investigated the optical band gap of compound **1**.

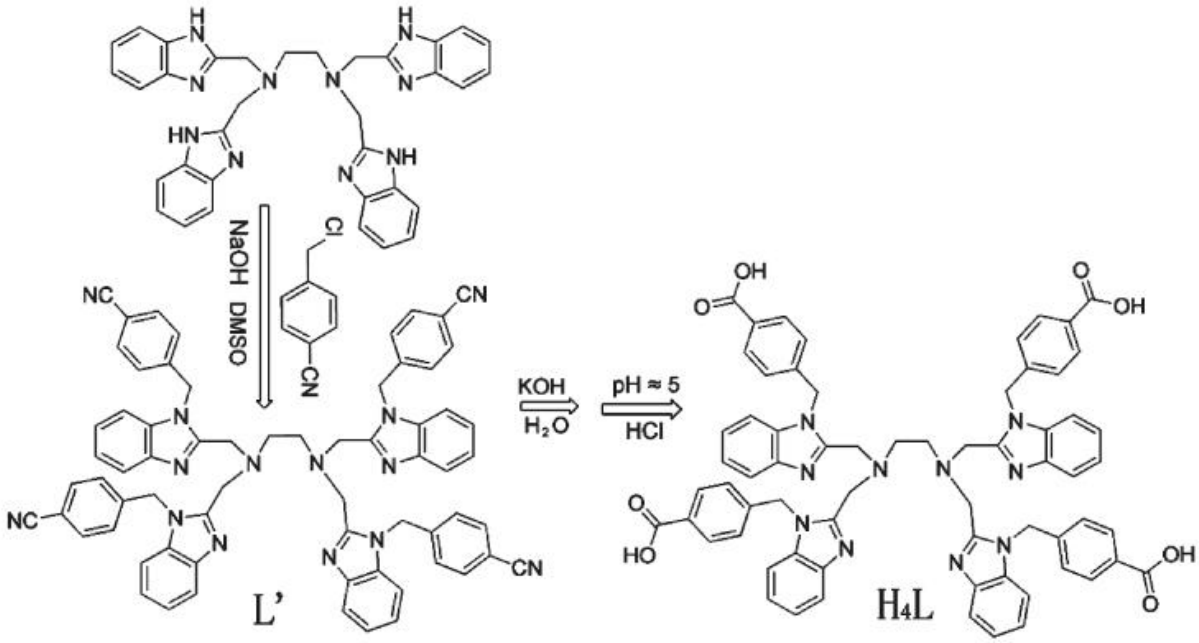


**Scheme 1.7**

Berding et al. [29] prepared nickel (II) halide complexes of novel chelating bidentate benzimidazole-based N-heterocyclic carbenes from $Ni(OAc)_2$ with bisbenzimidazolium salts and revealed a *cis*-geometry on a square-planar nickel center via single-crystal X-ray structure determination (Scheme 1.8 and Fig. 1.21). They found that these complexes are active catalysts for the Kumada coupling of 4-chloroanisole and 4-bromoanisole with phenylmagnesium chloride.

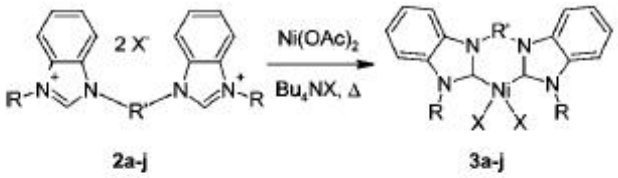


**2a-j** **3a-j**

**3a** R=Me, R'=1,3-propyl, X=Br **3f** R=Ph, R'=1,3-propyl, X=Br
**3b** R=Me, R'=1,3-propyl, X=Cl **3g** R=Me, R'=1,4-butyl, X=Br
**3c** R=Pr, R'=1,3-propyl, X=Br **3h** R=Me, R'=1,4-butyl, X=Cl
**3d** R=$^{i}$Pr, R'=1,3-propyl, X=Br **3i** R=Me, R'=1,1'-$SiMe_4$, X=Br
**3e** R=Bn, R'=1,3-propyl, X=Br **3j** R=Me, R'=α,α'-o-xylyl, X=Br

**Scheme 1.8** Different substitution over **3a-3j**

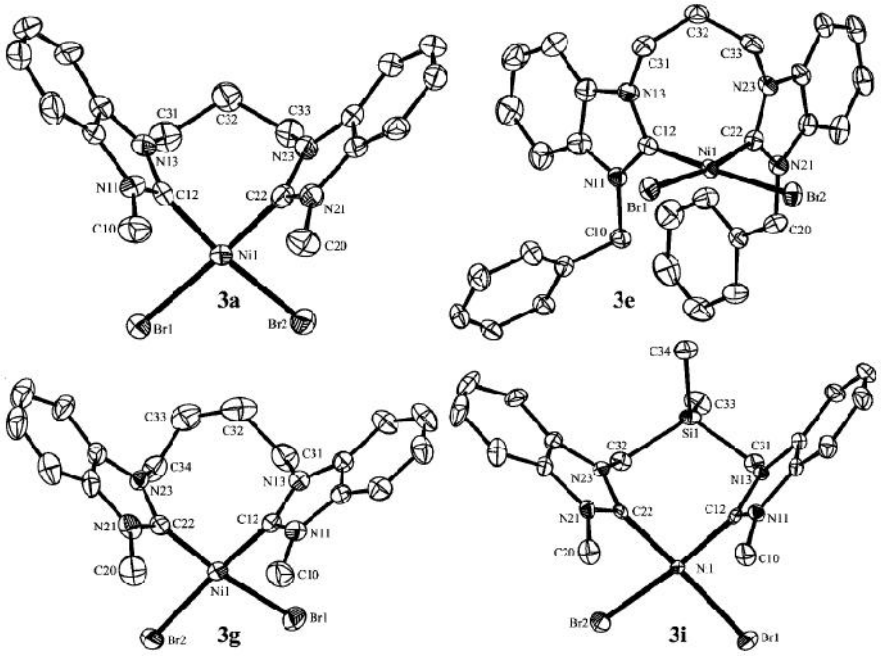


**Fig 1.21** Crystal structure of **3a**, **3e**, **3g** and **3i**

Panja et al. [30] reported four new metal complexes *mer*-$[Fe(bbp)(CN)_3]^{2-}$ **(1)**, trinuclear $\{[Ni(ntb)(MeOH)]_2[Fe(bbp)(CN)_3][ClO_4]_2\}\cdot 2MeOH$ **(2),** tetranuclear rectangular $\{[Ni(tren)]_2[Fe(bbp)(CN)_3]_2\}\cdot 7MeOH$ **(3)** and bimetallic $\{[Ni(dpd)_2]_2[Fe(bbp)(CN)_3]_2\}\cdot 9MeOH\cdot 3H_2O$ **(4)**. They characterized them by IR, UV-Vis and single crystal diffraction method and established that these complexes are stabilized in the solid state by extensive hydrogen bonding and moderate strong π···π stacking interactions (Fig. 1.22-1.23).

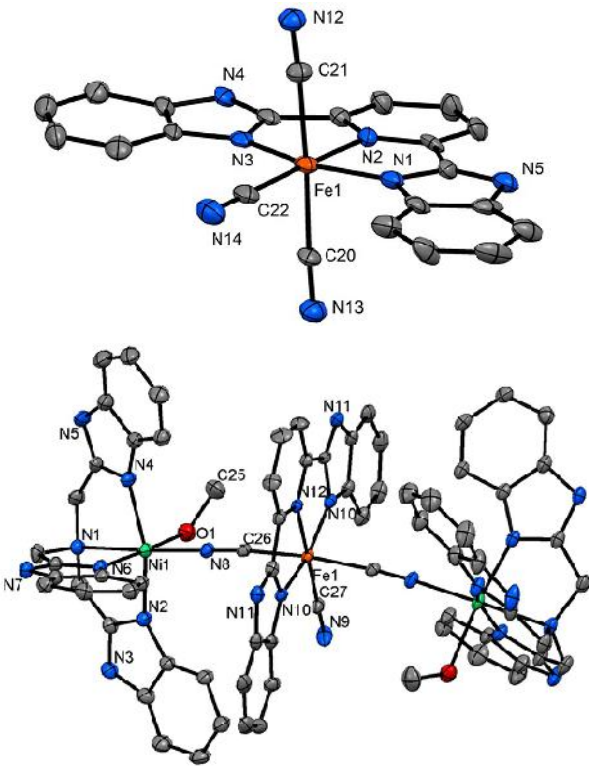


**(a)** **(b)**

**Fig 1.22 (a)** Crystal structure of **1** and **(b) 2**

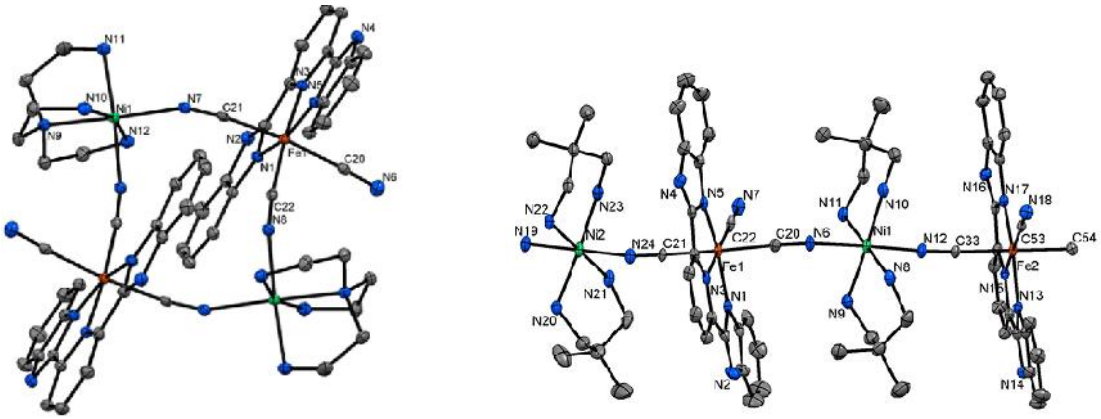


**(a)** **(b)**

**Fig 1.23 (a)** Crystal structure of **3** and **(b) 4**

Along with nickel, zinc and cadmium, various other metals e.g. iron, cobalt, copper, silver, ruthenium, palladium are also reported in literature which formed metal complexes with benzimidazole as well as derivatives of benzimidazole ligands with various applications in different field.

Lai et al. [31] reported two novel benzimidazole-bridged dinuclear ferrocenyl derivative viz., 1-ferrocenyl methyl-2-ferrocenyl-3-methylbenzimidazolium iodide **(1)** and 1-ferrocenyl methyl-2-ferrocenyl-3-ethylbenzimidazolium iodide **(2)** and

characterized by X-ray crystallography, IR, $^{1}H$ and $^{13}C$ NMR and elemental analysis (Fig. 1.24). They demonstrated that these complexes are of great value in preparing high-burning-rate catalyst for composite solid propellants.

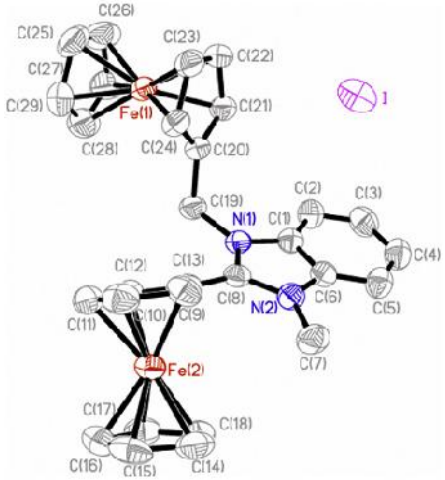


**Fig 1.24** Crystal structure of **1**

Sun et al. [32] synthesized two novel helical supramolecular architectures by self-assembly of cobalt (II) (**1**) and copper (II) (**2**) complexes with 1-[(5-methyl-2-furyl)methylene]-2-(5-methyl-2-furyl)benzimidazole, which were stabilized through the intra- and intermolecular π···π interactions between benzimidazole rings (Fig. 1.25). They observed that when the methylfuran fragment of the ligand was replaced by a furan group, the cobalt complex (**3**) of 1-(2-furylmethylene)-2-(2-furyl)benzimidazole formed another type of supramolecular network through π···π interactions under similar reaction conditions (Fig. 1.26). They investigated the spectral and thermal behaviors of complexes **1**-**3** by ultraviolet, chiral dichroism, and fluorescence spectral and thermogravimetric techniques.

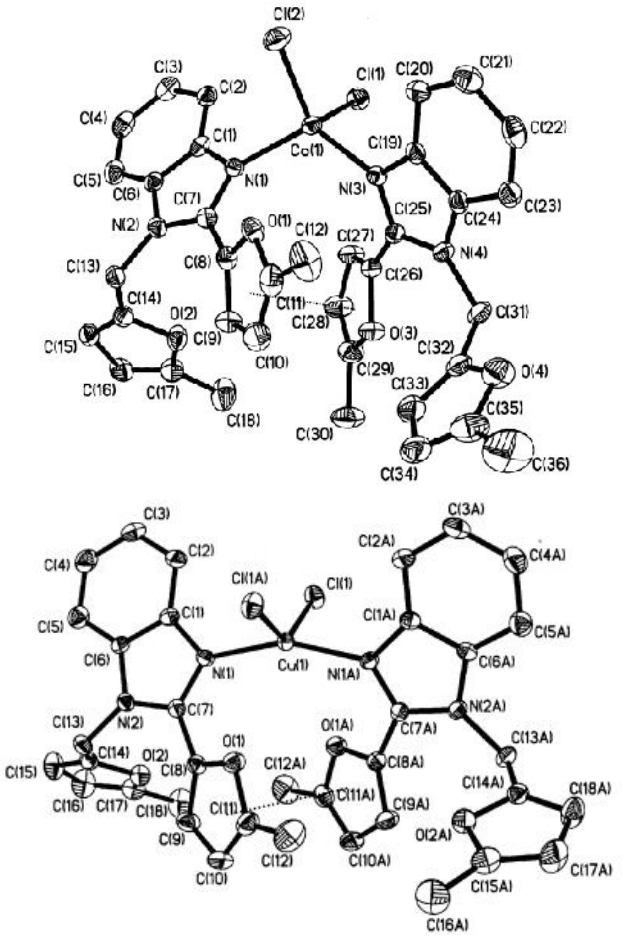


**(a)** **(b)**

**Fig 1.25 (a)** Crystal structures of **1**and **(b) 2**

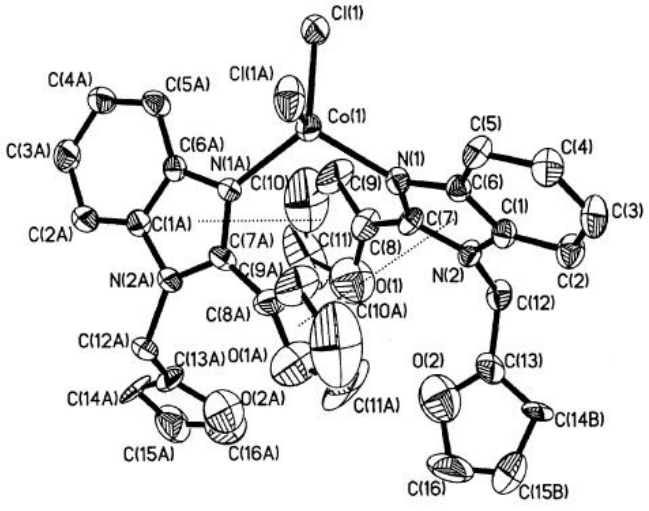


**Fig 1.26 (a)** Crystal structure of **3**

Payra et al. [33] reported dimethyl-substituted bis(benzimidazole) ($Me_2BBZ$) and synthesized its metal complexes with a variety of metals e.g., Mn(II), Fe(II), Co(II), Ni(II) and Cu(II) (Fig. 1.27).

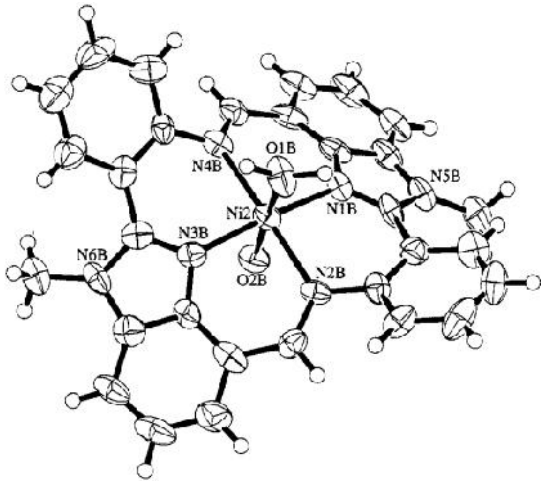


**Fig 1.27** Crystal structure of $[Ni(Me_2BBZ)(H_2O)_2](ClO_4)_2$

Gupta et al. [34] synthesized pentacoordinated copper (II) complex $[CuCl(GMBHA)]Cl.H_2O.CH_3OH$ from tetradentate ligand N,N′-bis(2-methyl-N-methylbenzimidazolyl)hexanediamide and characterized on the basis of elemental analysis, electronic spectra, IR studies, conductance data, magnetic properties, EPR and X-ray studies (Fig. 1.28). They found the stoichiometry of the complexes as 1:1 metal to ligand ratio from analytical data. They demonstrate that the metal was coordinated with tetradentate ligand through two benzimidazolyl nitrogen and two amide oxygen atoms and the fifth coordination site of the metal was occupied by the anion from metal salt.

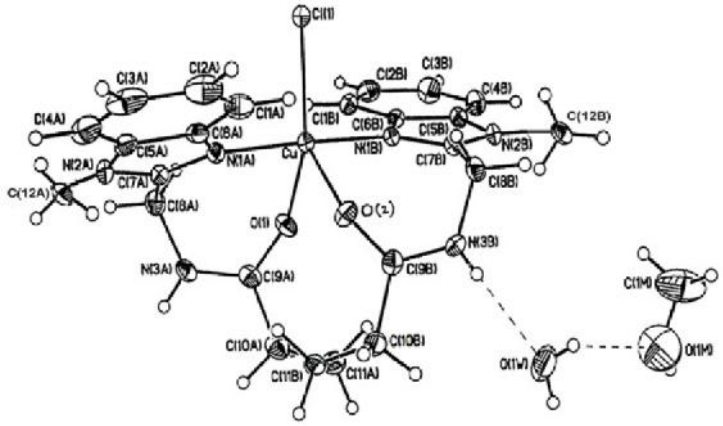


**Fig. 1.28** Crystal structure of $[CuCl(GMBHA)]Cl.H_2O.CH_3OH$

Devereux et al. [35] reported a new series of Cu(II) complexes $[Cu(BZA)_2(bipy)(H_2O)]$ **(1)**, $[Cu(CH_3COO)_2(5,6\text{-}DMBZDH)_2]$ **(2)** and $[Cu(salH)_2(BZDH)_2]$ **(3)** **(**BZDH = benzimidazole, 5,6-DMBZDH = 5,6-dimethylbenzimidazole, $SalH_2$ = salicylic acid, BZAH = benzoic acid,) They

demonstrated that complex **1** had square pyramidal, whereas **2-3** were square planar geometry (Fig. 1.29-1.30). They observed that all the complexes exhibit an excellent superoxide dismutase (SOD) mimetic activity and the two phen derivatives [$Cu(CH_3COO)_2$(phen)] and [Cu(sal)(phen)] displays a potent *in vitro* cytotoxicity against human hepatic (Hep-G), renal (A-498) and lung (A-549) cancer cell lines.

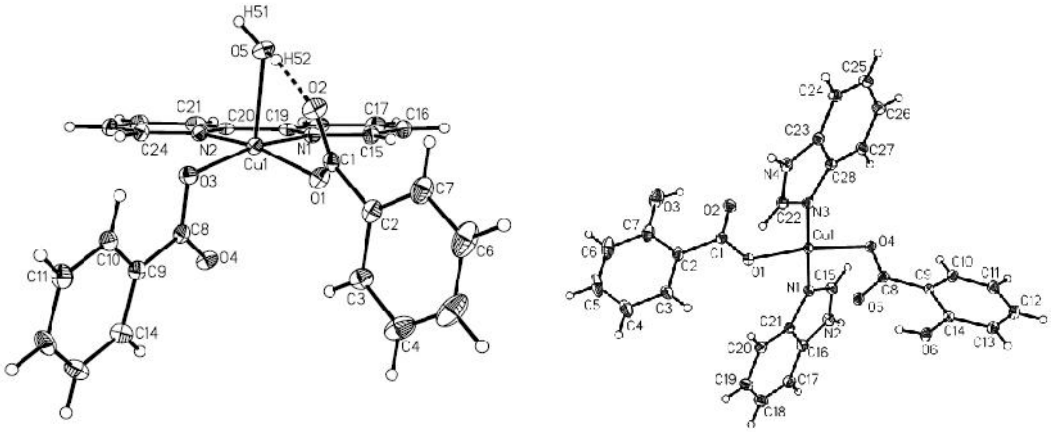


**(a)** **(b)**

**Fig 1.29 (a)** Crystal structure of [$Cu(BZA)_2$(bipy)($H_2O$)] and **(b)** [$Cu(salH)_2(BZDH)_2$]

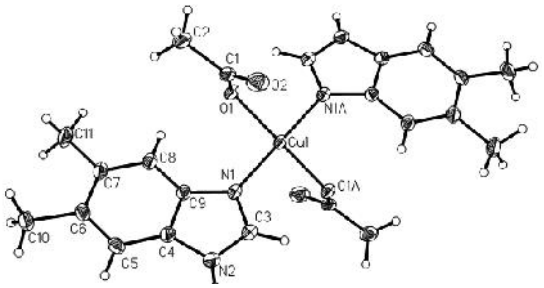


**Fig 1.30** Crystal structure of [$Cu(CH_3COO)_2$(5,6-DMBZDH)$_2$]

Tehlan et al. [36] prepared Cu(II) complexes of general composition [Cu(L)X]X (L = O-ABHA or O-GBHA and X = $Cl^-$ or $NO_3^-$ ) with the new N-octylated benzimidazole-based diamide ligands N,N´-bis(N-octylbenzimidazolyl-2-ethyl)hexanediamide (O-ABHA) and N,N´-bis(N-octylbenzimidazolyl-2-methyl)hexanediamide (O-GBHA). They obtained the X-ray structure of one of the complexes, [Cu(O-GBHA)$NO_3$]$NO_3$ where the Cu(II) ion is in distorted octahedral geometry and the N2O2 equatorial plane comprises an amide carbonyl O, a nitrate O, and the two benzimidazole imine N atoms while another amide carbonyl O and nitrate O take up the axial positions (Fig. 1.31). They found that these complexes can oxidize

aromatic alcohols to aldehydes in the presence of cumenyl hydroperoxide at 40-45 °C and act as catalyst with turnovers varying between 13- and 27-fold.

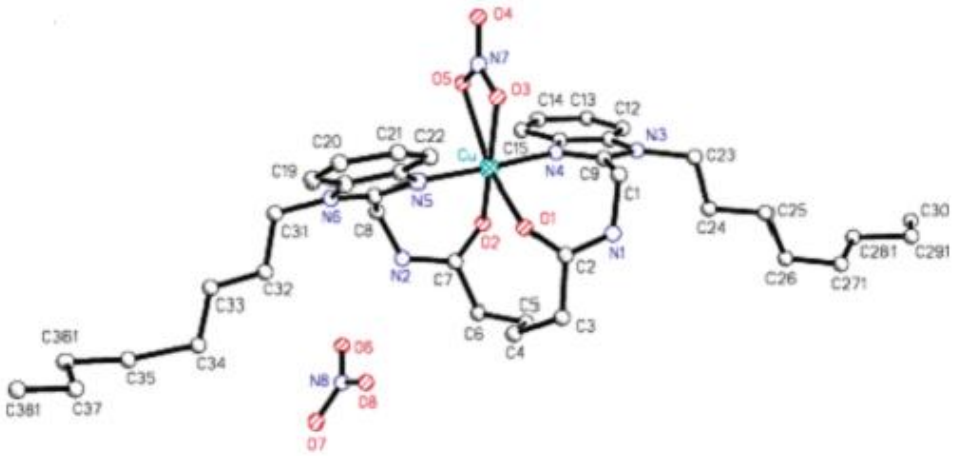


**Fig 1.31** Crystal structure of $[Cu(O\text{-}GBHA)(NO_3)](NO_3)$

Xia et al. [37] synthesized three novel silver (I) metal complexes namely, $[Ag_2(PyBIm)_2(H_2O)_2]SO_4.H_2O$ **(1)**, $[Ag_3(PyBIm)_3(\mu_2\text{-}SO_4)(HSO_4)].3H_2O$ **(2)** and $[Ag_2(PyBIm)_2(\mu_2\text{-}SO_4)].4H_2O$ **(3)** **(**PyBIm = 2-(4-pyridyl)benzimidazole) by hydrothermal methods (Fig. 1.32). They found that the N-H groups of benzimidazoyl did not coordinate to silver (I) atoms and formed strong hydrogen bonding with lattice water or uncoordinated sulfate groups and contribute to the packing of the complexes. They observed that all these complexes exhibit photoluminescence in the visible region and characterized them, using standard analytical and spectroscopic techniques.

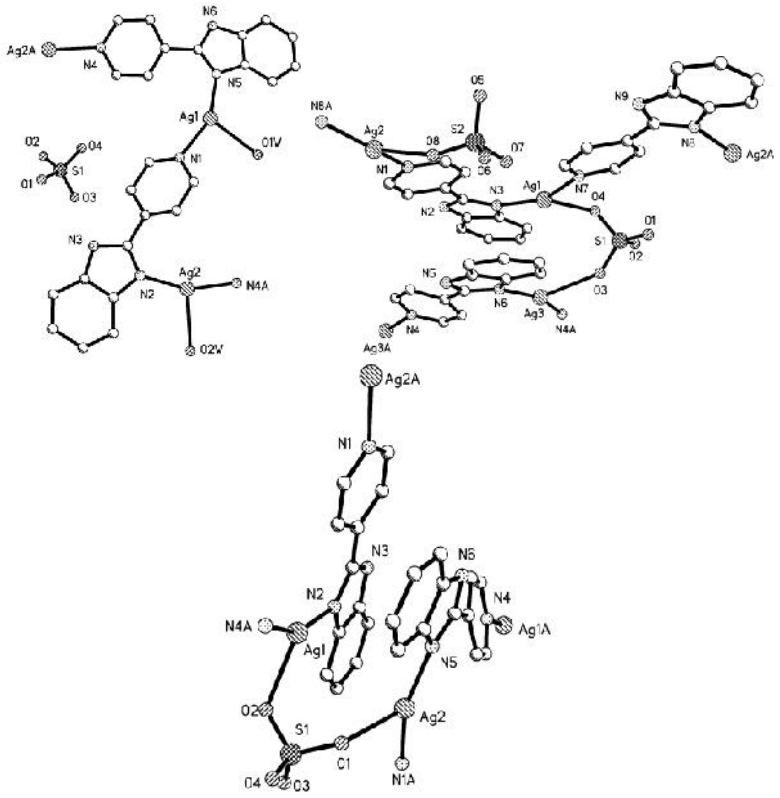


**(a)** **(b)** **(c)**

**Fig 1.32** Crystal structure of complexes **1-3**

Sharma et al. [38] synthesized and structurally characterized oligodentate pyridyl-(**1**) and benzimidazole ligands (**2-3**) and their ruthenium (II) and (III) complexes viz., $([Ru(L1)(Cl)(PPh_3)]^+$ (**4**), $([Ru(L2)(Cl)(PPh_3)]^+$ (**5**) and $([Ru(L3)(Cl)(H_2O)]^{2+}$ (**6**) (Scheme 1.9). Their investigations revealed that if the coordination sphere of the metal ion carries a strong coordinating $PPh_3$ ligand (complexes **4** and **5**), the framework was not suitable for anion binding at all, however, coordination of solvent ($H_2O$) to the metal centre (complex **6**) generate a receptor for anion recognition through fluorescence spectroscopy.

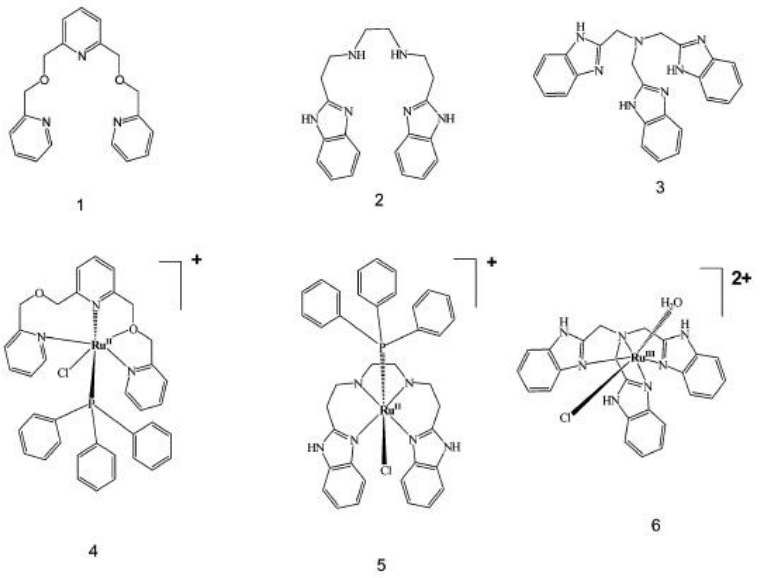

**Scheme 1.9**

Araki et al. [39] treated the protic N-heterocyclic carbine (NHC) complex [Cp*RuCl(LH)] (**2**) **(**LH = N-(2-pyridyl)benzimidazolin-2-ylidene-$\kappa^2$N,C) (Scheme 1.10) with $AgNO_2$ which gives the nitrosyl–imidazolyl complex [Cp*Ru(NO)(L)][OTf] (OTf = $OSO_2CF_3$), which undergoes in a reversible protonation to afford the NHC complex [Cp*Ru(NO)(LH)][OTf]$_2$. They found that the bifunctional complex **2** also catalyzes the dehydrative condensation of N-(2-pyridyl)benzimidazole and allyl alcohol, which leads to the formation of *trans*- and *cis*-2-(1-propenyl)-N-(2-pyridyl)benzimidazole.

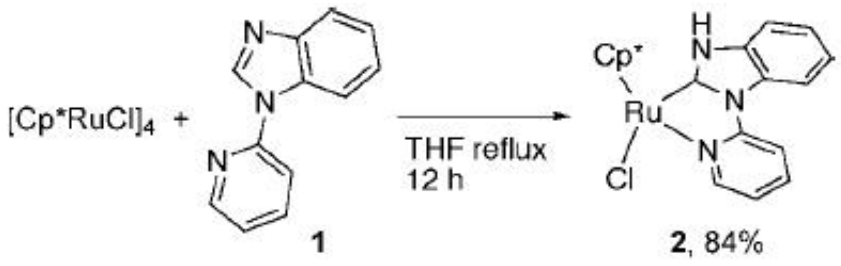


**Scheme 1.10** Synthesis of [Cp*RuCl(LH)]

Yutaka et al. [40] reported three novel Ir(III) complexes [Ir(L1)$_2$](PF$_6$)$_3$.3CH$_3$CN **(1)**, [Ir(L1)(bpy)Cl](PF$_6$)$_2$.2CH$_3$CN **(2)** [Ir(L1)(L2)](BPh$_4$)$_2$.CH$_3$CN **(3) (**L1=2,6-bis(1-methyl-benzimidazol-2-yl)pyridine, L2

= 1,3-bis-(1-methyl-benzimidazol-2-yl)benzene, bpy = 2,2′-bipyridine) and characterized all the three metal complexes by X-ray crystallography, IR, $^1$H NMR and elemental analysis and studied their photophysical and electrochemical properties (Fig. 1.33). They found that Ir(III) complexes exhibits phosphorescent emissions in the 500−600 nm, with lifetimes ranging from approximately 1-10 µs at 295 K.

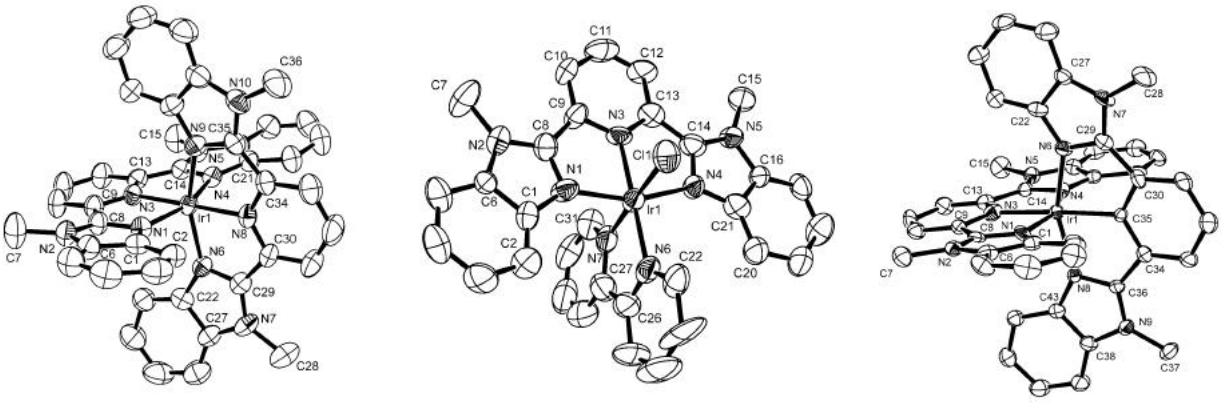


**Fig 1.33** Crystal structure of **(a)** $[Ir(L1)_2](PF_6)_3.3CH_3CN$ **(1) (b)** $[Ir(L1)(bpy)Cl](PF_6)_2.2CH_3CN$ **(2)** and **(c)** $[Ir(L1)(L2)](BPh_4)_2.CH_3CN$ **(3)**

Hahn et al. [41] reported the reaction of the xylene-bridged bisbenzimidazolium salts 2,6-bis(N-alkyl-N´-methylenebenzimidazolium)-1-bromophenylene dibromide (**1**, alkyl = ethyl; **2**, alkyl = *n*-propyl; **3**, alkyl = *n*-butyl) with $[Pd_2(dba)_3]$ yields the palladium pincer complexes of type [Pd(L)Br] (**4**-**6**) (L = 2,6-bis(N-alkyl-N´-methylenebenzimidazolin-2-ylidene) phenylene) (Fig. 1.34) and tested **4**-**6** as precatalysts in Heck and Suzuki coupling reactions of various aryl bromides with styrene and phenylboronic acid.

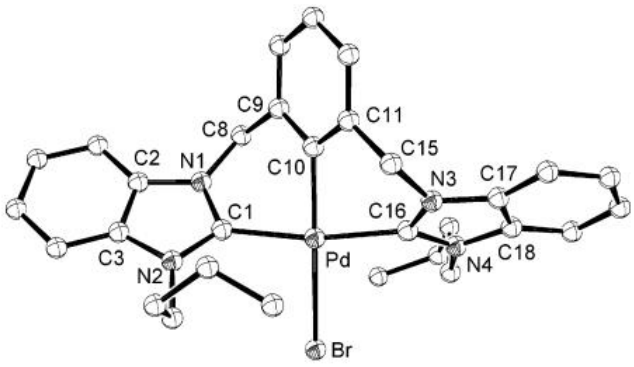


**Fig 1.34** Crystal structure of **6**

Not only transition metal complex, but lanthanides are also reported in literature forming metal complexes with the ligands derived from the benzimidazole moiety.

Hong et al. [42] reported the temperature-driven single-crystal to single-crystal transformation of a new erbium (III) coordination polymer $\{[Er(bidc)(ClO_4)((H_2O)_3].3H_2O\}_n$ (**1**) to $[Er(bidc)(ClO_4)]_n$ (**2**) ($H_2$bidc = benzimidazole-5,6-dicarboxylic acid) and studied their thermal stability by thermogravimetric analysis (TGA) (Scheme 1.11). They demonstrated the oxo-affinity-induced and temperature-driven SC-SC transformation, involving the release of coordinated aqua molecules, from the 1-D Er(III) complex **1** to the 2-D Er(III) coordination polymer **2** without any coordination of water molecules. They found from the photoluminescent analysis that the NIR emission of the Er(III) ion in compound **2** could be enhanced as compared to that in **1**, which indicates the energy transfer from the ligand to the $Er^{3+}$ ion in **2** was more effective than in **1**.

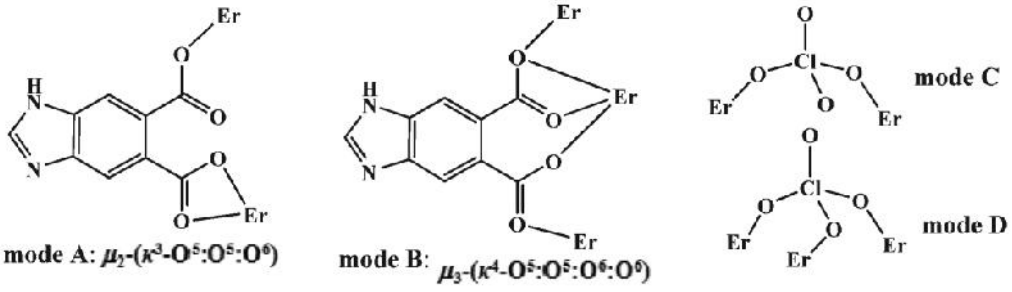


**Scheme 1.11** The coordination modes of the ligand and $ClO_4$ in complexes **1** and **2**

Muller et al. [43] synthesized the ligand neopentyl 2,6-bis[(1-methylbenzimidazol-2-yl)]-pyridine-4-carboxylate (L) and its lanthanide $[Ln(L)_3]^{3+}$ complexes (Fig. 1.35). They found the helical wrapping of the ligand strands around the Ln(III) ions through Chiro-optical data.

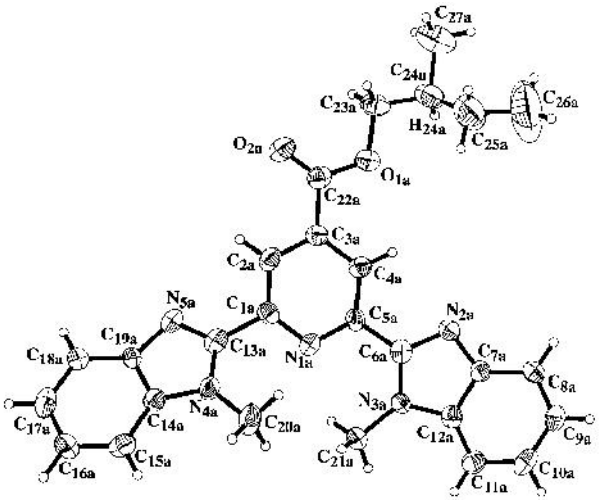


**Fig. 1.35** Molecular structure of **L**

The above literature revealed that various benzimidazole derivatives can dramatically change the structural chemistry of the salt/co-crystal or metal complexes which in turn can tune the supramolecular assemblies in the crystalline material and in turn can also change their physical properties.

Since very few salts of benzimidazole ligand with the various positional isomers of pyridine dicarboxylic acid are present in the literature, in present thesis an attempt has been made for the preparation of salts with various positional isomer of pyridine dicarboxylic acid in the present thesis. In addition, salts of benzimidazole derivative ligand with inorganic acids have been also synthesized. Furthermore nickel, zinc and cadmium complexes were also synthesized with these ligands.

**References**


1. Kamal, A., Kumar, P. P., Sreekanth, K., Seshadri, B. N. and Ramulu, P., "Synthesis of new benzimidazole linked pyrrolo[2,1-c][1,4]benzodiazepine conjugates with efficient DNA-binding affinity and potent cytotoxicity", *Bioorg. Med. Chem. Lett*., **18**, 2594 (2008).
2. Göker, H., Kuş, C., Boykin, D. W., Yildiz, S. and Altanlar, N., "Synthesis of some new 2-substituted-phenyl-1H-benzimidazole-5-carbonitriles and their potent activity against candida species", *Bioorg. Med. Chem*., **10**, 2589 (2002).
3. Güven, Ö. Ö., Erdoğan, T., Göker, H. and Yildiz, S., "Synthesis and antimicrobial activity of some novel phenyl and benzimidazole substituted benzyl ethers", *Bioorg. Med. Chem. Lett*., **17**, 2233 (2007).
4. Nobilis, M., Jira, T., Lísa, M., Holčapek, M., Szotáková, B., Lamka, J. and Skálová, L., "Achiral and chiral high-performance liquid chromatographic determination of flubendazole and its metabolites in biomatrices using UV photodiode-array and mass spectrometric detection", *J. Chromatogr. A*., **1149**, 112 (2007).
5. Elderfield, R. C., "Heterocyclic compounds", vol 5. Wiley, New York (1957).
6. Katritzky, A. R. and Rees, C. W., "Comprehensive heterocyclic chemistry", vol 5. Pergamon, Oxford (1984).
7. Hobrecker, F., "Ueber reductionsprodukte der nitracetamidverbindungen", *Ber. Dtsch. Chem. Ges*., **6**, 920 (1872).
8. VanVliet, D. S., Gillespie, P. and Scicinski, J. J., "Rapid one-pot preparation of 2-substituted benzimidazoles from 2-nitroanilines using microwave conditions", *Tetrahedron Lett*., **46**, 6741 (2005).
9. Ibrahim, M. N. "Synthesis and characterization of 2-arylbenzimidazoles by reactions of *o*-nitroaniline and aromatic aldehyde derivatives via reductive cyclization", *Asian J. Chem*., **19**, 2419 (2007).
10. Shao, J., Qiao, Y., Lin, H. and Lin, H., "Rational design of novel benzimidazole-based sensor molecules that display positive and negative fluorescence responses to anions", *J. Fluoresc*., **19**, 183 (2009).
11. Hranjec, M., Pavlovic, G. and Karminski-Zamola, G., "Spectroscopic characterization, crystal structure determination and interaction with DNA of novel cyano substituted benzimidazole derivative", *Struct. Chem*., **18**, 943 (2007).

12. Li, L. and Clarkson, G. J., “New bis(benzimidazole) cations for threading through dibenzo-24-crown-8”, *Org. Lett*., **9**, 497 (2007).
13. Rachocki, A., Pogorzelec-Glaser, K., Ławniczak, P., Pugaczowa-Michalska, M., Łapiński, A., Hilczer, B., Matczak, M. and Pietraszko A., “Protonc conducting compound of benzimidazole with sebacic acid: Structure, molecular dynamics, and proton conductivity”, *Cryst. Growth Des*., **14**, 1211 (2014).
14. Jin, S., Guo, J., Liu, L. and Wang, D., “Five organic salts assembled from carboxylic acids and bis-imidazole derivatives through collective noncovalent interactions”, *J. Mol. Struct*., **1004**, 227 (2011).
15. Jin, S. and Wang, D., “Eight supramolecular assemblies constructed from bis(benzimidazole) and organic acids through strong classical hydrogen bonding and weak noncovalent interactions”, *J. Mol. Struct*., **1065**, 120 (2014).
16. Wang, Y., Xu, H. -B., Su, Z. -M., Shao, K. -Z., Zhao, Y. -H., Cui, H. -P., Lan,Y. -Q. and Hao, X. -R., “Anion-directed assembly of two novel cadmium (II) complexes constructed by 2,20-(1,4-butanediyl)bis(1H-benzimidazole) ligand”, *Inorg. Chem. Commun*., **9**, 1207 (2006).
17. Esparza-Ruiz, A., Peña-Hueso, A., Mijangos, E., Osorio-Monreal, G., Nöth, H., Flores-Parra, A., Contreras, R. and Barba-Behrens, N., “Cobalt (II), nickel (II) and zinc (II) coordination compounds derived from aromatic amines”, *Polyhedron*, **30**, 2090 (2011).
18. Liu, S., Cao, W., Yu, L., Zheng, W., Li, L., Fana, C. and Chen, T., “Zinc (II) complexes containing bis-benzimidazole derivatives as a new class of apoptosis inducers that trigger DNA damage-mediated p53 phosphorylation in cancer cells”, *Dalton Trans*., **42**, 5932 (2013).
19. Dey, A., Mandal, S. K. and Biradha, K., “Metal–organic gels and coordination networks of pyridine-3,5-bis(1-methyl-benzimidazole-2-yl) and metal halides: Self sustainability, mechano, chemical responsiveness and gas and dye sorptions”, *Cryst. Eng. Comm*., **15**, 9769 (2013).
20. Meng, W., Xu, Z., Ding, J., Wu, D., Han, X., Hou, H. and Fan, Y., “A systematic research on the synthesis, structures, and application in photocatalysis of cluster-based coordination complexes”, *Cryst. Growth Des*., **14**, 730 (2014).
21. Tarulli, S. H., Quinzani, O. V., Piro, O. E., Castellano, E. E. and Baran, E. J., “Structural and spectroscopic characterization of

bis(thiosaccharinato)bis(benzimidazole) cadmium (II)", *J. Mol. Struct*., **797**, 56 (2006).

22. Sokol, V. I., Sergienko, V. S., Baikalova, L. V. and Parshinab, L. N., "Synthesis and crystal structure of copper and zinc chloride complexes with bidentate imidazol- benzimidazole ligands", *Russ. J. Inorg. Chem*., **57**, 1313 (2012).
23. Liu, Q. -X., Zhao, Z. -X. Zhao, X. -J., Yao, Z. -Q., Li, S. -J. and Wang, X. -G., "Zinc (II), cobalt (II), and copper (II) complexes based on dibenzimidazolyl bidentate ligands with oligoether linkers: Crystal structure and weak interactions", *Cryst. Growth Des*., **11**, 4933 (2011).
24. Catalano, V. J. and Moore, A. L., "Mono-, di-, and trinuclear luminescent silver (I) and gold (I) N-heterocyclic carbene complexes derived from the picolyl-substituted methylimidazolium salt: 1-Methyl-3-(2-pyridinylmethyl)-1H-imidazolium tetrafluoroborate", *Inorg. Chem*., **44**, 6558 (2005).
25. Yam, V. W. W., Yu, K. L., Wong, K. M. C. and Cheung, K. K., "Synthesis and structural characterization of a novel luminescent tetranuclear mixed-metal platinum (II)−copper (I) complex", *Organometallics*, **20**, 721 (2001).
26. Li, S. -L., Lan, Y. -Q., Ma, J. -C., Ma, J. -F. and Su, Z. -M., "Metal-organic frameworks based on different benzimidazole derivatives: Effect of length and substituent groups of the ligands on the structures", *Cryst. Growth Des*., **10**, 1161 (2010).
27. Guo, Q., Xu, C., Zhao, B. Jia, Y., Hou, H. and Fan, Y., "Syntheses, characterizations, and properties of five interpenetrating complexes based on 1,4-benzenedicarboxylic acid and a series of benzimidazole-based linkers", *Cryst. Growth Des*., **12**, 5439 (2012).
28. Liu, H. -S., Lan, Y. -Q. and Li, S. -L., "Metal-organic frameworks with diverse structures constructed by using capsule-like ligand and Ni(II) based on ionothermal and hydrothermal methods", *Cryst. Growth Des*., **10**, 5221 (2010).
29. Berding, J., Lutz, M., Spek, A. L. and Bouwman, E., "Synthesis of novel chelating benzimidazole-based carbenes and their nickel (II) complexes: Activity in the Kumada coupling reaction", *Organometallics*, **28**, 1845 (2009).
30. Panja, A., Guionneau, P., Jeon, I. -R., Holmes, S. M., Clerac, R. and Mathoniere, C., "Syntheses, structures, and magnetic properties of a novel mer-$[(bbp)FeIII(CN)_3]^{2-}$ building block (bbp: Bis(2-benzimidazolyl)pyridine

dianion) and its related heterobimetallic Fe(III)−Ni(II) complexes", *Inorg. Chem*., **51**, 12350 (2012).

31. Lai, Z. -M., Ye, H. -M., Wan, Q., Xie, X. -X., Bai, X. and Yuan, Y. -F., "Synthesis, crystal structure and properties of benzimidazole-bridged dinuclear ferrocenyl derivatives", *J. Mol. Struct*., **1059**, 33 (2014).
32. Sun, W. -H., Shao, C., Chen, Y., Hu, H., Sheldon, R. A., Wang, H., Leng, X. and Jin, X., "Controllable supramolecular assembly by π···π interactions: Cobalt (II) and copper (II) complexes with benzimidazole derivatives", *Organometallics*, **21**, 4350 (2002).
33. Payra, P., Zhang, H., Kwok, W. H., Duan, M., Gallucci, J. and Chan, M. K., "Structural trends in first-row transition-metal bis(benzimidazole) complexes", *Inorg. Chem*., **39**, 1076 (2000).
34. Gupta, S. and Maheshwari, M. K., "Synthesis, spectral and structural studies of some copper (II) complexes of N,N′-bis(2-methyl-N-methylbenzimidazolyl)hexanediamide ligand", *Chem. Sci. Trans*., **2**, 927 (2013).
35. Devereux, M., O'Shea, D., O'Connor, M., Grehan, H., Connor, G., McCann, M., Rosair, G., Lyng, F., Kellett, A., Walsh, M., Egan, D. and Thati, B., "Synthesis, catalase, superoxide dismutase and antitumour activities of copper (II) carboxylate complexes incorporating benzimidazole, 1,10-phenanthroline and bipyridine ligands: X-ray crystal structures of $[Cu(BZA)_2(bipy)(H_2O)]$, $[Cu(SalH)_2(BZDH)_2]$ and $[Cu(CH_3COO)_2(5,6\text{-}DMBZDH)_2]$ ($SalH_2$ = salicylic acid; BZAH = benzoic acid; BZDH = benzimidazole and 5,6-DMBZDH = 5,6-dimethylbenzimidazole)", *Polyhedron*, **26**, 4073 (2007).
36. Tehlan, S., Hundal, M. S. and Mathur, P., "Copper (II) complexes of N-octylated bis(benzimidazole) diamide ligands and their peroxide-dependent oxidation of aryl alcohols", *Inorg. Chem*., **43**, 6589 (2004).
37. Xia, C. -K., Lu, C. -Z., Zhang, Q. -Z., He, X., Zhang, J. -J. and Wu, D. -M., "Syntheses, structures, and photoluminescent properties of three silver (I) coordination polymers with 2-(4-pyridyl)benzimidazole", *Cryst. Growth Des*., **5**, 1569 (2005).
38. Sharma, H., Guadalupe, H. J., Narayanan, J., Hofeld, H., Pandiyan, T. and Singh, N., "Pyridyl- and benzimidazole-based ruthenium (III) complex for

selective chloride recognition through fluorescence spectroscopy", *Anal. Methods*, **5**, 3880 (2013).

39. Araki, K., Kuwata, S. and Ikariya, T., "Isolation and interconversion of protic N-heterocyclic carbene and imidazolyl complexes: Application to catalytic dehydrative condensation of *N*-(2-pyridyl)benzimidazole and allyl alcohol", *Organometallics*, **27**, 2176 (2008).
40. Yutaka, T., Obara, S., Ogawa, S., Nozaki, K., Ikeda, N., Ohno, T., Ishii, Y., Sakai, K. and Haga, M., "Syntheses and properties of emissive iridium (III) complexes with tridentate benzimidazole derivatives", *Inorg. Chem*., **44**, 4737 (2005).
41. Hahn, F. E., Jahnke, M. C. and Pape, T., "Synthesis of pincer-type bis(benzimidazolin-2-ylidene) palladium complexes and their application in C-C coupling reactions", *Organometallics*, **26**, 150 (2007).
42. Hong, X. -J., Wang, M. -F., Jin, H. -G., Zhan, Q. -G., Liu, Y. -T., Jia, H. -Y., Liua, X. and Cai, Y. -P., "Single-crystal to single-crystal transformation from a 1-D chain-like structure to a 2-D coordination polymer on heating", *Cryst. Eng. Comm*., **15**, 560 (2013).
43. Muller, G., Riehl, J. P., Schenk, K. J., Hopfgartner, G., Piguet, C. and Bünzli, J. -C. G., "Lanthanide triple helical complexes with a chiral bis(benzimidazole)pyridine derivative", *Eur. J. Inorg. Chem*., 3101 (2002).

# *Chapter 2*

# *Synthesis and Structural Studies of Salts of Various Pyridine Dicarboxylic Acids with Benzimidazole Ligands and Their Metal Complexes*

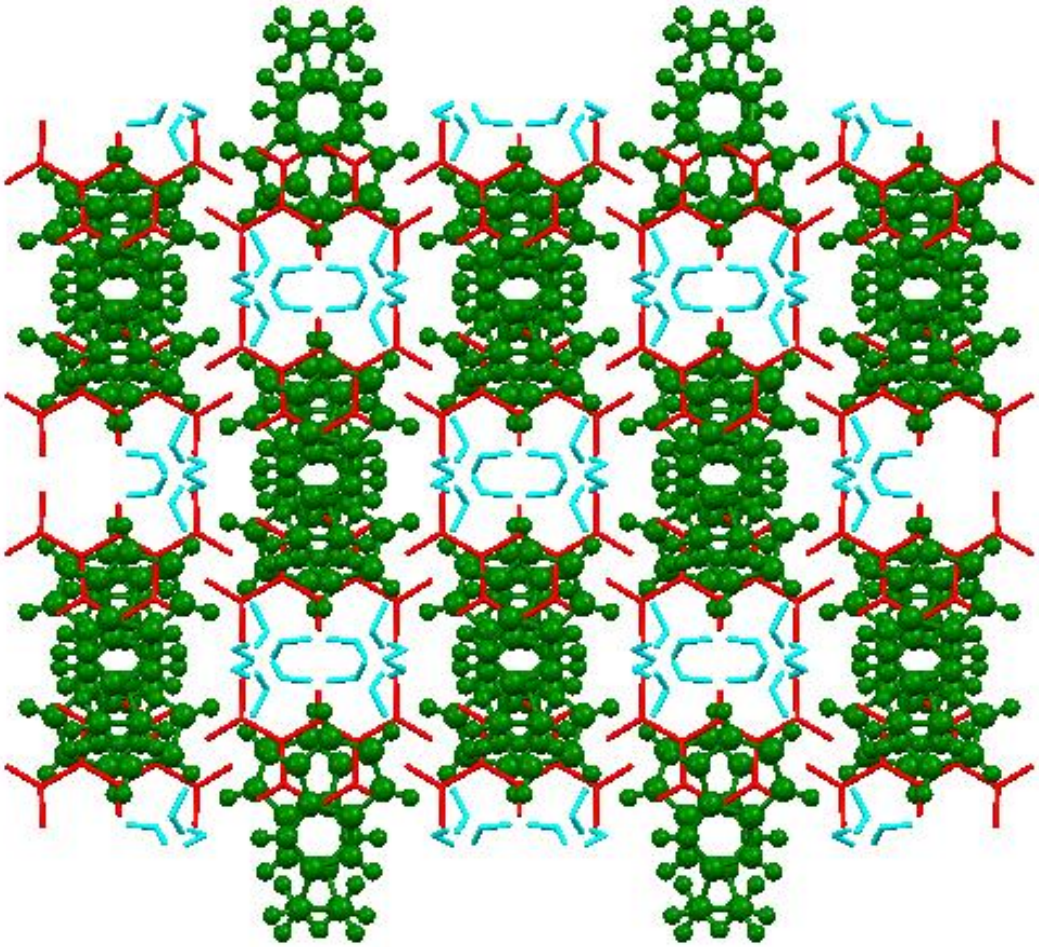

Crystal engineering is an interesting area of research for the designing of new co-crystals and salts which exhibit the structural novelty and supramolecular diversity. It has various applications in different scientific disciplines like, material science, nanotechnology and pharmaceutical industry [1-12].

The carboxylic acids are the most important functional group and play a significant role in crystal engineering because of its capability in forming the directional and robust synthons [13-14]. It has been recognized that the carboxylic acids have both a hydrogen bond donor and acceptor that are self-associated through O-H···O hydrogen bonds and are involved in the formation of stable supramolecular homosynthons. This functional group has also been extensively used as a strong hydrogen bond donor to a variety of nitrogen containing hydrogen bond acceptors [15-16].

A variety of substituted pyridine dicarboxylic acid ($PDCAH_2$) may have different orientation of the carboxylate groups which can interact with the accompanied molecules in the different direction and thereby can afford either discrete or consecutive structure [17]. In addition of being an effective tridentate chelating ligand, pyridine dicarboxylic acid also participates in the construction of extensive H-bonding networks. The pyridine dicarboxylic acid can act as a hydrogen-bond donor as well as acceptor due to the presence of two carboxylic acid groups and the pyridyl nitrogen. Literature reveals that $PDCAH_2$ exists in the form of zwitter ion, where the pyridyl nitrogen gets protonated by one of the carboxylic acid groups due to the proton transfer. A remarkable alternation has been noticed in the supramolecular landscape of pyridine dicarboxylic acid because the molecule can act as a hydrogen bond donor by the virtue of its nitrogen atom [18].

The pyridine dicarboxylic acid is now also recognized to be a major component of bacterial spores [19-21], which is used in a variety of processes as an enzyme inhibitor, plant preservative and food sanitizer [22-26].

Despite considerable studies on the solid state behaviour of the systems containing pyridine and carboxylic acid moeities, the impact of other structural features still remains ambiguous and demands more exhaustive investigations. Such studies would offer greater levels of predictability regarding the persistent structural motifs and favoured arrangements in the solid state assemblies precipitated by the number and arrangement of the structural elements present therein [27]. It is interesting to note that although the polycarboxylate ligands with transition and lanthanide metal ions have

given thermally stable polymeric materials, however the systems derived from pyridine dicarboxylate are still very less explored [28].

Hadadzadeh et al. [29] prepared a new co-crystal of pyridine-2,6-dicarboxylic acid and 1,10-phenanthroline-5,6-dione (phen-dione) (**1**) and a mixed ligand Ni(II) complex, [Ni(phen)(dipic)($H_2O$)].4$H_2O$ (**2**). They characterized them by analytical, spectroscopic, thermogravimetric and crystallographic methods. They found an interesting feature that the co-crystal exhibits no direct hydrogen bonding between these two components (pyridine-2,6-dicarboxylic acid and 1,10-phenanthroline-5,6-dione), however a three dimensional supramolecular architecture was formed by hydrogen bonding interactions between dipic···water and phen-dione···water in the crystal structure and probably responsible for the co-crystallization of pyridine-2,6-dicarboxylic acid and 1,10-phenanthroline-5,6-dione (Fig. 2.1a). They observed that dipic ligand coordinates to Ni(II) in a O,N,O-tridentate coordination mode in the complex **2** and a distorted octahedral coordination at Ni(II) was formed by the three donor atoms of dipic, two N atoms of phen and one O atom of water. They found that O atoms of dipic ligand are trans to each other and the phen ligand chelates to the Ni(II) and $H_2O$ ligand is trans to the phen N atom (Fig. 2.1b).

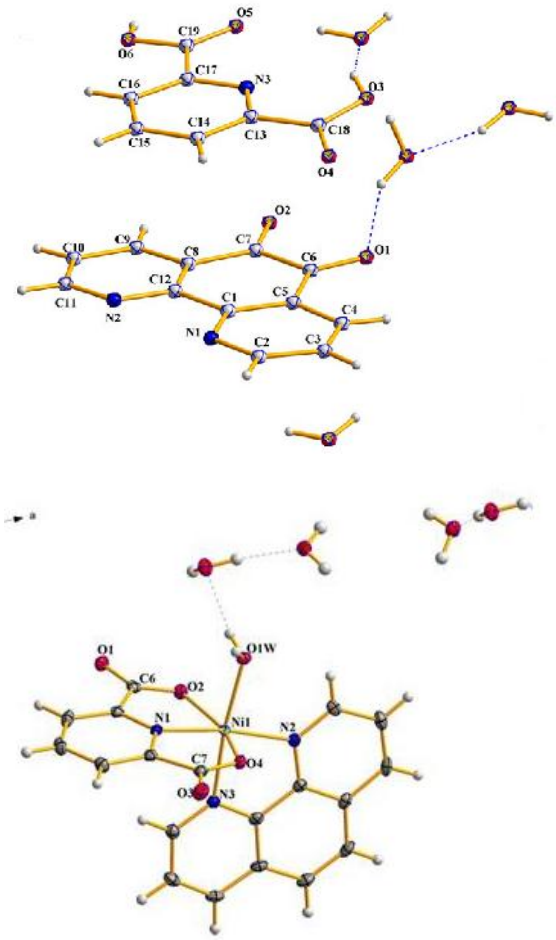


**(a)** **(b)**

**Fig. 2.1** Crystal structure of **(a)** pyridine-2,6-dicarboxylic acid, 1,10-phenanthroline-5,6-dione and water molecules **(b)** [Ni(phen)(dipic)($H_2O$)].4$H_2O$

Babulal et al. [30] reported the formation of co-crystals of caffeine and theophylline viz., caf.dpa (**1**), caf.pzca (**2**), 2caf.trimel (**3**), theo.2dpa (**4**) and 2theo.2pzca (**5**) (where caf = caffeine, theo = theophylline, dpa = dipicolinic acid, pzca = 3,5-pyrazole dicarboxylic acid, trimel = trimellitic acid) and their characterization by X-ray diffraction and conventional spectroscopic techniques. They found that co-crystal **1** forms a hydrogen-bonded assembly through one of the carboxylic acids with the imidazole moiety of caffeine, whereas the other carboxylic acid group is involved in strong hydrogen bonding with the crystallized water molecule. Thus, water-assisted assemblies are formed in which the water molecules are held by the nitrogen atom and also by the two carboxylic acid groups of dpa (Fig. 2.2).

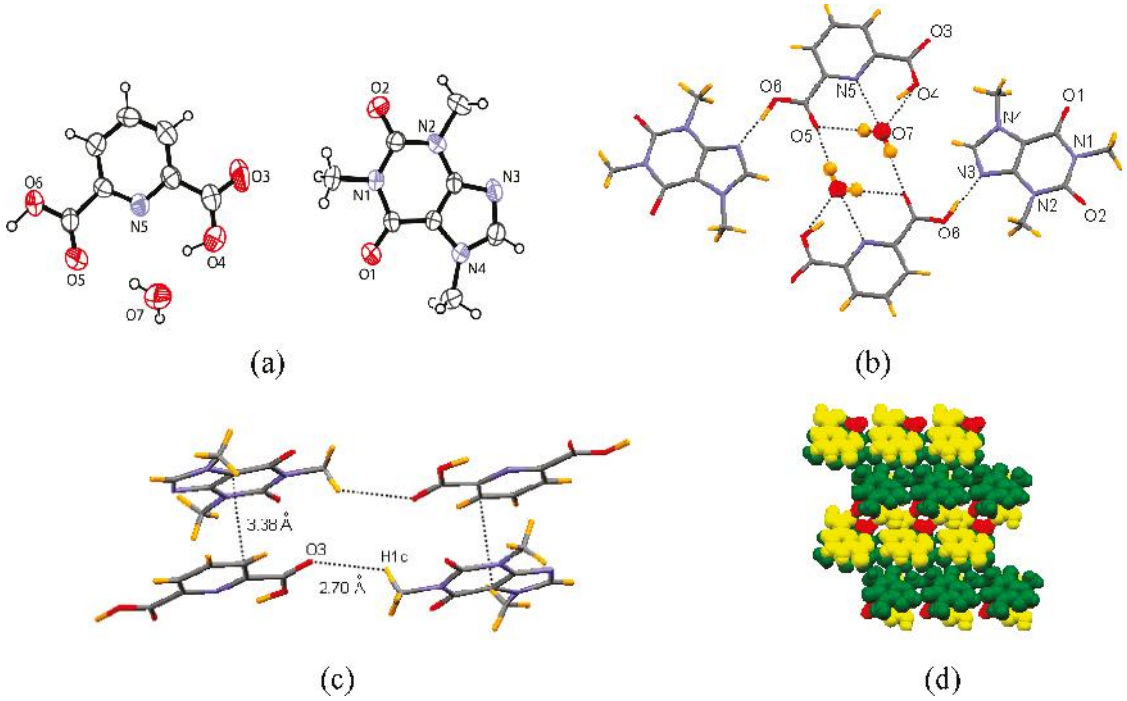


**Fig 2.2 (a)** ORTEP view of **1**. **(b)** A perspective view of hydrogen bonded crystallized water bridged assembly. **(c)** π-π stacking and C-H...O interactions. **(d)** A space filling model of the crystal packing of stacked (green = caffeine, yellow = dpa, red = water)

Thompson et al. [31] reported the melting point alternation behaviour of odd and even alkanedicarboxylic acids which was mimicked in a set of co-crystals where isonicotinamide was combined in a 1 : 1 stoichiometry with pimelic acid, suberic acid and azelaic acid (Fig. 2.3). They observed that all the three structures contain hydrogen bonded chains of alternating acid and amide molecules in which acid–pyridine and acid–amide synthons were formed. They found that both isonicotinamide:pimelic acid and isonicotinamide:azelaic acid form structures in which the acid moiety adopts a twisted alkyl backbone conformation similar to that observed in the pure odd alkanediacid materials whereas the isonicotinamide:suberic acid co-crystal differs from the others by retaining both the elevated melting point and the planar acid conformation displayed by even alkanediacid materials.

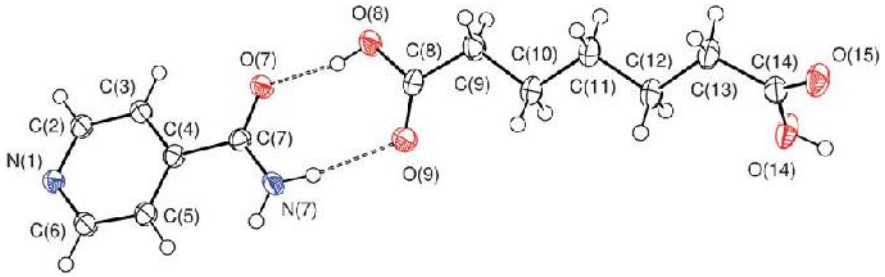


**Fig 2.3** Crystal structure of **1**

Bučar et al. [32] synthesized a group of caffeine-containing co-crystals of hydroxy-2-naphthoic acids and analyzed via single-crystal X-ray diffraction and IR analysis. They observed imidazolecarboxylic acid synthon in co-crystals of 1-hydroxy-2-naphthoic and 3-hydroxy-2-naphthoic acid whereas in the case of 6-hydroxy-2-naphthoic acid, the co-crystal exhibits a hydrogen-bonded carboxylic acid dimer along with a hydroxyl-caffeine heterosynthon (Fig. 2.4).

**(a)** **(b)**

**Fig. 2.4 (a)** A perspective view of the neutral 1:1 caffeine:3-hydroxy-2-naphthoic acid assembly. **(b)** and 1:1 caffeine:6-hydroxy-2-naphthoic acid

Batchelor et al. [33] reported the co-crystallisation of phenazine and dicarboxylic acids and found that the complexes of phenazine with succinic and glutaric acid comprised in 1:1 and 1:2 stoichiometric ratios, respectively. Szafran et al. [34] reported crystalline complex comprised of N-methylpiperidinebetaine (MPB) and L(+)-tartaric acid (TA) which formed a six-molecular non-centrosymmetric hydrogen bonds through two O-H···O=C and four COO···HOOC interactions (Fig. 2.5). They also studied that the core of the cluster is formed by two tartaric acid molecules linked by O-H···O=C hydrogen bonds into a cyclic asymmetric dimer.

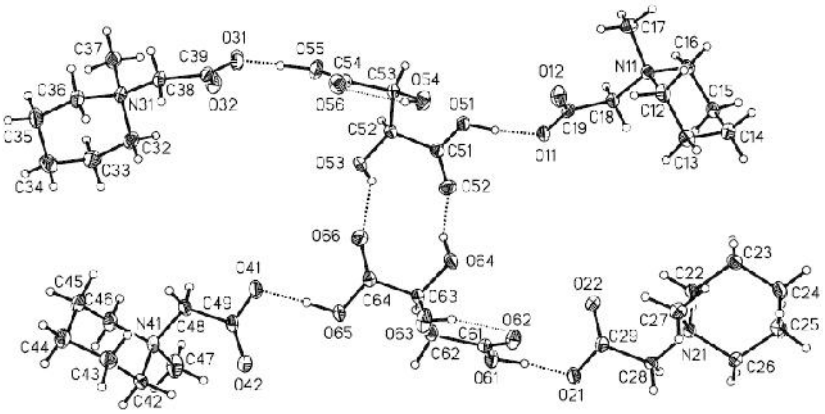


**Fig. 2.5** Hydrogen bonds in the cluster of $[(MBP)_2TA]_2$

Aghabozorg et al. [35] prepared homonuclear water-soluble and air stable compounds $(dmpH)(H_5O_2)[M(pydc)_2].0.5H_2O$ in aqueous solution at room temperature (M = Ni(II) (**1**), Cu(II) (**2**), Zn(II) (**3**); $pydcH_2$ = pyridine-2,6-dicarboxylic acid, dmp = 2,9-dimethyl-1,10-phenanthroline) (Scheme 2.1) and characterized by IR, $^1$H NMR, $^{13}$C NMR, elemental analysis and X-ray diffraction single crystal analyses. They observed that all the complexes **1-3** represent the isostructural features and extensive hydrogen bonding interactions involving all aqua ligands, dipicolinate oxygens and lattice water molecules which further stabilize the complex units by linking them to form a three dimensional polymeric networks (Fig. 2.6). They investigated the stoichiometry and stability of all the three complexes in aqueous solution by potentiometric *p*H titration.

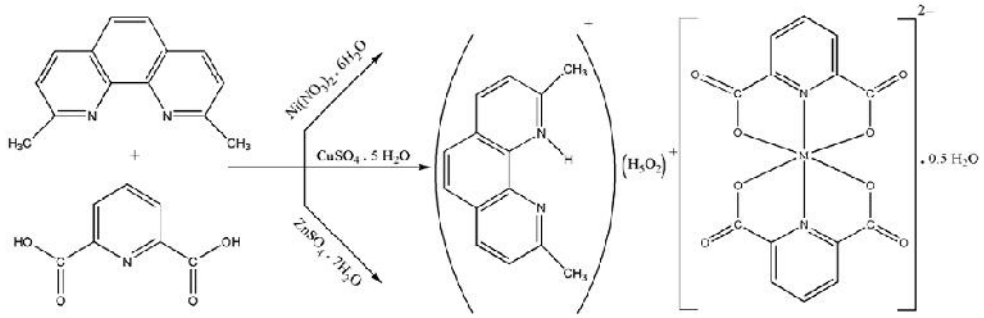


**Scheme 2.1** Synthesis of Ni(II), Cu(II) and Zn(II) compounds

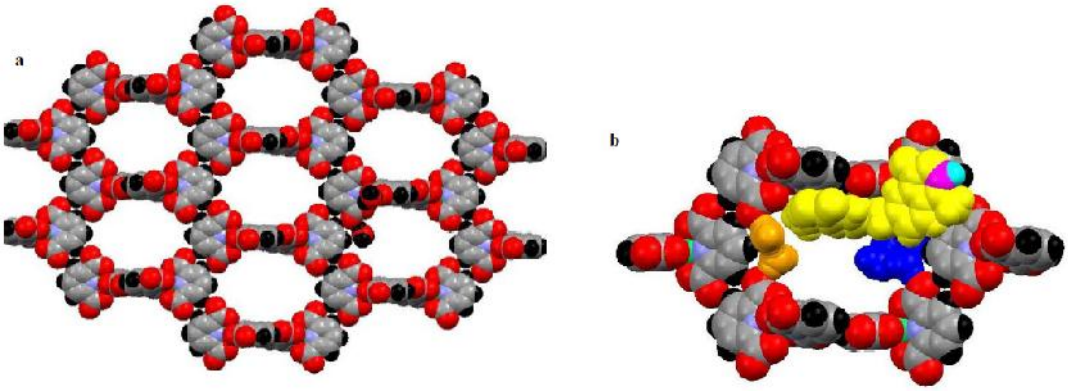


**(a)** **(b)**

**Fig. 2.6 (a)** Honey-comb framework resulted by C-H···O interactions in the crystal lattice. **(b)** Inside each room. Blue: water tetramer; Orange: $(H_5O_2)^+$; Yellow $(dmpH)^+$

Kirillova et al. [36] synthesized heteronuclear water-soluble and air-stable compounds $[M(H_2O)_5M'(dipic)_2].mH_2O$ (M/M´ = CuII/CoII (**1**), CuII/NiII (**2**), CuII/ZnII (**3**), ZnII/CoII (**4**), NiII/CoII (**5**), *m* = 2–3; $H_2$dipic = dipicolinic acid) in aqueous solution at room temperature (Scheme 2.2) and characterized them by IR, UV-Vis and atomic absorption spectroscopies, elemental and X-ray diffraction single crystal (for **1** and **2**) analyses (Fig. 2.7). They reported that complexes **1–5** represent the first examples of heteronuclear dipicolinate compounds with 3d metals and studied their extensive hydrogen bonding interactions involving all aqua ligands, dipicolinate oxygens and lattice water molecules which further stabilize the dimetallic units by linking them to form three-dimensional polymeric networks.

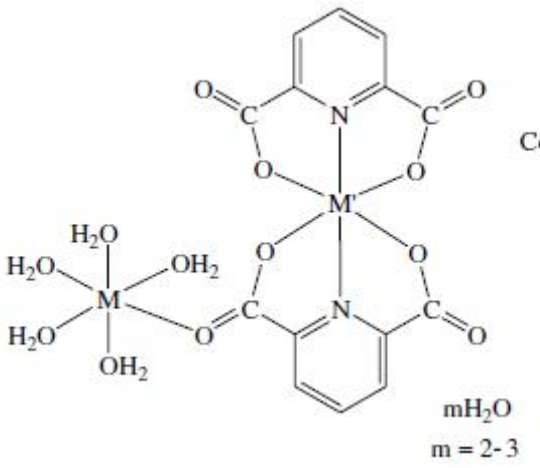


| Compound | M | M' |
|---|---|---|
| 1 | Cu | Co |
| 2 | Cu | Ni |
| 3 | Cu | Zn |
| 4 | Zn | Co |
| 5 | Ni | Co |

**Scheme 2.2** Schematic representation of complexes **1–5**

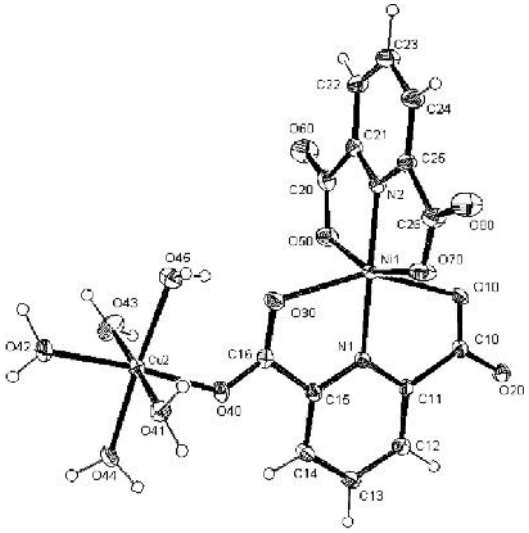


**Fig. 2.7** Thermal ellipsoid view of **2**

Park et al. [37] prepared two new nickel (II) complexes of the composition $[Ni(cyclam)(Hdipic)_2].2H_2O$ (**1**) and $[Ni(cyclam)(H_2O)_2][Ni(dipic)_2].2.5H_2O$ (**2**) (dipic = 2,6-pyridinedicarboxylate, dipicolinate; cyclam = 1,4,8,11-tetraazacyclotetradecane) and structurally characterized by a combination of analytical, spectroscopic, thermogravimetric and crystallographic methods. They found that the central nickel (II) ion is coordinated axially by two monodentate Hdipic ligands in **1** and the discrete neutral complex further extends its structure by hydrogen bonding interactions in a one-dimensional supramolecule (Fig. 2.8). They also found that complex **2** consists of two independent nickel (II) centers and the water molecules prefer to coordinate to the Ni ion instead of dipic ligands resulting in a divalent cation $[Ni(cyclam)(H_2O)_2]^{2+}$ and two dipic ligands coordinate to the second Ni ion forming a divalent anion $[Ni(dipic)_2]^{2-}$ .(Fig. 2.9). Both the divalent cations and anions are balancing the charge, resulting in a molecular salt and are interconnected by multiple types of hydrogen bonding interactions.

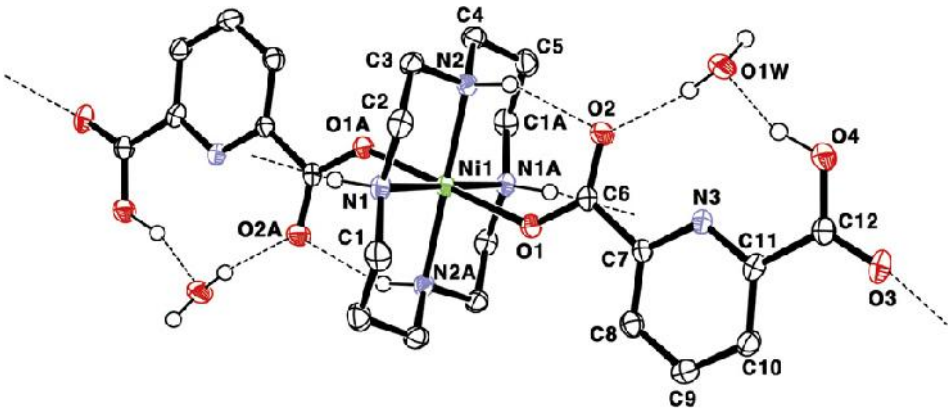


**Fig. 2.8** Crystal structure of **1**

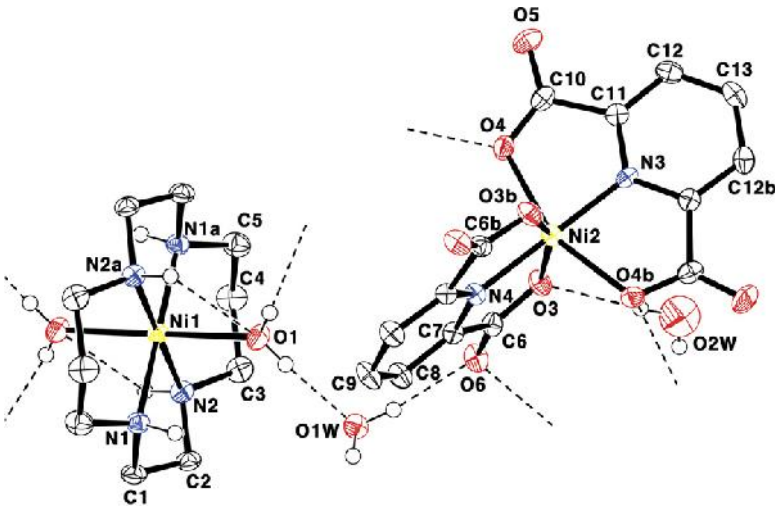


**Fig. 2.9** Crystal structure of **2** with atom-labeling scheme

Ghosh et al. [38] synthesized Co(II) and Ni(II)-nitrate metal-organic framework (MOF) [M(pdc)(4,4´-bpy)].1/2MeOH (M = Co(II), **1** and Ni(II), **2**) and found rectangular voids of approximate dimension 8.9 x 5.5 Å in both the structures (Fig. 2.10). They demonstrated that each 2-D sheet formed is stacked on top of each other with an intricate array of hydrogen bonding, shows a perpendicular distance of 8.1 and 7.8 Å in **1** and **2**, respectively. When they used 1,2-di(4-pyridyl)ethylene in place of 4,4´-bipyridyl to construct the MOFs, only Ni(II)-nitrate affords crystals whose structure differs greatly from that of **1** or **2**. They found that 1,2-di(4-pyridyl)ethylene is not bonded to the metal but exists in the lattice in diprotonated form and a hydrogen-bonded 3-D structure of discrete $(dpeH_2)[Ni(pdc)_2].5H_2O$ (**3**) units is formed. In complex **3** they also highlight the presence of an acyclic trimeric water cluster which is hydrogen bonded to the spacer and a free carboxylate O atom (Fig. 2.11).

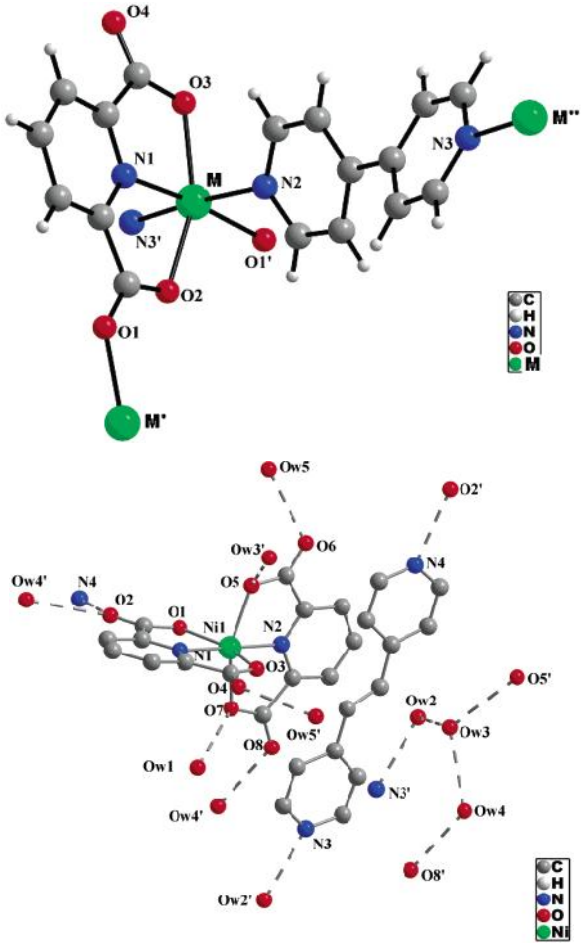


**(a)** **(b)**

**Fig. 2.10 (a)** The coordination geometry around the metal. **(b)** Non-covalent interactions in **2**

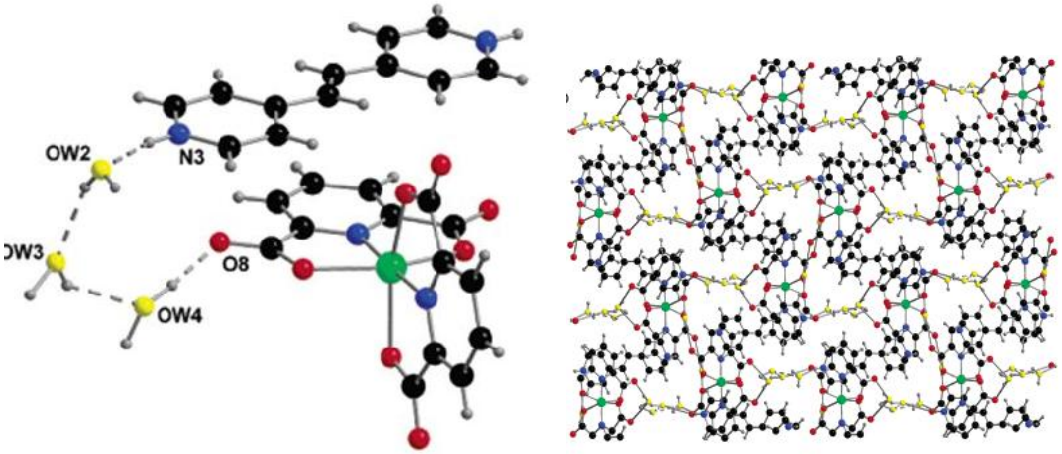


**(a)** **(b)**

**Fig. 2.11 (a)** Close view of the hydrogen-bonded acyclic water trimer. **(b)** Hydrogen-bonded 3-D metal-organic framework structure in **3**

Çolak et al. [39] prepared two new compounds $(8\text{-}H_2Q)_2[M(dipic)_2].6H_2O$ (M = Co (**1**) and Ni (**2**) (8-HQ = 8-hydroxyquinoline, dipic = dipicolinate) (Fig 2.12) and characterized them by elemental analysis, spectral (IR and UV-Vis), thermal analyses, magnetic measurements and single-crystal X-ray diffraction techniques. They found that both the complex **1** and **2** consists of two 8-hydroxyquinolinium cations, one bis(dipicolinate)M(II) anion [M = Co(II), Ni(II)] and six uncoordinated water molecules. In the anionic part of the compounds, each dipic ligand exhibits tridentate coordination modes through one nitrogen atom of pyridine ring and two oxygen atoms of the carboxylate groups. They also evaluated *in vitro* antibacterial and antifungal activities of **1** and **2** by the agar well diffusion method via MIC tests and found that both the new compounds showed the same antimicrobial activity against Gram-positive bacteria, yeast and fungi.

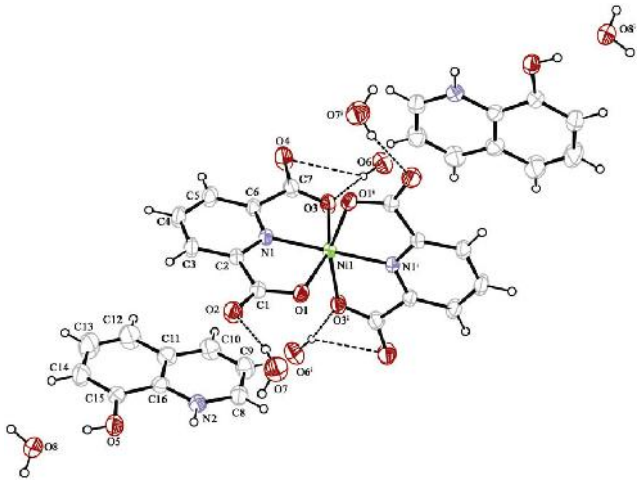


**Fig. 2.12** The molecular structure of $(8\text{-}H_2Q)_2[Ni(dipic)_2].6H_2O$

Zhang et al. [40] prepared nickel complex $[Ni(NIT_2Py)(PDA)(H_2O)].(MeOH).H_2O$ using ligands ($NIT_2Py$ = 2-(2´-pyridyl)-4,4,5,5-tetramethylimidazoline-oxyl-3-oxide; PDA = pyridine- 2,6-dicarboxylic acid). They found that Ni(II) ion was in distorted octahedral geometry and was stabilized in one dimension chain by intermolecular hydrogen bonds (Fig. 2.13).

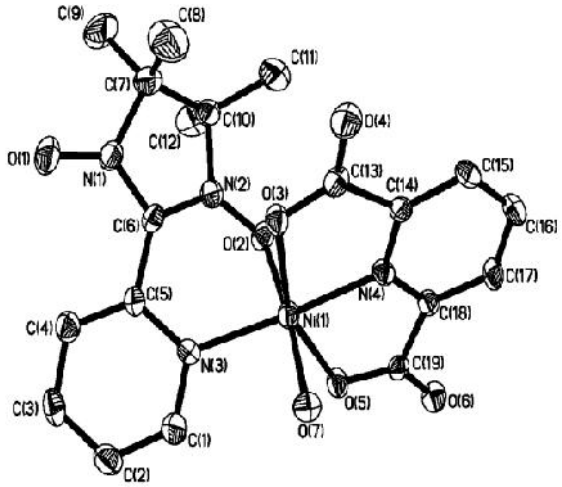


**Fig 2.13** Crystal Structure of [Ni($NIT_2Py$)(PDA)($H_2O$)].(MeOH).$H_2O$

The metal complexes of pyridine dicarboxylic acid are not only limited to transition metals but few lanthanide complexes with the same ligands are also reported in literature. .

Prasad et al. [41] synthesized a series of new heterometallic compounds containing cerium (IV) and lanthanide (III) with pyridine-2,6-dicarboxylic acid ($dipicH_2$). They obtained four types of compounds depending on the Ln(III) ion and the preparation conditions, Type-I: one-dimensional coordination polymer, [Ln(dipicH)$(H_2O)_4$Ce$(dipic)_3$].7H2O; Ln = La (**1**), Ce (**2**) or Pr (**3**). Type-II: ionic compound, [Ln(dipicH)$(H_2O)_6$][Ce$(dipic)_3$].7$H_2O$; Ln = Nd (**4**), Sm(**5**), Eu (**6**), Gd (**7**), or Dy (**8**). Type-III: octanuclear cluster incorporating a six-membered coordination ring, [Ln$(H_2O)_7$Ln(dipic)$(H_2O)_4$-$(Ce(dipic)_3)_2]_2$.*n*$H_2O$; Ln = La (**9**) *n* = 24, Ce (**10**) *n* = 24, Pr (**11**) *n* = 24, or Nd (**12**) *n* = 26. Type-IV: hexanuclear cluster incorporating a four-membered coordination ring, [$(Ln(H_2O)_5)_2$$(Ce(dipic)_3)_4$(2Hþ)].nH2O; Ln = Nd (**13**) *n* =34, Sm (**14**) *n* = 26, Eu (**15**) *n* = 26, or Gd (**16**) *n* = 26 (Fig. 2.14). They examined that Tb and heavier lanthanides form compounds isomorphous with Type-IV compounds and observed metal-centered luminescence sensitized by dipic ligand in compounds containing EuIII and DyIII ions.

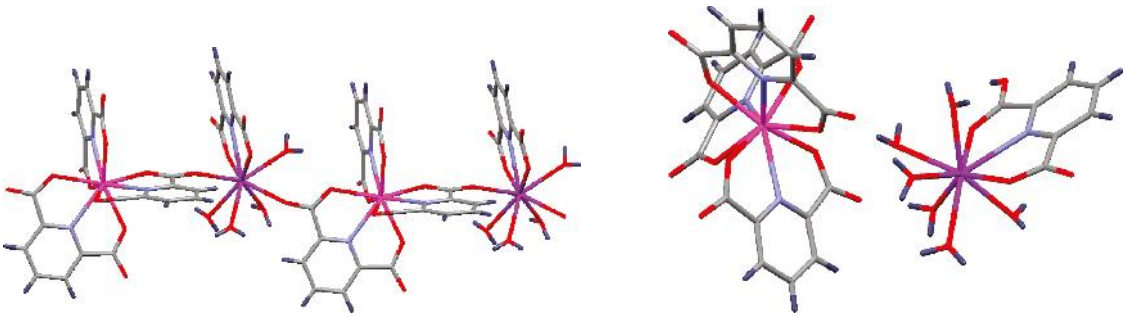

**(a)** **(b)**

**Fig. 2.14 (a)** 1D polymeric structure of compound **1**. **(b)** Structure of compound **4**

The above literature revealed that carboxylic acids play an important role in co-crystallization and crystal engineering but their use in co-crystallization using benzimidazole as one component and pyridine dicarboxylic acid derivatives as other component are not yet reported. Benzimidazole and its derivates are important organic compounds with successful applications in several areas, such as biological chemistry, materials science, organic synthesis, medicinal and pharmaceutical field [42-43]. These can be synthesiszed easily by the condensation reaction between *o*-phenylene diamine and aliphatic dicarboxylic acid which leads to the formation of a benzimidazole linkage together with the release of two water molecules. These ligands play a vital role in assembling diverse architectures in the area of supramolecular chemistry as molecular building blocks.

The present chapter describes the co-crystallization of various pyridine dicarboxylic acids with the derivatives of benzimidazole to study the structural diversity. Along with that attempts were made to incorporate zinc and nickel metal ion in the above prepared binary salts.

**Results and discussion**

Ligands 1,4-bis(1H-benzimidazol-2-yl)butane ($H_2$BBBu) and tris(1H-benzimidazol-2-yl)methyl)amine ($H_3$NTB) were synthesized by the literature methods (scheme 2.3-2.4) . The reactions of various pyridine dicarboxylic acids [pyridine-2,3-dicarboxylic acid (2,3-PDCA$H_2$); pyridine-2,4-dicarboxylic acid (2,4-PDCA$H_2$); pyridine-2,5-dicarboxylic acid (2,5-PDCA$H_2$); pyridine-2,6-dicarboxylic acid (2,6-PDCA$H_2$); pyridine-3,4-dicarboxylic acid (3,4-PDCA$H_2$) and pyridine-3,5-dicarboxylic acid (3,5-PDCA$H_2$)] with $H_4$BBBu and $H_3$NTB resulted in the formation of salts $[(H_4BBBu)^{2+}.(2,3\text{-}PDCA)^{2-}]$ (**2a**), $[(H_4BBBu)^{2+}.(2,4\text{-}PDCA)^{2-}]$ (**2b**), $[(H_4BBBu)^{2+}.(2,5\text{-}PDCA)^{2-}]$ (**2c**), $[(H_4BBBu)^{2+}.(2,6\text{-}PDCA)^{2-}.H_2O]$ (**2d**), $[(H_4BBBu)^{2+}.2(3,4\text{-}PDCAH)^{-}.2H_2O]$ (**2e**), $[(H_4BBBu)^{2+}.(3,5\text{-}PDCA)^{2-}.3H_2O]$ (**2f**), $[(H_5NTB)^{2+}.2(2,3\text{-}PDCAH)^{-}.DMF]$ (**2g**), $[(H_4NTB)^{+}.(2,4\text{-}PDCH)^{-}.2CH_3OH\ .H_2O]$ (**2h**), $[(H_5NTB)^{2+}.(2,5\text{-}PDCA)^{2-}.DMF]$ (**2i**), $[(H_4NTB)^{+}.(2,6\text{-}PDCAH)^{-}.C_2H_5OH.CH_3OH.H_2O]$ (**2j**), $[(H_5NTB)^{2+}.(3,4\text{-}PDCA)^{2-}.DMF]$ **(2k)** and $[(H_6NTB)^{3+}.(3,5\text{-}PDCA)^{2-}.(3,5\text{-}PDCAH)^{-}.DMF]$ (**2l**) (Scheme 2.5-2.6). The different formulations were confirmed by elemental analysis, infrared spectroscopy and X-ray crystallography. The suitable single crystals of salt **2d-2l** for X-ray diffraction analysis were achieved by slow evaporation of methanolic or a binary solution of methanolic and DMF containing the receptor and requisite amounts of organic acids.

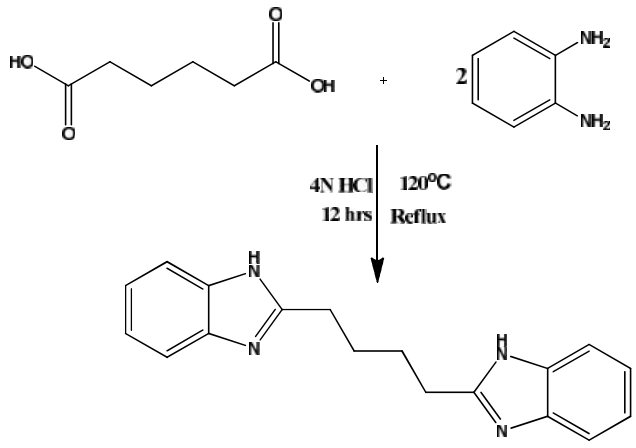


**Scheme 2.3**

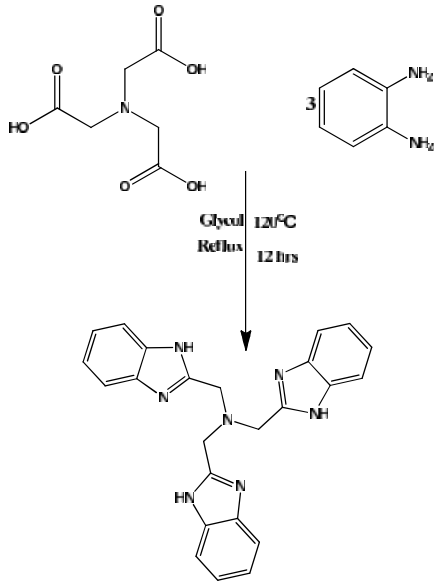


**Scheme 2.4**

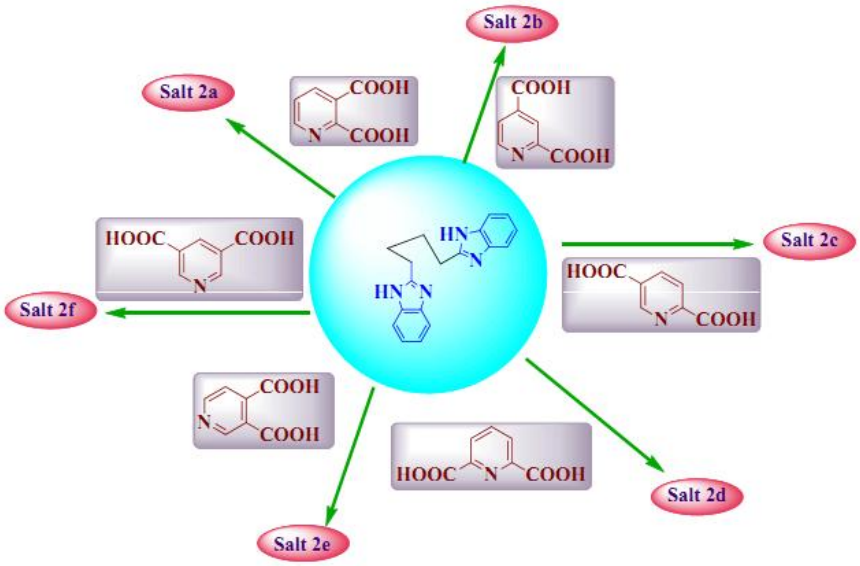


**Scheme 2.5**

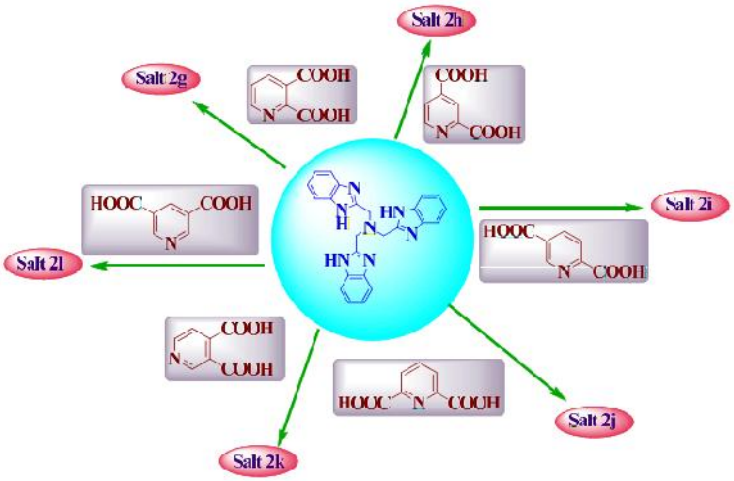


**Scheme 2.6**

**Infrared Spectra**

During crystallization the proton has been transferred from the acid to the benzimidazole nitrogen. The proton transfer has been confirmed by the shifting of position of carboxyl C=O stretching bands. Generally it presents in between 1676 and 1735 $cm^{-1}$ in the spectra of the corresponding neutral carboxylic acids and shifted to 1590 and 1655 $cm^{-1}$ during salt formation. The NH stretching vibration is normally observed at 3505-3405 $cm^{-1}$ which is shifted to lower wave number (3106-3060 $cm^{-1}$) due to the attraction of the –NH protons by the carboxylate anion leading to an increase in –NH bond length in salts [44]. The shifting towards lower frequency, is due to the hydrogen bonded non-covalent interactions between donor (-NH protons) and acceptor (carboxylate anion) moiety [45].

**Crystal Structures of $[(H_4BBBu)^{2+}.(2,6\text{-}PDCA)^{2-}.H_2O]$ (2d)**

Salt **2d** crystallizes in the monoclinic crystal system with C2/c space group and the asymmetric unit consists of one protonated molecule of 1,4-bis(1H-benzimidazol-2-yl)butane $(H_4BBBu)^{2+}$, one molecule of pyridine-2,6-dicarboxylate anion $(2,6\text{-}PDCA)^{2-}$ and one molecule of water (Fig. 2.15). The crystal data and experimental details are given in Table 2.1 and important bond lengths and angles are summarized in Table 2.2. Both the proton from pyridine-2,6-dicarboxylic acid has been transferred to the 1,4-bis(1H-benzimidazol-2-yl)butane resulted in the formation of salt **2d**. Both the benzimidazoloyl NH as well as the protonated NH are available for extensive hydrogen bonding (N-H···O) with the oxygen atoms of pyridine-2,6-dicarboxylic acid (N2-H2B···O5, 1.864(5) Å; N1-H1···O2, 1.856(3) Å; N1-H1···O1, 2.922(5) Å) (Fig. 2.16).

The phenyl rings of the benzimidazole moiety exhibited π-stacking interaction with the pyridyl rings of PDCA at a distance of 3.978(6) Å. It has also observed that the $H_2O$ molecules present in the lattice are also involved in O-H···O interactions (O5-H6W···O3, 1.891(9); O5-H5W···O4, 1.983(6) Å) (Table 2.25). The three dimensional packing diagram of salt **2d** is shown in Fig. 2.17.

**Crystal Structures of $[(H_4BBBu)^{2+}.2(3,4\text{-}PDCAH)^{-}.2H_2O]$ (2e)**

The co-crystallization of pyridine-3,4-dicarboxylic acid and 1,4-bis(1H-benzimidazol-2-yl)butane resulted in the formation of salt **2e** due to proton transfer. Salt **2e** crystallizes in the triclinic crystal system with P-1 space group and the unit cell consists of one molecule of protonated 1,4-bis(1H-benzimidazol-2-yl)butane cation $(H_4BBBu)^{2+}$, two molecules of pyridine-3,4-dicarboxylate anion $(3,4\text{-}PDCAH)^{-}$ and two molecules of water (Fig 2.18). The PDCA and water molecule are present on crystallographic symmetry axis. The crystal data and refinement details are given in Table 2.3 and important bond lengths and angles are summarized in Table 2.4. Unlike to the salt **2d**, in salt **2e**, only one proton from each acid moiety has been transferred to the 1,4-bis(1H-benzimidazol-2-yl)butane. Salt **2e** also shows various intermolecular interactions viz., N-H···O and C-H···O interactions are tabulated in Table 2.25 (Fig 2.19). However no significant C-H···π or π···π interactions has been observed in the crystal structure of **2e**. The three dimensional packing diagram of salt **2d** is shown in Fig 2.20.

**Crystal Structures of $[(H_4BBBu)^{2+}.(3,5\text{-}PDCA)^{2-}.3H_2O]$ (2f)**

Salt **2f** crystallized in the monoclinic system with C2/c space group. In salt **2f**, there is one molecule of pyridine-3,5-dicarboxylate anion, one molecule of protonated 1,4-bis(1H-benzimidazol-2-yl)butane cation and three water is present in the asymmetric unit. Similar to the case of salt **2d**, both the acidic hydrogen of carboxyl groups of pyridine-3,5-dicarboxylic acid has been transferred to the nitrogen atoms of 1,4-bis(1H-benzimidazol-2-yl)butane as shown in Fig 2.21. The crystal data and experimental details are given in Table 2.5 and important bond lengths and angles are summarized in Table 2.6. In the crystal structure of salt **2f**, each cation and anion is non-covalently hydrogen bonded to each other via, N-H···O (N1-H1···O5, 1.834(1); N2-H1B···O1, 2.060(1); N2-H1B···O2, 2.274(1) Å), C-H···O (C5-H5···O2, 2.665(1); C8-H8B···O1, 2.889(1) Å) and O-H···O interactions (O5-H1W···O3, 1.942(3); O4-H5W···O3, 2.034(2); O3-H3W···O1, 1.840(3); O3-H4W···O2, 11.963(2); O5-H2W···O2, 1.912(2); O4-H6W···O2, 1.983(3) Å). The cation is wrapped around the

anion to permit π stacking interactions between both phenyl ring of benzimidazole moiety in cation and pyridine ring of anion at a distance of 3.624(4) Å (Fig. 2.22). The presence of different non-covalent interactions resulted in the three dimensional packing as shown in Fig.2.23.

**Crystal Structures of $[(H_5NTB)^{2+}.2(2,3\text{-}PDCAH)^{-}.DMF]$ (2g)**

The reaction of tris(1H-benzimidazol-2-yl)methyl)amine ($H_3NTB$) with pyridine-2,3-dicarboxylic acid (2,3-$PDCAH_2$) resulted in the formation of salt **2g** because of proton transfer and crystallized in triclinic system with P-1 space group. The asymmetric unit of salt **2g** consists of two pyridine-2,3-dicarboxylate anions (2,3-$PDCAH)^{-}$, one protonated tris(1H-benzimidazol-2-yl)methyl) amine cation $(H_5NTB)^{2+}$ and one molecule of dimethylformaide (Fig 2.24). It has been observed that transfer of two acidic hydrogen atoms took place from two molecules of pyridine-2,3-dicarboxylic acid to two nitrogens of the three benzimidazole rings of tris(1H-benzimidazol-2-yl)methyl)amine resulting in the formation of cationic-anionic pairs while the third nitrogen of benzimidazole ring bearing lone pair of electron remained unprotonated. The crystal data and experimental details are given in Table 2.7 and important bond lengths and angles are summarized in Table 2.8. The molecular packing analysis shows the existence of several non-covalent interactions. The protonated NH as well as benzimidazoloyl NH are extensively involved in N-H···O interactions with the oxygens of carboxylate and DMF molecules (N1-H1A···O3, 1.801(2); N2-H2B···O6, 1.884(2); N5-H5B···O6, 2.736(2); N4-H4B···O6, 1.805(2); N3-H3B···O9, 1.836(4) Å) (Fig. 2.25).The methylene CH and phenyl CH are also involved in C-H···O interactions (C8-H8B···O1, 2.800(4); C23-H23···O2, 2.942(3); C40-H40C···O4, 2.870(4); C15-H15···O8, 2.765(2); C17-H17B···O1, 2.975(3); C17-H17B···O2, 2.463(3); C5-H5···O5, 2.632(2); C3-H3···O3, 2.731(2); C8-H8B···O5, 2.528(3); C8-H8A···O6, 2.662(4); C39-H39A···O7, 2.809(2); C21-H21···O5, 2.522(3); C22-H22···O7, 2.639(3); C27-H27···O7 , 2.504(3); C36-H36···O4, 2.868(2) Å), wheras few O-H···O interactions are also noticed in the crystal structure (O8-H8···O4, 2.855(3) Å). The self assembly of cations resulted in the formation of supramolecular host architecture accommodating anions and the solvent molecule as the guest species (Fig 2.26).

**Crystal Structures of $[(H_4NTB)^{+}.(2,4\text{-}PDCAH)^{-}.2CH_3OH.H_2O]$ (2h)**

Salt **2h** crystallizes in the triclinic system with P-1 space group. The crystal structure of salt **2h** demonstrates that the asymmetric unit contains pyridine-2,4-dicarboxylate anion, one protonated tris(1H-benzimidazol-2-yl)methyl)amine cation,

two molecules of methanol and one molecule of water (Fig. 2.27). The crystal data and collection details are tabulated Table 2.9 and important bond lengths and angles are given in Table 2.10. The ionic species is formed by the transfer of one proton from the oxygen atom of one carboxyl group of pyridine-2,4-dicarboxylic acid to the one nitrogen atom (N1) of tris(1H-benzimidazol-2-yl)methyl)amine, whereas the remaining two nitrogens of benzimidazole rings of cation remained unprotonated. The crystal structure of salt **2h** featured several non-covalent interactions e.g., N-H···O (N1-H1···O1, 1.908(7); N5-H5A···O1, 1.977(1); N4-H4B···N6, 1.917(9) Å), C-H···O (C31-H31···O2, 2.366(3); C12-H12···O2, 2.393(2); C9-H9B···O6, 2.658(2); C17-H17A···O6, 2.963(4); C23-H23···O2, 2.891(1); C17-H17B···O6, 2.536(4) Å), O-H···O interactions (O7-H7···O6, 1.861(1) Å) and N-H···N (N4-H4B···N6, 1.917(9) Å) due to the involvement of protonated NH, benzimidazoloyl NH, phenylic CH with the variety of oxygens of methanol, water and carboxyl group (Fig 2.28). All these interactions are involved in the formation of three dimensional supramolecular motif as shown in the Fig 2.29, where the pyridine-2,4-dicarboxylate anions are sandwiched between the channels formed by the host $(H_4NTB)^+$ molecules.

**Crystal Structures of $[(H_5NTB)^{2+}.(2,5\text{-}PDCA)^{2-}.DMF]$ (2i)**

Salt **2i** crystallizes in the triclinic system with P-1 space group. The asymmetric unit consists of one protonated tris(1H-benzimidazol-2-yl)methyl)amine cation, one pyridine-2,5-dicarboxylate anion and one dimethylformamide molecule as solvent of crystallization (Fig 2.30). The crystal data and collection details are tabulated in Table 2.11 and important bond lengths and angles are given in Table 2.12. Two of the three benzimidazole nitrogen gets protonated by pyridine-2,5-dicarboxylic acid, resulted in the formation of the ion pair. The different non-covalent interactions present in the crystal structure of salt **2h** are N-H···O (N1-H1···O1, 2.823(5); N2-H1···O2, 1.913(2); N3-H3···O2, 2.018(4); N6-H6···O2, 2.019(2) Å), C-H···O [C2-H2···O1, 2.726(4); C8-H8A···O3, 2.913(1); C17-H17B···O3, 2.571(8); C17-H17B···O4, 2.302(8); C20-H20···O1, 2.482(5); C29-H29A···O3, 2.809(8); C29-H29B···O1, 2.569(5) Å) and N-H···N interactions (N5-H5···N2, 1.917(5); N2-H2···N5, 1.974(5) Å) (Fig 2.31). The self association of cations formed a supramolecular architecture which served as host to accommodate the guest carboxylate anions and solvent molecules (Fig. 2.32).

**Crystal Structures of $[(H_4NTB)^+.(2,6\text{-}PDCAH)^-.C_2H_5OH.CH_3OH.H_2O]$ (2j)**

The asymmetric unit of salt **2j** contains one pyridine-2,6-dicarboxylate anion and one tris(1H-benzimidazol-2-yl)methyl)amine cation along with one molecule each

of methanol, ethanol and water which co-crystallizes in triclinic crystal system with P-1 space group (Fig. 2.33). The formation of salt **2j** occurred by the transfer of only one acidic hydrogen from one of the carboxylic acid group of pyridine-2,6-dicarboxylic acid to one of the benzimidazole ring of tris(1H-benzimidazol-2-yl)methyl)amine similar to case of salt **2h**. The crystal data and collection details are tabulated in Table 2.13 and important bond lengths and angles are given in Table 2.14. In crystal packing, it has been observed that cations, anions and solvent molecules were actively participate in non-covalent interactions like N-H···O (N2-H2A···O1, 1.817(2); N3-H5A···O1, 2.074(2); N5-H5Z···O1, 2.227(3); N4-H4A···O8, 1.851(4) Å) and C-H···O interactions (27-H27···O2, 2.578(2); C29-H29···O4, 2.638(5); C15-H15···O2, 2.817(2); C34-H34C···O7, 2.917(2) Å) (Fig. 2.34). The self association of $H_4NTB^+$ cations in the crystal structure of salt **2j** afforded a supramolecular architecture decorated with distinct voids to accommodate the guest anions and solvent molecules (Fig 2.35).

**Crystal Structures of [$(H_5NTB)^{2+}$.$(3,4\text{-PDCA})^{2-}$.DMF ] (2k)**

Salt **2k** crystallizes in monoclinic system with space group $P2_1/n$. The asymmetric unit consists of one pyridine-3,4-dicarboxylate anion $(3,4\text{-PDCA})^{2-}$, one tris(1H-benzimidazol-2-yl)methyl)amine cation $(H_5NTB)^{2+}$ and one molecule of dimethylformamide (Fig. 2.36). The ionic species was formed by the transfer of two proton from oxygen atom of the carboxyl group of pyridine-3,4-dicarboxylic acid to, two of the nitrogen atom of benzimidazole rings in tris(1H-benzimidazol-2-yl)methyl)amine similar to salt **2i**. The crystal data and refinement parameters are tabulated in Table 2.15 and selected bond length and bond angles are summarised in Table 2.16. The cations, anions and the solvent molecule were held together in the crystal lattice through a number of non-covalent interactions viz., N-H···N (N9-H3B'···N4, 1.724(3) Å), N-H···O (N5-H4B'···O3, 1.903(2); N7-H2B'···O3, 2.047(3); N7-H2B'···O4, 2.861(3); N8-H1B···O3, 1.863(2) Å) and C-H···O interactions (C21-H21···O4, 2.587(2); C31-H31A···O5, 2.506(3); C5-H5···O1, 2.618(2); C31-H31B···O5, 2.807(3); C15-H15B···O5, 2.619(3); C26-H26···O1, 2.782(8) Å) (Fig. 2.37). The host-guest supramolecular framework present in the crystal structure of salt **2k** is manifested in Fig 2.38 where the guest entities are situated within the interstitial spaces of polymeric structure formed by the self association of $(H_4NTB)^+$ cations.

**Crystal Structures of [$(H_6NTB)^{3+}$.$(3,5\text{-PDCA})^{2-}$.$(3,5\text{-PDCAH})^-$.DMF] (2l)**

Salt **2l** crystallizes in triclinic system with space group P-1. The asymmetric unit of salt **2l** contains one protonated tris(1H-benzimidazol-2-yl)methyl)amine, two pyridine-3,5-dicarboxylate anions and one molecule of dimethylformamide as solvent of crystallization (Fig. 2.39). The formation of salt in case of **2l** occurs in entirely different manner. One pyridine-3,5-dicarboxylic acid donates its both the proton to the tris(1H-benzimidazol-2-yl)methyl)amine, whereas the second molecule of pyridine-3,5-dicarboxylic acid contributes only one proton for the salt formation [**(**3,5-PDCA)$^{2-}$ and (3,5-PDCAH)$^{-}$]. The crystal data and refinement parameters are tabulated in Table 2.17 and selected bond length and bond angles are summarised in Table 2.18. Various non-covalent interactions were supporting the three dimensional structure which include N-H···O (N9-H9···O3, 1.765(3); N9-H9···O4, 2.786(3); N6-H6···O6, 2.824(2); N3-H3B···O6, 1.887(2); N2-H2B···O6, 2.111(2); N3-H3B···O5, 2.822(3); N6-H6···O5, 2.033(2); N5-H5B···O2, 1.833(2); N5-H5B···O1, 2.687(4); N8-H8···O7, 1.859(2) Å), C-H···O (C2-H2···O4, 2.855(3); C9-H9A···O9, 2.369(2); C8-H8B···O9, 2.947(3); C9-H9B···O9, 2.444(3); C39-H38A···O6, 2.940(2); C39-H39B···O7, 2.872(3); C17-H17B···O1, 2.422(2); C14-H14···O9, 2.762(2); C40-H40B···O9, 2.762(2) Å) and N-H···N interactions (N1-H1···N4, 2.116(2); N4-H4A···N1, 2.037(2) Å) (Fig. 2.40). The presence of different non-covalent interactions between pyridine-3,5-dicarboxylate anions and $(H_6NTB)^{3+}$ cation is responsible for the formation of three dimensional tetragonal channel like supramolecular networks (Fig. 2.41).

In another set of experiment, attempts were made to insert the metal ion in the above prepared ionic salts. 1,3-bis(1H-benzimidazol-2-yl)propane ($H_2$BBPr) and 1,6-bis(1H-benzimidazol-2-yl)hexane ($H_2$BBHex) were prepared by the literature methods (Scheme 2.7-2.8). The reaction of $Zn(NO_3)_2.6H_2O$ and $Ni(NO_3)_2.6H_2O$ with 1,3-bis(1H-benzimidazol-2-yl)propane ($H_2$BBPr), 1,4-bis(1H-benzimidazol-2-yl)butane ($H_2$BBBu), 1,6-bis(1H-benzimidazol-2-yl)hexane ($H_2$BBHex), in presence of pyridine-2,3-dicarboxylic acid (2,3-PDCA$H_2$) and pyridine-2,6-dicarboxylic acid (2,6-PDCA$H_2$) resulted in the formation of $(H_3BBPr)^{+}[Zn(2,3\text{-}PDCAH)_3]^{-}$ (**2m**), $(H_3BBBu)^{+}[Zn(2,3\text{-}PDCAH)_3]^{-}$ (**2n**), $(H_3BBHex)^{+}[Zn(2,3\text{-}PDCAH)_3]^{-}$ (**2o**), $(H_4BBPr)^{2+}[Ni(2,6\text{-}PDCA)_2]^{2-}.7H_2O$ (**2p**), $(H_4BBBu)^{2+}[Ni(2,6\text{-}PDCA)_2]^{2-}$ (**2q**) $(H_4BBHex)^{2+}[Ni(2,6\text{-}PDCA)_2]^{2-}.CH_3OH$ (**2r**) (Scheme 2.9).The different formulations were confirmed by elemental analysis, infrared spectroscopy and X-ray crystallography.

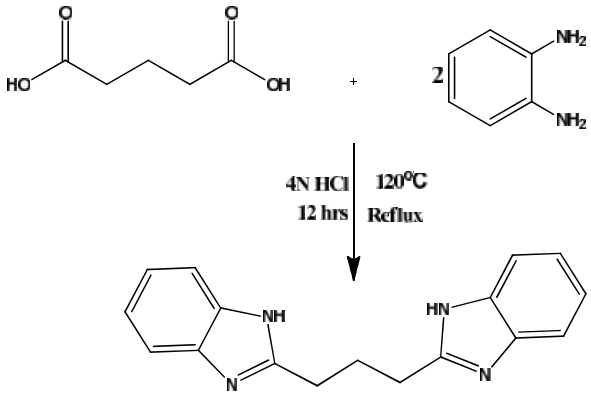


**Scheme 2.7**

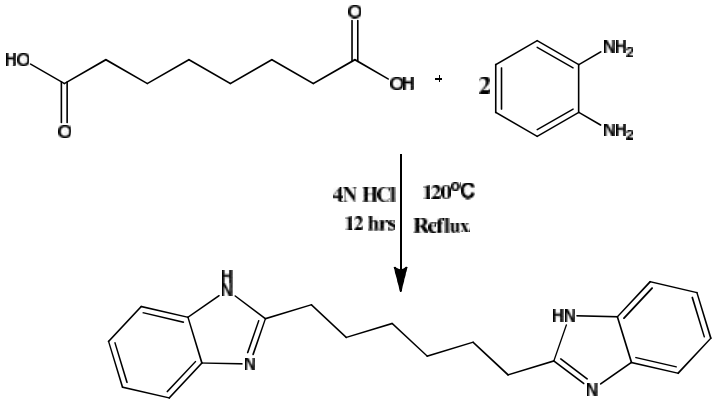


**Scheme 2.8**

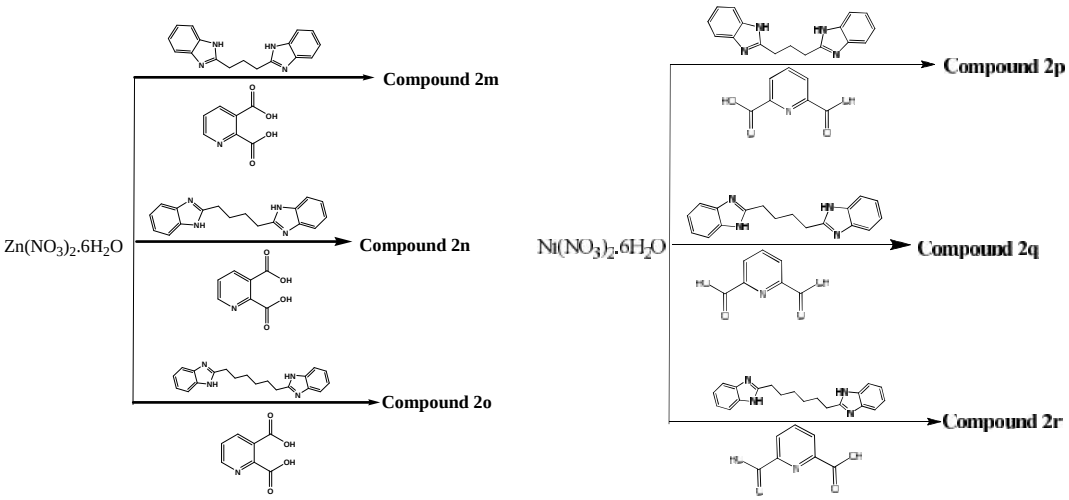


**Scheme 2.9**

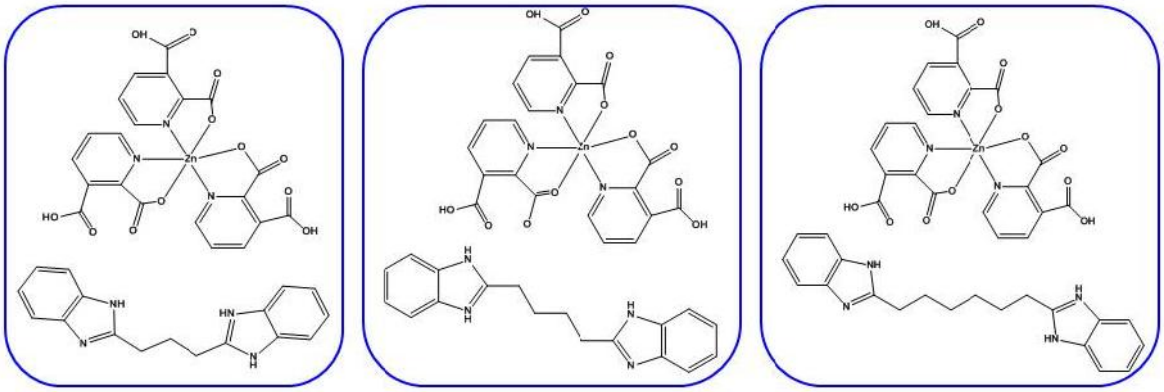

**2m** **2n** **2o**

**Scheme 2.10**

**Crystal structure of $(H_3BBBu)^+[Zn(2,3\text{-}PDCAH)_3]^-$ (2n)**

The single crystal X-ray diffraction studies confirmed the formulation of complex **2n** as $(H_3BBBu)^+[Zn(2,3\text{-}PDCAH)_3]^-$. Complex **2n** crystallizes in the monoclinic crystal system with $P2_1/n$ space group. The crystal structure of complex **2n** is illustrated in Fig 2.42 (Scheme 2.10). The crystallographic data and experimental details are listed in Table 2.19 and important bond lengths and bond angles are summarized in Table 2.20. The asymmetric unit contains one mono-protonated 1,4-bis(1H-benzimidazol-2-yl)butane molecule $(H_3BBBu)^+$ having uni-positive charge along with a mononuclear anionic zinc complex. In the anionic zinc complex the Zn(II) ion is coordinated with the three pyridyl nitrogen and three oxygens of carboxylate group present on 2 position of pyridine dicarboxylic acid. The complex revealed a distorted octahedral geometry around the metal centre. The donor atoms around the Zn(II) ion were oriented in two mutually perpendicular planes passing through the Zn(II) ion: the first plane contains the pyridine nitrogen donors (N5, N6 and N7) while the second plane contains the oxygen donors (O1, O5 and O9) from the coordinating carboxylate group. The coordinating pyridine rings of the three 2,3-PDCAH molecules were roughly perpendicular to one another. The geometry of anionic zinc complex in **2n** revealed a considerable distortion which could be explained in terms of the bond angles (O9-Zn1-N7, 75.97(9); O5-Zn-N7, 77.08(9); O1-Zn1-N7, 162.44(9) and O9-Zn-O5, 166.04(9) °) deviating significantly from the ideal values. The mean Zn(II)-N and Zn(II)-O bond distances were 2.172 Å and 2.092 Å which were close to the reported values in similar compounds [46-47]. The molecules were engaged in extensive hydrogen bonding interactions extending over a range of 1.862(2)-2.870(2) Å which

have been listed in detail in Table 2.25 (Fig. 2.43). Certain intermolecular CH···π interactions were also evident in the crystal structure of **2n** which include the interactions of pyridine hydrogen atoms (H36) with pyridine rings and phenyl hydrogen atoms (H16) with phenyl rings. These interactions were responsible for stabilizing the three dimensional packing of molecules in the lattice which has been illustrated in Fig 2.44**.**

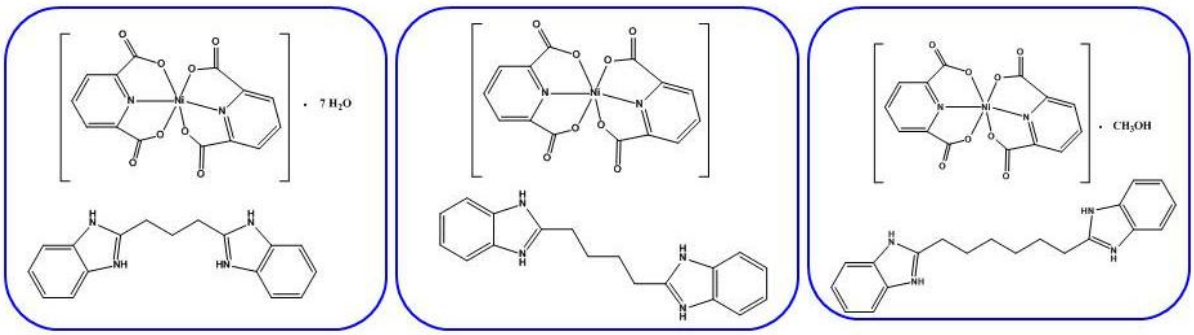

**2p** **2q** **2r**

**Scheme 2.11**

**Crystal structure of $(H_4BBPr)^{2+}[Ni(2,6\text{-}PDCA)_2]^{2-}.7H_2O$ (2p)**

The single crystal X-ray diffraction studies confirmed the formulation of complex **2p** as $(H_4BBPr)^{2+}[Ni(2,6\text{-}PDCA)_2]^{2-}.7H_2O$. The compound crystallizes in the monoclinic system with space group $P2_1/c$. The crystal structure of complex **2p** is illustrated in Fig. 2.45 (Scheme 2.11) and the crystal data and refinement parameter are tabulated in Table 2.21, whereas the selected bond lengths and bond angles are listed in Table 2.22. The asymmetric unit of **2p** consists of a di-protonated 1,3-bis(1H-benzimidazol-2-yl)propane molecule $(H_4BBPr)^{2+}$ having bi-positive electrical charge along with an octahedral Ni(II) di-anionic species bearing two molecules of pyridine-2,6-dicarboxylic acid. In addition, seven molecules of water were also present in the crystal lattice as solvent of crystallization. In the anionic Ni complex, the Ni(II) metal center is six coordinated, where the four coordination is completed by four oxygen atoms of carboxyl group and rest two sites are occupied by the two pyridyl nitrogen. The doubly deprotonated PDCA molecules coordinated with Ni(II) centre in a meridional fashion affording a bis species and a *trans* orientation of two pyridine nitrogen donors. The large deviations of the bond angles (N5-Ni1-O7, 73.33(5); N6-Ni1-O1, 114.40(6); O7-

Ni1-O6, 154.47(6); O1-Ni1-O4, 155.47(5)°) from the ideal values marked a considerable distortion in the octahedral geometry of Ni(II) di-anion. The mean Ni(II)-N and Ni(II)-O bond distances were found 1.968(2) Å and 2.131(2) Å respectively which are consistent with the values reported in the literature for analogous compounds [48]. The non-covalent interactions in the crystal structure of **2p** includes weak hydrogen bonding and π-π interactions. The various hydrogen bonding interactions encountered in the crystal structure of **2p** spanning over the range 1.821(2)-2.996(4) Å which have been listed in Table 2.25 (Fig.2.46). The similar pyridine rings in two different molecules were involved in π stacking interactions with a distances of 3.650(2) and 3.830(3) Å respectively which resulted in the formation of a polymeric chain along *c* axis in the crystal lattice. Furthermore the benzimidazole rings on two different sides were also involved in intermolecular π stacking interactions with a centroid to centroid distance of 3.721(3) Å resulted in a zig-zag chain. The three dimensional packing diagram of the complex **2p** is shown in Fig 2.47 where a continuous chain of anionic nickel complex runs parallel on either side of the chain formed by the doubly protonated 1,3-bis(1H-benzimidazol-2-yl)propane molecule.

**Crystal structure of $(H_4BBHex)^{2+}[Ni(2,6\text{-}PDCA)_2]^{2-}.CH_3OH$ (2r)**

The single crystal X-ray diffraction studies confirmed the formulation of complex **2r** as $(H_4BBHex)^{2+}[Ni(2,6\text{-}PDCA)_2]^{2-}.CH_3OH$. The compound crystallizes in the triclinic system with P-1 space group. The crystal structure of complex **2r** is illustrated in Fig 2.48 (Scheme 2.11). The crystal data and refinement parameters are tabulated in Table 2.23 and selected bond lengths and bond angles are listed in Table 2.24. The structural features of compound **2r** are very much similar to those observed for compound **2p** except that 1,6-bis(1H-benzimidazol-2-yl)hexane crystallized as dication in place of 1,3-bis(1H-benzimidazol-2-yl) propane and a methanol molecule was present as solvent of crystallization. The mean Ni(II)-N and Ni(II)-O bond distances were found to be 1.968(4) Å and 2.120(4) Å respectively which matched well with the values reported in the literature for analogous compounds [49]. The non-covalent interactions in the crystal structure of compound **2r** could be explain in terms of hydrogen bonding and CH···π interactions. The hydrogen bonding interactions involved the association of imidazole hydrogen atoms with carboxylate oxygen atoms with the distances of 1.747(3) and 2.037(4) Å. A detailed list of these interactions has been summarized in Table 2.25 (Fig. 2.49). Moreover, the aryl hydrogen atom (H4) of

benzimidazole ring also involved in CH··π interaction with the phenyl ring of benzimidazole moiety of neighbouring molecule. A perspective view of three dimensional packing of complex **2r** is shown in Fig 2.50 which is similar to the packing of **2p** where chain of anionic complex runs parallel to the chain of cationic ligand molecules.

For complex **2m, 2o** and **2q**, the structure has been proposed on the basis of elemental analysis and FT-IR.

**CONCLUSION**

The present chapter demonstrates the synthesis of binary salts based on different substitute of pyridine dicarboxylic acids and benzimidazole derived ligands i.e., 1,4-bis(1H-benzimidazol-2-yl)butane ($H_2$BBBu) and tris(1H-benzimidazol-2-yl)methyl)amine ($H_3$NTB). The structural analysis revealed that the benzimidazole is an excellent building block which is involved in the creation of entirely different three dimensional packing. The diversity of supramolecular structures in present chapter may be due to the difference in the structures of bases and the position of carboxylic group over the pyridine ring. Further metal complexes were also prepared by inserting the metal salts in the above prepared binary salts and characterized them through elemental analysis, FT-IR spectroscopy and single crystal X-ray diffraction.

**Table 2.1: Crystal data and collection details of $[(H_4BBBu)^{2+}.(2,6\text{-}PDCA)^{2-}.H_2O]$ (2d)**

| | |
|---|---|
| Emprical formula | $C_{32}H_{30}N_6O_{10}$ |
| Formula weight | 658.62 |
| Crystal system | Monoclinic |
| Space group | C2/c |
| *a*/ Å | 30.3196(10) |
| *b*/ Å | 6.8281(3) |
| *c*/ Å | 15.7608(5) |
| α/ $^o$ | 90.00 |
| *β*/ $^o$ | 110.571(3) |
| γ/ $^o$ | 90.00 |
| *V* / Å$^3$ | 3054.8(2) |
| *Z* | 4 |
| $D_{calc}$ (g cm$^{-3}$) | 1.432 |
| $\mu$/mm$^{-3}$ | 0.109 |
| $\theta$ range/ $^o$ | 1.45-25.30 |
| Reflections collected | 25830 |
| Independent reflections | 5160 |
| Parameters/ Restraints | 226/0 |
| GOF ($F^2$) | 1.163 |
| $R_1$; w$R_2$ [$I>2\sigma(I)$] | 0.0675; 0.1931 |
| $R_1$; w$R_2$ (all data) | 0.0988; 0.2143 |

**Table 2.2: Selected bond distances (Å) and bond angles ($^{o}$) for [$(H_4BBBu)^{2+}$.(2,6-PDCA)$^{2-}$.$H_2O$] (2d)**

| | | | |
|---|---|---|---|
| **Bond Distances** | | | |
| O1-C10 | 1.248(7) | O2-C10 | 1.222(7) |
| O3-C16 | 1.234(8) | O4-C16 | 1.239(7) |
| N3-C11 | 1.332(6) | N3-C15 | 1.356(6) |
| N1-C7 | 1.318(7) | N1-C1 | 1.393(6) |
| N2-C7 | 1.344(7) | N2-C6 | 1.371(7) |
| C1-C2 | 1.379(7) | C1-C6 | 1.390(7) |
| C2-C3 | 1.379(8) | C3-C4 | 1.400(9) |
| C4-C5 | 1.360(9) | C5-C6 | 1.393(7) |
| C7-C8 | 1.472(8) | C8-C9 | 1.386(9) |
| **Bond Angles** | | | |
| C11-N3-C15 | 123.4(5) | C7-N1-C1 | 108.5(4) |
| C7-N2-C6 | 108.3(4) | C2-C1-C6 | 121.3(5) |
| C2-C1-N1 | 132.4(5) | C6-C1-N1 | 106.2(4) |
| C1-C2-C3 | 116.8(5) | C2-C3-C4 | 121.4(6) |
| C5-C4-C3 | 122.3(5) | C4-C5-C6 | 116.2(5) |
| N2-C6-C1 | 107.1(4) | N2-C6-C5 | 131.0(5) |
| C1-C6-C5 | 121.9(5) | N1-C7-N2 | 109.9(5) |
| N1-C7-C8 | 126.6(5) | N2-C7-C8 | 123.5(5) |
| C9 C8 C7 | 120.4(6) | C8 C9 C9 | 119.3(7) |

**Table 2.3: Crystal data and collection details of $[(H_4BBBu)^{2+}.2(3,4\text{-}PDCAH)^{-}.H_2O]$ (2e)**

| | |
|---|---|
| Emprical formula | $C_{32}H_{32}N_6O_{10}$ |
| Formula weight | 660.64 |
| Crystal system | Triclinic |
| Space group | P-1 |
| *a*/ Å | 7.3442(7) |
| *b*/ Å | 8.3025(8) |
| *c*/ Å | 13.8227(14) |
| α/ $^{o}$ | 98.472(6) |
| *β*/ $^{o}$ | 103.510(5) |
| γ/ $^{o}$ | 104.565(6) |
| *V* / Å$^3$ | 773.93(14) |
| *Z* | 1 |
| $D_{calc}$ (g cm$^{-3}$) | 1.418 |
| $\mu$/mm$^{-3}$ | 0.107 |
| $\theta$ range/ $^{o}$ | 2.77-26.75 |
| Reflections collected | 22270 |
| Independent reflections | 2882 |
| Parameters/ Restraints | 203/0 |
| GOF ($F^2$) | 1.057 |
| $R_1$; w$R_2$ [$I>2\sigma(I)$] | 0.0437; 0.1144 |
| $R_1$; w$R_2$ (all data) | 0.0616; 0.1257 |

**Table 2.4: Selected bond distances (Å) and bond angles ($^{o}$) for $(H_4BBBu)^{2+}.2(3,4\text{-}PDCAH)^{-}.H_2O]$ (2e)**

| | | | |
|---|---|---|---|
| **Bond Distances** | | | |
| C1-N1 | 1.380(2) | C1-C6 | 1.391(2) |
| C1-C2 | 1.395(2) | C6-C5 | 1.381(2) |
| C6-N2 | 1.391(2) | C7-N1 | 1.325(2) |
| C7-N2 | 1.329(2) | C7-C8 | 1.486(2) |
| C9-C9 | 1.496(3) | C9-C8 | 1.503(2) |
| C2-C3 | 1.371(3) | C4-C3 | 1.393(3) |
| C5-C4 | 1.376(2) | C15-C14 | 1.399(2) |
| C15-C11 | 1.407(2) | C12-C13 | 1.364(3) |
| C15-C16 | 1.516(3) | C12-C11 | 1.390(3) |
| **Bond Angles** | | | |
| C14-C15-C16 | 113.54(15) | C11-C15-C16 | 129.70(15) |
| C13-C12-C11 | 121.42(18) | O3-C16-O4 | 120.87(18) |
| O3-C16-C15 | 119.43(17) | O4-C16-C15 | 119.70(17) |
| C12-C11-C15 | 116.92(15) | C12-C11-C10 | 114.50(16) |
| C15-C11-C10 | 128.57(16) | N3-C14-C15 | 125.54(17) |
| N3-C13-C12 | 122.65(18) | C14-N3-C13 | 116.67(16) |
| O1-C10-O2 | 123.63(17) | O1-C10-C11 | 118.22(17) |

**Table 2.5 Crystal data and collection details of $[(H_4BBBu)^{2+}.(3,5\text{-}PDCA)^{2-}.3H_2O]$ (2f)**

| | |
|---|---|
| Emprical formula | $C_{25}H_{35}N_5O_{10}$ |
| Formula weight | 565.58 |
| Crystal system | Monoclinic |
| Space group | C2/c |
| *a*/ Å | 13.8116(4) |
| *b*/ Å | 12.0304(4) |
| *c*/ Å | 18.1278(6) |
| α/ $^o$ | 90.00 |
| *β*/ $^o$ | 111.041(2) |
| γ/ $^o$ | 90.00 |
| $V$ / Å$^3$ | 1456.8(5) |
| $Z$ | 4 |
| $D_{calc}$ (g cm$^{-3}$) | 1.336 |
| $\mu$/mm$^{-3}$ | 0.104 |
| $\theta$ range/ $^o$ | 2.83-29.18 |
| Reflections collected | 27518 |
| Independent reflections | 6146 |
| Parameters/ Restraints | 206/0 |
| GOF ($F^2$) | 1.006 |
| $R_1$; w$R_2$ [$I>2\sigma(I)$] | 0.0641; 0.1309 |
| $R_1$; w$R_2$ (all data) | 0.1109; 0.1429 |

**Table 2.6: Selected bond distances (Å) and bond angles ($^{o}$) for [$(H_4BBBu)^{2+}$.(3,5-PDCA)$^{2-}$.3$H_2O$] (2f)**

| | | | |
|---|---|---|---|
| **Bond Distances** | | | |
| O1-C10 | 1.2456(17) | O4-H6W | 0.90(3) |
| O2-C10 | 1.2594(17) | O5-H2W | 0.84(2) |
| O3-H4W | 0.85(3) | O5-H1W | 0.91(3) |
| O3-H3W | 0.96(3) | N1-C7 | 1.3328(17) |
| O4-H5W | 0.88(2) | N1-C1 | 1.3781(18) |
| N2-C7 | 1.3275(18) | N1-H1 | 0.8600 |
| N3-C13 | 1.3877(18) | N3-C13 | 1.3355(15) |
| **Bond Angles** | | | |
| H4W-O3-H3W | 107(2) | H5W-O4-H6W | 107(2) |
| H2W-O5-H1W | 107(2) | C7-N1-C1 | 109.65(11) |
| C7-N1-H1 | 125.2 | C1-N1-H1 | 125.2 |
| C7-N2-C6 | 109.45(11) | C7-N2-H1B | 125.3 |
| C6-N2-H1B | 125.3 | C13-N3-C13 | 117.01(15) |
| N3-C13-C11 | 124.13(12) | N3-C13-H13 | 117.9 |
| C11-C13-H13 | 117.9 | C13-C11-C12 | 117.28(11) |
| C13-C11-C10 | 122.35(11) | C12-C11-C10 | 120.36(12) |

**Table 2.7: Crystal data and collection details of $[(H_5NTB)^{2+}.2(2,3\text{-}PDCAH)^{-}.DMF]$ (2g)**

| | |
|---|---|
| Emprical formula | $C_{41}H_{38}N_{10}O_9$ |
| Formula weight | 814.81 |
| Crystal system | Triclinic |
| Space group | P-1 |
| *a*/ Å | 12.457(1) |
| *b*/ Å | 13.0137(10) |
| *c*/ Å | 14.3789(11) |
| α/ $^o$ | 65.736(4) |
| *β*/ $^o$ | 72.646(4) |
| γ/ $^o$ | 70.684(4) |
| $V$ / Å$^3$ | 1969.4(3) |
| $Z$ | 2 |
| $D_{calc}$ (g cm$^{-3}$) | 1.374 |
| $\mu$/mm$^{-3}$ | 0.100 |
| $\theta$ range/ $^o$ | 2.98-25.00 |
| Reflections collected | 37123 |
| Independent reflections | 5529 |
| Parameters/ Restraints | 549/0 |
| GOF ($F^2$) | 1.062 |
| $R_1$; w$R_2$ [$I>2\sigma(I)$] | 0.0424; 0.1045 |
| $R_1$; w$R_2$ (all data) | 0.0537; 0.1131 |

**Table 2.8: Selected bond distances (Å) and bond angles ($^{o}$) for [$(H_5NTB)^{2+}$.2(2,3-PDCAH)$^{-}$.DMF] (2g)**

| | | | |
|---|---|---|---|
| **Bond Distances** | | | |
| O1-C25 | 1.305(4) | O2-C25 | 1.211(4) |
| O3-C31 | 1.235(4) | O4-C31 | 1.256(3) |
| O5-C32 | 1.226(3) | O6-C32 | 1.278(3) |
| O7-C38 | 1.205(3) | O8-C38 | 1.312(3) |
| O9-C41 | 0.997(11) | N1-C7 | 1.325(3) |
| N1-C1 | 1.385(4) | N2-C7 | 1.330(3) |
| N2-C6 | 1.393(3) | N3-C10 | 1.319(3) |
| N3-C11 | 1.382(4) | N4-C10 | 1.322(3) |
| N4-C16 | 1.391(3) | N5-C18 | 1.345(3) |
| **Bond Angles** | | | |
| C7-N1-C1 | 109.0(2) | C7-N2-C6 | 108.9(2) |
| C10-N3-C11 | 108.7(3) | C10-N4-C16 | 108.4(2) |
| C18-N5-C19 | 107.8(2) | C18-N6-C24 | 105.8(2) |
| C8-N7 C9 | 111.7(2) | C8-N7-C17 | 113.3(2) |
| C9-N7-C17 | 110.3(2) | C27-N8-C26 | 117.3(3) |
| C36-N9-C37 | 118.4(3) | C41-N10-C39 | 133.3(9) |
| C41-N10-C40 | 115.6(9) | C39-N10-C40 | 111.1(6) |
| C6-C1-N1 | 106.7(2) | C6-C1-C2 | 121.8(3) |
| N1-C1-C2 | 131.5(3) | C3-C2-C1 | 116.7(3) |

**Table 2.9: Crystal data and collection details of $[(H_4NTB)^+.(2,4\text{-}PDCH)^-.2CH_3OH.H_2O]$ (2h)**

| | |
|---|---|
| Emprical formula | $C_{33}H_{33}N_8O_7$ |
| Formula weight | 653.67 |
| Crystal system | Triclinic |
| Space group | P-1 |
| *a*/ Å | 10.660(18) |
| *b*/ Å | 13.03(2) |
| *c*/ Å | 14.35(2) |
| α/ $^o$ | 90.46(5) |
| *β*/ $^o$ | 109.68(4) |
| γ/ $^o$ | 102.48(5) |
| $V$ / Å$^3$ | 1825.00(5) |
| $Z$ | 2 |
| $D_{calc}$ (g cm$^{-3}$) | 1.190 |
| $\mu$/mm$^{-3}$ | 0.086 |
| $\theta$ range/ $^o$ | 1.74-25.10 |
| Reflections collected | 26939 |
| Independent reflections | 6695 |
| Parameters/ Restraints | 438/117 |
| GOF ($F^2$) | 1.505 |
| $R_1$; w$R_2$ [$I>2\sigma(I)$] | 0.0439; 0.1368 |
| $R_1$; w$R_2$ (all data) | 0.0525; 0.1462 |

**Table 2.10: Selected bond distances (Å) and bond angles ($^{o}$) for [$(H_4NTB)^{+}$.(2,4-PDCH)$^{-}$.$2CH_3OH.H_2O$] (2h)**

| | | | |
|---|---|---|---|
| **Bond Distances** | | | |
| C7-N2 | 1.295(11) | C7-N1 | 1.355(12) |
| C7-C8 | 1.554(13) | C1-C2 | 1.329(13) |
| C1-C6 | 1.377(14) | C1-N1 | 1.390(12) |
| C18-N6 | 1.340(11) | C18-N5 | 1.334(12) |
| C18-C17 | 1.495(13) | C26-C31 | 1.330(13) |
| C26-N8 | 1.335(12) | C26-C25 | 1.574(14) |
| C19-C24 | 1.367(14) | C19-C20 | 1.381(14) |
| C19-N5 | 1.369(11) | C31-C29 | 1.404(13) |
| C16-N4 | 1.349(13) | C16-C11 | 1.407(14) |
| **Bond Angles** | | | |
| N2-C7-N1 | 114.1(10) | N2-C7-C8 | 123.3(10) |
| N1-C7-C8 | 122.5(10) | C2-C1-C6 | 123.5(12) |
| C2-C1-N1 | 131.4(12) | C6-C1-N1 | 105.0(10) |
| N6-C18-N5 | 113.3(8) | N6-C18-C17 | 122.1(9) |
| N5-C18-C17 | 124.5(10) | C31-C26-N8 | 126.2(9) |
| C31-C26-C25 | 117.4(10) | N8-C26-C25 | 116.2(11) |
| C24-C19-C20 | 120.6(10) | C24-C19-N5 | 108.7(9) |
| C20-C19-N5 | 130.7(11) | C26-C31-C29 | 117.8(10) |
| N4-C16-C11 | 108.4(10) | N4-C16-C15 | 130.9(10) |

**Table 2.11 Crystal data and collection details of $[(H_5NTB)^{2+}.(2,5\text{-}PDCA)^{2-}.DMF]$ (2i)**

| | |
|---|---|
| Emprical formula | $C_{31}H_{25}N_8O_3$ |
| Formula weight | 557.59 |
| Crystal system | Triclinic |
| Space group | P-1 |
| *a*/ Å | 10.2326(4) |
| *b*/ Å | 10.8277(4) |
| *c*/ Å | 13.9349(5) |
| α/ $^o$ | 99.072(2) |
| *β*/ $^o$ | 108.474(2) |
| γ/ $^o$ | 94.329(2) |
| $V$ / Å$^3$ | 1433.01(9) |
| $Z$ | 4 |
| $D_{calc}$ (g cm$^{-3}$) | 1.292 |
| $\mu$/mm$^{-3}$ | 0.087 |
| $\theta$ range/ $^o$ | 2.38-25.71 |
| Reflections collected | 31170 |
| Independent reflections | 3215 |
| Parameters/ Restraints | 258/0 |
| GOF ($F^2$) | 1.062 |
| $R_1$; w$R_2$ [$I>2\sigma(I)$] | 0.0523; 0.1235 |
| $R_1$; w$R_2$ (all data) | 0.0855; 0.1466 |

**Table 2.12: Selected bond distances (Å) and bond angles ($^o$) for [$(H_5NTB)^{2+}$.(2,5-PDCA)$^{2-}$.DMF] (2i)**

| | | | |
|---|---|---|---|
| **Bond Distances** | | | |
| O1-C25 | 1.225(6) | O2-C25 | 1.276(6) |
| O3-C31 | 1.277(19) | N1-C7 | 1.321(6) |
| N1-C1 | 1.366(6) | N1-H1 | 0.8600 |
| N2-C7 | 1.341(6) | N2-C6 | 1.378(6) |
| N2-H2 | 0.8600 | N3-C10 | 1.337(6) |
| N3-C11 | 1.404(6) | N3-H3 | 0.8600 |
| N4-C10 | 1.304(6) | N4-C16 | 1.389(7) |
| N4-H4 | 0.8600 | N5-C18 | 1.334(6) |
| N5-C19 | 1.379(6) | N5-H5 | 0.8600 |
| **Bond Angles** | | | |
| C7-N1-C1 | 108.4(4) | C7-N1-H1 | 125.8 |
| C1-N1-H1 | 125.8 | C7-N2-C6 | 107.3(4) |
| C7-N2-H2 | 126.4 | C6-N2-H2 | 126.4 |
| C10-N3-C11 | 106.5(4) | C18-N5-H5 | 126.4 |
| C10-N3-H3 | 126.7 | C18-N5-C19 | 107.3(4) |
| C11-N3-H3 | 126.7 | C16-N4-H4 | 127.0 |
| C10-N4-C16 | 106.0(4) | C10-N4-H4 | 127.0 |
| C19-N5-H5 | 126.4 | C18-N6-C24 | 108.2(4) |
| C18-N6-H6 | 125.9 | C24-N6-H6 | 125.9 |

**Table 2.13 Crystal data and collection details of $[(H_4NTB)^+.(2,6\text{-}PDCAH)^-.C_2H_5OH.CH_3OH.H_2O]$ (2j)**

| | |
|---|---|
| Emprical formula | $C_{34}H_{38}N_8O_7$ |
| Formula weight | 670.72 |
| Crystal system | Triclinic |
| Space group | P-1 |
| *a*/ Å | 11. 0199(3) |
| *b*/ Å | 13.0798(4) |
| *c*/ Å | 14.0511(6) |
| α/ $^o$ | 66.3020(10) |
| *β*/ $^o$ | 73.191(2) |
| γ/ $^o$ | 78.798(2) |
| $V$ / Å$^3$ | 1768.23(11) |
| $Z$ | 2 |
| $D_{calc}$ (g cm$^{-3}$) | 1.260 |
| $\mu$/mm$^{-3}$ | 0.090 |
| $\theta$ range/ $^o$ | 1.80-25.84 |
| Reflections collected | 26301 |
| Independent reflections | 5628 |
| Parameters/ Restraints | 459/0 |
| GOF ($F^2$) | 1.090 |
| $R_1$; w$R_2$ [$I>2\sigma(I)$] | 0.0408; 0.0992 |
| $R_1$; w$R_2$ (all data) | 0.0626; 0.1083 |

**Table 2.14: Selected bond distances (Å) and bond angles ($^{o}$) for [$(H_4NTB)^{+}$.(2,6-PDCAH)$^{-}$.$C_2H_5OH$.$CH_3OH$.$H_2O$] (2j)**

| | | | |
|---|---|---|---|
| **Bond Distances** | | | |
| O1-C25 | 1.264(3) | O1-H1 | 0.8200 |
| O2-C25 | 1.238(3) | O3-C31 | 1.274(3) |
| O4-C31 | 1.181(4) | N2-C7 | 1.341(3) |
| N2-C6 | 1.383(3) | N2-H2A | 0.8600 |
| N7-C8 | 1.468(3) | N7-C9 | 1.468(3) |
| N7-C17 | 1.467(3) | N8-C30 | 1.336(3) |
| N8-C26 | 1.338(3) | N3-C10 | 1.348(3) |
| N3-C11 | 1.386(3) | N3-H5A | 0.8600 |
| N6-C18 | 1.320(3) | N6-C24 | 1.392(4) |
| N1-C7 | 1.322(3) | N1-C1 | 1.387(3) |
| **Bond Angles** | | | |
| C25-O1-H1 | 109.5 | C7-N2-C6 | 107.6(2) |
| C7-N2-H2A | 126.2 | C6-N2-H2A | 126.2 |
| C8-N7-C9 | 111.95(19) | C8-N7-C17 | 110.99(19) |
| C9-N7-C17 | 111.6(2) | C30-N8-C26 | 118.1(2) |
| C10-N3-C11 | 108.0(2) | C10-N3-H5A | 126.0 |
| C11-N3-H5A | 126.0 | C18-N6-C24 | 105.4(2) |
| C7-N1-C1 | 106.0(2) | C18-N5-C19 | 108.2(2) |
| C18-N5-H5Z | 125(2) | C19-N5-H5Z | 126(2) |
| C10-N4-C16 | 107.2(2) | C10-N4-H4A | 126.4 |
| C16-N4-H4A | 126.4 | O2-C25-O1 | 125.9(2) |

**Table 2.15: Crystal data and collection details of $[(H_5NTB)^{2+}.(3,4\text{-}PDCA)^{2-}.DMF]$ (2k)**

| | |
|---|---|
| Emprical formula | $C_{34}H_{31}N_9O_5$ |
| Formula weight | 645.68 |
| Crystal system | Monoclinic |
| Space group | $P2_1/n$ |
| *a*/ Å | 11.3486(4) |
| *b*/ Å | 22.5144(9) |
| *c*/ Å | 13.3740(6) |
| α/ $^o$ | 90.00 |
| *β*/ $^o$ | 102.905(2) |
| γ/ $^o$ | 90.00 |
| *V* / Å$^3$ | 3330.8(2) |
| *Z* | 4 |
| $D_{calc}$ (g cm$^{-3}$) | 1.288 |
| $\mu$/mm$^{-3}$ | 0.090 |
| $\theta$ range/ $^o$ | 2.47-27.62 |
| Reflections collected | 30584 |
| Independent reflections | 5624 |
| Parameters/ Restraints | 437/0 |
| GOF ($F^2$) | 1.494 |
| $R_1$; w$R_2$ [$I>2\sigma(I)$] | 0.0398; 0.1122 |
| $R_1$; w$R_2$ (all data) | 0.0538; 0.1459 |

**Table 2.16: Selected bond distances (Å) and bond angles ($^o$) for [$(H_5NTB)^{2+}$.(3,4-PDCA)$^{2-}$.DMF ] (2k)**

| | | | |
|---|---|---|---|
| **Bond Distances** | | | |
| O1-C25 | 1.196(4) | O2-C25 | 1.303(4) |
| O3-C31 | 1.269(3) | O4-C31 | 1.229(4) |
| O5-C34 | 1.164(7) | N1-C15 | 1.334(4) |
| N1-C9 | 1.399(4) | N2-C15 | 1.339(3) |
| N2-C14 | 1.398(4) | N3-C8 | 1.465(3) |
| N3-C16 | 1.469(3) | N3-C24 | 1.471(3) |
| N4-C7 | 1.345(3) | N4-C1 | 1.388(4) |
| N5-C7 | 1.318(3) | N6-C23 | 1.347(3) |
| N5-C6 | 1.396(4) | N6-C17 | 1.379(3) |
| **Bond Angles** | | | |
| C15-N1-C9 | 107.6(2) | C15-N2-C14 | 107.2(2) |
| C8-N3-C16 | 110.1(2) | C8-N3-C24 | 111.9(2) |
| C16 N3-C24 | 110.5(2) | C7-N4-C1 | 107.7(2) |
| C7-N5-C6 | 105.3(2) | C23-N6-C17 | 107.9(2) |
| C23-N7-C22 | 104.7(2) | C27-N8-C30 | 115.5(3) |
| C34-N9-C33 | 125.4(6) | C34-N9-C32 | 119.1(5) |
| C33-N9-C32 | 115.5(5) | C2-C1-N4 | 133.2(3) |
| C2-C1-C6 | 121.9(3) | N4-C1-C6 | 104.9(2) |
| C3-C2-C1 | 116.5(3) | C4-C3-C2 | 122.5(3) |

**Table 2.17: Crystal data and collection details of $[(H_6NTB)^{3+}.(3,5\text{-}PDCA)^{2-}.(3,5\text{-}PDCAH)^{-}.DMF]$ (2l)**

| | |
|---|---|
| Emprical formula | $C_{41}H_{39}N_{10}O_9$ |
| Formula weight | 815.82 |
| Crystal system | Triclinic |
| Space group | P-1 |
| *a*/ Å | 11.6941(7) |
| *b*/ Å | 13.4776(8) |
| *c*/ Å | 13.5714(8) |
| α/ $^o$ | 67.644(2) |
| *β*/ $^o$ | 87.023(3) |
| γ/ $^o$ | 84.563(3) |
| *V* / Å$^3$ | 1969.0(2) |
| *Z* | 2 |
| $D_{calc}$ (g cm$^{-3}$) | 1.376 |
| $\mu$/mm$^{-3}$ | 0.100 |
| $\theta$ range/ $^o$ | 2.37-28.45 |
| Reflections collected | 48294 |
| Independent reflections | 10184 |
| Parameters/ Restraints | 544/0 |
| GOF ($F^2$) | 1.258 |
| $R_1$; w$R_2$ [$I>2\sigma(I)$] | 0.0417; 0.1460 |
| $R_1$; w$R_2$ (all data) | 0.0508; 0.1522 |

**Table 2.18: Selected bond distances (Å) and bond angles (°) for $[(H_6NTB)^{3+}.(3,5\text{-}PDCA)^{2-}.(3,5\text{-}PDCAH)^{-}.DMF]$ (2l)**

| | | | |
|---|---|---|---|
| **Bond Distances** | | | |
| O1-C25 | 1.211(4) | O2-C25 | 1.294(4) |
| O3-C29 | 1.305(4) | O4-C29 | 1.193(4) |
| O5-C32 | 1.243(3) | O6-C32 | 1.266(3) |
| O7-C36 | 1.310(4) | O8-C36 | 1.194(4) |
| O9-C41 | 1.231(4) | N1-C7 | 1.314(3) |
| N1-C1 | 1.395(3) | N2-C7 | 1.357(3) |
| N2-C6 | 1.379(3) | N3-C10 | 1.323(3) |
| N3-C11 | 1.381(3) | N4-C10 | 1.324(3) |
| N4-C16 | 1.389(3) | N5-C18 | 1.315(3) |
| **Bond Angles** | | | |
| C7-N1-C1 | 105.5(2) | C7-N2-C6 | 107.2(2) |
| C10-N3-C11 | 108.6(2) | C10-N4-C16 | 108.8(2) |
| C18-N5-C19 | 106.7(2) | C18-N6-C24 | 107.5(2) |
| C8-N7-C9 | 109.64(18) | C8-N7-C17 | 111.48(19) |
| C9-N7-C17 | 111.51(18) | C30-N8-C31 | 117.8(3) |
| C37-N9-C38 | 118.8(2) | C41-N10-C39 | 121.3(3) |
| C41-N10-C40 | 119.8(3) | C39-N10-C40 | 118.8(3) |
| C2-C1-C6 | 120.6(2) | C2-C1-N1 | 130.3(2) |
| C6-C1-N1 | 109.1(2) | C3-C2-C1 | 117.3(3) |

**Table 2.19: Crystal data and collection details of $(H_3BBBu)^+[Zn(2,3\text{-}PDCAH)_3]^-$ (2n)**

| | |
|---|---|
| Emprical formula | $C_{39}H_{30}N_7O_{12}Zn$ |
| Formula weight | 854.09 |
| Crystal system | Monoclinic |
| Space group | $P2_1/n$ |
| *a*/ Å | 7.8725(2) |
| *b*/ Å | 26.4725(6) |
| *c*/ Å | 17.3774(4) |
| α/ $^o$ | 90.00 |
| *β*/ $^o$ | 100.269(1) |
| γ/ $^o$ | 90.00 |
| $V$ / Å$^3$ | 3563.52(15) |
| $Z$ | 4 |
| $D_{calc}$ (g cm$^{-3}$) | 1.592 |
| $\mu$/mm$^{-3}$ | 0.769 |
| $\theta$ range/ $^o$ | 2.34-28.39 |
| Reflections collected | 7284 |
| Independent reflections | 1756.0 |
| Parameters/ Restraints | 500/0 |
| GOF ($F^2$) | 1.166 |
| $R_1$; w$R_2$ [$I>2\sigma(I)$] | 0.056, 0.210 |
| $R_1$; w$R_2$ (all data) | 0.073,0.230 |

**Table 2.20: Selected bond distances (Å) and bond angles (°) for $(H_3BBBu)^+[Zn(2,3\text{-}PDCAH)_3]^-$ (2n)**

| | | | |
|---|---|---|---|
| **Bond Distances** | | | |
| Zn1-O1 | 2.073(2) | Zn1-N5 | 2.195(3) |
| Zn1-O9 | 2.091(2) | Zn1-N6 | 2.203(3) |
| Zn1-N7 | 2.123(2) | | |
| **Bond Angles** | | | |
| O1-Zn1-O9 | 95.31(9) | O5-Zn1-N7 | 77.08(9) |
| O1-Zn1-O5 | 89.33(9) | O5-Zn1-N5 | 97.87(9) |
| O1-Zn1-N7 | 162.44(9) | O5-Zn1-N6 | 90.49(9) |
| O1-Zn1-N5 | 76.76(9) | N7-Zn1-N5 | 93.93(9) |
| O1-Zn1-N6 | 95.57(9) | N7-Zn1-N6 | 95.61(9) |
| O9-Zn1-O5 | 166.04(9) | N5-Zn1-N6 | 168.51(12) |
| O9-Zn1-N7 | 100.51(9) | O9-Zn1-N6 | 75.97(9) |
| O9-Zn1-N5 | 96.01(9) | | |

**Table 2.21: Crystal data and collection details of $(H_4BBPr)^{2+}[Ni(2,6\text{-}PDCA)_2]^{2-}.7H_2O$ (2p)**

| | |
|---|---|
| Emprical formula | $C_{31}H_{22}N_6NiO_{15}$ |
| Formula weight | 777.24 |
| Crystal system | Monoclinic |
| Space group | $P2_1/c$ |
| *a*/ Å | 14.3133(4) |
| *b*/ Å | 17.3652(5) |
| *c*/ Å | 15.5842(4) |
| α/ $^o$ | 90.00 |
| *β*/ $^o$ | 115.195(1) |
| γ/ $^o$ | 90.00 |
| *V* / Å$^3$ | 3505.00(17) |
| *Z* | 4 |
| $D_{calc}$ (g cm$^{-3}$) | 1.473 |
| $\mu$/mm$^{-3}$ | 0.633 |
| $\theta$ range/ $^o$ | 2.34-28.39 |
| Reflections collected | 7420 |
| Independent reflections | 1592.0 |
| Parameters/ Restraints | 478/0 |
| GOF ($F^2$) | 1.109 |
| $R_1$; w$R_2$ [$I>2\sigma(I)$] | 0.055; 0.190 |
| $R_1$; w$R_2$ (all data) | 0.073; 0.210 |

**Table 2.22: Selected bond distances (Å) and bond angles ($^{o}$) for $(H_4BBPr)^{2+}[Ni(2,6\text{-}PDCA)_2]^{2-}.7H_2O$ (2p)**

| | | | |
|---|---|---|---|
| **Bond Distances** | | | |
| Ni1-O1 | 2.128(1) | Ni1-O7 | 2.116(2) |
| Ni1-O4 | 2.143(2) | Ni1-N5 | 1.969(1) |
| Ni1-O6 | 2.139(1) | Ni1-N6 | 1.967(2) |
| **Bond Angles** | | | |
| N6-Ni1-N5 | 166.86(6) | N6-Ni1-O1 | 114.40(6) |
| N6-Ni1-O7 | 78.13(6) | N6-Ni1-O6 | 77.74(6) |
| N6-Ni1-O4 | 90.07(6) | O7-Ni1-O6 | 154.47(6) |
| N5-Ni1-O7 | 96.81(6) | O6-Ni1-O4 | 90.21(5) |
| N5-Ni1-O1 | 77.33(5) | O1-Ni1-O6 | 89.23(5) |
| N5-Ni1-O6 | 108.53(5) | O1-Ni1-O4 | 155.47(5) |
| N5-Ni1-O4 | 77.74(5) | O6-Ni1-O4 | 98.02(5) |
| O7-Ni1-O1 | 93.22(6) | | |

**Table 2.23: Crystal data and collection details of for $[(H_4BBHex)^{2+}[Ni(2,6\text{-}PDCA)_2]^{2-}.CH_3OH$ (2r)**

| | |
|---|---|
| Emprical formula | $C_{35}H_{32}N_6O_9Ni$ |
| Formula weight | 739.36 |
| Crystal system | Triclinic |
| Space group | P-1 |
| *a*/ Å | 9.3519(5) |
| *b*/ Å | 12.7449(6) |
| *c*/ Å | 14.9462(7) |
| α/ $^o$ | 75.210(3) |
| *β*/ $^o$ | 75.637(3) |
| γ/ $^o$ | 87.960(3) |
| *V* / Å$^3$ | 1667.83(15) |
| *Z* | 2 |
| $D_{calc}$ (g cm$^{-3}$) | 1.472 |
| $\mu$/mm$^{-3}$ | 0.648 |
| $\theta$ range/ $^o$ | 2.34-28.39 |
| Reflections collected | 4806 |
| Independent reflections | 6285 |
| Parameters/ Restraints | 466/0 |
| GOF ($F^2$) | 1.261 |
| $R_1$; w$R_2$ [$I>2\sigma(I)$] | 0.035; 0.200 |
| $R_1$; w$R_2$ (all data) | 0.061; 0.230 |

**Table 2.24: Selected bond distances (Å) and bond angles ($^{o}$) for $[(H_4BBHex)^{2+}[Ni(2,6\text{-}PDCA)_2]^{2-}.CH_3OH$ (2r)**

| | | | |
|---|---|---|---|
| **Bond Distances** | | | |
| Ni1-N6 | 1.966(4) | Ni1-N5 | 1.969(4) |
| Ni1-O2 | 2.101(4) | Ni1-O8 | 2.122(4) |
| Ni1-O6 | 2.127(4) | Ni1-O4 | 2.129(4) |
| **Bond Angles** | | | |
| N6-Ni1-N5 | 176.53(9) | O2-Ni1-O6 | 93.82(8) |
| N6-Ni1-O2 | 78.31(8) | O2-Ni1-O4 | 155.85(8) |
| N6-Ni1-O8 | 99.99(8) | O8-Ni1-O6 | 155.81(8) |
| N6-Ni1-O6 | 104.21(8) | O8-Ni1-O4 | 93.24(8) |
| N6-Ni1-O4 | 77.54(8) | O6-Ni1-O4 | 91.90(8) |
| N5-Ni1-O2 | 103.99(9) | N1-Ni1-N4 | 100.15(9) |
| N5-Ni1-O8 | 77.47(9) | O2-Ni1-O8 | 91.10(7) |
| N1-Ni1-O6 | 78.35(9) | | |

**2.25: Non-covalent interactions for 2d-2r (Å and $^{o}$)**

| S.N | D-H···A | d(D-H) | d(H-A) | d(D-A) | <(DHA)> |
|---|---|---|---|---|---|
| **1.** | **2d** | | | | |
| | N2-H2B···O5 | 0.860(5) | 1.864(5) | 2.718(7) | 171.67 |
| | O5-H6W···O3 | 0.880(9) | 1.891(9) | 2.725(7) | 157.29 |
| | C2-H2···O1 | 0.930(6) | 2.502(3) | 3.315(6) | 146.11 |
| | N1-H1···O2 | 0.860(4) | 1.856(3) | 2.711(5) | 172.20 |
| | N1-H1···O1 | 0.860(4) | 2.922(5) | 3.544(6) | 130.78 |
| | C9-H9B···O2 | 0.970(9) | 2.739(4) | 3.250(8) | 113.49 |
| | C9-H9A···O2 | 0.970(9) | 2.861(4) | 3.250(8) | 104.99 |
| | C4-H4···O5 | 0.930(5) | 2.962(5) | 3.732(7) | 141.19 |
| | O5-H5W···O4 | 0.803(6) | 1.983(6) | 2.738(6) | 156.42 |
| | C5-H5···O4 | 0.930(5) | 2.587(5) | 3.472(8) | 159.27 |
| | C13-H13···O5 | 0.930(7) | 2.741(5) | 3.599(8) | 153.76 |
| | C3-H3···O1 | 0.930(7) | 2.441(4) | 3.364(8) | 172.06 |
| **2.** | **2e** | | | | |
| | C9-H9A···O1 | 0.970(2) | 2.636(2) | 3.589(3) | 167.28 |
| | N1-H1B···O2 | 0.821(2) | 1.848(2) | 2.669(2) | 178.49 |
| | O4-H4A···O2 | 0.820(2) | 1.599(2) | 2.419(2) | 178.28 |
| | O1-H1···O2 | 0.970(2) | 2.636(2) | 3.589(3) | 167.68 |
| | N2-H2B···O2 | 0.870(2) | 1.926(2) | 2.794(2) | 176.66 |
| | C9-H9B···O4 | 0.970(2) | 2.673(2) | 3.603(2) | 145.37 |
| | C9-H9B···O2 | 0.970(2) | 2.503(2) | 3.362(2) | 147.65 |
| | C5-H5···O1 | 0.930(2) | 2.439(1) | 3.252(2) | 146.07 |
| | N2-H2B···O1 | 0.870(2) | 2.903(2) | 3.501(2) | 127.49 |
| | C2-H2···O3 | 0.930(2) | 2.898(2) | 3.734(2) | 150.26 |
| | C4-H4···O1 | 0.930(2) | 2.977(2) | 3.891(2) | 168.02 |
| | C13-H14···O3 | 0.930(2) | 2.871(2) | 3.691(3) | 147.68 |
| | C8-H8A···O4 | 0.970(2) | 2.504(1) | 3.414(2) | 156.18 |
| | O5-H6W···O3 | 0.952(3) | 2.909(4) | 3.574(2) | 127.88 |
| | O5-H5W···N3 | 0.952(3) | 1.897(3) | 2.827(2) | 164.65 |

| | | | | | |
|---|---|---|---|---|---|
| **3.** | **2f** | | | | |
| | N1-H1···O5 | 0.860(1) | 1.834(1) | 2.689(2) | 172.60 |
| | C9-H9B···N3 | 0.970(2) | 2.811(1) | 3.419(2) | 121.47 |
| | C5-H5···O2 | 0.930(2) | 2.665(1) | 3.319(2) | 127.94 |
| | N2-H1B···O1 | 0.860(1) | 2.060(1) | 2.880(2) | 159.02 |
| | C8-H8B···O1 | 0.970(2) | 2.889(1) | 3.569(2) | 127.99 |
| | N2-H1B···O2 | 0.860(1) | 2.274(1) | 2.984(2) | 139.97 |
| | C13-H13···O3 | 0.930(1) | 2.880(1) | 3.771(2) | 160.82 |
| | O5-H1W···O3 | 0.908(1) | 1.942(3) | 2.841(2) | 169.67 |
| | O4-H5W···O3 | 0.880(2) | 2.034(2) | 2.907(2) | 171.53 |
| | C8-H8B···O3 | 0.970(2) | 2.902(1) | 3.840(2) | 162.86 |
| | C4-H4···O5 | 0.930(2) | 2.770(2) | 3.557(3) | 142.89 |
| | C5-H5···O4 | 0.930(2) | 2.756(2) | 3.613(2) | 153.09 |
| | O3-H3W···O1 | 0.959(3) | 1.840(3) | 2.792(2) | 171.26 |
| | O3-H4W···O2 | 0.855(2) | 1.963(2) | 2.811(2) | 171.43 |
| | O5-H2W···O2 | 0.840(2) | 1.912(2) | 2.736(2) | 166.88 |
| | O4-H6W···O2 | 0.900(1) | 1.983(3) | 2.861(2) | 164.59 |
| **4** | **2g** | | | | |
| | O1-H1···N6 | 0.820(2) | 1.814(2) | 2.611(3) | 163.59 |
| | N1-H1A···O3 | 0.860(2) | 1.801(2) | 2.653(3) | 170.39 |
| | C8-H8B···O1 | 0.970(3) | 2.800(4) | 3.622(5) | 143.00 |
| | C23-H23···O2 | 0.930(4) | 2.942(3) | 3.662(5) | 135.33 |
| | C40-H40C···O4 | 0.960(1) | 2.870(4) | 3.704(1) | 145.81 |
| | O8-H8···O4 | 0.820(3) | 2.855(3) | 3.346(5) | 120.39 |
| | C15-H15···O8 | 0.930(3) | 2.765(2) | 3.619(4) | 153.05 |
| | C17-H17B···O1 | 0.970(3) | 2.975(3) | 3.662(4) | 128.80 |
| | N2-H2B···O6 | 0.860(2) | 1.884(2) | 2.741(3) | 173.68 |
| | C17-H17B···O2 | 0.970(3) | 2.463(3) | 3.386(4) | 159.02 |
| | N5-H5B···O6 | 0.860(3) | 2.736(2) | 3.217(4) | 116.84 |
| | C5-H5···O5 | 0.930(3) | 2.632(2) | 3.462(4) | 148.46 |
| | C34-H34···N5 | 0.930(2) | 1.983(2) | 2.877(3) | 160.57 |

| | | | | | |
|---|---|---|---|---|---|
| | N4-H4B···O6 | 0.860(2) | 1.805(2) | 2.662(3) | 174.76 |
| | N3-H3B···O9 | 0.860(2) | 1.836(4) | 2.666(4) | 161.44 |
| | C3-H3···O3 | 0.930(3) | 2.731(2) | 3.565(4) | 149.67 |
| | C8-H8B···O5 | 0.970(4) | 2.528(3) | 3.471(5) | 164.10 |
| | C8-H8A···O6 | 0.970(4) | 2.662(4) | 3.432(4) | 136.57 |
| | C39-H39A···O7 | 0.960(8) | 2.809(2) | 3.485(7) | 128.20 |
| | C12-H12···N8 | 0.930(4) | 2.929(3) | 3.808(4) | 158.14 |
| | C21-H21···O5 | 0.930(5) | 2.522(3) | 3.353(6) | 148.92 |
| | C22-H22···O7 | 0.930(7) | 2.639(3) | 3.560(8) | 171.09 |
| | C27-H27···O7 | 0.930(5) | 2.504(3) | 3.376(5) | 156.31 |
| | C36-H36···O4 | 0.930(3) | 2.868(2) | 3.717(4) | 152.34 |
| **5** | **2h** | | | | |
| | C31-H31···O2 | 0.930(2) | 2.366(3) | 2.691(2) | 100.81 |
| | C20-H20···N8 | 0.930(2) | 2.638(1) | 3.481(2) | 151.04 |
| | C12-H12···O2 | 0.930(2) | 2.393(2) | 3.164(2) | 140.26 |
| | C8-H8B···N5 | 0.970(2) | 2.920(9) | 3.316(2) | 109.35 |
| | N1-H1···O1 | 0.860(8) | 1.908(7) | 2.765(1) | 174.46 |
| | N5-H5A···O1 | 0.860(9) | 1.977(1) | 2.798(2) | 159.40 |
| | O7-H7···O6 | 0.820(4) | 1.861(1) | 2.398(4) | 121.90 |
| | N4-H4B···N6 | 0.860(1) | 1.917(9) | 2.704(2) | 151.57 |
| | C9-H9B···O6 | 0.970(1) | 2.658(2) | 3.579(2) | 158.61 |
| | C14-H14···N2 | 0.930(1) | 2.793(1) | 3.602(2) | 145.95 |
| | C17-H17A···O6 | 0.970(1) | 2.963(4) | 3.735(2) | 137.33 |
| | C5-H5···N8 | 0.930(2) | 2.727(1) | 3.625(2) | 162.52 |
| | C4-H4···N5 | 0.930(1) | 2.985(9) | 3.545(2) | 120.17 |
| | C23-H23···O2 | 0.930(1) | 2.891(1) | 3.489(2) | 123.95 |
| | C17-H17B···O6 | 0.970(1) | 2.536(4) | 3.308(2) | 136.33 |
| | C33-H33B···N5 | 0.960(2) | 2.827(9) | 3.700(3) | 151.62 |
| **6.** | **2i** | | | | |
| | N1-H1···O1 | 0.860(4) | 2.823(5) | 3.592(6) | 136.11 |
| | N2-H1···O2 | 0.860(4) | 1.913(2) | 2.743(4) | 161.76 |

| | | | | | |
|---|---|---|---|---|---|
| | N3-H3···O2 | 0.860(4) | 2.018(4) | 2.830(6) | 157.17 |
| | N6-H6···O2 | 0.860(5) | 2.019(2) | 2.852(6) | 162.82 |
| | C2-H2···O1 | 0.930(6) | 2.726(4) | 3.513(7) | 142.96 |
| | C27-H27···N3 | 0.930(5) | 2.650(4) | 3.507(6) | 153.53 |
| | N5-H5···N2 | 0.860(5) | 1.917(5) | 2.765(7) | 168.30 |
| | N2-H2···N5 | 0.860(4) | 1.974(5) | 2.765(7) | 153.31 |
| | C8-H8A···O3 | 0.970(5) | 2.913(1) | 3.766(1) | 147.27 |
| | C17-H17B···O3 | 0.970(6) | 2.571(8) | 3.375(1) | 140.26 |
| | C17-H17B···O4 | 0.970(5) | 2.302(8) | 3.069(1) | 135.44 |
| | C20-H20···O1 | 0.930(7) | 2.482(5) | 3.334(9) | 152.29 |
| | C28-H28···N4 | 0.970(7) | 2.959(5) | 3.685(2) | 136.00 |
| | C29-H29A···O3 | 0.960(2) | 2.809(8) | 3.755(2) | 168.48 |
| | C29-H29B···O1 | 0.960(2) | 2.569(5) | 3.477(1) | 157.75 |
| **7.** | **2j** | | | | |
| | N2-H2A···O1 | 0.860(3) | 1.817(2) | 2.909(3) | 175.11 |
| | N3-H5A···O1 | 0.860(2) | 2.074(2) | 2.909(3) | 163.61 |
| | N3-H5A···N8 | 0.860(2) | 2.753(2) | 3.354(4) | 128.25 |
| | N5-H5Z···O1 | 0.767(3) | 2.227(3) | 2.944(3) | 156.08 |
| | N5-H5Z···N8 | 0.767(3) | 2.587(3) | 3.155(3) | 132.35 |
| | N4-H4A···O8 | 0.860(3) | 1.851(4) | 2.685(5) | 162.98 |
| | C12-H12···N8 | 0.930(4) | 2.733(2) | 3.397(4) | 129.03 |
| | C27-H27···O2 | 0.930(3) | 2.578(2) | 3.493(3) | 167.77 |
| | C3-H3···N6 | 0.930(3) | 2.929(2) | 3.567(4) | 126.03 |
| | C29-H29···O4 | 0.930(4) | 2.638(5) | 3.544(6) | 164.32 |
| | C15-H15···O2 | 0.930(4) | 2.817(2) | 3.728(5) | 166.73 |
| | O8-2W···O2 | 0.970(5) | 1.581(5) | 2.747(4) | 178.64 |
| | C34-H34C···O7 | 0.960(2) | 2.917(2) | 3.787(2) | 151.20 |
| **8.** | **2k** | | | | |
| | C21-H21···O4 | 0.930(3) | 2.587(2) | 3.360(3) | 140.78 |
| | C31-H31A···O5 | 0.970(2) | 2.506(3) | 3.277(3) | 136.38 |
| | N5-H4B'···O3 | 0.927(3) | 1.903(2) | 2.828(3) | 175.42 |

| | | | | | |
|---|---|---|---|---|---|
| | N7-H2B'···O3 | 0.853(3) | 2.047(3) | 2.896(2) | 173.83 |
| | N7-H2B'··O4 | 0.853(3) | 2.861(3) | 3.519(3) | 135.25 |
| | N8-H1B···O3 | 0.886(2) | 1.863(2) | 2.748(2) | 175.76 |
| | C5-H5···O1 | 0.930(2) | 2.618(2) | 3.244(3) | 125.18 |
| | C12-H12···N1 | 0.930(2) | 2.590(2) | 3.476(3) | 159.95 |
| | C5-H5···N6 | 0.930(2) | 2.698(2) | 3.672(3) | 151.37 |
| | O2-H2···N6 | 0.820(2) | 1.870(2) | 2.674(2) | 166.26 |
| | C31-H31B···O5 | 0.970(2) | 2.807(3) | 3.543(4) | 133.32 |
| | C15-H15B···O5 | 0.970(2) | 2.619(3) | 3.526(4) | 168.38 |
| | N9-H3B'···N4 | 0.927(3) | 1.724(3) | 2.732(3) | 168.22 |
| | C26-H26··O1 | 0.930(3) | 2.782(8) | 3.600(4) | 134.63 |
| **9.** | **2l** | | | | |
| | C2-H2···O4 | 0.930(3) | 2.855(3) | 3.570(4) | 134.62 |
| | C9-H9A···O9 | 0.970(2) | 2.369(2) | 3.092(3) | 130.87 |
| | C8-H8B···O9 | 0.970(3) | 2.947(3) | 3.779(4) | 144.48 |
| | N1-H1···N4 | 0.860(2) | 2.116(2) | 2.895(2) | 150.35 |
| | C9-H9B···O9 | 0.970(3) | 2.444(3) | 3.270(4) | 142.81 |
| | N9-H9···O3 | 0.860(3) | 1.765(3) | 2.598(5) | 162.36 |
| | N9-H9···O4 | 0.860(3) | 2.786(3) | 3.356(4) | 125.20 |
| | N4-H4A···N1 | 0.860(2) | 2.037(2) | 2.895(3) | 175.15 |
| | N6-H6···O6 | 0.860(2) | 2.824(2) | 3.536(3) | 141.26 |
| | N3-H3B···O6 | 0.860(2) | 1.887(2) | 2.701(3) | 157.38 |
| | N2-H2B···O6 | 0.860(2) | 2.111(2) | 2.837(3) | 141.79 |
| | N3-H3B···O5 | 0.860(2) | 2.822(3) | 3.532(4) | 140.97 |
| | N6-H6···O5 | 0.860(2) | 2.033(2) | 2.807(3) | 149.32 |
| | C39-H38A···O6 | 0.960(4) | 2.940(2) | 3.740(3) | 141.63 |
| | C39-H39B···O7 | 0.960(4) | 2.872(3) | 3.783(3) | 158.78 |
| | N5-H5B···O2 | 0.860(2) | 1.833(2) | 2.667(3) | 162.91 |
| | N5-H5B···O1 | 0.860(2) | 2.687(4) | 3.394(4) | 140.42 |
| | C17-H17B···O1 | 0.970(3) | 2.422(2) | 3.349(4) | 159.79 |
| | N8-H8···O7 | 0.860(3) | 1.859(2) | 2.669(3) | 156.53 |

| | | | | | |
|---|---|---|---|---|---|
| | C14-H14···O9 | 0.930(3) | 2.762(2) | 3.667(3) | 164.53 |
| | C40-H40B···O9 | 0.930(3) | 2.762(2) | 3.667(3) | 164.53 |
| **10** | **2n** | | | | |
| | C24-H24···N7 | 0.930(4) | 2.941(2) | 3.399(4) | 111.87 |
| | C38-H38···O5 | 0.930(4) | 2.668(2) | 3.209(4) | 114.90 |
| | C2-H2···O12 | 0.930(4) | 2.727(3) | 3.606(5) | 156.61 |
| | C14-H14···O1 | 0.930(3) | 2.477(2) | 3.210(4) | 135.83 |
| | C15-H15···O11 | 0.930(4) | 2.792(3) | 3.575(5) | 140.56 |
| | C4-H4···O4 | 0.930(4) | 2.513(2) | 3.325(5) | 144.02 |
| | C5-H5···O9 | 0.930(4) | 2.558(2) | 3.423(4) | 153.52 |
| | C9-H9A···O10 | 0.970(4) | 2.509(2) | 3.261(5) | 132.43 |
| | C9-H9A···O11 | 0.970(4) | 2.509(2) | 3.621(5) | 128.33 |
| | N2-H2A···O10 | 0.860(3) | 1.862(2) | 2.701(4) | 163.05 |
| | C17-H17···O7 | 0.930(4) | 2.600(3) | 3.395(5) | 141.68 |
| | C10-H10A···O8 | 0.970(4) | 2.590(2) | 3.180(4) | 117.22 |
| | N4-H4B···O7 | 0.860(3) | 2.870(2) | 3.515(4) | 130.62 |
| | N4-H4B···O8 | 0.860(3) | 1.990(2) | 2.828(4) | 162.92 |
| | C22-H22···O6 | 0.930(4) | 2.893(3) | 3.696(5) | 143.55 |
| | O4-H4A···O7 | 0.820(3) | 1.874(3) | 2.629(4) | 150.82 |
| | C30-H30···O1 | 0.930(3) | 2.457(2) | 3.150(4) | 128.62 |
| | C30-H30···O5 | 0.930(3) | 2.368(2) | 3.102(4) | 133.11 |
| | C23-H23···O3 | 0.930(3) | 2.763(3) | 3.648(4) | 158.28 |
| | C24-H24···O2 | 0.930(2) | 2.774(2) | 3.490(4) | 134.27 |
| **11** | **2p** | | | | |
| | C9-H9A···O13 | 0.970(2) | 2.830(2) | 3.742(5) | 156.14 |
| | C20-H20···O11 | 0.930(2) | 2.824(2) | 3.524(5) | 132.65 |
| | N2-H2B···O3 | 0.860(2) | 1.821(1) | 2.677(2) | 173.68 |
| | N3-H3B···O5 | 0.860(2) | 1.874(2) | 2.715(3) | 163.93 |
| | N3-H3B···O6 | 0.860(2) | 2.927(1) | 3.579(2) | 131.63 |
| | C13-H13···O1 | 0.930(2) | 2.823(2) | 3.625(3) | 143.17 |
| | C13-H13···O6 | 0.930(2) | 2.626(2) | 3.427(3) | 142.69 |

| | | | | | |
|---|---|---|---|---|---|
| | C14-H14···O2 | 0.930(2) | 2.885(2) | 3.664(3) | 140.28 |
| | C3-H3···O11 | 0.930(3) | 2.766(2) | 3.615(3) | 150.69 |
| | C8-H8B···O14 | 0.970(2) | 2.996(4) | 3.945(4) | 166.12 |
| | C9-H9B···O11 | 0.970(3) | 2.723(2) | 3.499(3) | 137.44 |
| | C10-H10B···O12 | 0.970(3) | 2.662(3) | 3.579(4) | 157.05 |
| | C20-H20···O15 | 0.930(2) | 2.905(3) | 3.388(5) | 113.74 |
| | C21-H21···O15 | 0.930(2) | 2.455(4) | 3.175(5) | 134.22 |
| | C16-H16···O8 | 0.930(2) | 2.598(2) | 3.378(3) | 141.41 |
| | C28-H28···O15 | 0.930(3) | 2.844(4) | 3.668(5) | 148.39 |
| | C27-H27···O12 | 0.930(2) | 2.869(2) | 3.711(3) | 151.19 |
| **12** | **2r** | | | | |
| | C5-H5···O9 | 0.930(4) | 2.520(3) | 3.393(5) | 156.33 |
| | C35-H35C···O8 | 0.960(6) | 2.799(2) | 3.595(5) | 140.78 |
| | C8-H8B···O3 | 0.970(3) | 2.477(3) | 3.265(4) | 138.24 |
| | O9-H9··O4 | 0.820(4) | 1.952(2) | 2.769(3) | 174.48 |
| | N2-H2B··O3 | 0.860(2) | 1.941(4) | 2.727(4) | 151.21 |
| | N3-H3B···O5 | 0.974(38) | 1.762(38) | 2.711(3) | 163.59 |
| | C12-H12A···O5 | 0.970(3) | 2.772(2) | 3.523(4) | 134.74 |
| | C16-H16···O6 | 0.930(2) | 2.767(2) | 3.621(4) | 153.27 |
| | C9-H9A···N2 | 0.970(2) | 2.735(2) | 3.582(4) | 146.12 |
| | C8-H8A···O7 | 0.970(3) | 2.484(3) | 3.293(4) | 140.73 |
| | C9-H9B···O8 | 0.970(3) | 2.812(2) | 3.598(4) | 138.69 |
| | C9-H9B···O4 | 0.970(3) | 2.661(2) | 3.545(4) | 151.59 |
| | C19-H19···N5 | 0.930(4) | 2.980(2) | 3.843(4) | 154.96 |
| | C13-H13A···O1 | 0.970(3) | 2.847(2) | 3.558(4) | 130.86 |
| | C13-H13B···O6 | 0.970(3) | 2.850(2) | 3.786(4) | 162.22 |
| | C3-H3···O1 | 0.930(3) | 2.654(2) | 3.465(4) | 146.06 |
| | C24-H24···O6 | 0.930(3) | 2.816(2) | 3.528(3) | 134.12 |
| | C31-H31···O9 | 0.930(3) | 2.433(3) | 3.363(5) | 177.32 |

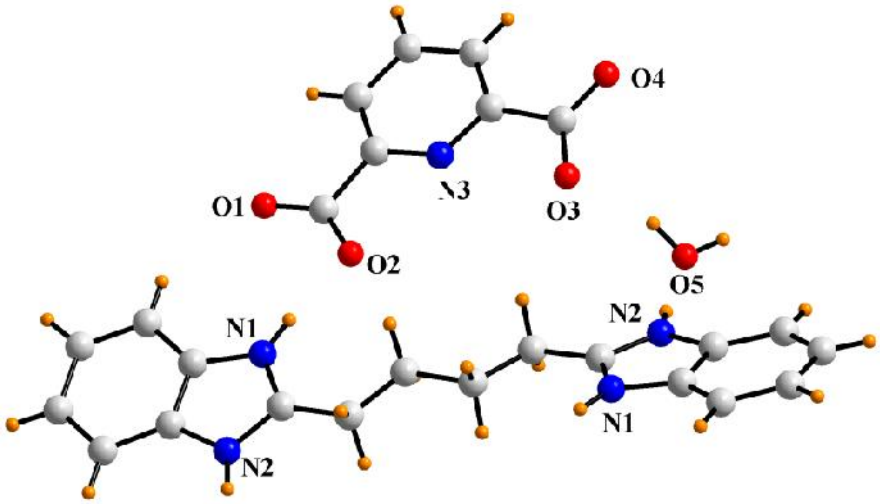


**Fig. 2.15** Crystal structure of $[(H_4BBBu)^{2+}.(2,6\text{-}PDCA)^{2-}.H_2O]$ **2d**. Color code: C, grey; N, blue; O, red

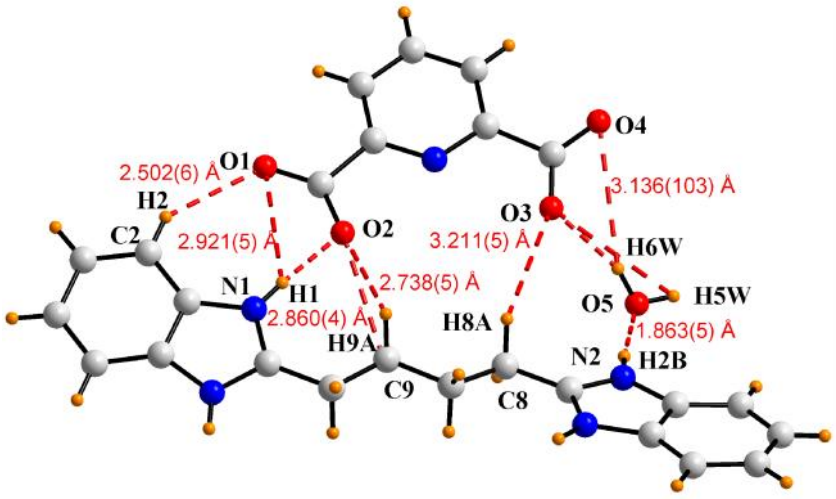


**Fig. 2.16** Various non-covalent interactions in **2d**. Color code: C, grey; N, blue; O, red

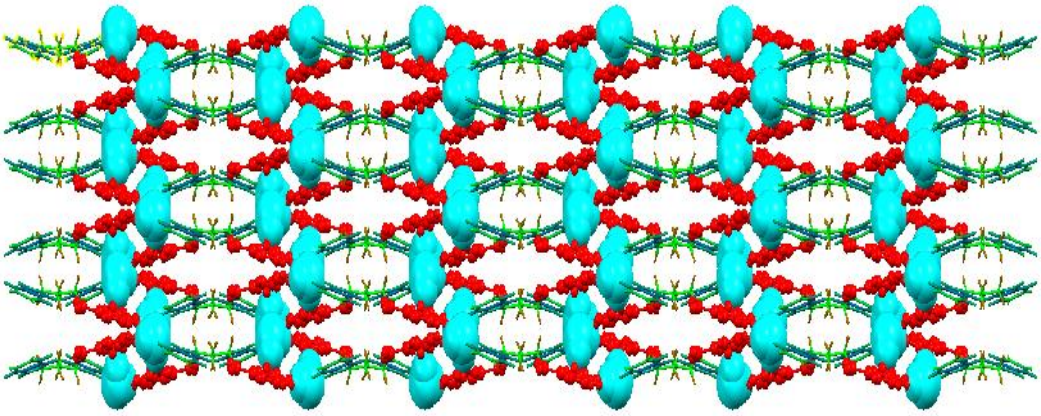

**Fig. 2.17** Three dimensional host-guest supramolecular architecture in **2d.** Color code: $(H_4BBBu)^{2+}$, green; $(2,6\text{-}PDCA)^{2-}$, red; $H_2O$, cyan

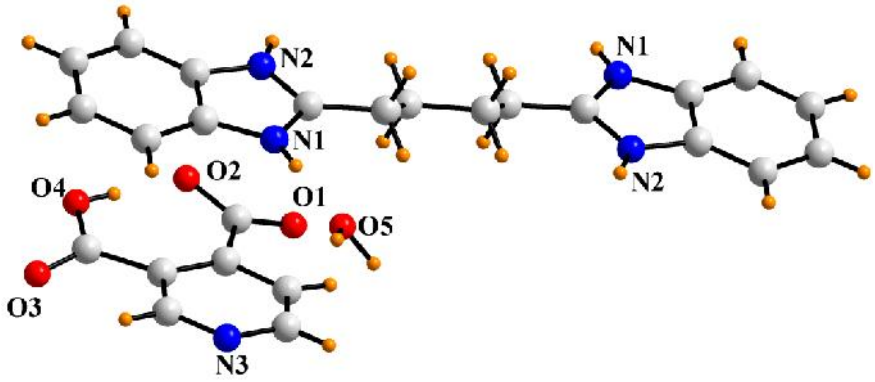


**Fig. 2.18** Crystal structure of $[(H_4BBBu)^{2+}.2(3,4\text{-}PDCAH)^{-}.2H_2O]$ **2e**. Color code: C, grey; O, red; N, blue

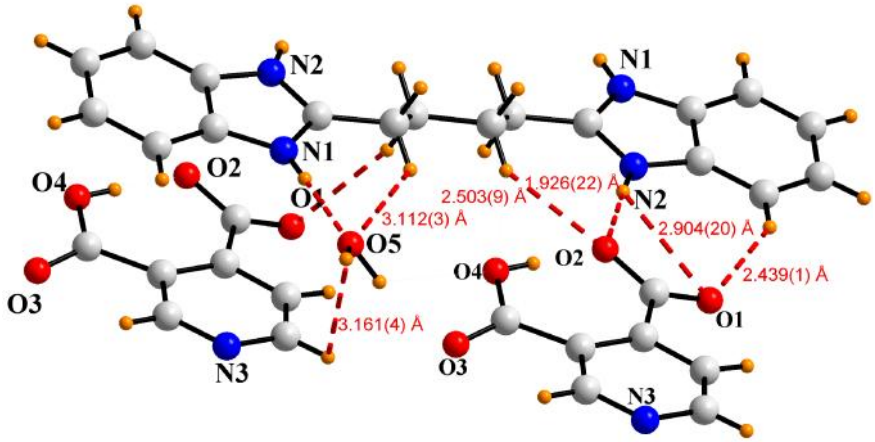


**Fig. 2.19** Various N-H···O, C-H···O and O-H···O non-covalent interactions in **2e.** Color code: C, grey; H, orange; O, red; N, blue

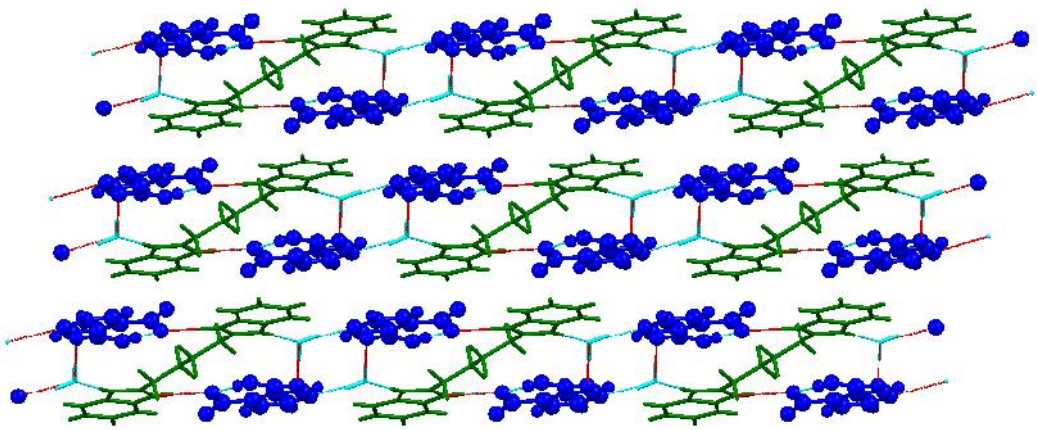

**Fig. 2.20** Three dimensional host-guest supramolecular architecture with guest anionic molecule in **2e.** Color code: $(H_4BBBu)^{2+}$, green; $(3,4\text{-PDCAH})^{-}$, blue; $H_2O$, cyan

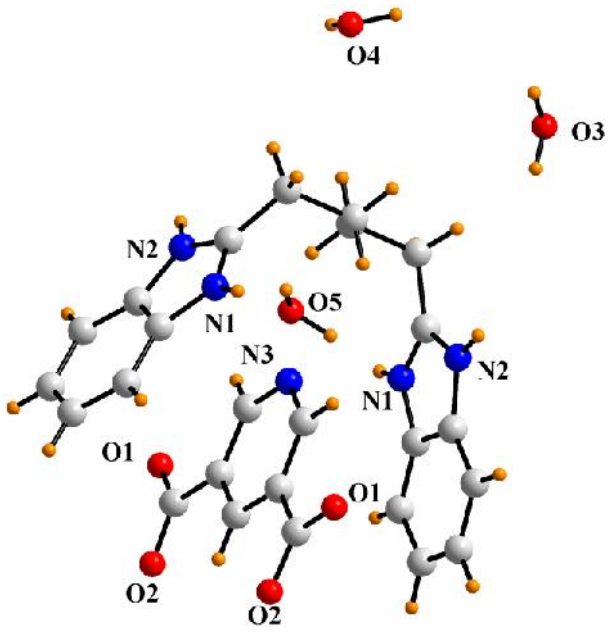


**Fig. 2.21** Crystal structure of $[(H_4BBBu)^{2+}.(3,5\text{-PDCA})^{2-}.3H_2O]$ **2f**. Color code: C, grey; H,orange; O, red; N, blue

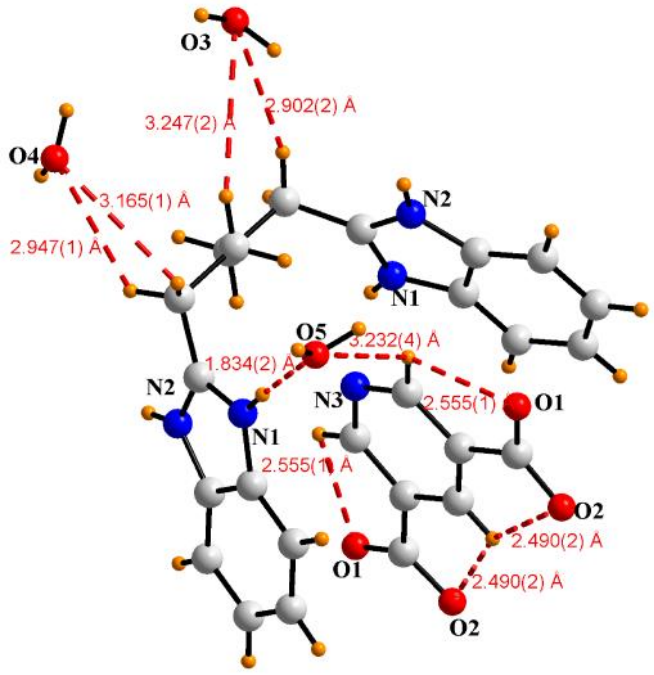


**Fig. 2.22** N-H···O, C-H···O and O-H···O interactions in **2f.** Color code: C, grey; H, orange; O, red; N, blue

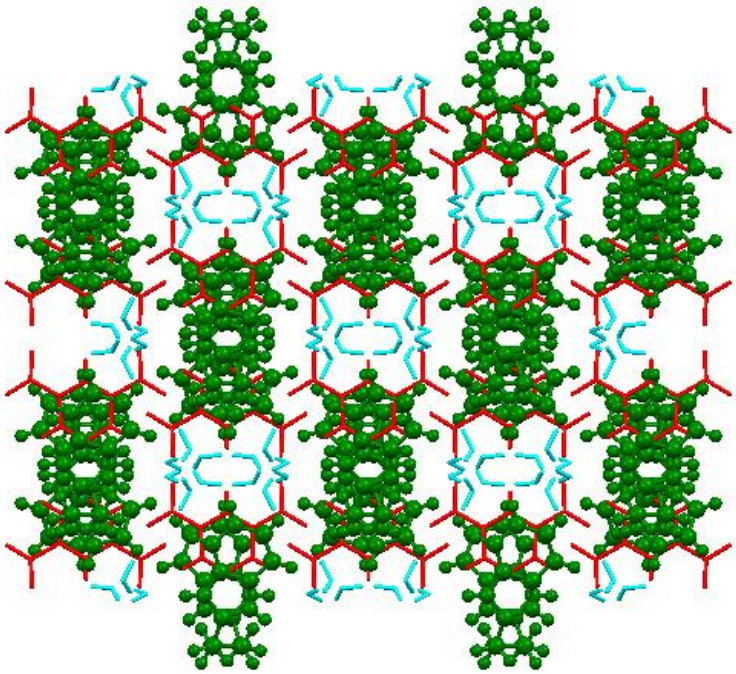

**Fig. 2.23** Three dimensional packing in **2f**. Color code: $(H_4BBBu)^{2+}$, green; $(3,5\text{-}PDCA)^{2-}$, red; $H_2O$, light blue

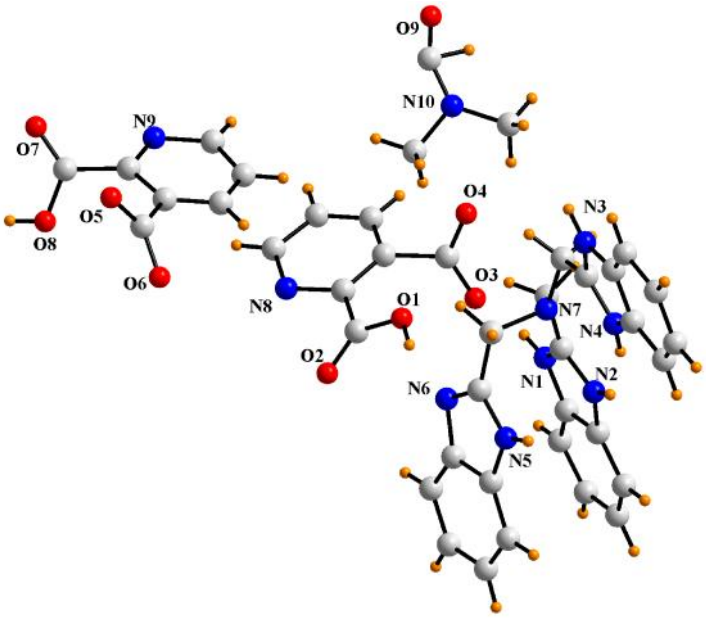


**Fig. 2.24** Crystal structure of $[(H_5NTB)^{2+}.2(2,3\text{-}PDCAH)^{-}.DMF]$ **2g**. Color code: C, grey; O, red; N, blue

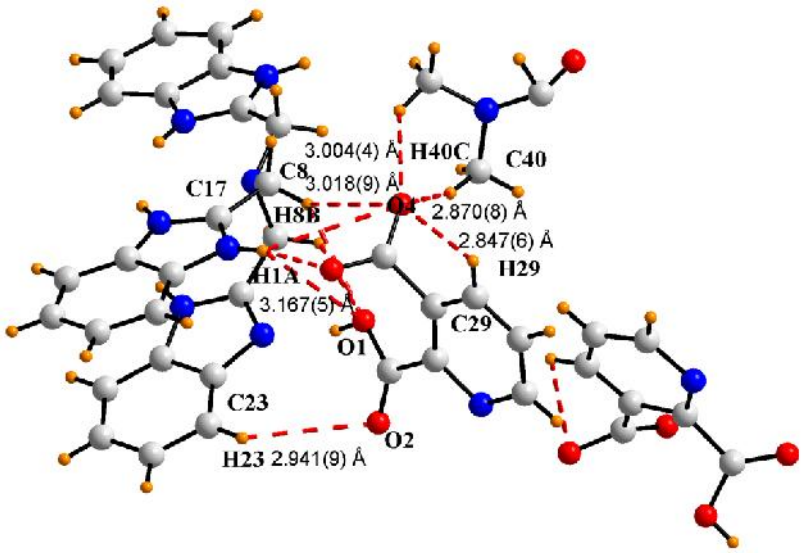


**Fig. 2.25** Various N-H···O, C-H···O and O-H···O non-covalent interactions in **2g.** Color code: C, grey; H, orange; O, red; N, blue

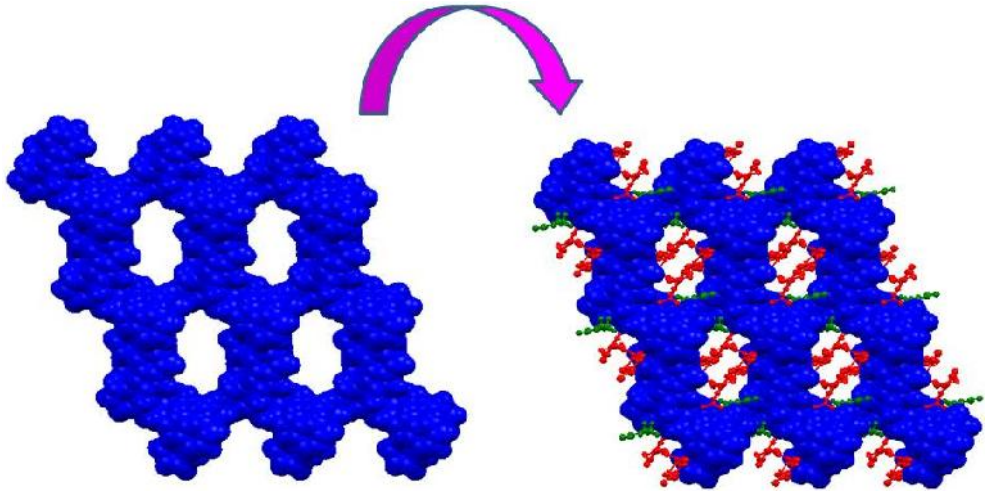

**(a)** **(b)**

**Fig. 2.26 (a)** Three dimensional host-guest supramolecular architecture without guest, **(b)** with guest in **2g**. Color code: $(H_5NTB)^{2+}$, blue; $(2,3\text{-}PDCAH)^-$, red; DMF, green

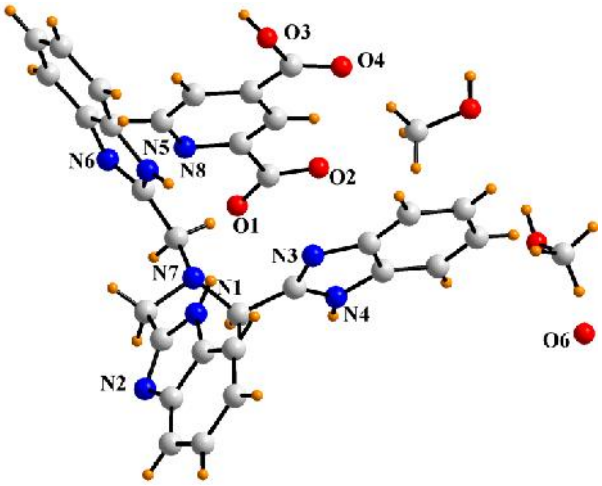


**Fig. 2.27** Crystal structure of $[(H_4NTB)^+.(2,4\text{-}PDCH)^-.2CH_3OH.H_2O]$ **2h**. Color code: C, grey; H, orange; O, red; N, blue

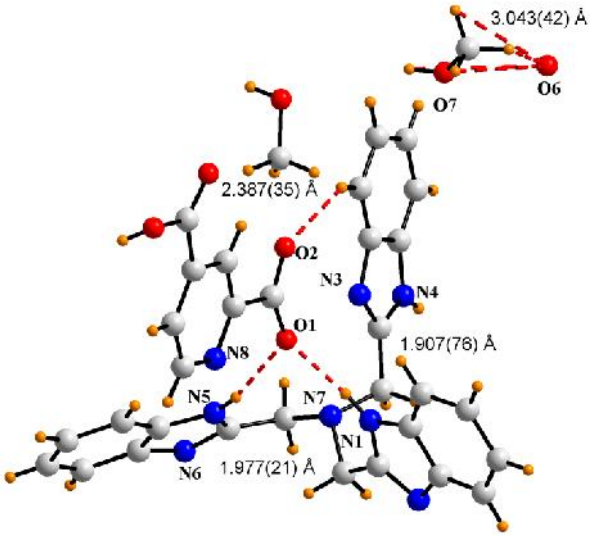


**Fig. 2.28** Different non-covalent interactions in **2h** Color code: C, grey; H, orange; O, red; N, blue

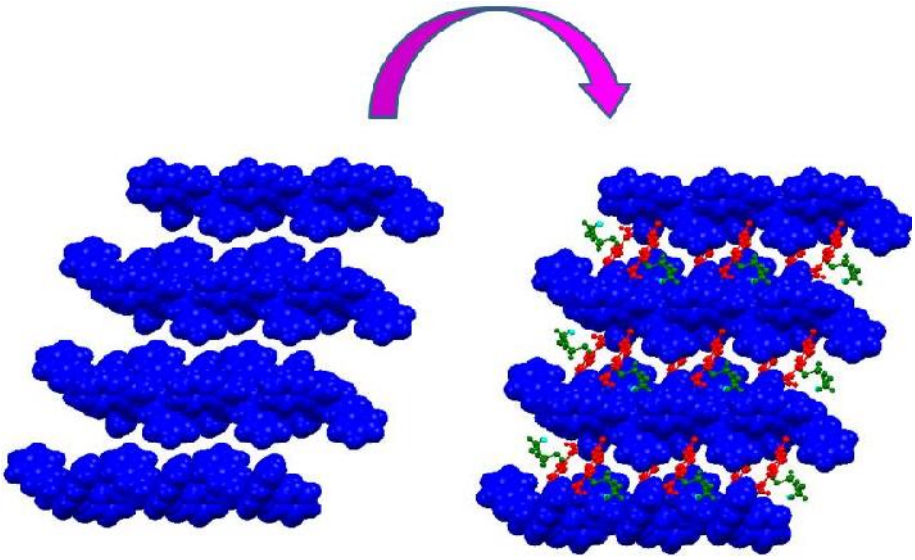

**Fig. 2.29** Alternate channels of host framework formed by the self-assembly of the cationic protonated ligand with guest pyridine-3,4-dicarboxylate anions in salt **2h.** Color code: $(H_4NTB)^+$, blue; $(2,4\text{-}PDCH)^-$, red; $CH_3OH$, green

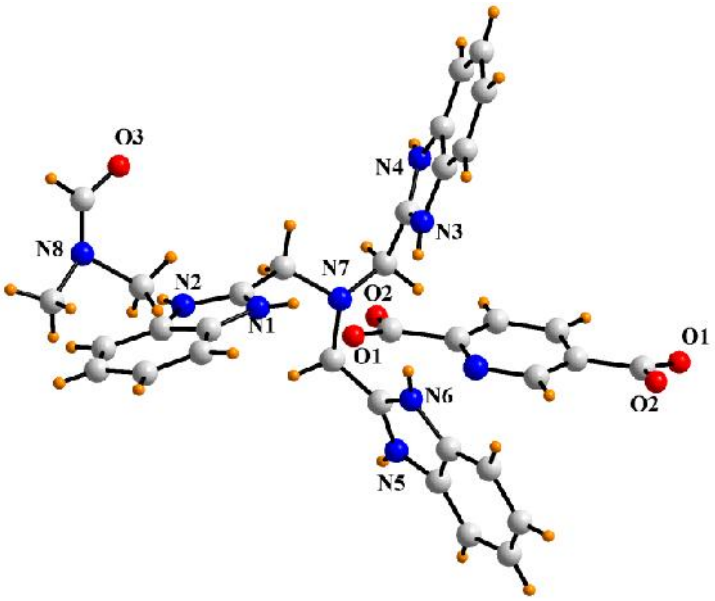


**Fig. 2.30** Crystal structure of $[(H_5NTB)^{2+}.(2,5\text{-}PDCA)^{2-}.DMF]$ **2i**. Color code: C, grey; H, orange; O, red; N, blue

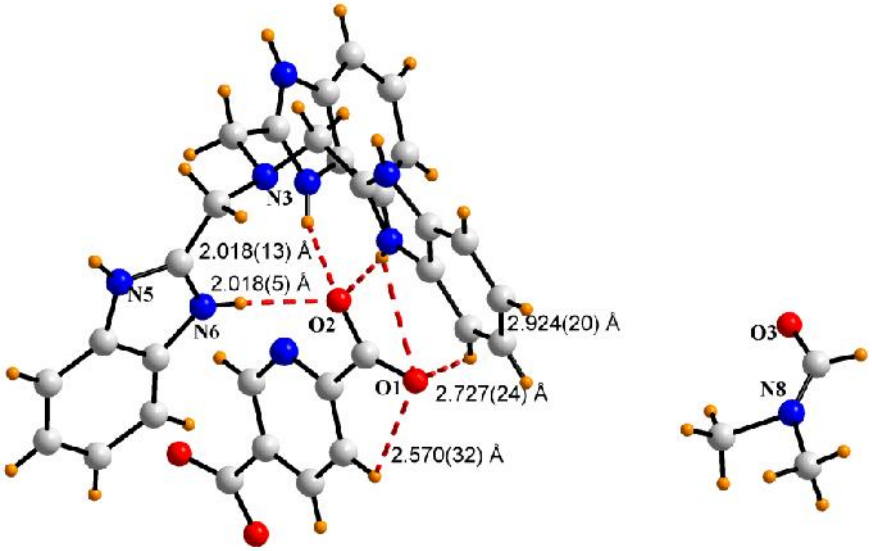


**Fig. 2.31** Various non-covalent interactions in **2i.** Color code: C, grey; H, orange; O, red; N, blue

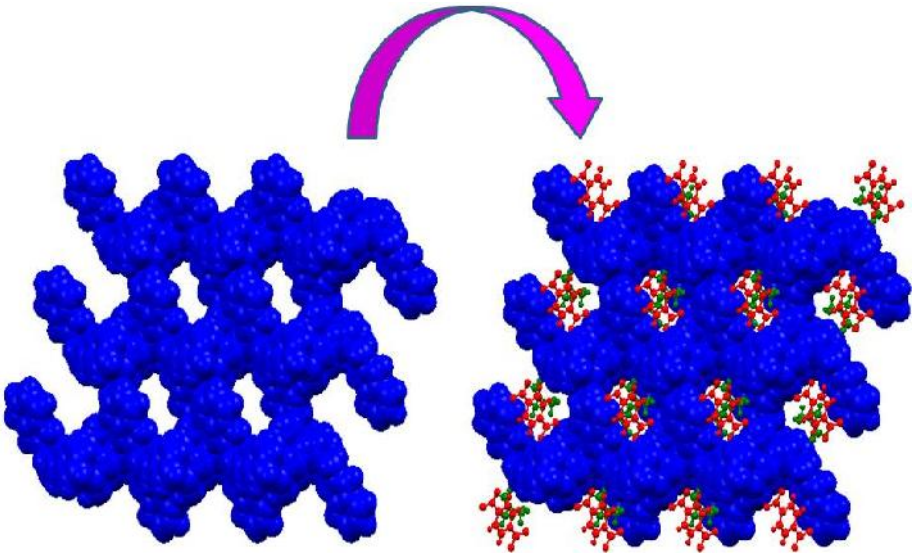

**(a)** **(b)**

**Fig. 2.32 (a)** Three dimensional host-guest supramolecular architecture without guest, **(b)** with guest molecule in **2i**. Color code: $(H_5NTB)^{2+}$, blue; $(2,5\text{-}PDCA)^{2-}$, red; DMF, greeen

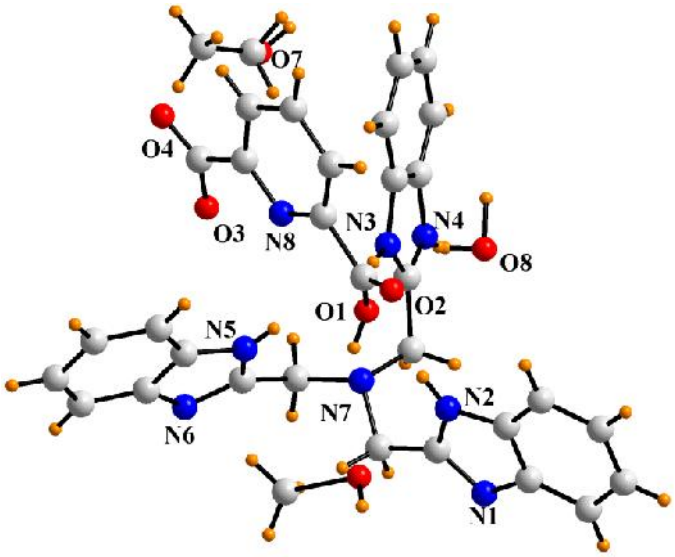


**Fig. 2.33** Crystal structure of $[(H_4NTB)^{+}.(2,6\text{-}PDCAH)^{-}.C_2H_5OH.CH_3OH.H_2O]$ **2j**. Color code: C, grey; H, orange; O, red; N, blue

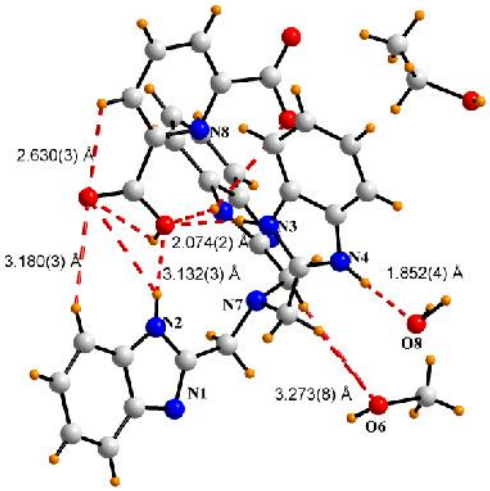


**Fig. 2.34** Various N-H···O and C-H···O interactions in **2j.** Color code: C, grey; H, orange; O, red; N, blue

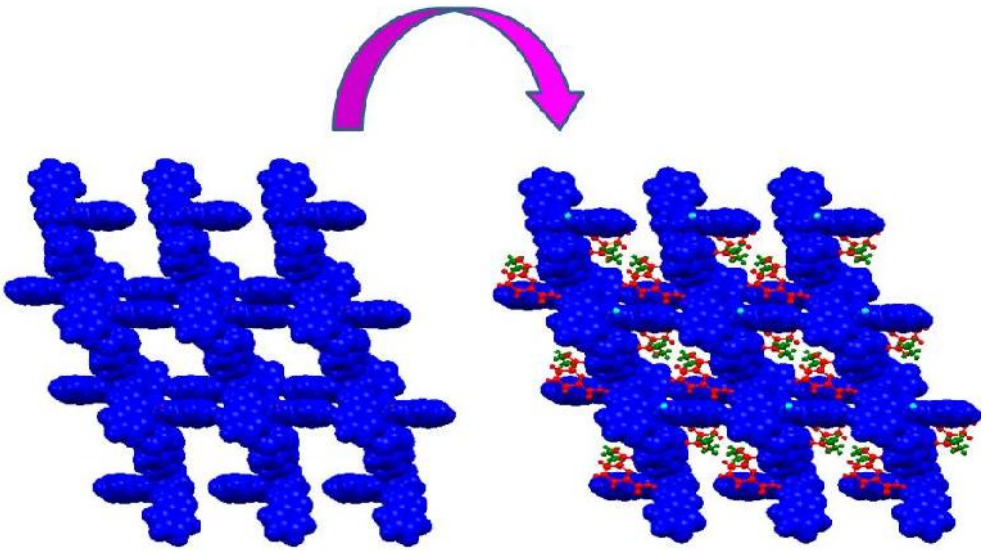

**Fig. 2.35 (a)** Three dimensional host-guest supramolecular architecture without guest, **(b)** with guest in **2j**. Color code: $(H_4NTB)^+$, blue; $(2,6\text{-}PDCAH)^-$, red; $C_2H_5OH$.& $CH_3OH$, green; $H_2O$, cyan

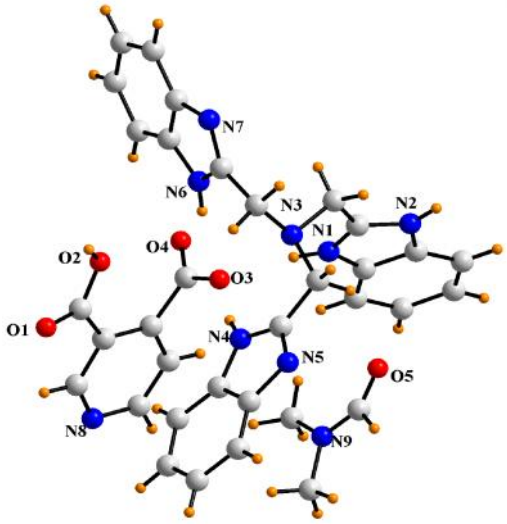


**Fig. 2.36** Crystal structure of $[(H_5NTB)^{2+}.(3,4\text{-}PDCA)^{-}.DMF\ ]$ **2k**. Color code: C, grey; H, orange; O, red; N, blue

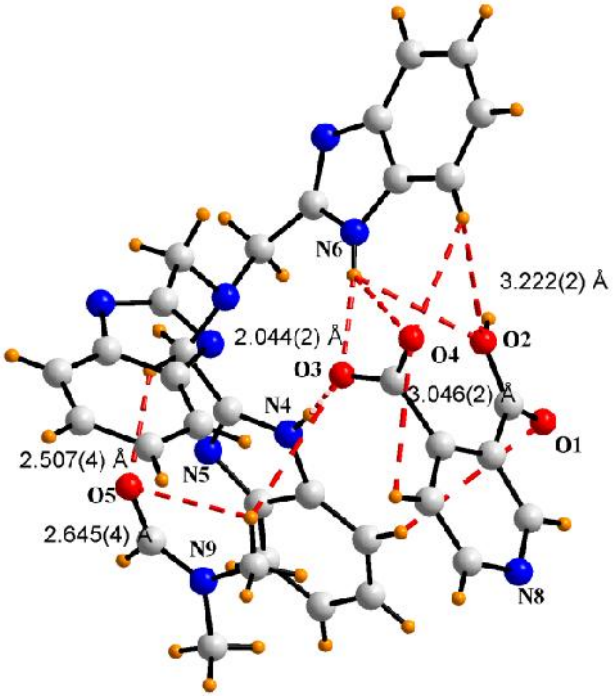


**Fig. 2.37** Various non-covalent interactions in **2k.** Color code: C, grey; H, orange; O, red; N, blue

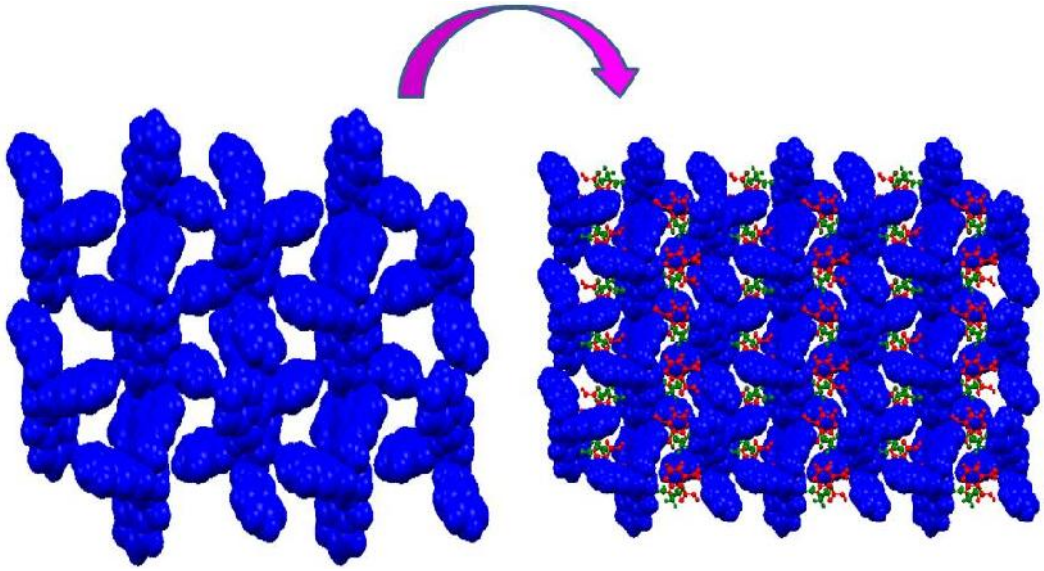

**(a)** **(b)**

**Fig. 2.38 (a)** Three dimensional host-guest supramolecular architecture without guest, **(b)** with guest in **2k**. Color code: $(H_5NTB)^{2+}$, blue; $(3,4\text{-PDCA})^{-}$, red; DMF, green

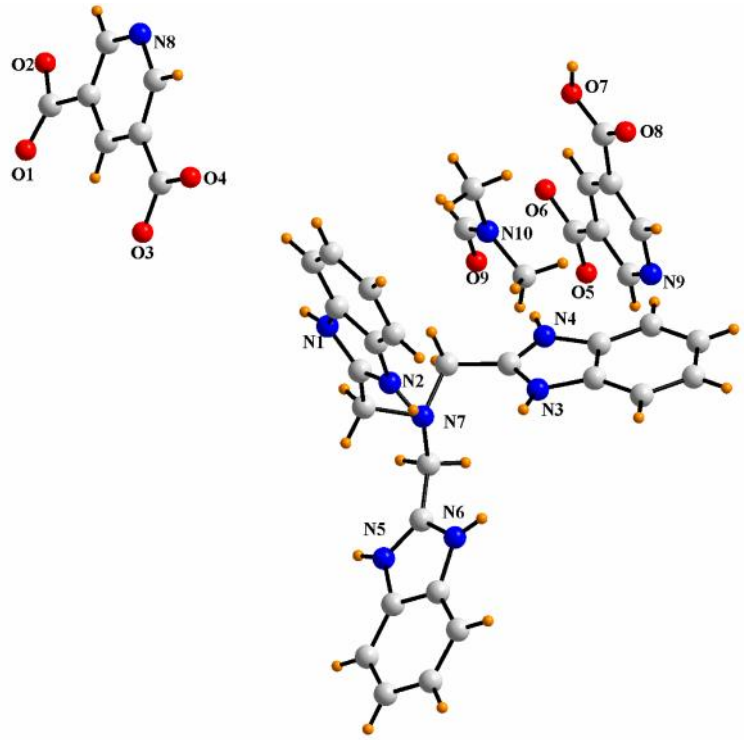


**Fig. 2.39** Crystal structure of $[(H_6NTB)^{3+}.(3,5\text{-PDCA})^{2-}.(3,5\text{-PDCAH})^{-}.DMF]$ **2l**. Color code: C, grey; H, orange; O, red; N, blue

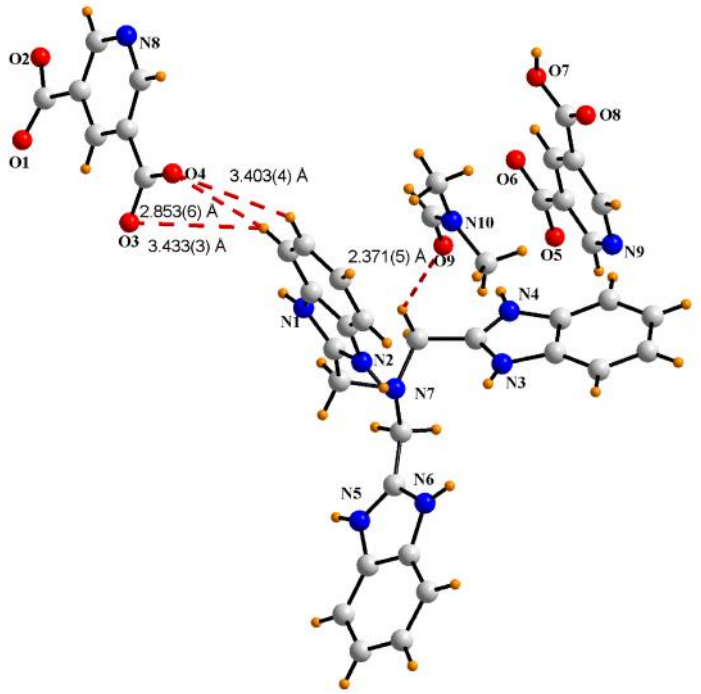


**Fig. 2.40** Different non-covalent interactions in **2l**. Color code: C, grey; O, red; N, blue

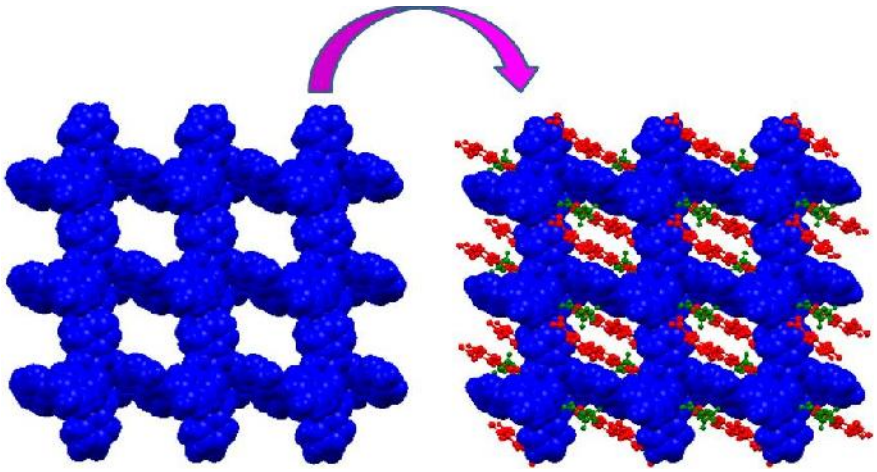

**(a)** **(b)**

**Fig. 2.41 (a)** Cavity designed by the ligand **(b)** entrapping pyridine-3,5-dicarboxylate anion and DMF molecules in **2l**. Color code: $(H_6NTB)^{3+}$, blue; $(3,5\text{-}PDCA)^{2-}$ and $(3,5\text{-}PDCAH)^{-}$, red; DMF, green

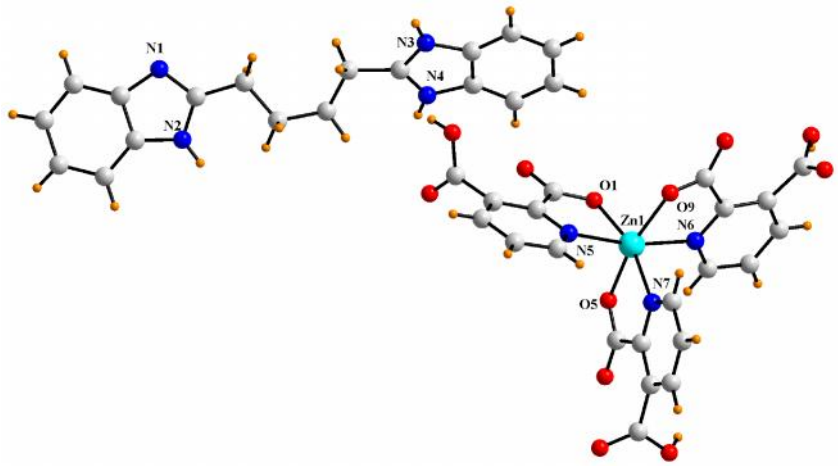


**Fig. 2.42** Crystal Structure of $(H_3BBBu)^+[Zn(2,3\text{-}PDCAH)_3]^-$ **2n**. Color code: C, grey; N, blue; O, red; Zn, cyan

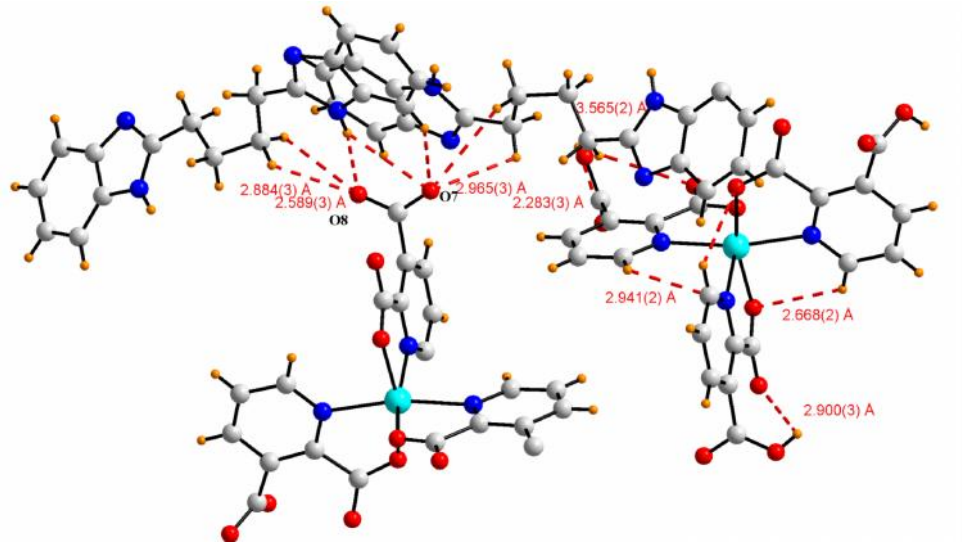


**Fig. 2.43** Different non-covalent interactions in **2n** Color code: C, grey; N, blue; H, orange; O, red; Zn, Cyan

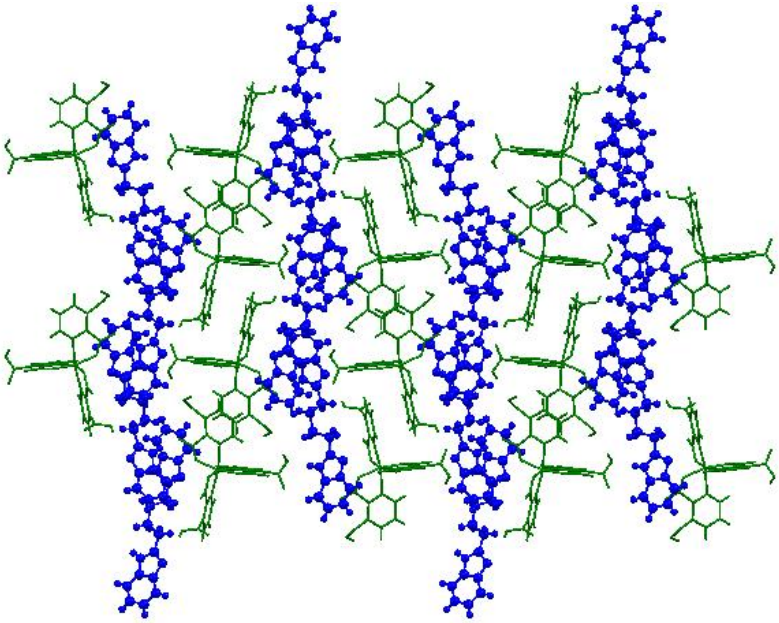

**Fig 2.44** 3D packing diagram of **2n** viewed down along *a*-axis

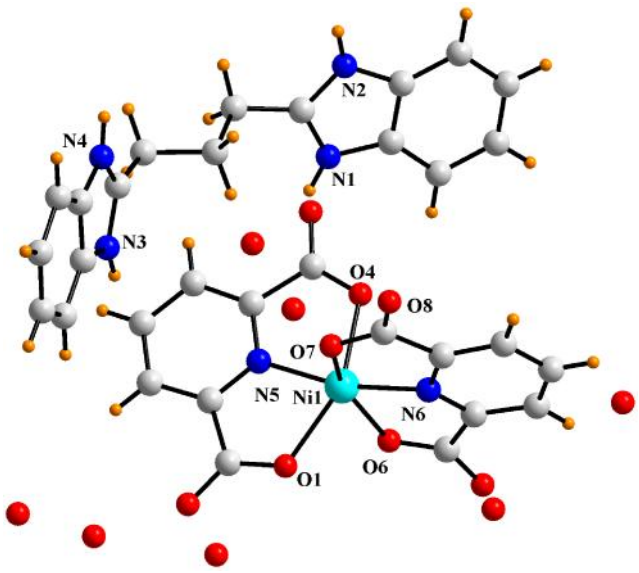


**Fig. 2.45** Crystal Structure of $(H_4BBPr)^{2+}[Ni(2,6\text{-}PDCA)_2]^{2-}.7H_2O$ **2p**. Color code: C, grey; N, blue; O, red; Ni, cyan

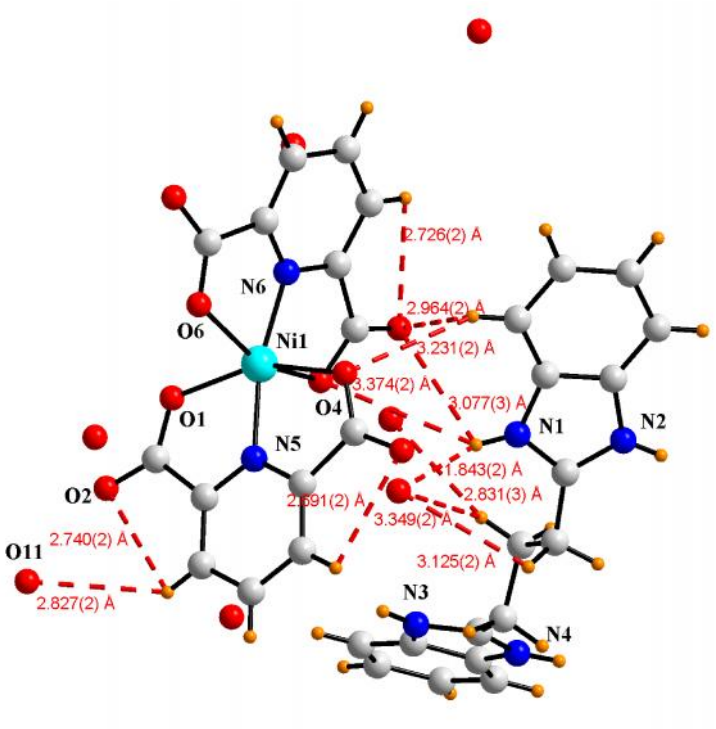


**Fig. 2.46** Different non-covalent interactions in **2p** Color code: C, grey; N, blue; H, orange; O, red; Ni, cyan

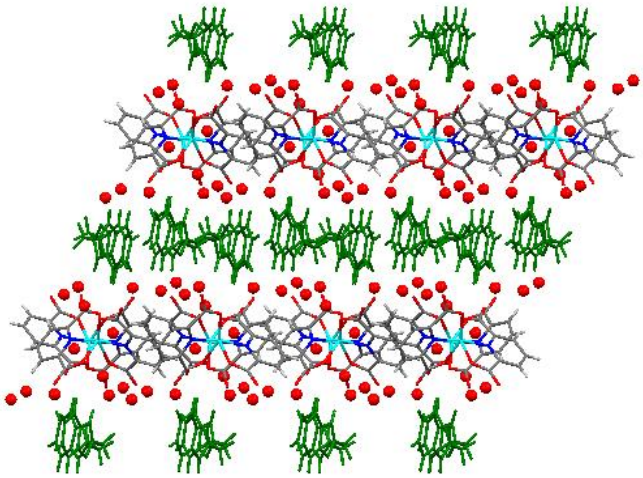

**Fig.2.47** 3D packing diagram of **2p** viewed down along *b*-axis

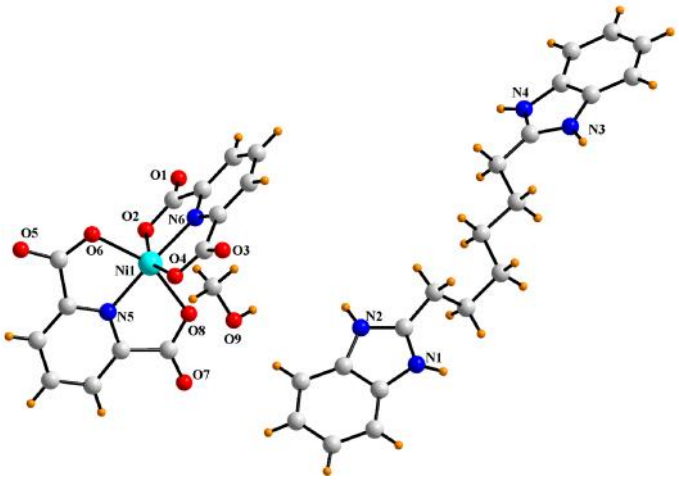


**Fig. 2.48** Crystal Structure of $(H_4BBHex)^{2+}[Ni(2,6\text{-}PDCA)_2]^{2-}.CH_3OH$ **2r**. Color code: C, grey; N, blue; H, orange; O, red; Ni, cyan

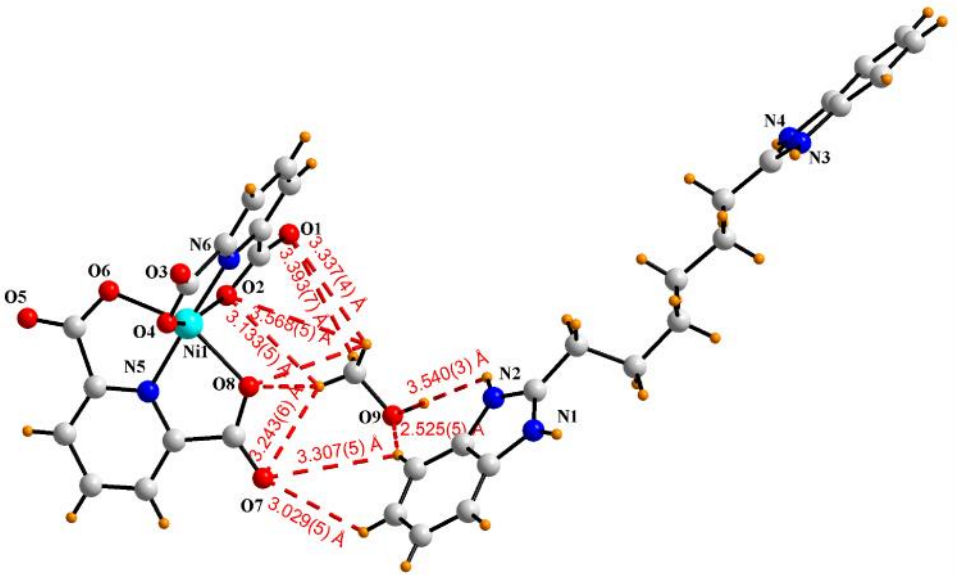


**Fig. 2.49** Different non-covalent interactions in **2r** Color code: C, grey; N, blue; O, red; Ni, cyan

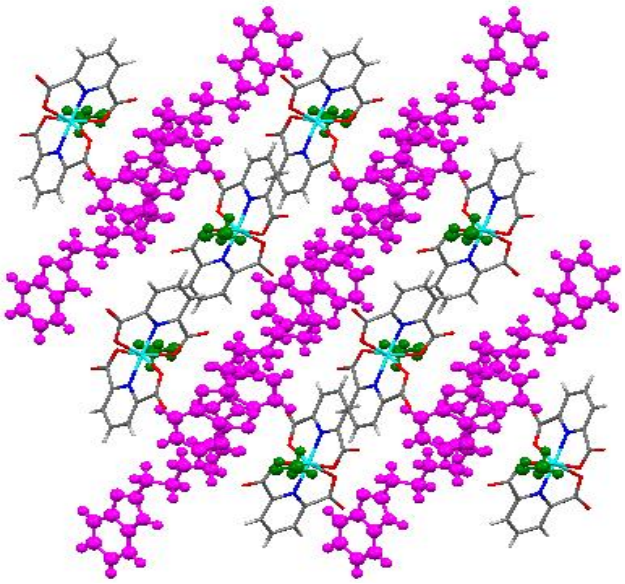

**Fig 2.50** 3D packing diagram of **2r** viewed down along *a*-axis

**References**


1. Pepinsky, R., "Crystal engineering: New concepts in crystallography", *Phys. Rev*., **100**, 971 (1955).
2. Braga, D., "Crystal engineering, where from? Where to", *Chem. Commun*., 2751 (2003).
3. Trask, A. V. and Jones, W., "Crystal engineering of organic co-crystals by the solid-state grinding approach", *Top. Curr. Chem*., **254**, 41 (2005).
4. Desiraju, G. R., "Crystal engineering: A brief overview", *J. Chem. Sci*., **122**, 667 (2010).
5. Desiraju, G. R., "In crystal engineering: The design of organic solids", *Elsevier*, Amsterdam, The Netherlands (1989).
6. Desiraju, G. R., "Supramolecular synthons in crystal engineering: A new organic synthesis", *Angew. Chem. Int. Ed. Engl*., **34**, 2311 (1995).
7. Desiraju, G. R., "Hydrogen bridges in crystal engineering: Interactions without borders", *Acc. Chem. Res*., **35**, 565 (2002).
8. Braga, D., Desiraju, G. R., Miller, J. S., Orpen, A. G. and Price, S. L., "Innovation in crystal engineering", *Cryst. Eng. Comm*., **4**, 500 (2002).
9. Moorthy, J. N., "Crystal engineering with sterically-hindered molecular modules: Unique supramolecular synthons and novel molecular self assembly", *J. Indian Inst. Sci*., **88**, 131 (2008).
10. Burrows, A. D., "Crystal engineering using multiple hydrogen bonds", *Struct. Bond*., **108**, 55 (2004).
11. Guru Row, T. N., "Hydrogen and fluorine in crystal engineering: Systematics from crystallographic studies of hydrogen bonded tartrate–amine complexes and fluoro-substituted coumarins, styrylcoumarins and butadienes", *Coord. Chem. Rev*., **183**, 81 (1999).
12. Tiekink, E. R. and Vittal, J. J., "Frontiers in crystal engineering", Wiley, Chichester (2005).
13. Kuduva, S. S., Craig, D. C., Nangia, A. and Desiraju, G. R., "Cubanecarboxylic acids: Crystal engineering considerations and the role of C-H···O hydrogen bonds in determining O-H···O networks", *J. Am. Chem. Soc*., **121**, 1936 (1999).

14. Steiner, T., “Competition of hydrogen-bond acceptors for the strong carboxyl donor”, *Acta. Crystallogr.*, B **57**, 103 (2001).
15. Ugono, O., Rath, N. P. and Beatty, A. M., “Synthesis and control of single layer and polar 2-D layered architectures in a series of organic layered solids”, *Cryst. Growth Des*., **9**, 4595 (2009).
16. Basu, T., Sparkes, H. A. and Mondal, R., “Construction of extended molecular networks with heterosynthons in co-crystals of pyrazole and acids”, *Cryst. Growth Des*., **9**, 5164 (2009).
17. Gao, H. -L., Yi, L., Zhao, B., Zhao, X. -Q., Cheng, P., Liao, D. -Z. and Yan, S. -P., “Synthesis and characterization of metal−organic frameworks based on 4-hydroxypyridine-2,6-dicarboxylic acid and pyridine-2,6-dicarboxylic acid ligands”, *Inorg. Chem*., **45**, 5980 (2006).
18. Sander, J. R. G., Bucar, D. –K., Henry, R. F., Baltrusaitis, J., Zhang, G. G. Z. and Macgillivray, L. R., “A red zwitterionic co-crystal of acetaminophen and pyridine-2,4-dicarboxylic acid”, *J. Pharm. Sci*., **99**, 9 (2010).
19. Douki, T., Setlow, B. and Setlow, P., “Effects of the binding of α/β-type small, acid-soluble spore proteins on the photochemistry of DNA in spores of bacillus subtilis and in vitro”, *Photochem. Photobiol. Sci*., **81**, 163 (2005).
20. Slieman, T.A., Nicholson, W. L., “Role of dipicolinic acid in survival of bacillus subtilis spores exposed to artificial and solar UV radiation”, *Appl. Environ. Microbiol*., **67**, 1274 (2001).
21. Errington, J., “Bacillus subtilis sporulation: Regulation of gene expression and control of morphogenesis”, *Microbiol. Rev*., **57**, 1 (1993).
22. Murakami, K., Tanemura, Y. and Yoshino, M., “Dipicolinic acid prevents the copper-dependent oxidation of low density lipoprotein”, *J. Nutr. Biochem*., **14**, 99 (2003).
23. Couper, L., Mckendrick, J. E., Robins, D. J. and Chrystal, E. J. T., “Pyridine and piperidine derivatives as inhibitors of dihydrodipicolinic acid synthase, a key enzyme in the diaminopimelate pathway to L-lysine”, *Bioorg. Med. Chem. Lett*., **4**, 2267 (1994).
24. Griggs, D. L., Hedden, P., Templesmith, K. E. and Rademacher, W., “Inhibition of gibberellin 2β-hydroxylases by acylcyclohexanedione derivatives”, *Phytochemistry*, **30**, 2513 (1991).

25. Nathan, L. C., “Coordination complexes of pyridine-2,6-dicarboxylic acid and pyridine-2,6-dicarboxylic acid N-oxide”, *Trends Inorg. Chem*., **3**, 415 (1993).
26. Yang, L., Crans, D. C., Miller, S. M., la Cour, A., Anderson, O. P., Kaszynski, P. M., Godzala, M. E. III., Austin, L. D. and Willsky, G. R., “Cobalt (II) and cobalt (III) dipicolinate complexes: Solid state, solution and in vivo insulin-like properties”, *Inorg. Chem*., **41**, 4859 (2002).
27. Grossel, M. C., Dwyer, A. N., Hursthouse, M. B. and Orton, J. B., “Polymorphism in pyridine-2,6-dicarboxylic acid: Competition between‘‘robust’’ synthons”, *Cryst. Eng. Comm*., **8**, 123 (2006).
28. Zarracino, R. G. and Hopfl, H., “Self-Assembly of diorganotin (IV) oxides (R= Me, nBu, Ph) and pyridine-2,5-dicarboxylic acid to polymeric and trinuclear macrocyclic hybrids with porous solid-state structures: Influence of substituents and solvent on the supramolecular structure”, *J. Am. Chem. Soc*., **127**, 3120 (2005).
29. Hadadzadeh, H., Rezvani, A. R., Abdolmaleki, M. K., Ghasemi, K., Esfandiari, H. and Daryanavard, M., “Pyridine-2,6-dicarboxylic acid (Dipic): Crystal structure from co-crystal to a mixed ligand nickel (II) complex”, *J. Chem. Crystallogr*., **40**, 48 (2010).
30. Das, B. and Baruah, J. B., “Water bridged assembly and dimer formation in co-crystals of caffeine or theophylline with polycarboxylic acids”, *Cryst. Growth Des*., **11**, 278 (2011).
31. Thompson, L. J., Voguri, R. S., Male, L. and Tremayne, M., “The crystal structures and melting point properties of isonicotinamide co-crystals with alkanediacids $HO_2C(CH_2)_n$-$2CO_2H$ $n$ = 7–9”, *Cryst. Eng. Comm*., **13**, 4188 (2011).
32. Bučar, D. K., Henry, R. F., Lou, X., Borchardt, T. B. and Zhang, G. G. Z., “A ‘‘hidden’’ co-crystal of caffeine and adipic acid”, *Chem. Commun.*, 525 (2007).
33. Batchelor, E., Klinowski, J. and Jones, W., “Crystal engineering using co-crystallisation of phenazine with dicarboxylic acids”, *J. Mater. Chem.*, **10**, 839 (2000).
34. Szafran, Z. D., Fojud, Z., Katrusiak, A. and Szafran, M., “Structure of an inclusive compound of bis(piperidinium-4-carboxylate)hydrogen semi-tartrate with water and methanol studied by X-ray diffraction, NMR, FTIR and DFT methods”, *J. Mol. Struct.*, **928**, 99 (2009).

35. Aghabozorg, H., Sadr-khanlou, E., Shokrollahi, A., Ghaedi, M. and Shamsipur, M., "Synthesis, characterization, crystal structures, and solution studies of Ni(II), Cu(II) and Zn(II) complexes obtained from pyridine-2,6-dicarboxylic acid and 2,9-Dimethyl-1,10-phenanthroline", *J. Iran. Chem. Soc*., **6,** 55 (2009).

36. Kirillova, M. V., Guedes da Silva, M. F. C., Kirillov, A. M., Frau´sto da Silva, J. J., Pombeiro, R. A. J. L., "3D Hydrogen bonded heteronuclear $Co^{II}$, $Ni^{II}$, $Cu^{II}$ and $Zn^{II}$ aqua complexes derived from dipicolinic acid", *Inorg. Chim. Acta*., **360**, 506 (2007).

37. Park, H., Lough, A. J., Kim, J. C., Jeong, M. H. and Kang, Y. S., "Different coordination modes of Hdipic and dipic ligands to nickel (II) ions in a same environment (dipic = pyridine-2,6-dicarboxylate, dipicolinate)", *Inorg. Chim. Acta*., **360**, 2819 (2007).

38. Ghosh, S. K., Ribas, J. and Bhardadwaj, P. K., "Characterization of 3-D metal−organic frameworks formed through hydrogen bonding interactions of 2-D networks with rectangular voids by Co(II)- and Ni(II)-pyridine-2,6-dicarboxylate and 4,4'-bipyridine or 1,2-di(pyridyl)ethylene", *Cryst. Growth Des*., **5**, 623 (2005).

39. Çolak, A. T., Çolak, F., Yesilel, O. K. and Büyükgüngör, O., "Synthesis, spectroscopic, thermal, voltammetric studies and biological activity of crystalline complexes of pyridine-2,6-dicarboxylic acid and 8-hydroxyquinoline", *J. Mol. Struct*., **936**, 67 (2009).

40. Zhang, C. -X., Liao, D. -Z., Jiang, Z. -H. and Yan, S. -P., "Synthesis, crystal structure and magnetic properties of a nickel (II) complex with pyridine-substituted nitronyl nitroxide radicals", *Transit. Met. Chem*., **28,** 621 (2003).

41. Prasad, T. K. and Rajasekharan, M. V., "Cerium (IV)-Lanthanide (III)-pyridine-2,6-dicarboxylic acid system: Coordination salts, chains, and rings", *Inorg. Chem*., **48**, 11543 (2009).

42. Pedireddi, V. R., Chatterjee, S., Ranganathan, A. and Rao, C. N. R., "A study of supramolecular hydrogen bonded complexes formed by aliphatic dicarboxylic acids with azaaromatic donors", *Tetrahedron*, **54**, 9457 (1998).

43. Naiya, S., Sarkar, B., Song, Y., Ianelli, S., Drew, M. G. B. and Ghosh, A., "Carbonyl compound dependent hydrolysis of mono-condensed Schiff bases: A trinuclear Schiff base complex and a mononuclear mixed-ligand ternary complex of copper (II)", *Inorg. Chim. Acta*., **363**, 2488 (2010).

44. Ikeda, C., Nagahara, N., Motegi, E., Yoshioka, N. and Inoue, H., "Self-assembly of monopyrazolporphyrins by hydrogen bonding in solution", *Chem. Commun*., **43**, 1759 (1999).

45. Silverstein, R. M., Bassler, G. C. and Morrill, T. C., "Spectrometric identification of organic compounds", 5th Ed., John Wiley, New York (1991).

46. Yin, H. and Liu, S. -X., "Copper and zinc complexes with 2,3-pyridinedicarboxylic acid or 2,3-pyrazinedicarboxylic acid: Polymer structures and magnetic properties", *J. Mol. Struct*., **918**, 165 (2009).

47. Chen, L., Lin, X. -M., Ying, Y., Zhan, Q. -G., Hong, Z. H., Li, J. Y., Weng, N. S. and Cai, Y. P., "Synthesis, crystal structures and photoluminescence of Zn-Ln heterometallic polymers based on pyridine-2,3-dicarboxylic acid", *Inorg. Chem. Commun*., **12**, 761 (2009).

48. Sun, L. -P., Niu, S. -Y., Jin, J., Yang, G. -D. and Ye, L., "Crystal structure and surface photovoltage of a series of Ni(II) coordination supramolecular polymer", *Inorg. Chem. Commun*., **9**, 679 (2006).

49. Ghosh, S. K. and Bharadwaj, P. K., "Supramolecularly assembled pentameric and octameric water clusters stabilized by a mixed complex of Ni(II)", *Inorg. Chim. Acta*., **359**, 1685 (2006).

# *Chapter 3*

# *Effect of Anions on Supramolecular Architecture of Benzimidazole Based Ionic Salts*

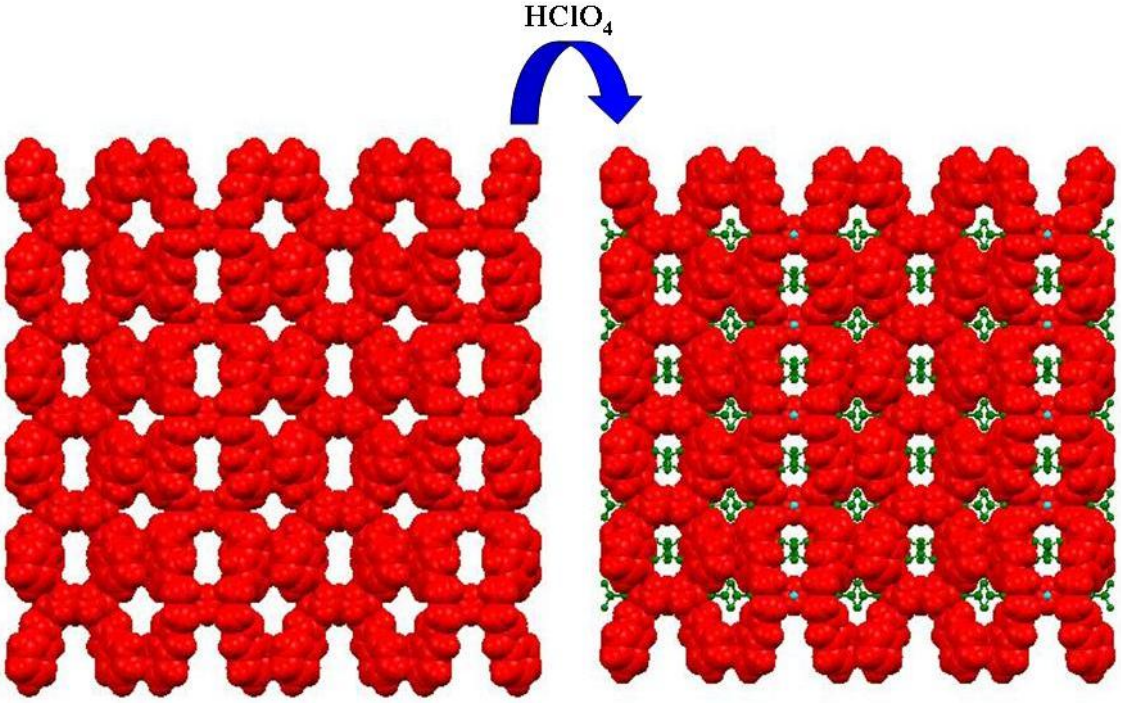
HClO4

Anion-selected sensing and recognition is of great interest because anions are known to play numerous fundamental roles not only in the supramolecular chemistry but also in the environmental, ion exchange, anion separation in nuclear waste, catalysis, water purification and in biological field [1-5]. A variety of new synthetic molecules capable of anion-recognition have been synthesized that offer hydrogen bonding, which includes amides [6-8], protonated amine [9], guanidinium [10], indole [11-13], pyrroles [14-15] and urea/thiourea [16-17]. Some interesting works of anion sensing based on benzimidazole are also available in literature. Benzimidazole, a hetero-aryl compound is an essential pharmacophore in the drug discovery and used as variety of drugs, like thiabendazole and flubendazole (anthelmintic), omeprazole and lansoprazole (antiulcerative) and astemizole (antihistaminic) [18-25]. The different crystal structures of numerous benzimidazole based ligands, illustrate their potential as excellent hydrogen bond donors for the anions, and for that reason they could be used as selective anion sensors as well as anion receptors. Because of the amphoteric nature of N-atom in imidazole ring of benzimidazole moiety, it can be used as a receptor molecule for selective and effective anion or cation and netural organic molecules.

**Importance of anion sensing**

The field of anion supramolecular chemistry has received considerable interest in the last two decades due to the crucial role that anions play in the natural world. In mammalian physiology anions, especially chloride, have important roles to play in many biological processes. Some anions are very crucial to maintain life, whereas others are acutely toxic; cyanide inhibits the action of cytochrome c oxidase (an important respiratory enzyme) and oxalate ingestion can cause permanent kidney and liver damage. Environmentally, phosphates and nitrates from agricultural fertilizers, cause eutrophication if they leech into rivers, and nitrate and sulfate cause acid rain. Furthermore, the release of pertechnetate, a radioactive by-product of nuclear fuel processing, constitutes an example of the serious pollution impact. Now-a-days, the designing of hosts for anionic guest species has become very significant because of the importance of anions in biological systems, along with their impact in the environment and their numerous chemical roles etc.

**Factors responsible for anion selectivity**

The field of anion supramolecular chemistry is less developed as compared to that of cations due to the inherent characteristics of anions which make it more challenging to design appropriate receptor (host) systems. Firstly, the anions are

significantly larger than their isoelectronic cations (e.g. r($Cl^-$) = 1.69Å, r($K^+$) = 1.52 Å) and accordingly their charge to size ratio is smaller. Therefore the diffuse nature results in diminished electrostatic interactions between an anion and its receptor. Along with size, shape also plays an important role and that is why the anions possessing a wide range of geometries require a receptor with a complementary binding cleft for selective complexation (Fig. 3.1). It should be highlighted that many biologically relevant anions such as DNA and ATP with complex geometries requires receptor with complicating structures. In contrast to cations, most of the anions are spherical in shape, making it facile to design an appropriate receptor.

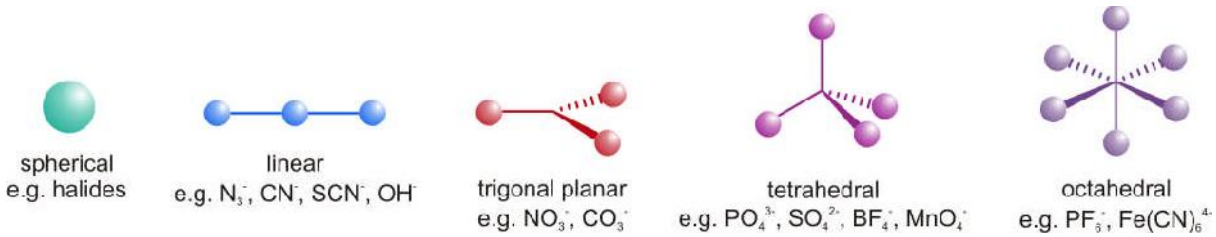


**Fig 3.1** Geometries of different anions

**Anion receptor chemistry**

The field of anion receptor can be broadly classified in two groups: those possessing positive charge; and those that are neutral. The positively charged receptors utilise electrostatic interactions and can compete with protic polar solvents, such as water and methanol. Neutral receptors however, may be able to function in more competitive polar solvents if the binding domain is effectively shielded from solvent molecules.

**Positively charged anion receptors**

The most discernable feature of anions is their negative charge therefore, for a potential receptor has to be positively charged which can exploit strong electrostatic interactions between the oppositely charged species. Park and Simmons utilized the strength of electrostatic interactions in combination with hydrogen bonds to create the first anion receptor in 1968. The acidic ammonium protons were shown by $^1H$ NMR spectroscopy (and later by X-ray crystallography) to cooperatively bind the halide guest. This receptor signalled the beginning of the emergence of pH dependent polyammonium receptors for anion complexation.

In more recent work, the tripodal tren-based polyammonium receptor reported by Hossain and co-workers [26], was shown to strongly complex dihydrogen phosphate through three N-H···O hydrogen bonds, both in the solid as well as in solution state ($^1$H-NMR titration experiments in $CDCl_3$) (Fig. 3.2).

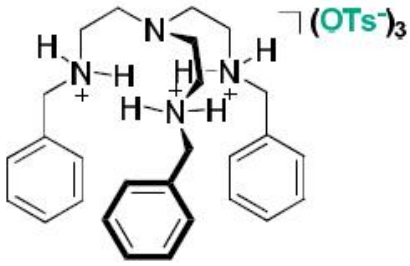


**Fig. 3.2** Tripodal tren-based polyammonium receptor

In recent years positively charged imidazolium and to a lesser extent triazolium motifs have emerged as important anion complexing groups due to their acidic C-H protons, capable of undergoing charge-assisted hydrogen bonding with an anionic species. Kim et al. [27] designed a receptor with a glycouril backbone bearing two imidazolium groups capable of orienting themselves for the strong binding of acetate (Fig. 3.3) in 9:1 $CD_3CN/d_6$-DMSO.

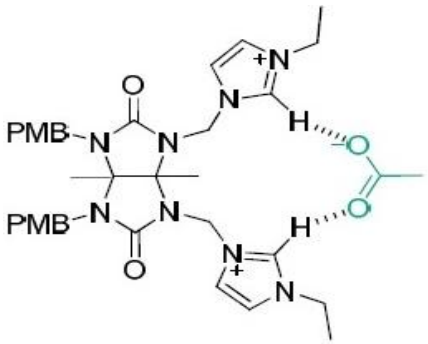


**Fig. 3.3** Glycouril receptor with imidazolium groups

**Neutral anion receptors**

Neutral anion receptors are based on weaker non-covalent interactions to bind the anion, and consequently operate in less competitive aprotic organic media. However, it may be possible for these receptors to achieve greater selectivity than their positively charged counterparts if they utilize multiple directional hydrogen bonding interactions for anion complexation. Much focus has been paid to amide based receptors, probably due to the extensive use of amide hydrogen bonding interactions in the anion binding domain of proteins. The closely related to the amide groups, ureas

and thioureas are also used for the same. These motifs have been incorporated into many anion receptors and benefit from two parallel N-H hydrogen bond donor groups spaced a suitable distance apart to allow for interaction with a number of anionic species, especially Y-shaped anions such as carboxylate and nitrate. Pyrroles also provide an acidic hydrogen bond donor which can bind to different anions through various non-covalent interactions and are also intrinsic to many anion binding groups such as indoles, indolocarbazoles and calixpyrroles.

**Metal containing anion receptors**

A final class of anion receptors consists of complexes possessing a metal centre, which may act to enhance binding affinity either through an attractive columbic interaction with the anion, or by organizing the receptor so that binding groups take their correct orientation for effective association. Specific transition and lanthanide metals may also act as a reporter groups, signalling the occurrence of such an anion recognition event. An elegant example of a transition metal directed cage (Fig. 3.4) capable of anion recognition is provided by Fabbrizzi, where the iron (II) prefers an octahedral coordination by a tripodal imidazolium bipyridyl structure. In the cage structure the three imidazolium C-H hydrogen bond donor fragments converge into the cavity which is of the correct size for complexing halide anions and azide in 4:1 MeCN/$H_2O$ [28].

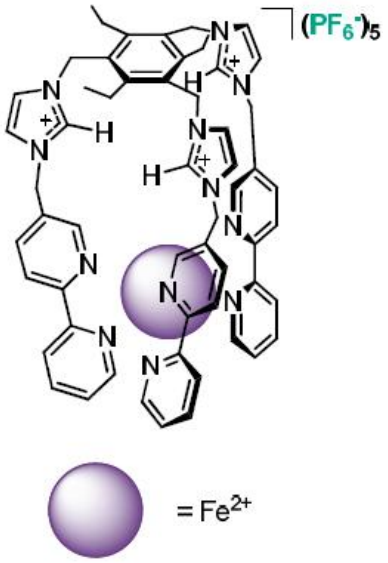


**Fig. 3.4** Transition metal directed cage for anion recognition

**Anion Sensing**

The interaction between anion recognition site and receptor group is basically responsible for the signalling of recognition events (Fig. 3.5).

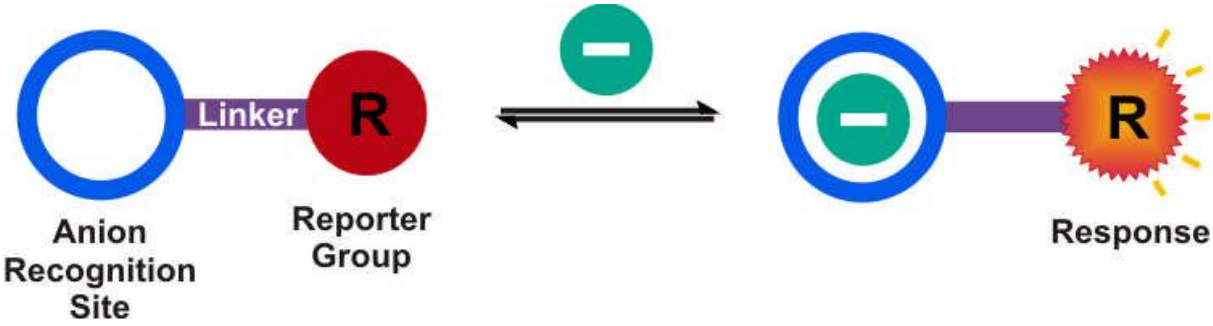


**Fig. 3.5** Schematic representation of anion sensing. Addition of an anion to the receptor induces a change in the physical properties of the reporter group

Therefore, the binding of the anion to a specific receptor induces a macroscopic physical change in an optical (colorimetric or luminescent) or electrochemical property. During the recent emergence of anion receptor chemistry numerous anion sensors have been reported.

**Colorimetric Sensors**

The induced signal in terms of color change in the presence of anions has received a great interest, because the fluorophore needs no equipment and the detection can be achieved by the naked eye. Dickson and co-workers [29] have developed a viologen based sensor (Fig. 3.6) that undergoes a colour change from colorless to deep purple upon addition of succinate, malonate and acetate, but remains unchanged by other anions including chloride and nitrate. This colour change is suggestive of the formation of a charge-transfer complex between the carboxylate anions and the viologen.

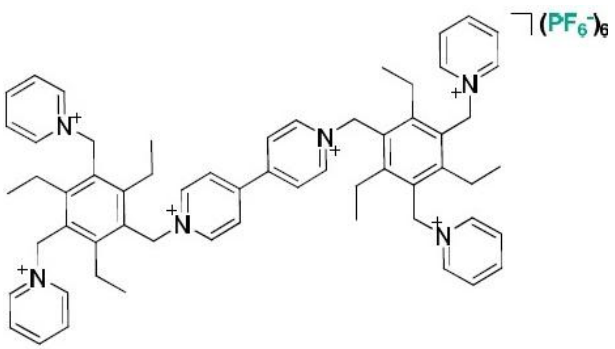


**Fig. 3.6** Viologen based sensor

A number of chromophore appended thiourea receptors have been reported, which sense anions such as fluoride and acetate colorimetrically. Often the addition of these basic anions induces deprotonation of the acidic urea protons leading to increased conjugation in the system and thus a colour change is observed.

**Luminescent sensors**

Receptors integrated with a luminescent functional group are attractive for anion sensing because the detection can be done at very low concentrations, thus requiring only small quantities of the host species, coupled with the high sensitivity of luminescence detection techniques. The luminescence of a reporter group can be modulated upon anion binding by one of the four mechanisms:

(i) Photoelectron transfer (PET)

(ii) Electronic energy transfer

(iii) Switching between monomers and excimers

(iv) Rigidity effect.

These phenomena can act to either enhance or quench luminescent emission intensity and may also alter the wavelength at which an excited state emits.

Arunachalam et al. [30] studied anion-assisted formation of discrete homodimeric and heterotetrameric assemblies by benzene based protonated heteroaryl receptors $L^1$−$L^6$ by single crystal X-ray diffraction studies (Fig. 3.7) and found the fact that protonated tripodal receptor $L^1$ formed staggered homodimeric capsular assemblies with $CF_3COO^-$ (Fig. 3.8) and $ClO_4^-$ anion (Fig. 3.9). They also found the formation of homodimeric assembly, due to the protonation of $L^3$ with trimesic acid and established that in all these cases the anions are hydrogen bonded to the receptor molecules and show remarkable influence on the outcome of the self-assembly process to form discrete capsules.

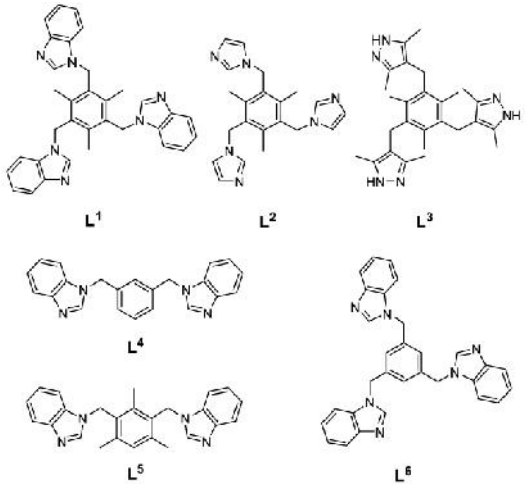


**Fig. 3.7** Molecular structures of $L^1$-$L^6$

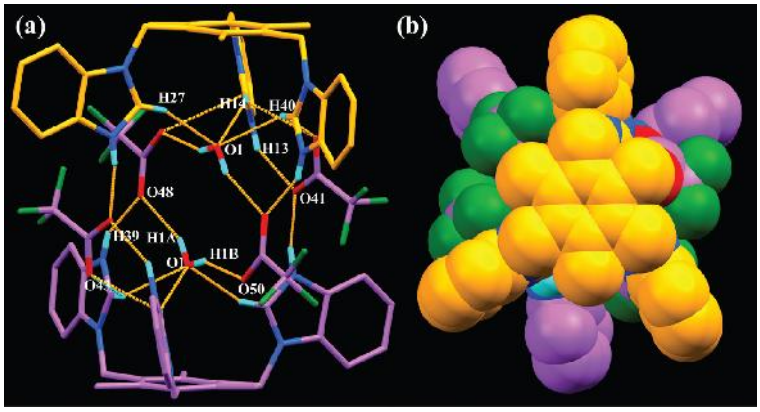


**(a)** **(b)**

**Fig. 3.8 (a)** MERCURY diagram showing the $CF_3COO^-$ stitched capsular aggregate of $[H_3L^1]^{3+}$ with encapsulated water molecules. **(b)** Space filling view of the staggered assembly along the benzene cap

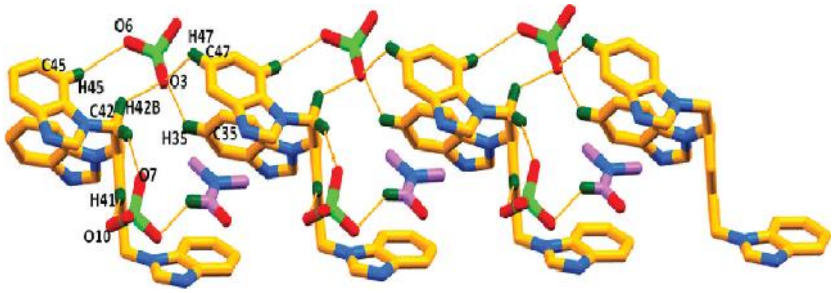


**Fig. 3.9** View showing the hydrogen bonding interactions between $ClO_4^-$ and $L^6$ showing trapped DMF molecules in the clefts

Gogoi and Das [31] carried out the reactions of two benzimidazole-based receptors ($L^1$ and $L^2$) (Fig. 3.10) bearing -OH functionality forming crystalline salts with different inorganic and organic acids viz. $[L^1H^+][Cl^-]$ (**1**) (Fig. 3.11) , $[L^1H^+][NO_3^-]$ (Fig. 3.12) (**2**), $[L^1H^+][OAc^-]$ (Fig. 3.13) (**3**), $[L^1H^+][DNB^-]\cdot DMF$ (**4**), $[L^1H^+][H_2PO_4^-]$ (**5**), $[L_2H^+][OAc^-]\cdot AcOH$ (**6**), $[L_2H^+]^-$ $[DNB^-]$ (**7**) and $[L^2H^+][HSO_4^-]\cdot H_2O$ (**8**) where the shape of the counter anion drives the solid structure from a one dimensional polymeric chain to a three-dimensional structure. They further rationalized on the basis of structural analyses that the anion binding in all eight complexes was attributed entirely to $NH^+\cdots$anion, NH$\cdots$anion, OH$\cdots$anion, and multiple CH$\cdots$anion hydrogen bonding interactions. They found the planar nitrate anion formed a cyclic structure with receptor $L^1$, whereas the acetate anion with the same receptor lead to a molecular barrel type structure. Again the tetrahedral dihydrogen phosphate anion formed a polymeric interanionic chain structure with $L^1$ and the other tetrahedral hydrogen sulfate anion formed hydrogen sulfate−$(water)_2$−hydrogen sulfate adducts with charged $L^2$.

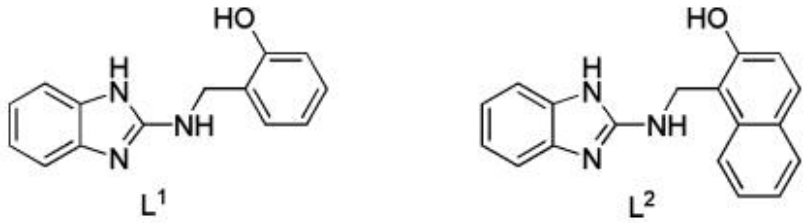


**Fig. 3.10** Molecular structures of the receptors ($L^1$ and $L^2$)

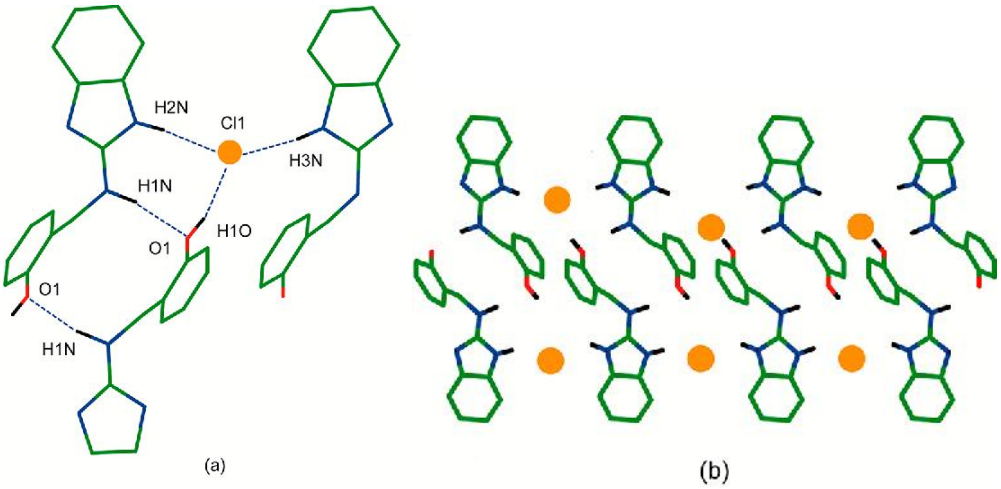


**Fig. 3.11 (a)** Illustration of various nonbonding interactions (dotted lines) between spherical chloride anion and receptor $L^1$ in salt **1** and **(b)** the one-dimensional polymeric chain structure along *a* axis

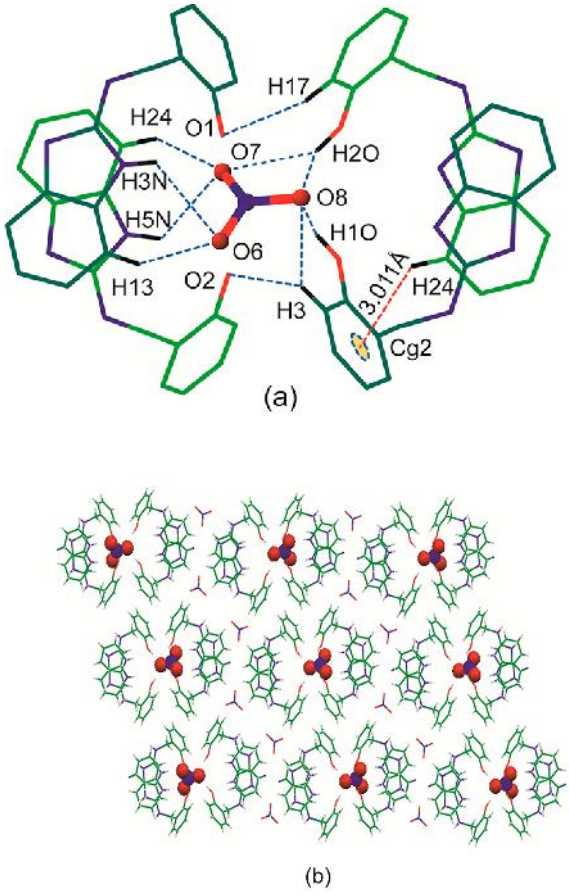


**Fig. 3.12 (a)** Coordination mode of $NO_3^-$ anion in the salt **2. (b)** 2D structure of the salt **2** with the same nitrate in space fill and the other nitrate in ball and stick model

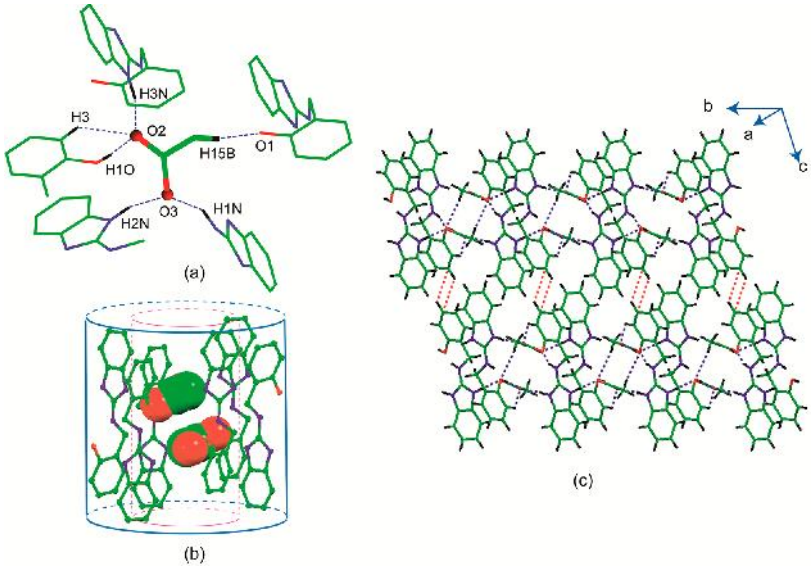


**Fig. 3.13 (a)** Crystal structure of $[L^1H^+][OAc^-]$. **(b)** The acetate anion induced molecular barrel with spacefill guest molecules along *c* axis. **(c)** Its three-dimensional packing

Singh and Jang [32] synthesized novel tripodal fluorescent receptor (Fig. 3.14) bearing benzimidazole motifs as recognition sites in the pods of the receptor. They evaluated the recognition behavior of the receptor toward various anions in $CH_3CN/H_2O$ (9:1, v/v) solution and found that the receptor showed change in fluorescent intensity only with $I^-$, but no significant change was observed on addition of other anions such as $F^-$, $Cl^-$, $Br^-$, $HSO_4^-$, $NO_3^-$, $CH_3COO^-$ and $H_2PO_4^-$ .

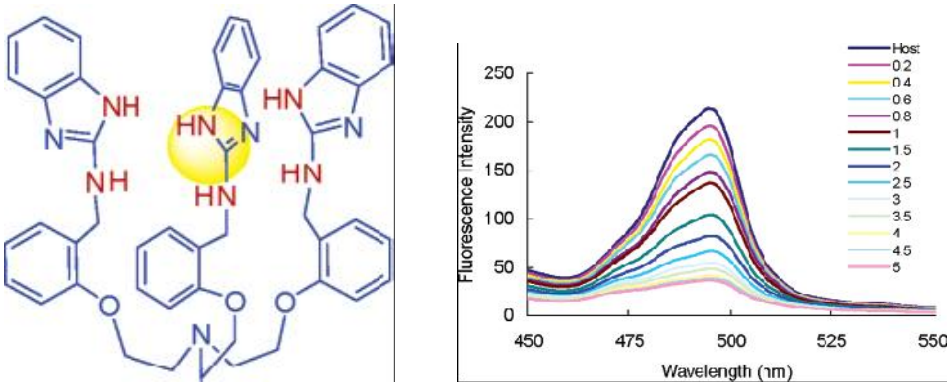


**(a)** **(b)**

**Fig. 3.14 (a)** Molecular structure of ligand **(b)** and its fluorescence spectra

Lee et al. [33] synthesized a novel 1,3,5-substituted triethylbenzene derivative with a 2-aminobenzimidazole moiety (Scheme 3.1) as a binding and signaling subunit. They tested the sensor in a buffered $CH_3CN/H_2O$ (99:1, v/v) solution and demonstrated that this is selective for iodide by the photophysical properties obtained through UV-Vis absorption and fluorescence spectroscopy (Fig. 3.15 (a-b)) analysis.

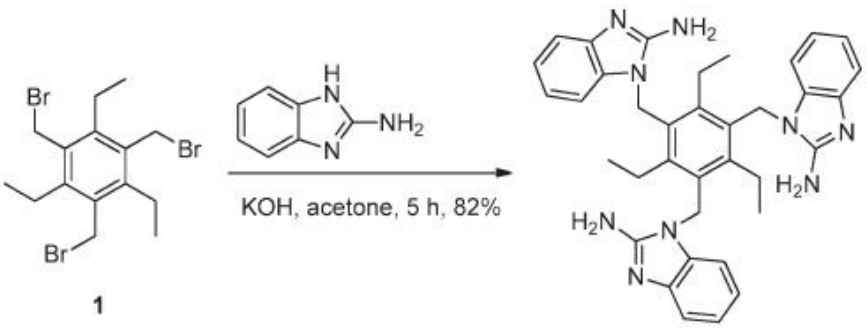


**Scheme 3.1**

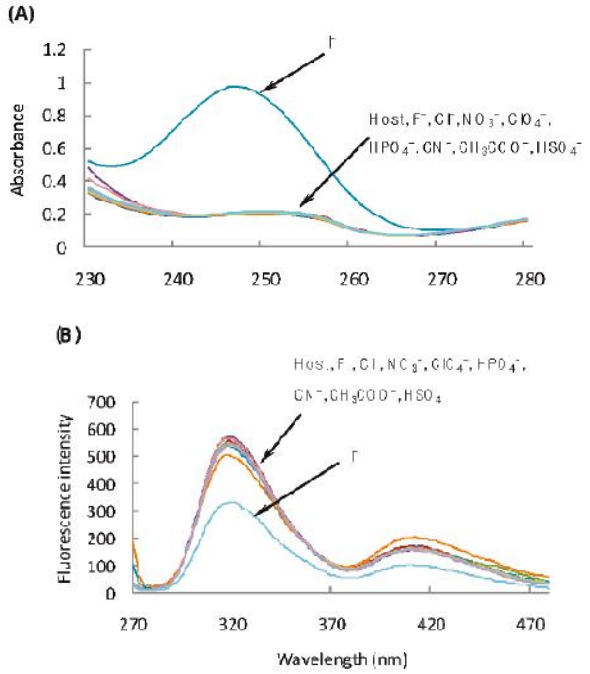


**(a)** **(b)**

**Fig. 3.15 (a)** UV-Vis absorption spectra and **(b)** Fluorescence spectra of receptor

Joo et al. [34] synthesized a novel fluorescent receptor bearing benzimidazole moieties as recognition sites (Scheme 3.2). The recognition behavior of the receptor towards various anions has been evaluated in $CH_3CN$. The receptor showed ratiometric fluorescent changes only with $CH_3COO^-$ and it showed no significant response to any of other anions such as $Cl^-$, $Br^-$, $I^-$, $HSO_4^-$, $NO_3^-$, $C_6H_5COO^-$ and $H_2PO_4^-$.

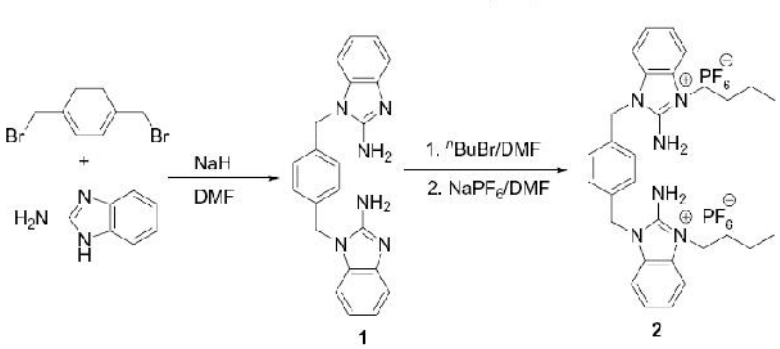


**Scheme 3.2**

Yu et al**.** [35] designed and synthesized a benzimidazole-based anion receptor (Fig. 3.16 (a)) and characterized their single crystal X-ray diffraction analysis. They carried out anion-binding studies using $^1H$ NMR and UV–Visible which revealed that the compound exhibits selective recognition toward $F^-$ over other halide anions. The

highest selectivity for $F^-$ among the halides is attributed mainly to the strongest hydrogen-bond interaction of the receptor with $F^-$. In addition, the higher match in geometry between the receptor and $F^-$ also plays a important role in the selective recognition of the receptor for $F^-$. They also found change in color of compound from light-yellow to red in presence of tetrabutylammonium fluoride and moreover, $F^-$ induced color changes remained the same even in the presence of a large excess of $Cl^-$, $Br^-$, $I^-$ (Fig. 3.16 (b)).

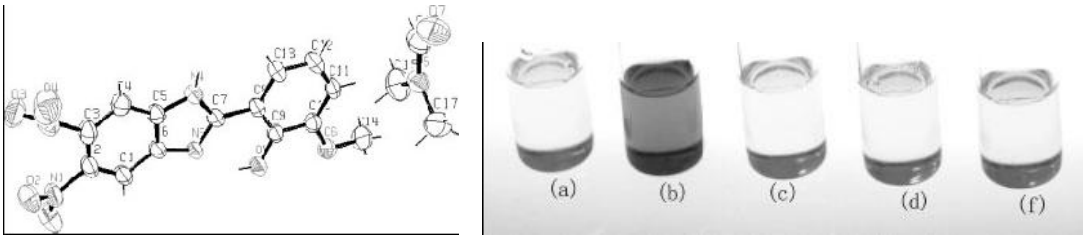


**(a)** **(b)**

**Fig. 3.16 (a)** Crystal structure of benzimidazole-based anion receptor. **(b)** Colorimetric experiment

Ghosh and Kar [36] synthesized a new flexible anthracene linked benzimidazolium-based receptor (Fig. 3.17) and studied its binding properties by NMR, UV-Vis and fluorescence spectroscopic techniques. They found that the compound exhibits a greater change in emission in the presence of tetrabutylammonium dihydrogenphosphate in $CH_3CN$ over the other anions and iodide is selectively preferred in $CHCl_3$ containing 0.1% $CH_3CN$. They found that upon complexation of dihydrogen phosphate and iodide, the emission gradually decreases without showing any other characteristic change in the spectra and suggest that hydrogen bonding and charge–charge interactions interplay simultaneously in a cooperative manner for selectivity in the binding process.

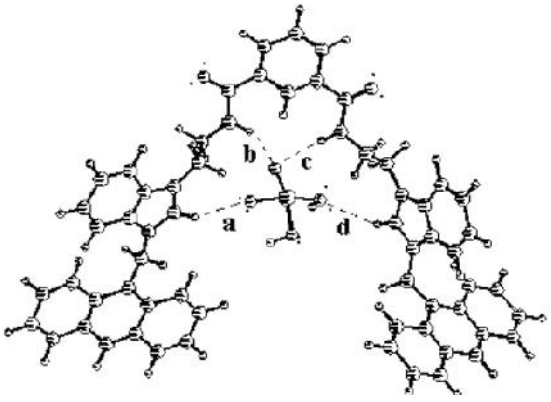

**Fig. 3.17** Crystal structure of anthracene linked benzimidazolium based receptor

Molina et al. [37] reviewed that the amphoteric nature of the imidazole ring can function as selective and effective receptor system for both cation and / or anion and even for neutral organic molecules. Therefore they concluded that the design of new multichannel imidazole-based receptors (Fig. 3.18 and Fig. 3.19) are capable of recognizing different types of analytes and summarized the most recent and relevant advances in this area.

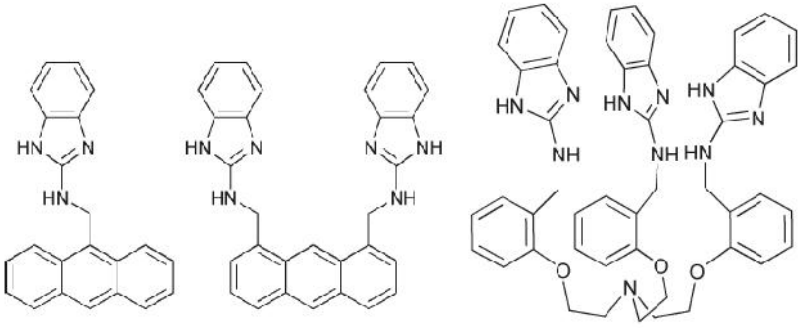

**(a)** **(b)**

**Fig. 3.18 (a)** Fluorescent receptors based on 2-aminobenzimidazole **(b)** Benzimidazole-based tripodal receptor

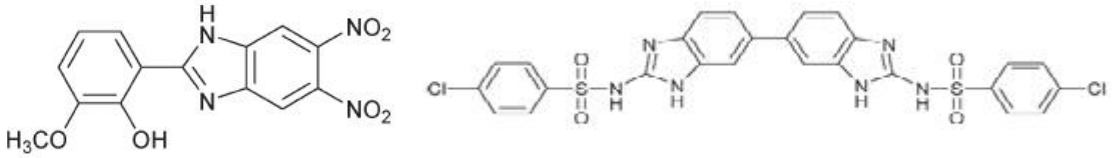

**(a)** **(b)**

**Fig. 3.19 (a)** Chromogenic functionalized benzimidazole receptor **(b)** Bis-benzimidazole-based conformationally restricted receptor

Lirag et al. [38] reported new family of half cruciform benzimidazole based fluorophores (Fig. 3.20), which exhibits fluorescence change in response to bases, acids and anions. They found that the two members of this series retained their fluorescence properties even in their deprotonated form and justified their potential as building blocks in zeolitic imidazolate frameworks (ZIFs).

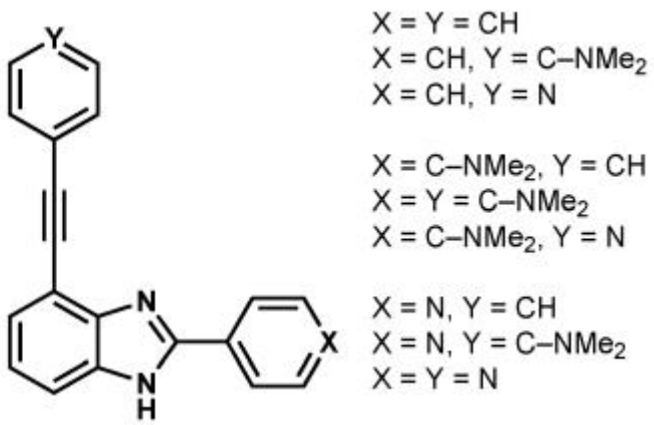


**Fig. 3.20** Schmatic diagram of L-shaped benzimidazole fluorophores

Gale et al. [39] described tautomeric switching in benzimidazole based anion receptor (Fig. 3.21) induced by the presence of basic anions. They highlighted the role of substitutents in controlling the selectivity of benzimidazole-based receptor towards a variety of guest anions capable to form hydrogen bonds with guests that functions in polar solvent mixtures.

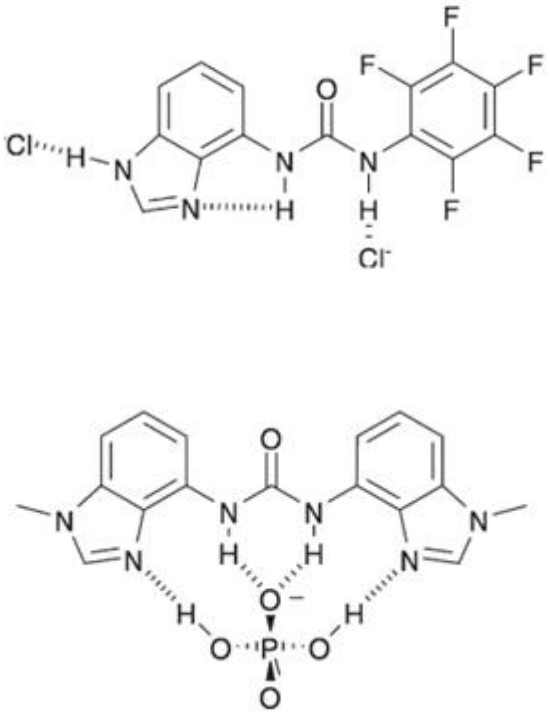

**Fig. 3.21** Schematic diagram of benzimidazole salts

Lee et al. [40] synthesized salts of N,N'-dihexylbenzimidazolium with three anions $Br^-$, $I^-$, $PF_6^-$ and characterized by single-crystal X-ray diffraction (Fig. 3.22).

They demonstrated some anion-independent structural properties, which include the U-shaped conformation, bilayer packing and the thickness of the ionic layer.

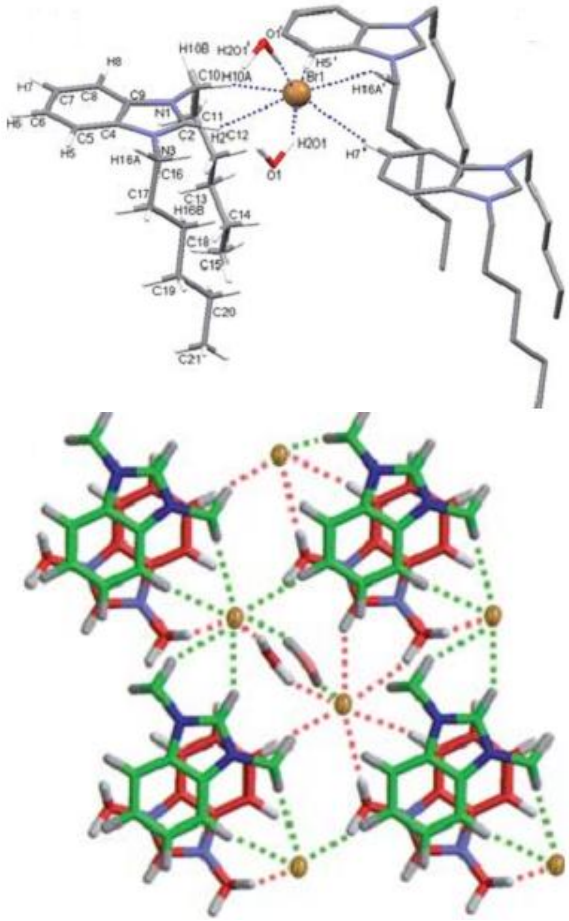


**(a)** **(b)**

**Fig. 3.22 (a)** Hydrogen bonding of $Br^-$ anion with benzimidazolium cations. **(b)** Two dimensional hydrogen bonding network via non-covalent interactions

Fisher et al. [41] reported a series of 2,6-dicarboxamidopyridine clefts bearing benzimidazole moieties, which crystallized in DMSO and reported the most important feature in the crystal structure, that the DMSO molecules were held by amide NH groups and could be replaced by neutral gas molecules thereby forming the guest binding sites. They discussed the role of various intermolecular hydrogen bonding interactions in this host guest chemistry (Fig. 3.23).

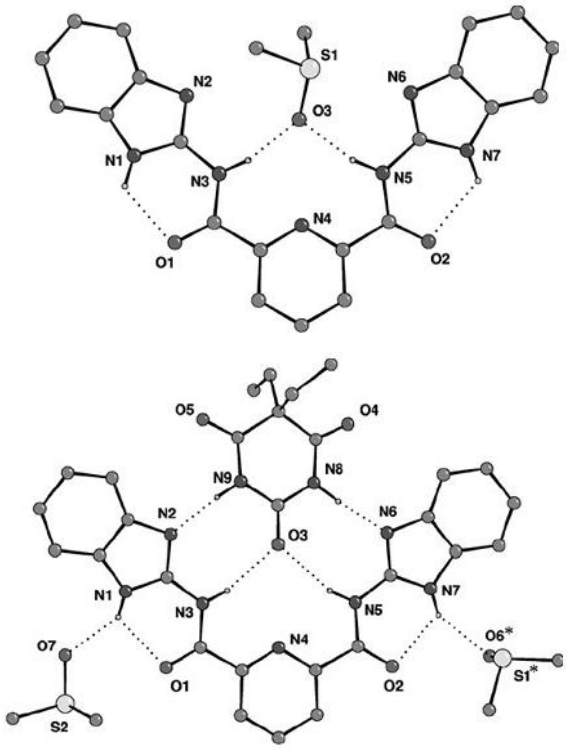


**(a)** **(b)**

**Fig. 3.23 (a)** X-ray crystal structure of the DMSO solvate **(b)** Barbital and 2,6-dicarboxamidopyridine benzimidazole

Hiscock et al. [42] studied the influence of anions on tautomerism in benzimidazole containing anion receptors via a variety of techniques in both solution and the solid state. They showed that hydrogen bonding interactions between the receptors and guests (Fig. 3.24) have a significant effect of the nature of the tautomer present in and the compounds have a preference for complexation of lactate over pyruvate (Fig. 3.25).

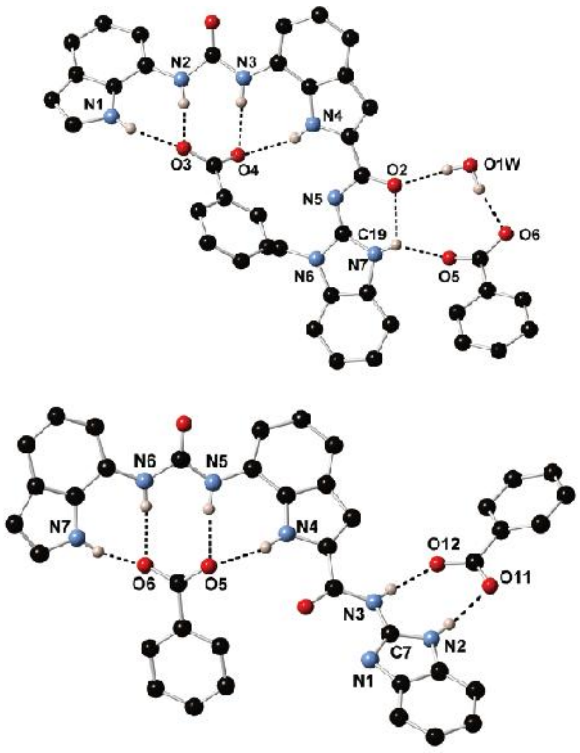


**(a)** **(b)**

**Fig. 3.24 (a)** Crystal structure of two polymorphs of $(TBA)_2 \cdot (C_6H_5CO_2)_2 \cdot (H_2O)$

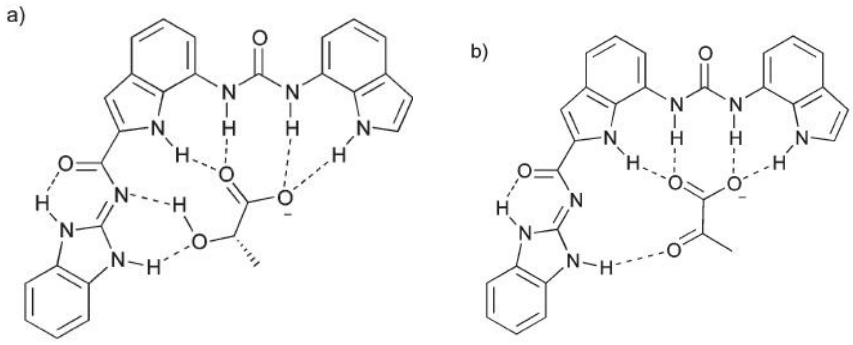


**(a)** **(b)**

**Fig. 3.25** Proposed binding modes of receptor with **(a)** lactate and **(b)** pyruvate

Yoon et al. [43] studied imidazolium receptors for anion recognition according to their topological and structural classification, which includes benzene tripodal, cyclophane and caliximidazolium, fluorescent imidazolium, ferrocenyl imidazolium, cavitand and calixarene, and polymeric imidazolium systems.

Not only inorganic anions but the organic anions were also trapped by different ligands having benzimidazole skeleton.

Ji et al. [44] carried out a survey of the Cambridge Structural Database (CSD) and found that 79 % of complexes that contain both imidazole and carboxyl groups generated imidazolium-carboxylate supramolecular heterosynthons rather than carboxyl or imidazole supramolecular homosynthons (Fig. 3.26). They found crystal structures of seven new complexes that contain tris(2-benzimidazylmethyl)amine (TBMA) and a variety of carboxylic acids, including benzoic acid (HBA), *p*-methoxybenzoic acid (HPMBA), phthalic acid ($H_2PA$), terephthalic acid ($H_2TPA$), isophthalic acid ($H_2PIA$), trimesic acid ($H_3TMA$), and pyromellitic acid ($H_4PMA$) and in all seven complexes, ($H_2TBMA$).$(BA)_{2.}$DMF(**1**), (HTBMA).(PMBA).(TBMA).$(HPMBA)_{2.}$2DMF.$H_2O$ (**2**), (HTBMA).($H_2TBMA$).(HPA).(PA).3DMF3$H_2O$ (**3**), $(HTBMA)_{2.}$(TPA).2DMF (**4**), $(HTBMA)_{2.}$(PIA).2DMF (**5**), ($H_2TBMA$).(HTMA).0.5DMF.$H_2O$ (**6**) and $(HTBMA)_{2.}$($H_2PMA$).2DMF.$H_2O$ (**7**) the protons have been transferred from acid to aromatic nitrogen of benzimidazole (partial proton transfer for **3**, **6** and **7**). They analyzed the H-bonding synthons and their effect on crystal packing in the context of crystal engineering and host-guest chemistry.

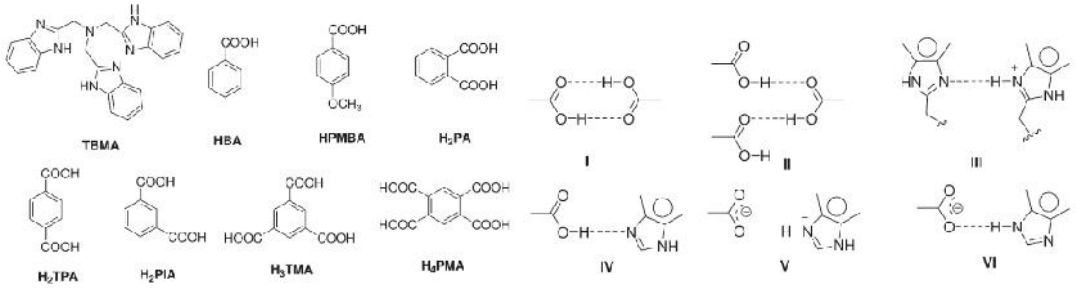


**(a)** **(b)**

**Fig. 3.26 (a)** Molecular components used **(b)** Supramolecular homosynthons (I, II, and III) and heterosynthons (IV, V, and VI)

Ghosh et al. [45] exploited benzimidazole framework to design anthracene based sensory system, which could distinguish the organic sulfonic acid from carboxylic acids (Fig. 3.27). They suggested that the molecule existed in the excimer form which was destructed in presence of organic sulfonic acids thereby enabling the system to differentiate them from carboxylic acids.

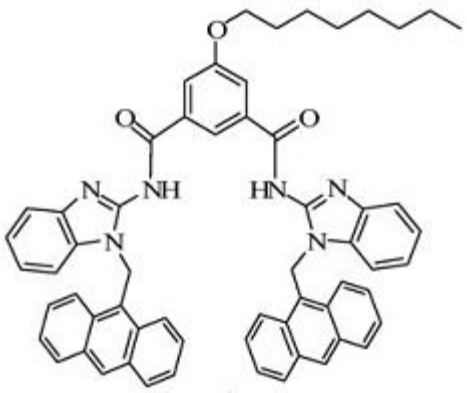

**Fig. 3.27** Schematic diagram of anthracene-linked benzimidazole diamide

The following literature revealed that not only the organic ligands but their metal complexes were also used for the anion sensing.

Cui et al. [46] developed a new anion sensor $[Ru(bpy)_2(H_2biim)](PF_6)_2$ (where bpy = 2,2'-bipyridine and $H_2biim$ = 2,2'-biimidazole), in which the Ru(II)-bpy moiety acts as a chromophore and the $H_2biim$ ligand as an anion receptor via hydrogen bonding and showed that the complex was an eligible sensor for various anions (Fig. 3.28). It donated protons for hydrogen bonding to $Cl^-$, $Br^-$, $I^-$, $NO_3^-$, $HSO_4^-$, $H_2PO_4^-$ and $OAc^-$ anions and further actualized monoproton transfer to the $OAc^-$ anion, changing color from yellow to orange brown. They found that the fluoride ion had high affinity towards the N-H group of the $H_2biim$ ligand for proton transfer, rather than hydrogen bonding, because of the formation of the highly stable $H_2F^-$ anion which results in stepwise deprotonation of the two N-H fragments. They concluded that these processes were signaled by vivid color changes from yellow to orange brown and then to violet because of second-sphere donor-acceptor interactions between Ru(II)-$H_2biim$ and the anions and the significant color changes can be distinguished visually (Fig. 3.29). The processes are not only determined by the basicity of anion but also by the strength of hydrogen bonding and the stability of the anion-receptor complexes.

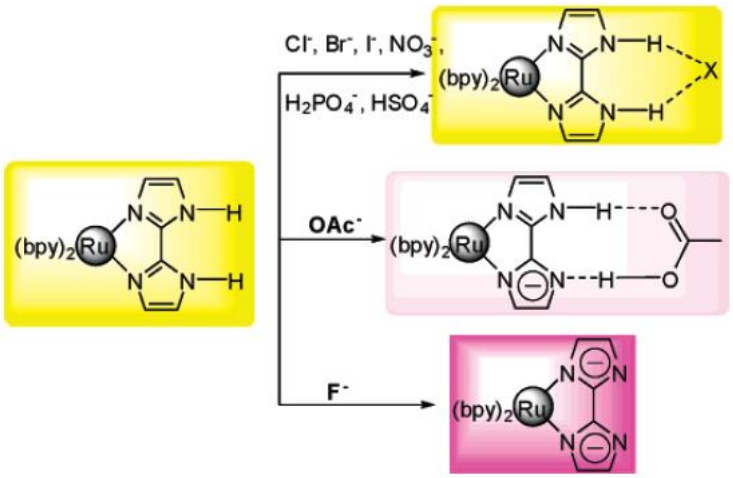


**Fig. 3.28** Schematic representation of the interaction between sensor and anions

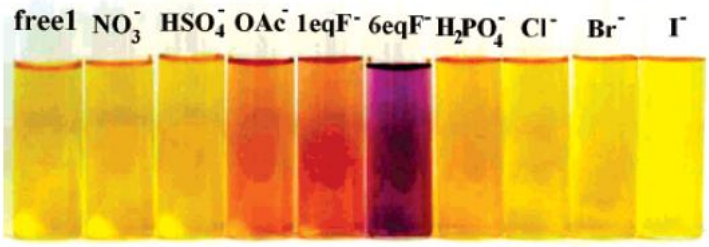


**Fig. 3.29** Color changes observed in MeCN solution

Saha et al. [47] synthesized mixed-ligand monometallic and bimetallic ruthenium(II) complexes of compositions $[(bpy)_2Ru(H_3Imbzim)](ClO_4)_2.2H_2O$ (Fig. 3.30 a) and $[(bpy)_2Ru(H_2Imbzim)Ru(bpy)_2](ClO_4)_3.3CH_2Cl_2$ (Fig. 3.30 b) (where $H_3Imbzim$ = 4,5-bis(benzimidazol-2-yl)imidazole and bpy = 2,2'-bipyridine) and characterized them using standard analytical and spectroscopic techniques. They investigated the anion binding properties of complexes as well as those of the parent $H_3Imbzim$ in an acetonitrile solution using absorption, emission, and $^1H$ NMR spectral studies, which revealed that both of the metalloreceptors act as sensors for $F^-$ and $AcO^-$ and to some extent, for $H_2PO_4^-$. They demonstrated that at a relatively lower concentration of anions, a 1:1 hydrogen-bonded adduct was formed. However, in the presence of an excess of anions, stepwise deprotonation of the two benzimidazole NH fragments occurred, and was signalled by the development of vivid colors visible with the naked eye (Fig. 3.31).

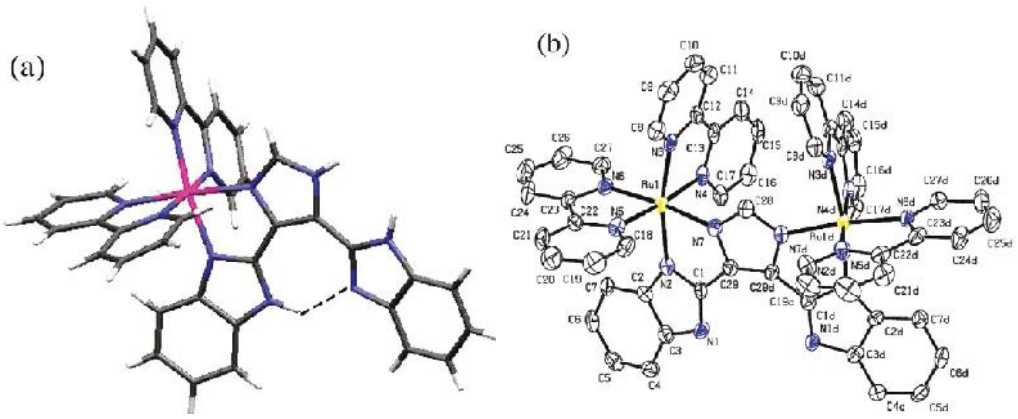


**Fig. 3.30 (a)** Crystal structures of $[(bpy)_2Ru(H_3Imbzim)](ClO_4)_2.2H_2O$ and **(b)** $[(bpy)_2Ru(H_2Imbzim)Ru(bpy)_2](ClO_4)_3.3CH_2Cl_2$


**Fig. 3.31** Color changes in metalloreceptor before and after the addition of anions

Matthews et al. [48] utilized two ligand frameworks namely 1,2-bis(1H-benzimidazol-2-yl)ethane and 1,3-bis(1H-benzimidazol-2-yl)propane, which gave rise to three dimensional network with tetrahalogenometallates in their diprotonated form (Fig. 3.32). They found three dimentional architecture derived from N–H···Cl hydrogen bonding interactions and stacking interactions between the protonated benzimidazole groups and predicted that the protonated benzimidazole moiety may serve as vital synthon in crystal engineering.

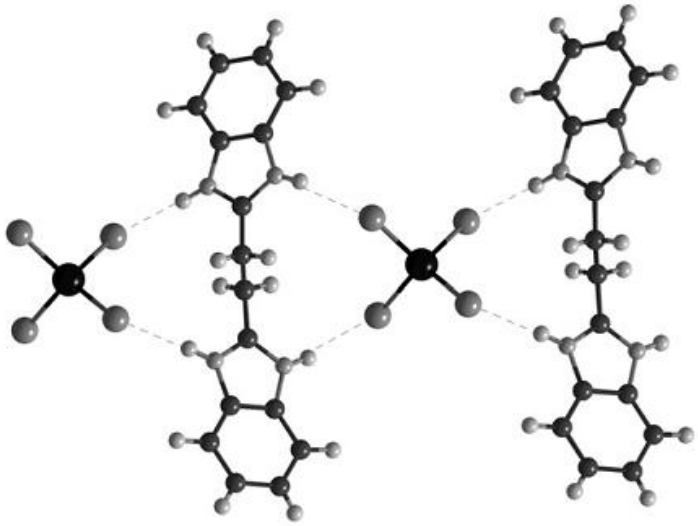

**Fig. 3.32** Crystal structure of benzimidazole cation and anion.

This chapter deals with the synthesis of two benzimidazole based ligands (N,N,N',N'-tetrakis(1H-benzimidazol-2yl)methyl)ethane-1,2-diamine ($H_4$EDTB) and N,N,N′,N′-tetrakis(1H-benzoimidazol-2ylmethyl)propane-1,3-diamine ($H_4$PDTB)) and preparation of their salts with various inorganic acids. This chapter also includes the characterization of the ligands and their salts by elemental analysis, FT-IR, crystal structure, colorimetric test and photo-physical properties and demonstrates the significant role of anions in their three dimensional structure.

**Results and discussion**

Ligands N,N,N',N'-tetrakis(1H-benzimidazol-2yl)methyl)ethane-1,2-diamine ($H_4$EDTB) and N,N,N′,N′-tetrakis(1H-benzoimidazol-2ylmethyl)propane-1,3-diamine ($H_4$PDTB) were synthesized by using 1,2-diaminoethane-N,N,N',N' tetra acetic acid and 1,3-diaminopropane-N,N,N',N' tetra acetic acid respectively by the reported procedure in the literature [49] (Scheme 3.3).

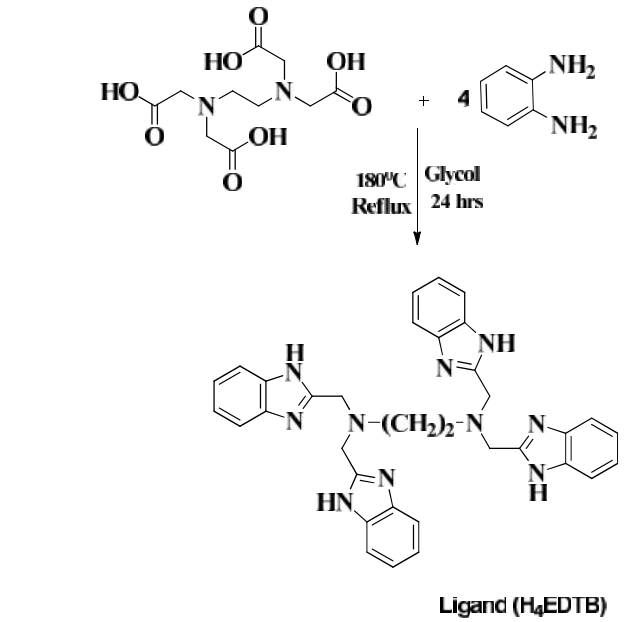


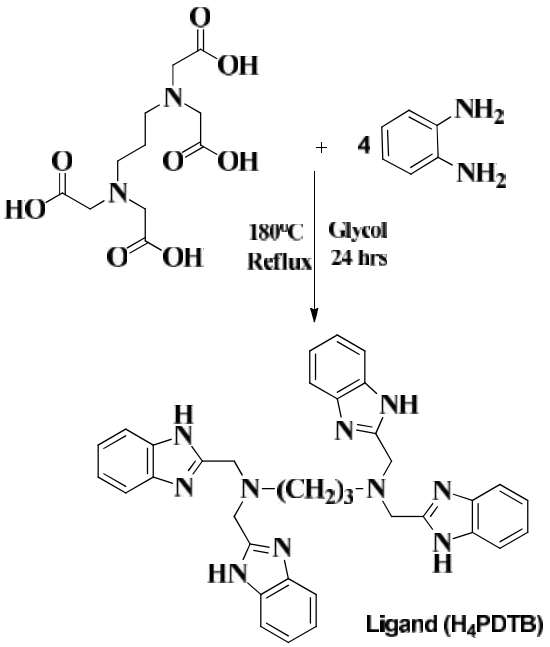


**A** **B**

**Scheme 3.3 Synthesis of $H_4$EDTB and $H_4$PDTB**

The reaction of N,N,N',N'-tetrakis(1H-benzimidazol-2yl)methyl)ethane-1,2-diamine ($H_4$EDTB) and N,N,N′,N′-tetrakis(1H-benzoimidazol-2ylmethyl)propane-1,3-diamine ($H_4$PDTB) with different inorganic acids i.e., $HClO_4$, HBr, HCl, HF, $HNO_3$, $H_3PO_4$, $CF_3COOH$ and $CH_3COOH$ in methanol/water/DMSO solution resulted in the formation of salts **3a-3k** and co-crystal **3e** (Scheme 3.4-3.5). The single crystals suitable for X-ray data collection were obtained by slow evaporation of solvent from reaction mixture. The different formulations were confirmed by elemental analysis, IR and crystallographic structure analyses of these salts.

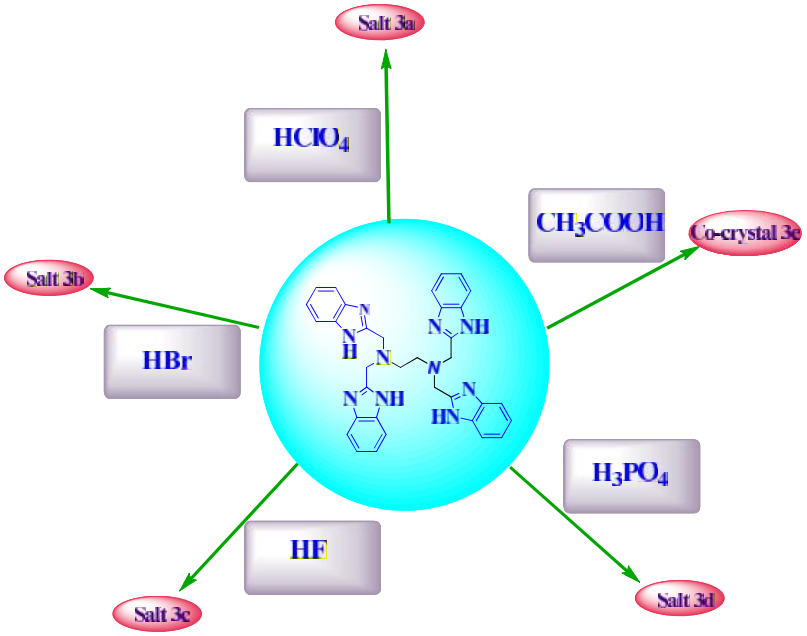


**Scheme 3.5** Preparation of salts derived from $H_4$EDTB

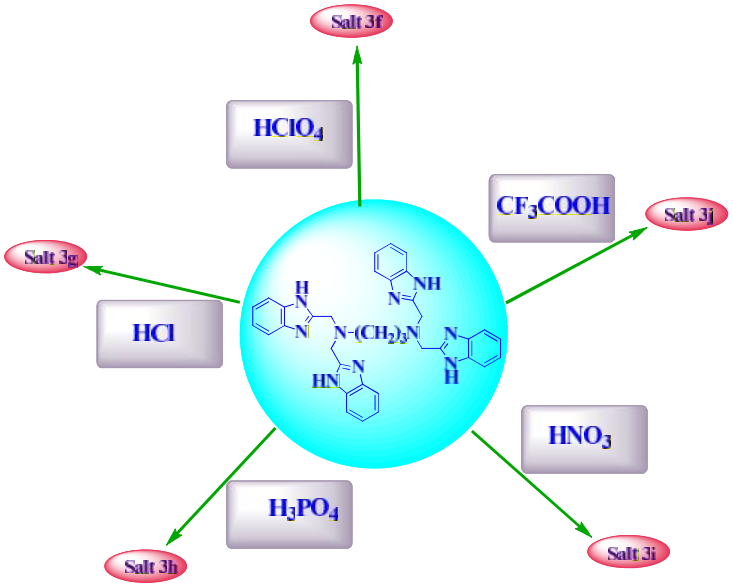


**Scheme 3.6** Preparation of salts derived from $H_4$PDTB

**Crystal structure of $[(H_8EDTB)^{4+}.4(ClO_4)^-.H_2O]$ (3a)**

Salt **3a** crystallizes in the triclinic crystal system P-1 space group. The asymmetric unit contains one protonated ligand $(H_8EDTB)^{4+}$ and four perchlorate anions along with four water molecules (Fig. 3.33) bonded together through a variety of hydrogen bonds (Fig. 3.34). Out of four perchlorate anions and water molecule, two are present on the symmetry axis. The proton has been transferred from the acid to the nitrogen bearing lone pair of electron resulting in the formation of salts. Since here four nitrogens are available, therefore four protons have been transferred from four acids. Hence the asymmetric unit consists of a protonated ligand with four positive charges and four perchlorate anions. The crystallographic data and structure refinement parameters are given in Table 3.1 and selected bond lengths and bond angles are summarized in Table 3.2. The selected hydrogen bonding data are summarized in Table 3.23. In the unit cell, deprotonated perchloric acid and protonated ligand form a cationic-anionic pair where all the imidazolium N-H as well as protonated N-H of ligand are involved in the hydrogen bonding with the oxygen of anion at their respective site. The two wings of the benzimidazole ring of the ligand are bridged by water and perchlorate molecule through N-H···O and C-H···O interactions on both side (N2-H2B···O9, 1.968(5); N4-H4B···O8, 1.972(3); C5-H5···O1, 2.680(3); C12-H12···O4, 2.638(3); C8-H8A···O3, 2.674(5); C8-H8B···O3, 3.476(5) Å) (Fig 3.35). The geometry around the chlorine in perchlorate is somewhat distorted tetrahedron with an average bond angle of 111.8 and 107.2 $^o$ (O4-Cl1-O3, 111.8(26); O2-Cl1-O3, 107.2(49); O4-Cl1-O2, 110.17(22); O1-Cl1-O2, 108.3(49); O5-Cl2-O6, 105.1(17); O5-Cl2-O7, 112.9(17); O5-Cl2-O8, 107.5(27); O6-Cl2-O8, 107.7(27); O7-Cl2-O8, 108.4(17)$^o$). The presence of different non-covalent interactions resulted in a continuous chain of perchlorate and water molecules that runs parallel on either side of the chain formed by the protonated ligands (Fig. 3.36).

**Crystal structure of $[(H_8EDTB)^{4+}.4(Br)^-.4DMSO]$ (3b)**

Salt **3b** crystallizes in the monoclinic crystal system with $P2_1/c$ space group. The asymmetric unit consists of a protonated ligand and four molecule of bromide anions and four dimethyl sulfoxide molecules (Fig. 3.37). The crystallographic data and structure refinement parameters are tabulated in Table 3.3 and selected bond lengths and bond angles are summarized in Table 3.4. The four protonated ligands interact with each other through C-H···π interaction. At one end the π electron density of phenyl ring

present on the ligand interact with the phenylic CH of the adjacent ligand molecule (C14-H14···π, 3.986(2) Å), however at the other end the π electron density of other phenyl ring present on the same ligand interacts with the hydrogen of dimethyl sulfoxide molecule (C21-H21···π, 3.468(5) Å). The oxygen of the same DMSO molecule interact via., N-H···O and C-H···O interaction (N1-H3A···O2, 1.895(3) C17-H17B···O2, 2429(5) Å) with the neighboring ligand molecule. All the interactions result in the formation of a cavity and is occupied by four molecules of bromide ion and four molecules of dimethyl sulfoxide through various non-covalent interactions (Fig. 3.38). The three dimensional host-guest packing of the salt **3b** is depicted in Figure 3.39.

**Crystal structure of $[2(H_7EDTB)^{3+}.3(SiF_6)^{2-}.14H_2O]$ (3c)**

Salt **3c** crystallizes in the triclinic crystal system with P-1 space group and its molecular structure is shown in Fig. 3.40. The asymmetric unit consists of two protonated ligands, six hexafluororo silicate anion and fourteen water molecules. The addition of HF to the aqueous-methanolic solution of ligand leads to the formation of $SiF_6^{2-}$ due to the corrosion effect of HF to the glass-vial [50]. In salt **3c**, unlike the above cases only three protons have been transferred instead of four from three benzimidazole nitrogen bearing lone pair of electrons. The crystallographic data and structure refinement parameters are given in Table 3.5 and selected bond lengths and bond angles are summarized in Table 3.6. The geometry around silicon in hexafluorosilicate ion is distorted octahedron with an average bond angle of 119.9$^o$ (F1-Si1-F2, 90.48(47); F1-Si1-F3, 90.40(47); F1-Si1-F4, 174.9(47): F1-Si1-F5, 85.00(60); F1-Si1-F6, 90.14(61); F2-Si1-F3, 102.10(61); F2-Si1-F4, 89.73(23); F2-Si1-F5, 170.40(62); F2-Si1-F6, 85.73(23); F3-Si1-F4, 94.48(12); F3-Si1-F5, 86.29(25); F3-Si1-F6, 172.00; F4-Si1-F5, 94.04(21); F4-Si1-F6, 84.85(45); F5-Si1-F6, 86.29(51)$^o$). Unlike salts **3a** and **3b** the molecular component of salt **3c** forms a pseudo cavity for trapping $SiF_6^{2-}$ ions. The distance of C-H···π interaction (π electron density of phenyl ring present on the ligand interact with the phenylic CH of the adjacent ligand molecule) in salt **3c** is found to be in the range of 4.4-4.7 Å (C13-H13··π, 4.764(3); C28-H28··π, 4.421(5) Å), which seems to be too large for the formation of a true cavity. Thus the pseudo cavity formed by ligand entrap single molecule of $SiF_6^{2-}$ through various N-H···F and C-H···F interactions (N1-H1···F9, 1.972(3); C2-H2···F8, 2.482(3); C17-H17···F9, 2.745(3); C25-H25A···F7, 2.693(3); C25-H25A···F9, 2.728(3) Å) (Fig. 3.41). The hexaflourosilicate anion and the water molecule form a

continuous chain through F-O interaction (Fig. 3.42). The cationic host assembly of protonated ligand in salt **3c** forms entirely different three dimensional packing as compared to salt **3a** and **3b** because of different orientation of the protonated ligand and $SiF_6^{2-}$ ions, and have both pseudo cavity as well as alternate channels as shown in Fig. 3.43.

**Crystal structure of $[(H_8EDTB)^{4+}.4(H_2PO_4)^{-}.2H_3PO_4]$ (3d)**

Salt **3d** crystallizes in the monoclinic crystal system with the space group $P2_1/n$. The asymmetric unit consists of a protonated ligand, three molecules of monohydrogen phosphate anion, three molecules of neutral phosphoric acid and two molecules of crystalline water (Fig. 3.44). The crystallographic data and structure refinement parameters are tabulated in Table 3.7 and selected bond lengths and bond angles are given in Table 3.8. In the unit cell, oxygens of monohydrogen phosphate, neutral phosphoric acids and water molecules are extensively involved in the hydrogen bonding with the protonated ligand (Fig. 3.45). The geometry around the phosphorus atom in phosphate anion is almost regular tetrahedron. The two phosphoric acid self-dimerized in $R_2^2(8)$ motif through O-H···O interactions (O9-H9···O21, 1.718(3) O23-H23A···O11, 1.719(2)Å, i.e., OH group of one dihydrogen phosphate interact with the oxygen of the other dihydrogen phosphate and vice-versa) as reported in other cases (Fig. 3.46 a) [51-52]. Along with dimerization, head-to-tail hydrogen bonding also exists in the same system (O18-H18···O10, 1.707(3)Å) (Fig. 3.46 b). The oxygen of water molecules bridge the two adjacent phosphate molecules and stabilizes the three dimensional herring bone type of packing as shown in Fig. 3.47.

**Crystal structure of $[H_4EDTB.2CH_3COOH]$ (3e)**

The co-crystal **3e** crystallizes in the triclinic crystal system with P-1 space group and its molecular structure is shown in Fig. 3.48. The asymmetric unit consists of a neutral ligand ($H_4EDTB$) and two acetic acid molecules. In co-crystal **3e**, unlike the above cases, no proton has been transferred from the acid to the ligand as a result both the neutral species crystallized simultaneously. The crystallographic data and structure refinement parameters are given in Table 3.9 and selected bond lengths and bond angles are summarized in Table 3.10. The carboxylate oxygens are extensively involved in various C-H···O interactions, the phenyl CH forms C-H···O interaction with the carboxylate oxygen atom of acetic acid (C17-H17B···02; 2.615(5)Å) (Fig. 3.49). Both the imidazolyl NH as well as the protonated NH are involved in N-H···O

hydrogen bonding with the carboxylate oxygen as well oxygens of water molecules. The four neutral ligand interact with each other through π···π and C-H···π interactions (C3-H3··π, 3.411(4); C4-H4··π, 3.691(7); C14-H14··π, 3.807(49); π···π, 3.411(4); π···π, 3.668(5) Å, the π electron density of phenyl ring present on ligand and adjacent phenylic CH) results in the formation of a cavity and the methylene C-H is also involved in C-H···π interaction (C8-H8··π, 3.040(2) Å) (Fig. 3.50). This cavity is occupied by two acetic acid molecules through various non-covalent interactions. The three dimensional packing of co-crystal **3e** is shown in Fig. 3.51.

**Crystal structure of $[(H_8PDTB)^{4+}.4(ClO_4)^{-}.H_2O]$ (3f)**

Salt **3f** crystallizes in orthorhombic crystal system with the space group Cmcm. The asymmetric unit contains a protonated ligand $(H_8PDTB)^{4+}$ and four perchlorate anions along with one water molecule (Fig. 3.52) bonded together through a variety of hydrogen bonds (Fig. 3.53). Out of four perchloric acid molecules, two are present on the symmetry axis. The proton has been transferred from the acid to the nitrogen bearing lone pair of electron. The asymmetric unit consists of a protonated ligand with four positive charge and four perchlorate anions as the four protons were transferred from four acids to four nitrogen atoms of the ligand. The crystallographic data and structure refinement parameters are given in Table 3.11 and selected bond lengths and bond angles are tabulated in Table 3.12. In the unit cell, deprotonated perchlorate anion and protonated ligand form a cationic-anionic pair, where all the imidazoloyl N-H as well as protonated N-H of ligand are involved in the N-H··O hydrogen bonding with the oxygen of anion at their respective site. The phenyl C-H of the benzimidazole ring also forms C-H··O interaction with the perchlorate oxygen atom. The geometry around the chlorine atom in perchlorate is somewhat distorted tetrahedron with an average bond angle of 114.38 and 106.85 ° (O4-Cl3-O4, 118.74(28); O6-Cl3-O5, 114.86(49); O4-Cl3-O5, 109.07(22); O5-Cl3-O6, 114.86(49); O3-Cl1-O1, 110.49(17); O3-Cl1-O1, 110.49(17); O1-Cl1-O2, 103.30(27); O2-Cl1-O1, 103.30(27); O3-Cl1-O1, 110.49(17)°). In a horizontal layer the phenyl C-H of benzimidazole ring interact through C-H··π interaction with the electron density of the phenyl ring of the adjacent ligand molecule (C2-H7··π, 3.799 Å). In a vertical chain, the imidzolium N-H interact with the π electron density of phenyl group of the benzimidazole ring (N-H··π, 3.799 Å). The presence of different non-covalent interactions resulted in cationic and anionic host-guest structure where the ligand formed three types of cavities for the guest perchlorate anion (Fig. 3.54). The diamond and the rectangular shaped cavities are

engaged with perchlorate anion whereas the third small size cavity was busy to entrap the water molecule. To the best of our knowledge, the existence of three different types of cavities in the same salt using benzimidazole and perchlorate anion is not available in the literature till today.

**Crystal structure of $[(H_8PDTB)^{4+}.4(Cl)^{-}.2H_2O]$ (3g)**

The hydrochloride salt of ligand $H_4$PDTB (salt **3g**), crystallizes in the orthorhombic crystal system with Fmm2 space group and its molecular structure is shown in Fig. 3.55. The asymmetric unit consists of one protonated ligand with four positive charge and four chloride anions. The proton was transferred from the HCl to the ligand. The crystallographic data and structure refinement parameters are given in Table 3.13 and selected bond lengths and bond angles are summarized in Table 3.14. Both the imidazoloyl NH as well as the protonated NH are available for extensive hydrogen bonding and involved in the principle N-H···Cl interaction (N1-H1···Cl1, 2.285(2); N2-H2B···Cl2, 1.952(3) Å) (Fig. 3.56). The chloride ion shows the primary N-H···Cl as well as secondary C-H···Cl interactions as reported earlier [53-56]. Similar to the previous case, salt **3g**, also has three types of cavities due to various non-covalent interactions (Fig. 3.57). The diamond and the rectangular shaped cavities are engaged in entrapping chloride ion whereas the third smaller one is vacant and can be used for trapping other suitable ions of appropriate size.

**Crystal structure of $[(H_8PDTB)^{4+}.2(H_2PO_4)^{-}.(H_7P_3O_{12})^{2-}.3H_3PO_4]$ (3h)**

Salt **3h** crystallizes in monoclinic crystal structure with the space group $P2_1/n$. The asymmetric unit consists of a protonated ligand, three molecules of monohydrogen phosphate, two molecules of dihydrogen phosphate anion and three molecule of phosphoric acid (Fig. 3.58). The crystallographic data and structure refinement parameters are given in Table 3.15 and selected bond lengths and bond angles are summarized in Table 3.16. In the unit cell, monohydrogen phosphate, dihydrogen phosphate and neutral phosphoric acid are extensively involved in the hydrogen bonding with the protonated ligand (Fig. 3.59). The geometry around the phosphorus in dihydrogen phosphate atom is regular tetrahedron. The two phosphoric acid self-dimerized in $R_2^2(8)$ motif through O-H···O interaction (O18-H18A···O25, 1.594 Å; O26-H26A···O17, 1.944 Å, i.e. OH group of one dihydrogen phosphate with the oxygen of the other dihydrogen phosphate and vice-versa) as reported in other cases

(Fig. 3.60) [51, 57-60]. The presence of head-to-tail hydrogen bonding results in a stack of phosphate anion with alternate O-H···O interaction resulting in an entirely different type of three dimensional packing as alternate channels of monohydrogen phosphate, dihydrogen phosphate, neutral phosphoric acid and protonated ligands (Fig. 3.61).

**Crystal structure of [$(H_8PDTB)^{4+}.4(NO_3)^-$] (3i)**

Salt **3i** crystallizes in the monoclinic crystal system with $P2_1/c$ space group and the unit cell consists of protonated ligand and four molecules of nitrate anion (Fig. 3.62). The geometry around the nitrogen in nitrate ion is trigonal planar with an average bond angle of 119.90° (O3-N11-O2, 120.01(47); O1-N11-O2, 119.74(47); O3-N11-O1, 120.22(47); O6-N12-O4, 116.75(60); O4-N12-O5, 119.95(61); O5-N12-O6, 123.29(61); O9-N13-O7, 120.37(57); O7-N13-O8, 121.38(49); O9-N13-O8, 118.24(50); O11-N14-O10, 143.75(104); O10-N14-O12, 99.42(83); O11-N14-O12, 116.80(92)°). The crystallographic data and structure refinement parameters are given in Table 3.17 and selected bond lengths and bond angles are summarized in Table 3.18. Similar to the above cases, both the imidazolyl NH as well as the protonated NH are involved in hydrogen bonding with the nitrate oxygen. The phenyl CH of benzimidazole ring are also involved in hydrogen bonding through C-H···O interaction (C2-H2···O2, 3.058(6); C15-H15···O5, 2.567(6) Å)) (Fig. 3.63). The cationic host assembly of ligand in salt **3i** forms neither cavity nor channels (Fig. 3.64) as compared to the three dimensional packing in above salts because of the different orientation of the protonated ligand and the nitrate anions.

**Crystal structure of [$2(H_5PDTB)^+.2(CF_3COO)^-.5H_2O$] (3j)**

The salt **3j** crystallizes in the triclinic crystal system with P-1 space group and its molecular structure is shown in Fig. 3.65. The asymmetric unit consists of two protonated ligands $(H_5PDTB)^+$, two triflouroacetate anions and five water molecules. In salt **3j**, unlike above cases only one proton has been transferred to one nitrogen, out of four benzimidazole nitrogens bearing lone pair of electrons. The crystallographic data and structure refinement parameters are given in Table 3.19 and selected bond lengths and bond angles are tabulated in Table 3.22. The phenyl CH forms C-H···F interaction with the flouro group of triflouroacetate anion (C31–H34···F3, 2.526(3) A°) (Fig. 3.66). The water molecules present in the lattice as well as the carboxylate oxygen atoms are extensively involved in C-H···O interactions. Both the imidazolyl NH as well as the protonated NH are involved in N-H···Ohydrogen bonding with the carboxylate oxygen

as well oxygen atoms of water molecules. In salt **3j**, also, no regular pattern (Fig. 3.67) was observed in the three dimensional packing.

**Anion Selectivity**

Both the ligands N,N,N',N'-tetrakis(1H-benzimidazol-2yl)methyl)ethane-1,2-diamine ($H_4$EDTB) and ligand N,N,N′,N′-tetrakis(1H-benzoimidazol-2ylmethyl)propane-1,3-diamine ($H_4$PDTB), have strong tendency to form salts with different anions. An attempt has been made to test the selectivity of these ligands by performing a particular experiment under the same reaction condition in which various salts were prepared.

Thus an aqueous methanolic solution containing one equivalent of the ligand N,N,N',N'-tetrakis(1H-benzimidazol-2yl)methyl)ethane-1,2-diamine ($H_4$EDTB) was added to a solution containing one equivalent (1.0 mmol) of each of $HClO_4$, HBr, HF, $H_3PO_4$ and $CH_3COOH$. Suitable crystals were obtained by slow evaporation and subjected to characterization by single crystal X-ray method. The single crystal X-ray data clearly indicates ($a$=9.29(3) Å; $b$=11.49(3) Å; $c$=12.15(4) Å; $\alpha$=86.10; $\beta$=89.93; $\gamma$=66.99 deg; $V$=1173.0(6) Å$^3$) that in the mixture of the acids, the ligand was superiorly selective for perchloric acid because of the extensive electrostatic as well as non-covalent interactions.

Similar test was also performed for N,N,N′,N′-tetrakis(1H-benzoimidazol-2ylmethyl)propane-1,3-diamine ($H_4$PDTB) with one equivalent of all acids, which results in the formation of salt $[(H_8PDTB)^{4+}.3(ClO_4)^{-}.(H_2PO_4)^{-}]$ (**3k**). Suitable crystals of salt **3k** were obtained by slow evaporation and characterized via single crystal X-ray diffraction. The asymmetric unit of salt **3k** consists of protonated ligand $(H_8PDTB)^{4+}$, three molecules of perchlorate, and one molecule of dihydrogen phosphate anion (Fig. 3.68). The three protons from three perchloric acid molecules, and one from phosphoric acid were transferred to all four nitrogen of benzimidazole ring having lone pair of electron. All the oxygen of phosphate and perchlorate anions are widely involved in hydrogen bonding with the imidazolyl NH as well as the protonated NH. The phenyl CH also forms C-H···O interaction with the oxygen of phosphate and perchlorate anions (Fig. 3.69). The three-dimensional packing of salt **3k** is shown in Fig. 3.70. The above results suggest that the ligand is selective for both the perchlorate as well as phosphate anion. Furthermore an experiment was performed to know the exact selectivity of the ligand ($H_4$PDTB). The solution containing one equivalent of $HClO_4$ and $H_3PO_4$ were added to the aqueous methanolic solution containing one equivalent of the ligand

($H_4$PDTB) under the same experimental conditions. The single crystal X-ray data of resultant salt shows the asymmetric unit cell with $a$=17.3101(4) Å; $b$= 10.8324(4) Å; $c$= 24.4325(7) Å; $\alpha$= $\beta$= $\gamma$= 90.00 deg; $V$= 4623.3(2) Å$^3$, parameters, which clearly indicate that in the mixture of above acids, the ligand was superiorly selective for perchlorate anions [61-62].

**Colorimetric Test**

The induced signal in terms of color change due to the presence of anions has received a great interest, because the fluorophore needs no equipment and the detection can be achieved by the naked eye. In the naked-eye colorimetric experiment, the ligand undergoes a dramatic color change. One of the most attractive approaches in this field involves the construction of colorimetric chemo-sensors, since the naked eye detection can offer a qualitative and quantitative information [63]. Most of the known colorimetric chemo-sensors are based on the synthetic receptors generally containing some combination of anion binding unit and signal-reporting group (chromophore), either covalently attached or intermolecularly linked [64].

The methanolic solutions of the ligands ($H_4$EDTB and $H_4$PDTB) are orange-red in color but after addition of the acids the color changes to light blue to dark blue (Fig. 3.71-3.72). In order to understand the factor responsible for the colorimetric change, another experiment was performed. A solution containing one equivalent (1.0 mmol) of NaCl was added to the aqueous methanolic solution containing one equivalent of the ligand under the same experimental conditions and no color change was observed. This suggests that the protonation of ligand is basically responsible for the color change, because the protonation of ligands enhances the conjugation and simultaneously color change too.

**Powder XRD**

The structural homogeneity of bulk samples were also examined through a comparison of experimental and simulated powder X-ray diffraction (XRD) patterns. The experimental patterns correlate favorably with the simulated ones generated from single-crystal X-ray diffraction (Fig. 3.73).

**Fluorescence Study**

The change in the photophysical properties of the ligand ($H_4$EDTB and $H_4$PDTB) and their respective salts were observed in the UV-Vis absorption and fluorescence spectra. The UV-Vis absorption spectra of ligand ($H_4$EDTB) showed two

peaks at 230 and 270 nm, however the ligand ($H_4$PDTB) gave at 290 nm (Fig. 3.74-3.75). The trend for the neutral ligand ($H_4$EDTB) as well as for the co-crystal **3e** was found to be same, however drastic change was observed in case of salts **3a-3d** (Fig. 3.76). In case of ligand ($H_4$PDTB) and their salts similar pattern was observed except for salt **3h** (Fig. 3.77).

**Conclusion**

The present chapter reports the anion directed supramolecular frame work which involves a change in the number and type of interactions and the orientation of the molecules in the three dimensional space. The benzimidazole molecules hold different anions and neutral acid molecules by different type of interactions. Their angle and orientation in three dimensional space is very important for deciding the formation of cavity or pseudo cavity or alternate channel or herring-bone network as depicted in salt **3a-3e**. In salts **3f-3g**, the perchlorate and chloride anions reside in the cavity, whereas in salt **3h,** the protonated ligand and the phosphate anions forms alternate channels and the anions are sandwiched between two channels of host protonated ligand. In case of salts **3i-3j** the cavity as well as the channel disappears and no pattern was observed. To the best of our knowledge, this is the first example of the organic molecule ($H_4$PDTB) used as receptor for both perchlorate as well as phosphate simultaneously as in case of salt **3k.** In conclusion, it has been demonstrated that the variation of anion plays a significant role in controlling the structure of the salts. Addition of inorganic acids to the ligand results in the color change, where the protonation of the ligand plays an important role.

**Table 3.1: Crystal data and structure refinement for $[(H_8EDTB)^{4+}.4(ClO_4)^{-}.H_2O]$ (3a)**

| | |
|---|---|
| Empirical formula | $C_{34}H_{36}Cl_4N_{10}O_{20}$ |
| Color | White |
| Formula weight (g $mol^{-1}$) | 1046.53 |
| Crystal System | Triclinic |
| Space Group | P-1 |
| a (Å) | 9.327(3) |
| b (Å) | 11.496(3) |
| c (Å) | 12.090(3) |
| α ($^0$) | 93.384(16) |
| β($^0$) | 90.600(16) |
| γ ($^0$) | 112.474(14) |
| V ($Å^3$) | 1195.0(6) |
| Crystal size (mm) | 0.30 x 0.27 x 0.21 |
| Z | 1 |
| $\rho_{calcd}$ (g $m^{-3}$) | 1.454 |
| μ | 0.332 |
| F (000) | 538.0 |
| θ range for data collection | 2.71-31.49 |
| No. of measured reflections | 3065 |
| No. of observed reflections | 1902 |
| Data/ restraints/parameters | 3853/0/307 |
| R1(I>2σ(I)) | 0.0893 |
| R1 (all data) | 0.1331 |
| wR2(I>2σ(I)) | 0.2709 |
| wR2 (all data) | 0.2996 |

**Table 3.2: Selected bond distances (Å) and bond angles ($^{o}$) for $[(H_8EDTB)^{4+}.4(ClO_4)^{-}.H_2O]$ (3a)**

| | | | |
|---|---|---|---|
| **Bond Distances** | | | |
| **Bond Distances** | | | |
| Cl1-O1 | 1.397(6) | Cl1-O4 | 1.403(5) |
| Cl1-O2 | 1.425(5) | Cl1-O3 | 1.435(5) |
| Cl2-O8 | 1.226(9) | Cl2-O6 | 1.275(7) |
| Cl2-O7 | 1.379(5) | Cl2-O5 | 1.431(5) |
| N3-C10 | 1.324(7) | N3-C11 | 1.378(7) |
| N2-C7 | 1.328(7) | N2-C6 | 1.399(6) |
| N5-C9 | 1.464(6) | N5-C8 | 1.465(6) |
| N5-C17 | 1.484(5) | N1-C7 | 1.332(6) |
| N1-C1 | 1.386(8) | N4-C10 | 1.352(6) |
| N4-C16 | 1.372(7) | C10-C9 | 1.472(8) |
| **Bond Angles** | | | |
| O1-Cl1-O4 | 108.4(4) | O1-Cl1-O2 | 110.0(3) |
| O4-Cl1-O2 | 110.1(3) | O1-Cl1-O3 | 111.8(4) |
| O4-Cl1-O3 | 107.2(3) | O2-Cl1-O3 | 109.3(3) |
| O8-Cl2-O6 | 107.6(14) | O8-Cl2-O7 | 108.6(7) |
| O6-Cl2-O7 | 114.7(7) | O8-Cl2-O5 | 107.5(8) |
| O6-Cl2-O5 | 105.1(4) | O7-Cl2-O5 | 113.0(4) |
| C10-N3-C11 | 111.1(4) | C7-N2-C6 | 109.6(4) |
| C9-N5-C8 | 108.8(4) | C9-N5-C17 | 111.0(3) |
| C8-N5-C17 | 112.1(4) | C7-N1-C1 | 109.3(6) |
| C10-N4-C16 | 111.3(4) | N3-C10-N4 | 106.0(5) |

**Table 3.3: Crystal data and structure refinement for $[(H_8EDTB)^{4+}.4(Br)^{-}.4DMSO]$ (3b)**

| | |
|---|---|
| Empirical formula | $C_{42}H_{60}S_4N_{10}O_4Br_4S_4$ |
| Color | Blue |
| Formula weight (g $mol^{-1}$) | 1216.88 |
| Crystal System | Monoclinic |
| Space Group | $P2_1/c$ |
| a (Å) | 9.674(2) |
| b (Å) | 24.767(5) |
| c (Å) | 10.982(2) |
| α ($^0$) | 90.00 |
| β($^0$) | 90.232(10) |
| γ ($^0$) | 90.00 |
| V ($Å^3$) | 2631.2(9) |
| Crystal size (mm) | 0.23 x 0.20 x 0.17 |
| Z | 2 |
| $\rho_{calcd}$ (g $m^{-3}$) | 1.536 |
| μ | 3.267 |
| F (000) | 1236.0 |
| θ range for data collection | 2.18-29.73 |
| No. of measured reflections | 7248 |
| No. of observed reflections | 5559 |
| Data/ restraints/parameters | 7003/0/293 |
| R1(I>2σ(I)) | 0.073 |
| R1 (all data) | 0.102 |
| wR2(I>2σ(I)) | 0.200 |
| wR2 (all data) | 0.217 |

**Table 3.4: Selected bond distances (Å) and bond angles (°) for $[(H_8EDTB)^{4+}.4(Br)^{-}.4DMSO]$ (3b)**

| | | | |
|---|---|---|---|
| **Bond Distances** | | | |
| S1-O1 | 1.5198(19) | S1-C19 | 1.781(3) |
| S1-C18 | 1.786(3) | S2-O2 | 1.5084(19) |
| S2-C21 | 1.780(3) | S2-C20 | 1.788(3) |
| N1-C7 | 1.325(3) | N1-C1 | 1.393(3) |
| N1-H1 | 0.8600 | N2-C7 | 1.333(3) |
| N2-C6 | 1.388(3) | N2-H2A | 0.8600 |
| N3-C10 | 1.327(3) | N3-C11 | 1.390(3) |
| N3-H3A | 0.8600 | N4-C10 | 1.337(3) |
| N4-C16 | 1.396(3) | N4-H4A | 0.8600 |
| **Bond Angles** | | | |
| O1-S1-C19 | 105.56(12) | O1-S1-C18 | 105.79(12) |
| C19-S1-C18 | 98.38(14) | O2-S2-C21 | 106.12(12) |
| O2-S2-C20 | 106.27(12) | C21-S2-C20 | 96.64(15) |
| C7-N1-C1 | 108.6(2) | C7-N1-H1 | 125.7 |
| C1-N1-H1 | 125.7 | C7-N2-C6 | 108.7(2) |
| C7-N2-H2A | 125.7 | C6-N2-H2A | 125.7 |
| C10-N3-C11 | 109.6(2) | C10-N3-H3A | 125.2 |
| C11-N3-H3A | 125.2 | C10-N4-C16 | 108.75(19) |
| C10-N4-H4A | 125.6 | C16-N4-H4A | 125.6 |

**Table 3.5: Crystal data and structure refinement for $[2(H_7EDTB)^{3+}.3(SiF_6)^{2-}.14H_2O]$ (3c)**

| | |
|---|---|
| Empirical formula | $C_{68}H_{70}F_{18}N_{20}O_{14}Si_3$ |
| Color | White |
| Formula weight (g $mol^{-1}$) | 1817.71 |
| Crystal System | Triclinic |
| Space Group | P-1 |
| a (Å) | 8.9116(3) |
| b (Å) | 14.9883(4) |
| c (Å) | 16.2263(4) |
| α ($^0$) | 107.941(2) |
| β($^0$) | 94.4870(10) |
| γ ($^0$) | 97.4300(10) |
| V ($Å^3$) | 2028.56(10) |
| Crystal size (mm) | 0.26 x 0.18 x 0.14 |
| Z | 1 |
| $\rho_{calcd}$ (g $m^{-3}$) | 1.488 |
| μ | 0.174 |
| F (000) | 934.0 |
| θ range for data collection | 1.92-28.58 |
| No. of measured reflections | 7159 |
| No. of observed reflections | 4885 |
| Data/ restraints/parameters | 7148/3/556 |
| R1(I>2σ(I)) | 0.044 |
| R1 (all data) | 0.059 |
| wR2(I>2σ(I)) | 0.117 |
| wR2(all data) | 0.133 |

**Table 3.6: Selected bond distances (Å) and bond angles ($^{o}$) for $[2(H_7EDTB)^{3+}.3(SiF_6)^{2-}.14H_2O]$ (3c)**

| | | | |
|---|---|---|---|
| **Bond Distances** | | | |
| C1-C6 | 1.385(5) | C1-C2 | 1.385(6) |
| C1-N1 | 1.390(5) | C2-C3 | 1.388(6) |
| C3-C4 | 1.378(7) | C4-C5 | 1.384(7) |
| C5-C6 | 1.393(6) | C6-N2 | 1.387(6) |
| C7-N2 | 1.322(5) | C7-N1 | 1.334(5) |
| C7-C8 | 1.486(6) | C8-N9 | 1.457(5) |
| C9-N9 | 1.456(5) | C9-C10 | 1.491(6) |
| C10-N4 | 1.328(6) | C10-N3 | 1.333(5) |
| C11-C12 | 1.377(6) | C11-N3 | 1.385(5) |
| **Bond Angles** | | | |
| C6-C1-C2 | 122.0(4) | C6-C1-N1 | 106.1(3) |
| C2-C1-N1 | 132.0(4) | C4-C3-C2 | 122.5(5) |
| C1-C2-C3 | 115.7(4) | C3-C4-C5 | 122.0(5) |
| C4-C5-C6 | 115.8(4) | C1-C6-N2 | 106.3(4) |
| C1-C6-C5 | 122.0(4) | N2-C6-C5 | 131.7(4) |
| N2-C7-N1 | 108.7(4) | N2-C7-C8 | 124.9(4) |
| N1-C7-C8 | 126.4(4) | N9-C8-C7 | 111.5(3) |
| N9-C9-C10 | 111.5(3) | N4-C10-N3 | 108.0(4) |
| N4-C10-C9 | 124.3(4) | N3-C10-C9 | 127.4(4) |
| C12-C11-N3 | 132.8(4) | C12-C11-C16 | 121.1(4) |

**Table 3.7: Crystal data and structure refinement for $[(H_8EDTB)^{4+}.4(H_2PO_4)^-.2H_3PO_4]$ (3d)**

| | |
|---|---|
| Empirical formula | $C_{34}H_{49}N_{10}O_{25.98}P_6$ |
| Color | White |
| Formula weight (g $mol^{-1}$) | 1199.33 |
| Crystal System | Monoclinic |
| Space Group | $P2_1/c$ |
| a (Å) | 14.2830(4) |
| b (Å) | 16.7711(4) |
| c (Å) | 21.1030(5) |
| α ($^0$) | 90.00 |
| β($^0$) | 96.502(2) |
| γ ($^0$) | 90.00 |
| V ($Å^3$) | 5022.5(2) |
| Crystal size (mm) | 0.31 x 0.27 x 0.23 |
| Z | 4 |
| $\rho_{calcd}$ (g $m^{-3}$) | 1.586 |
| μ | 0.312 |
| F (000) | 2483.4 |
| θ range for data collection | 2.20-28.36 |
| No. of measured reflections | 12339 |
| No. of observed reflections | 8595 |
| Data/ restraints/parameters | 12230/0/699 |
| R1(I>2σ(I)) | 0.076 |
| R1 (all data) | 0.133 |
| wR2(I>2σ(I)) | 0.192 |
| wR2(all data) | 0.231 |

**Table 3.8: Selected bond distances (Å) and bond angles ($^{o}$) for $[(H_8EDTB)^{4+}.4(H_2PO_4)^{-}.2H_3PO_4]$ (3d)**

| | | | |
|---|---|---|---|
| **Bond Distances** | | | |
| P1-O4 | 1.495(3) | P1-O3 | 1.526(2) |
| P1-O1 | 1.537(2) | P1-O2 | 1.546(3) |
| P2-O5 | 1.420(4) | P2-O6 | 1.445(4) |
| P2-O7 | 1.469(4) | P2-O8 | 1.550(3) |
| P3-O10 | 1.484(3) | P3-O9 | 1.524(3) |
| P3-O11 | 1.539(2) | P3-O12 | 1.575(3) |
| P4-O14 | 1.492(3) | P4-O15 | 1.512(3) |
| P4-O13 | 1.554(3) | P4-O16 | 1.565(3) |
| P5-O20 | 1.486(3) | P5-O19 | 1.515(3) |
| P5-O18 | 1.540(3) | P5-O17 | 1.561(3) |
| **Bond Angles** | | | |
| O4-P1-O3 | 115.10(16) | O4-P1-O1 | 109.51(14) |
| O3-P1-O1 | 104.28(16) | O4-P1-O2 | 107.98(15) |
| O3-P1-O2 | 110.52(16) | O5-P2-O6 | 114.5(4) |
| O1-P1-O2 | 109.32(16) | O5-P2-O7 | 109.0(4) |
| O6-P2-O7 | 108.0(5) | O5-P2-O8 | 114.2(2) |
| O6-P2-O8 | 109.3(3) | O7-P2-O8 | 100.7(3) |
| O10-P3-O9 | 111.91(16) | O10-P3-O11 | 109.89(17) |
| O9-P3-O11 | 110.78(14) | O10-P3-O12 | 111.61(19) |
| O9-P3-O12 | 104.39(16) | O14-P4-O15 | 116.49(19) |
| O11-P3-O12 | 108.10(15) | O14-P4-O13 | 108.60(14) |

**Table 3.9: Crystal data and structure refinement for [$H_4$EDTB.2$CH_3COOH$] (3e)**

| | |
|---|---|
| Empirical formula | $C_{38}H_{40}N_{10}O_{3.70}$ |
| Color | White |
| Formula weight (g $mol^{-1}$) | 696.06 |
| Crystal System | Triclinic |
| Space Group | P-1 |
| a (Å) | 9.4045(3) |
| b (Å) | 10.1006(4) |
| c (Å) | 10.6257(4) |
| α ($^0$) | 101.059(2) |
| β($^0$) | 100.153(2) |
| γ ($^0$) | 109.647(2) |
| V (Å$^3$) | 900.72(6) |
| Crystal size (mm) | 0.31 x 0.25 x 0.21 |
| Z | 1 |
| $\rho_{calcd}$ (g $m^{-3}$) | 1.283 |
| μ | 0.086 |
| F (000) | 367.6 |
| θ range for data collection | 2.87-31.59 |
| No. of measured reflections | 3719 |
| No. of observed reflections | 1847 |
| Data/ restraints/parameters | 3670/0/250 |
| R1(I>2σ(I)) | 0.081 |
| R1 (all data) | 0.164 |
| wR2(I>2σ(I)) | 0.194 |
| wR2(all data) | 0.230 |

**Table 3.10: Selected bond distances (Å) and bond angles ($^{o}$) for [$H_4$EDTB.2$CH_3$COOH] (3e)**

| | | | |
|---|---|---|---|
| **Bond Distances** | | | |
| O1-C19 | 1.170(4) | N1-C7 | 1.336(4) |
| N2-C7 | 1.324(4) | N2-C6 | 1.402(4) |
| N1-C1 | 1.379(4) | N1-H1B | 0.8600 |
| O2-C19 | 1.294(5) | O2-H15A | 0.89(7) |
| N3-C10 | 1.314(4) | N3-C11 | 1.397(4) |
| N4-C10 | 1.347(4) | N4-C16 | 1.395(4) |
| N4-H4B | 0.8600 | N5-C9 | 1.455(4) |
| N5-C17 | 1.462(4) | N5-C8 | 1.466(4) |
| **Bond Angles** | | | |
| C19-O2-H15A | 105(4) | C7-N1-C1 | 108.0(2) |
| C7-N1-H1B | 126.0 | C1-N1-H1B | 126.0 |
| C7-N2-C6 | 104.4(3) | C10-N3-C11 | 105.3(3) |
| C10-N4-C16 | 107.0(3) | C10-N4-H4B | 126.5 |
| C16-N4-H4B | 126.5 | C9-N5-C17 | 110.5(2) |
| C9-N5-C8 | 109.6(2) | C17-N5-C8 | 112.2(2) |
| N1-C1-C6 | 105.2(3) | N1-C1-C2 | 132.5(3) |
| C6-C1-C2 | 122.3(3) | C3-C2-C1 | 116.8(4) |
| C3-C2-H2 | 121.6 | C1-C2-H2 | 121.6 |

**Table 3.11: Crystal data and structure refinement for $[(H_8PDTB)^{4+}.4(ClO_4)^{-}.H_2O]$ (3f)**

| | |
|---|---|
| Empirical formula | $C_{35}\ H_{38}Cl_4N_{10}O_{17}$ |
| Color | Colorless |
| Formula weight (g $mol^{-1}$) | 1012.55 |
| Crystal System | Orthorhombic |
| Space Group | cmcm |
| a (Å) | 17.4081(4) |
| b (Å) | 10.8627(4) |
| c (Å) | 24.4693(7) |
| α ($^0$) | 90 |
| β($^0$) | 90 |
| γ ($^0$) | 90 |
| V ($Å^3$) | 4627.1(2) |
| Crystal size (mm) | 0.25 x 0.23 x 0.21 |
| Z | 4 |
| $\rho_{calcd}$ (g $m^{-3}$) | 1.454 |
| μ | 0.336 |
| F (000) | 2088.0 |
| θ range for data collection | 1.66- 26.53 |
| No. of measured reflections | 10817 |
| No. of observed reflections | 6528 |
| Data/restraints/parameters | 10817/0/736 |
| *$R1^b$ (I>2σ(I)) | 0.0795 |
| R1 ( all data) | 0.2450 |
| *$wR2^c$(I>2σ(I)) | 0.1080 |
| wR2( all data) | 0.246 |

**Table 3.12: Selected bond distances (Å) and bond angles ($^{o}$) for $[(H_8PDTB)^{4+}.4(ClO_4)^{-}.H_2O]$ (3f)**

| | | | |
|---|---|---|---|
| **Bond Distances** | | | |
| N1-C7 | 1.329(4) | N1-C1 | 1.388(4) |
| N1-H1 | 0.8599 | N2-C7 | 1.326(4) |
| N2-C6 | 1.370(5) | N2-H2 | 0.8600 |
| N3-C8 | 1.458(4) | N3-C8 | 1.458(4) |
| N3-C9 | 1.471(6) | C1-C6 | 1.379(5) |
| C1-C2 | 1.390(5) | C2-C3 | 1.368(6) |
| C2-H7 | 0.9300 | C3-C4 | 1.382(7) |
| C3-H6 | 0.9300 | C4-C5 | 1.378(7) |
| C4-H5 | 0.9300 | C5-C6 | 1.394(5) |
| **Bond Angles** | | | |
| C7-N1-C1 | 109.3(3) | C7-N1-H1 | 125.3 |
| C1-N1-H1 | 125.5 | C7-N2-C6 | 110.0(3) |
| C7-N2-H2 | 124.9 | C6-N2-H2 | 125.1 |
| C8-N3-C8 | 109.3(4) | C8-N3-C9 | 113.6(3) |
| C8-N3-C9 | 113.6(3) | C6-C1-N1 | 106.1(3) |
| C6-C1-C2 | 122.2(3) | N1-C1-C2 | 131.7(3) |
| C3-C2-C1 | 116.1(4) | C3-C2-H7 | 122.0 |
| C1-C2-H7 | 122.0 | C2-C3-C4 | 122.3(4) |
| C2-C3-H6 | 118.8 | C4-C3-H6 | 118.8 |

**Table 3.13: Crystal data and structure refinement for $[(H_8PDTB)^{4+}.4(Cl)^{-}.2H_2O]$ (3g)**

| | |
|---|---|
| Empirical formula | $C_{35}H_{38}Cl_4N_{10}O_2$ |
| Color | Colourless |
| Formula weight (g $mol^{-1}$) | 772.55 |
| Crystal System | Orthorhombic |
| Space Group | Fmm2 |
| a (Å) | 25.7225(11) |
| b (Å) | 30.2444(12) |
| c (Å) | 4.7662(2) |
| α ($^0$) | 90.00 |
| β($^0$) | 90.00 |
| γ ($^0$) | 90.00 |
| V ($Å^3$) | 3707.9(3) |
| Crystal size (mm) | 0.25 x 0.22 x 0.20 |
| Z | 4 |
| $\rho_{calcd}$ (g $m^{-3}$) | 1.384 |
| μ | 0.367 |
| F (000) | 832 |
| θ range for data collection | 1.35- 26.36 |
| No. of measured reflections | 2461 |
| No. of observed reflections | 2006 |
| Data/restraints/parameters | 2461/0/128 |
| R1(I>2σ(I)) | 0.040 |
| R1 (all data) | 0.052 |
| wR2(I>2σ(I)) | 0.136 |
| wR2 (all data) | 0.153 |

**Table 3.14: Selected bond distances (Å) and bond angles ($^{o}$) for [$(H_8PDTB)^{4+}$.4$(Cl)^{-}$ .2$H_2O$] (3g)**

| | | | |
|---|---|---|---|
| **Bond Distances** | | | |
| C1-N2 | 1.373(7) | C7-N1 | 1.323(7) |
| C1-C6 | 1.388(8) | C7-C8 | 1.488(8) |
| C1-C2 | 1.389(8) | C7-N2 | 1.318(7) |
| C8-N3 | 1.444(6) | C6-N1 | 1.391(8) |
| C6-C5 | 1.381(8) | C5-C4 | 1.372(10) |
| C2-C3 | 1.366(8) | C3-C4 | 1.423(10) |
| N3-C8 | 1.444(6) | N3-C9 | 1.488(9) |
| C9-C10 | 1.508(9) | C10-C9 | 1.508(9) |
| **Bond Angles** | | | |
| N2 C1 C6 | 108.2(5) | N2-C1-C2 | 131.6(5) |
| C6 C1 C2 | 120.2(5) | N2-C7-N1 | 111.2(5) |
| N2 C7 C8 | 124.4(5) | N1-C7-C8 | 124.4(5) |
| N3 C8 C7 | 111.2(4) | C5-C6-C1 | 123.3(6) |
| C5 C6 N1 | 131.6(6) | C1-C6-N1 | 105.1(5) |
| C4 C5 C6 | 116.1(6) | C3-C2-C1 | 117.9(6) |
| C2 C3 C4 | 120.8(6) | C5-C4-C3 | 121.7(6) |
| C7 N2 C1 | 107.3(5) | C7-N1-C6 | 108.2(5) |

**Table 3.15: Crystal data and structure refinement for $[(H_8PDTB)^{4+}.2(H_2PO_4)^{-}.(H_7P_3O_{12})^{2-}.3H_3PO_4]$ (3h)**

| | |
|---|---|
| Empirical formula | $C_{35}H_{58}N_{10}O_{32}P_8$ |
| Color | Blue |
| Formula weight (g $mol^{-1}$) | 1378.67 |
| Crystal System | Monoclinic |
| Space Group | $P2_1/n$ |
| a (Å) | 14.2634(9) |
| b (Å) | 24.5799(18) |
| c (Å) | 15.9232(12) |
| α ($^0$) | 90 |
| β($^0$) | 91.822(3) |
| γ ($^0$) | 90 |
| V ($Å^3$) | 5579.7(7) |
| Crystal size (mm) | 0.21 x 0.19 x 0.17 |
| Z | 4 |
| $\rho_{calcd}$ (g $m^{-3}$) | 1.641 |
| μ | 0.355 |
| F (000) | 302 |
| θ range for data collection | 2.19 -30.68 |
| No. of measured reflections | 4249 |
| No. of observed reflections | 3548 |
| Data/restraints/parameters | 11551/0/846 |
| R1(I>2σ(I)) | 0.039 |
| R1 (all data) | 0.049 |
| wR2(I>2σ(I)) | 0.134 |
| wR2(all data) | 0.151 |

**Table 3.16: Selected bond distances (Å) and bond angles ($^{o}$) for $[(H_8PDTB)^{4+}.2(H_2PO_4)^{-}.(H_7P_3O_{12})^{2-}.3H_3PO_4]$ (3h)**

| | | | |
|---|---|---|---|
| **Bond Distances** | | | |
| P1-O1 | 1.4933(19) | P1-O4 | 1.5242(19) |
| P1-O3 | 1.547(2) | P4-O13 | 1.497(2) |
| P1-O2 | 1.580(2) | P4-O16 | 1.525(2) |
| P4-O14 | 1.541(2) | P4-O15 | 1.561(2) |
| P5-O17 | 1.489(2) | P5-O18 | 1.536(2) |
| P5-O19 | 1.536(3) | P5-O20 | 1.539(2) |
| P6-O21 | 1.491(3) | N6-C24 | 1.389(4) |
| N6-C18 | 1.321(3) | N10-C35 | 1.481(3) |
| N10-C25 | 1.467(3) | N1-C7 | 1.326(4) |
| N10-C17 | 1.473(3) | N1-C1 | 1.400(4) |
| **Bond Angles** | | | |
| O1-P1-O4 | 115.15(11) | O1-P1-O2 | 111.26(11) |
| O1-P1-O3 | 111.92(11) | O4-P1-O2 | 103.62(11) |
| O4-P1-O3 | 108.80(11) | O3-P1-O2 | 105.35(12) |
| O13-P4-O16 | 113.65(13) | O17-P5-O19 | 112.29(15) |
| O13-P4-O14 | 111.30(12) | O18-P5-O19 | 108.99(15) |
| O16-P4-O14 | 110.79(12) | O17-P5-O20 | 110.96(15) |
| O13-P4-O15 | 108.72(13) | O18-P5-O20 | 110.10(14) |
| O16-P4-O15 | 104.40(13) | O19-P5-O20 | 102.51(15) |
| O14-P4-O15 | 107.56(12) | O21-P6-O23 | 115.40(13) |
| O17-P5-O18 | 111.62(13) | O21-P6-O22 | 110.94(13) |

**Table 3.17: Crystal data and structure refinement for $[(H_8PDTB)^{4+}.4(NO_3)^-]$ (3i)**

| | |
|---|---|
| Empirical formula | $C_{35}H_{38}N_{14}O_{12}$ |
| Color | Colorless |
| Formula weight (g $mol^{-1}$) | 846.79 |
| Crystal System | Monoclinic |
| Space Group | $P2_1/c$ |
| a (Å) | 12.823(3) |
| b (Å) | 14.921(3) |
| c (Å) | 21.023(4) |
| α ($^0$) | 90 |
| β($^0$) | 105.955(12) |
| γ ($^0$) | 90 |
| V (Å$^3$) | 3867.4(14) |
| Crystal size (mm) | 0.23 x 0.21 x 0.18 |
| Z | 4 |
| $\rho_{calcd}$ (g $m^{-3}$) | 1.454 |
| μ | 0.113 |
| F (000) | 242 |
| θ range for data collection | 1.80-31.97 |
| No. of measured reflections | 4949 |
| No. of observed reflections | 4225 |
| Data/ restraints/parameters | 6815 / 0 /550 |
| R1(I>2σ(I)) | 0.040 |
| R1 (all data) | 0.052 |
| wR2(I>2σ(I)) | 0.105 |
| wR2 (all data) | 0.127 |

**Table 3.18: Selected bond distances (Å) and bond angles ($^o$) for $[(H_8PDTB)^{4+}.4(NO_3)^-]$ (3i)**

| | | | |
|---|---|---|---|
| **Bond Distances** | | | |
| N1-C7 | 1.313(5) | N3-C10 | 1.351(6) |
| N1-C1 | 1.412(6) | N3-C11 | 1.364(6) |
| N9-C8 | 1.454(6) | N5-C26 | 1.301(6) |
| N9-C9 | 1.475(6) | N5-C27 | 1.409(6) |
| N9-C35 | 1.477(5) | N4-C16 | 1.382(6) |
| N2-C7 | 1.349(5) | N6-C26 | 1.331(6) |
| N2-C6 | 1.365(6) | N6-C32 | 1.391(7) |
| N4-C10 | 1.314(6) | N10-C17 | 1.391(7) |
| N10-C33 | 1.449(6) | N10-C25 | 1.471(6) |
| N7-C18 | 1.359(8) | N7-C19 | 1.362(8) |
| **Bond Angles** | | | |
| C7-N1-C1 | 110.2(4) | C10-N3-C11 | 110.4(4) |
| C8-N9-C9 | 110.7(4) | C8-N9-C35 | 111.8(4) |
| C9-N9-C35 | 111.6(4) | C26-N5-C27 | 109.2(4) |
| C7-N2-C6 | 109.2(4) | C10-N4-C16 | 109.9(4) |
| C26-N6-C32 | 107.3(4) | C17-N10-C33 | 115.9(4) |
| C17-N10-C25 | 109.9(4) | C33-N10-C25 | 111.3(4) |
| C18-N7-C19 | 112.1(7) | C18-N8-C24 | 117.7(8) |
| N1-C7-N2 | 108.6(4) | N1-C7-C8 | 125.4(4) |
| N2-C7-C8 | 125.9(4) | C2-C1-C6 | 123.1(5) |

**Table 3.19: Crystal data and structure refinement for [2($H_5$PDTB)$^+$.2($CF_3COO$)$^-$ .5$H_2O$] (3j)**

| | |
|---|---|
| Empirical formula | $C_{74}H_{70}F_6N_{20}O_9$ |
| Color | Colorless |
| Formula weight (g $mol^{-1}$) | 1497.50 |
| Crystal System | Triclinic |
| Space Group | P-1 |
| a (Å) | 13.9803(9) |
| b (Å) | 17.4151(10) |
| c (Å) | 18.7014(11) |
| α ($^0$) | 98.268(4) |
| β($^0$) | 110.082(3) |
| γ ($^0$) | 112.344 |
| V (Å$^3$) | 3752.9(4) |
| Crystal size (mm) | 0.23 x 0.20 x 0.17 |
| Z | 2 |
| $\rho_{calcd}$ (g $m^{-3}$) | 1.325 |
| μ | 0.101 |
| F (000) | 2320.0 |
| θ range for data collection | 1.77-28.37 |
| No. of measured reflections | 6893 |
| No. of observed reflections | 4650 |
| Data/ restraints/parameters | 15332/0/977 |
| R1(I>2σ(I)) | 0.097 |
| R1 (all data) | 0.128 |
| wR2(I>2σ(I)) | 0.305 |
| wR2 (all data) | 0.320 |

**Table 3.20: Selected bond distances (Å) and bond angles ($^o$) for $[2(H_5PDTB)^+.2(CF_3COO)^-.5H_2O]$ (3j)**

| | | | |
|---|---|---|---|
| **Bond Distances** | | | |
| C26-N19 | 1.325(4) | C26-N20 | 1.326(4) |
| C26-C25 | 1.489(5) | C1-C6 | 1.385(5) |
| C1-C2 | 1.394(5) | C1-N11 | 1.394(4) |
| C24-C23 | 1.389(5) | C24-C19 | 1.392(5) |
| C24-N18 | 1.392(4) | C33-N16 | 1.463(4) |
| C33-C34 | 1.511(4) | C18-N18 | 1.318(4) |
| C18-N17 | 1.356(4) | C18-C17 | 1.485(5) |
| C19-N17 | 1.377(4) | C19-C20 | 1.386(5) |
| C7-N11 | 1.319(4) | C7-N12 | 1.348(4) |
| **Bond Angles** | | | |
| N19 C26 N20 | 109.8(3) | N19-C26-C25 | 125.0(3) |
| N20 C26 C25 | 125.2(3) | C6-C1-C2 | 120.2(3) |
| C6 C1 N11 | 109.3(3) | C19-C24-N18 | 109.9(3) |
| C2 C1 N11 | 130.5(3) | N16-C33-C34 | 112.6(3) |
| C23 C24 C19 | 120.4(4) | N18-C18-N17 | 112.4(3) |
| C23 C24 N18 | 129.7(4) | N18-C18-C17 | 124.4(3) |
| N17 C18 C17 | 123.2(3) | N11-C7-N12 | 112.5(3) |
| N17 C19 C20 | 133.9(4) | N11-C7-C8 | 124.5(3) |

**Table 3.21: Crystal data and structure refinement for [$(H_8PDTB)^{4+}.3(ClO_4)^-.(H_2PO_4)^-$] (3k)**

| | |
|---|---|
| Empirical formula | $C_{35}H_{38}Cl_3N_{10}O_{16}P$ |
| Color | Colorless |
| Formula weight (g $mol^{-1}$) | 992.07 |
| Crystal System | Monoclinic |
| Space Group | $P2_1/c$ |
| a (Å) | 12.429(2) |
| b (Å) | 15.403(3) |
| c (Å) | 22.864(4) |
| α ($^0$) | 90.00 |
| β($^0$) | 105.174(9) |
| γ ($^0$) | 90.00 |
| V ($Å^3$) | 105.174(9) |
| Crystal size (mm) | 0.21 x 0.19 x 0.17 |
| Z | 4 |
| $\rho_{calcd}$ (g $m^{-3}$) | 1.560 |
| μ | 0.340 |
| F (000) | 240 |
| θ range for data collection | 2.74-28.59 |
| No. of measured reflections | 2744 |
| No. of observed reflections | 1406 |
| Data/ restraints/parameters | 8689/0/618 |
| R1(I>2σ(I)) | 0.071 |
| R1 (all data) | 0.144 |
| wR2(I>2σ(I)) | 0.164 |
| wR2 (all data) | 0.206 |

**Table 3.22: Selected bond distances (Å) and bond angles ($^{o}$) for $[(H_8PDTB)^{4+}.3(ClO_4)^{-}.(H_2PO_4)^{-}]$(3k)**

| | | | |
|---|---|---|---|
| **Bond Distances** | | | |
| P4-O16 | 1.348(8) | P4-O13 | 1.357(4) |
| O1-Cl1 | 1.448(3) | O2-Cl1 | 1.412(3) |
| O3-Cl1 | 1.419(3) | O4-Cl1 | 1.420(4) |
| O5-Cl2 | 1.435(3) | O6-Cl2 | 1.398(4) |
| O7-Cl2 | 1.402(4) | O8-Cl2 | 1.392(3) |
| O9-Cl3 | 1.423(3) | O10-Cl3 | 1.441(3) |
| O11-Cl3 | 1.393(3) | N1-C1 | 1.383(5) |
| O12-Cl3 | 1.382(4) | N2-C7 | 1.327(5) |
| N1-C7 | 1.323(5) | N2-C6 | 1.394(5) |
| **Bond Angles** | | | |
| O15-P4-O13 | 110.3(7) | C7-N1-C1 | 109.0(4) |
| O14-P4-O13 | 117.6(3) | C7-N2-C6 | 109.5(3) |
| O16-P4-O13 | 107.0(4) | C10-N3-C11 | 109.7(4) |
| C10-N4-C16 | 110.0(3) | C26-N8-C32 | 109.7(3) |
| C18-N5-C19 | 109.9(4) | C9-N9-C8 | 109.5(3) |
| C18-N6-C24 | 110.0(4) | C9-N9-C33 | 109.9(3) |
| C26-N7-C27 | 109.8(3) | C8-N9-C33 | 111.0(3) |
| C17-N10-C25 | 111.6(3) | O2-Cl1-O4 | 110.5(3) |
| C17-N10-C35 | 113.7(3) | O3-Cl1-O4 | 109.9(3) |
| C25-N10-C35 | 114.6(3) | O2-Cl1-O1 | 110.2(2) |
| O2-Cl1-O3 | 109.7(2) | O3-Cl1-O1 | 106.9(2) |

**Table 3.23 Non-covalent interactions for salts and co-crystal (Å and $^{o}$)**

| S. N | D-H···A | d(D-H) | d(H-A) | d(D-A) | <(DHA)> |
|---|---|---|---|---|---|
| **1.** | **3[a]** | | | | |
| | N1-H1···O10 | 0.860(8) | 1.902(15) | 2.758(20) | 173.50 |
| | N2-H2B···O9 | 0.860(8) | 1.968(16) | 2.806(1) | 164.47 |
| | N3-H3B···O2 | 0.861(8) | 2.857(26) | 3.081(23) | 96.85 |
| | N3-H3B···O9 | 0.861(8) | 1.972(16) | 2.832(7) | 177.49 |
| | C2-H2···O6 | 0.929(12) | 2.770(4) | 3.634(33) | 155.15 |
| | C2-H2···O8 | 0.929(12) | 3.062(28) | 3.952(35) | 161.12 |
| | C2-H2···O10 | 0.929(12) | 3.549(25) | 3.989(25) | 111.77 |
| | C5-H5 ···O9 | 0.931(10) | 3.440(9) | 3.924(10) | 114.97 |
| | C8-H8B···O3 | 0.970(8) | 2.674(9) | 3.498(16) | 142.95 |
| | C8-H8B···O10 | 0.970(8) | 3.542(20) | 4.081(30) | 117.33 |
| | C8-H8A···O2 | 0.970(11) | 2.625(12) | 3.242(21) | 121.74 |
| | C8-H8A···O3 | 0.970(11) | 3.478(18) | 3.498(16) | 83.17 |
| | C12-H12···O1 | 0.930(9) | 3.194(30) | 3.599(24) | 108.48 |
| | C12-H12···O2 | 0.930(9) | 3.136(32) | 3.303(35) | 92.09 |
| | C12-H12···O4 | 0.930(9) | 3.607(29) | 4.279(30) | 131.34 |
| | C12-H12···O9 | 0.930(9) | 3.680(43) | 4.122(48) | 112.19 |
| | C2-H2···Cl2 | 0.929(12) | 3.382(25) | 4.310(34) | 176.12 |
| | C8-H8B···Cl1 | 0.970(8) | 3.415(15) | 3.986(9) | 119.64 |
| **2.** | **3b** | | | | |
| | N3-H3A···Br2 | 0.860(5) | 2.380(11) | 3.233(16) | 171.56 |
| | N4-H4A···Br1 | 0.859(4) | 2.376(11) | 3.214(14) | 164.71 |
| | C8-H8A ···Br1 | 0.970(3) | 3.264(9) | 3.759(12) | 113.57 |
| | C8-H8B ···Br1 | 0.971(3) | 3.308(8) | 3.759(12) | 110.45 |
| | C8-H8B ···Br2 | 0.971(3) | 3.489(11) | 4.024(15) | 117.07 |
| | C9-H9B ···Br2 | 0.969(5) | 3.245(10) | 4.055(16) | 142.24 |
| | C15-H15 ···Br1 | 0.929(5) | 3.540(1) | 4.115(5) | 122.58 |
| | C17-H17B ···Br2 | 0.970(3) | 2.922(2) | 3.851(12) | 160.53 |
| | C18-H18B ···Br1 | 0.960(3) | 2.839(6) | 3.750(5) | 158.79 |

| | | | | | |
|---|---|---|---|---|---|
| | C19-H19B ···Br1 | 0.960(3) | 3.257(16) | 4.070(19) | 143.52 |
| | C20-H20B ···Br2 | 0.960(4) | 3.110(1) | 3.743(7) | 148.20 |
| | C21-H21B ···Br2 | 0.960(2) | 2.842(7) | 3.959(3) | 156.51 |
| **3.** | **3c** | | | | |
| | N1-H1···F9 | 0.860(3) | 1.972(3) | 2.797(4) | 160.42 |
| | N3-H3B···F8 | 0.860(2) | 2.754(2) | 3.287(4) | 121.62 |
| | N3-H3B···F9 | 0.860(2) | 1.962(2) | 2.822(3) | 177.78 |
| | N7-H7··O1 | 0.860(2) | 1.875(2) | 2.710(3) | 163.30 |
| | N4-H4A···O3 | 0.860(3) | 2.100(5) | 2.875(6) | 154.14 |
| | N4-H4A···O7 | 0.860(3) | 2.454(7) | 3.118(8) | 134.45 |
| | N6-H6···O4 | 0.860(3) | 1.944(5) | 2.795(7) | 170.07 |
| | N2-H2B···F4 | 0.860(3) | 2.324(6) | 3.076(7) | 146.27 |
| | N2-H2B···F2 | 0.860(4) | 1.962(7) | 3.602(7) | 131.36 |
| | C17-H17A ···O5 | 0.970(4) | 2.915(5) | 3.841(6) | 160.07 |
| | C12-H12 ···F8 | 0.930(3) | 2.718(2) | 3.318(4) | 123.11 |
| | C12-H12 ···F7 | 0.930(3) | 2.593(2) | 3.415(6) | 147.70 |
| | C15-H15 ···F5 | 0.930(4) | 2.663(4) | 3.309(6) | 151.48 |
| | C14-H14 ···F4 | 0.930(5) | 2.778(5) | 3.530(7) | 138.66 |
| | C31-H31 ···O2 | 0.930(4) | 2.399(3) | 3.314(3) | 167.80 |
| | C33-H33A ···N3 | 0.970(4) | 2.763(3) | 3.314(5) | 116.74 |
| | C23-H23 ···F6 | 0.930(5) | 2.554(6) | 3.414(8) | 153.92 |
| | C9-H9A ···F1 | 0.970(5) | 2.823(5) | 3.768(6) | 164.97 |
| | C25-H25A ···N3 | 0.970(4) | 2.730(2) | 3.646(4) | 157.70 |
| | C17-H17A ···F9 | 0.970(4) | 2.748(2) | 3.622(4) | 150.17 |
| **4.** | **3d** | | | | |
| | O2-H2C···O13 | 0.820(3) | 1.876(2) | 2.648(3) | 156.43 |
| | O3-H3B···O20 | 0.820(3) | 1.719(3) | 2.481(4) | 153.73 |
| | O24-H22···O25 | 0.820(3) | 1.902(3) | 2.667(4) | 154.82 |
| | C2-H2···O13 | 0.930(4) | 2.898(2) | 3.822(5) | 172.57 |
| | C3-H3···O9 | 0.930(4) | 2.995(3) | 3.816(5) | 148.09 |
| | O28-H28···O17 | 0.930(4) | 2.411(3) | 3.288(5) | 157.22 |

| | | | | | |
|---|---|---|---|---|---|
| | O30-H30···O12 | 0.930(4) | 2.742(3) | 3.512(5) | 140.73 |
| | N5-H5A···O4 | 0.860(3) | 2.006(2) | 2.849(4) | 166.48 |
| | N7-H7···O4 | 0.860(3) | 2.908(3) | 3.337(4) | 168.97 |
| | O1-H1A···O6 | 0.820(3) | 1.807(6) | 2.564(7) | 152.72 |
| | N1-H1···O6 | 0.860(3) | 2.345(2) | 3.199(3) | 171.99 |
| | N4-H4A···O6 | 0.860(3) | 1.945(5) | 2.783(6) | 164.30 |
| | O8-H8D···O9 | 0.820(4) | 1.883(3) | 2.622(5) | 149.30 |
| | O7-H7A···O26 | 0.820(7) | 2.992(5) | 3.488(7) | 121.19 |
| | O12-H12A···O4 | 0.820(3) | 1.905(2) | 2.689(4) | 159.54 |
| | O9-H9···O21 | 0.820(3) | 1.718(3) | 2.511(4) | 162.07 |
| | O13-H13A···O22 | 0.820(2) | 1.689(3) | 2.489(4) | 164.38 |
| | C3-H3 ···O21 | 0.930(4) | 2.732(3) | 3.621(5) | 160.11 |
| | O17-H17 ···O22 | 0.820(3) | 1.811(3) | 2.572(4) | 153.66 |
| | C23-H23A ···O11 | 0.820(3) | 1.720(2) | 2.519(4) | 164.34 |
| | N2-H2B ···O14 | 0.860(3) | 1.849(2) | 2.700(4) | 170.86 |
| | C33-H33A ···O16 | 0.970(3) | 2.727(3) | 3.515(4) | 138.74 |
| | C8-H8B ···O16 | 0.970(4) | 2.688(3) | 3.455(5) | 136.32 |
| | N8-H8 ···O20 | 0.860(3) | 1.851(3) | 2.709(3) | 174.80 |
| | C8-H8A ···O21 | 0.970(4) | 2.871(3) | 3.820(5) | 166.17 |
| | C22-H22 ···O10 | 0.930(4) | 2.951(3) | 3.821(5) | 156.30 |
| | C23-H23 ···O23 | 0.930(4) | 2.921(3) | 3.807(5) | 159.87 |
| | C14-H14 ···O8 | 0.930(5) | 2.961(5) | 3.856(7) | 164.46 |
| **5.** | **3e** | | | | |
| | O2-H15A···N3 | 0.887(8) | 1.806(7) | 2.636(8) | 154.89 |
| | N1-H13···O1 | 0.860(3) | 1.929(5) | 2.777(5) | 168.46 |
| | N4-H4B···N2 | 0.860(3) | 2.015(3) | 2.851(4) | 163.87 |
| | C17-H17···N3 | 0.970(4) | 2.866(2) | 3.341(4) | 111.17 |
| | C15-H15···O1 | 0.930(4) | 2.905(3) | 3.574(5) | 129.96 |
| | C17-H17B···O2 | 0.970(3) | 2.615(3) | 3.499(4) | 151.65 |
| | C9-H9A···N1 | 0.970(3) | 2.923(3) | 3.392(4) | 110.91 |
| **6.** | **3f** | | | | |

| | | | | | |
|---|---|---|---|---|---|
| | N1-H1···O1 | 0.860(5) | 2.546(7) | 3.217(4) | 135.5 |
| | N1-H1···O2 | 0.860(3) | 2.546(3) | 3.065(1) | 160.2 |
| | N2-H1···O4 | 0.861(3) | 2.148(6) | 2.957(7) | 156.4 |
| | N2-H2B···O6 | 0.861(3) | 2.572(5) | 3.325(7) | 146.6 |
| | C2-H2···O1 | 0.930(4) | 2.688(4) | 3.365(6) | 130.3 |
| | C5-H5···O4 | 0.931(5) | 3.118(6) | 3.699(8) | 122.1 |
| | C8-H8B···O6 | 0.971(5) | 2.920(7) | 3.744(8) | 143.4 |
| | C8-H8B ···O7 | 0.971(5) | 3.134(23) | 3.90(23) | 138.0 |
| | C9-H9A···O2 | 0.971(3) | 3.313(8) | 3.524(10) | 94.48 |
| | C10-H10B···O6 | 0.969(7) | 3.217(9) | 4.186(11) | 178.1 |
| **7.** | **3g** | | | | |
| | N1-H1···Cl1 | 0.860(5) | 2.285(2) | 3.122(5) | 164.3 |
| | N2-H2B···Cl2 | 0.860(4) | 1.952(3) | 2.799(5) | 167.9 |
| | C8-H8B ···Cl1 | 0.972(5) | 3.0052(2) | 3.819(6) | 142.1 |
| **8.** | **3h** | | | | |
| | N1-H1···O29 | 0.861(4) | 1.904(3) | 2.764(4) | 176.9 |
| | N4-H4B···O29 | 0.860(2) | 1.881(2) | 2.730(3) | 168.7 |
| | O10-H10A···O13 | 0.689(47) | 1.869(47) | 2.556(5) | 176.1 |
| | O11-H11···O14 | 1.300(47) | 1.177(47) | 2.474(4) | 174.6 |
| | O16-H16A···O7 | 1.209(49) | 1.270(49) | 2.474(3) | 171.3 |
| | O18-H18···O25 | 0.928(44) | 1.594(44) | 2.517(3) | 172.8 |
| | O26-H26···O17 | 0.693(43) | 1.944(43) | 2.617(4) | 164.2 |
| | C2-H2···O32 | 0.930(3) | 2.550(4) | 3.347(5) | 143.8 |
| | C8-H8B···O22 | 0.969(3) | 2.442(2) | 3.192(4) | 133.9 |
| | C9-H57A···O24 | 0.970(3) | 2.611(2) | 3.411(4) | 139.8 |
| | C15-H15···O31 | 0.930(3) | 2.635(2) | 3.521(4) | 159.2 |
| **9.** | **3i** | | | | |
| | N1-H1···O1 | 0.860(4) | 2.364(5) | 3.129(7) | 148.4 |
| | N1-H1···O2 | 0.860(4) | 1.995(5) | 2.794(6) | 154.2 |
| | N2-H2B···O7 | 0.859(4) | 1.984(5) | 3.831(6) | 168.4 |
| | N2-H2B···O9 | 0.859(4) | 2.750(6) | 3.301(7) | 123.3 |

| | | | | | |
|---|---|---|---|---|---|
| | N4-H4B···O5 | 0.860(4) | 2.580(6) | 3.226(8) | 132.8 |
| | N4-H4B···O6 | 0.860(4) | 2.014(5) | 2.797(7) | 151.0 |
| | N4-H4B···O7 | 0.860(4) | 2.759(5) | 3.077(6) | 103.6 |
| | N8-H8···O11 | 0.859(4) | 2.892(11) | 3.177(13) | 101.5 |
| | N8-H8···O12 | 0.859(4) | 3.328(11) | 3.304(12) | 117.6 |
| | C8-H8B···O11 | 0.970(6) | 3.412(12) | 4.268(15) | 148.3 |
| | C8-H8B···O12 | 0.970(6) | 2.522(12) | 3.348(13) | 171.3 |
| | C15-H15···O5 | 0.929(6) | 2,569(6) | 3.267(9) | 132.4 |
| **10.** | **3j** | | | | |
| | N2-H2A···O7 | 0.860(4) | 1.960(5) | 2.770(7) | 156.5 |
| | N3-H3A···O7 | 0.859(4) | 1.946(5) | 2.799(7) | 171.5 |
| | N5-H5A···O1 | 0.859(4) | 2.029(6) | 2.873(8) | 167.2 |
| | N8-H8C···O2 | 0.861(4) | 3.053(13) | 3.711(15) | 134.8 |
| | C20-H20···F2 | 0.930(6) | 2.702(7) | 3.515(11) | 146.4 |
| | C29-H29···O2 | 0.931(7) | 3.066(5) | 3.795(9) | 136.3 |
| | C31-H31···O2 | 0.931(6) | 3.149(8) | 3.841(12) | 132.6 |
| | C44-H44A···O3 | 0.970(4) | 2.903(6) | 3.659(9) | 135.6 |
| | C55-H55···F4 | 0.930(6) | 2.872(9) | 3.522(12) | 128.1 |
| | C31-H34···F3 | 0.930(6) | 2.526(5) | 3.292(7) | 139.8 |
| | C69-H69B···O6 | 0.970(5) | 3.036(8) | 3.663(8) | 123.6 |
| **11.** | **3k** | | | | |
| | N1-H1B···Cl1 | 0.847(45) | 3.033(46) | 3.770(4) | 146.7 |
| | N2-H2B···Cl2 | 0.859(45) | 2.951(46) | 3.790(3) | 165.8 |
| | C12-H12···O14 | 0.929(7) | 2.906(5) | 3.331(10) | 109.3 |
| | C13-H13···O6 | 0.929(5) | 2.736(12) | 3.439(13) | 133.1 |

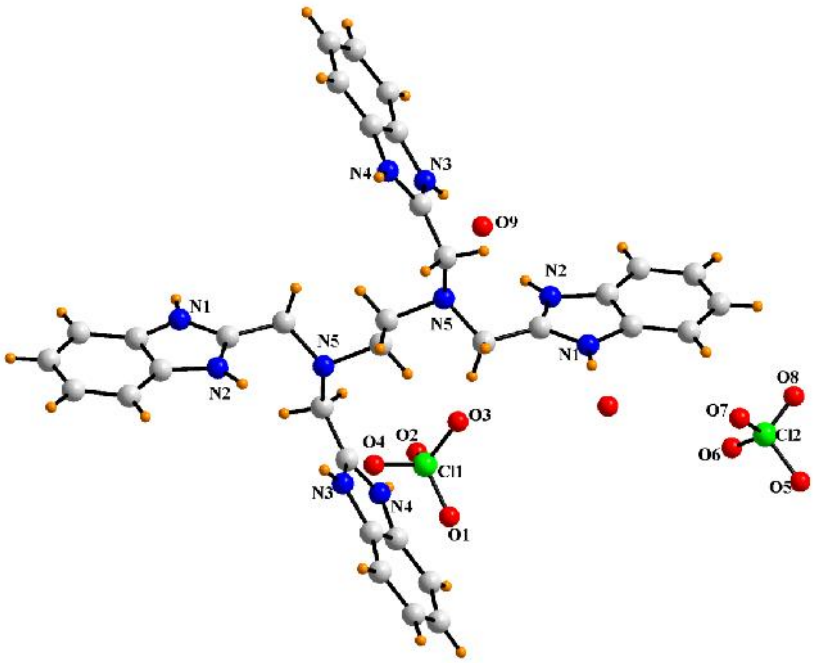


**Fig. 3.33** Crystal **s**tructure of salt $[(H_8EDTB)^{4+}.4(ClO_4)^{-}.H_2O]$ **3a**. Color code: C, grey; N, blue; H, orange; O, red; Cl, green

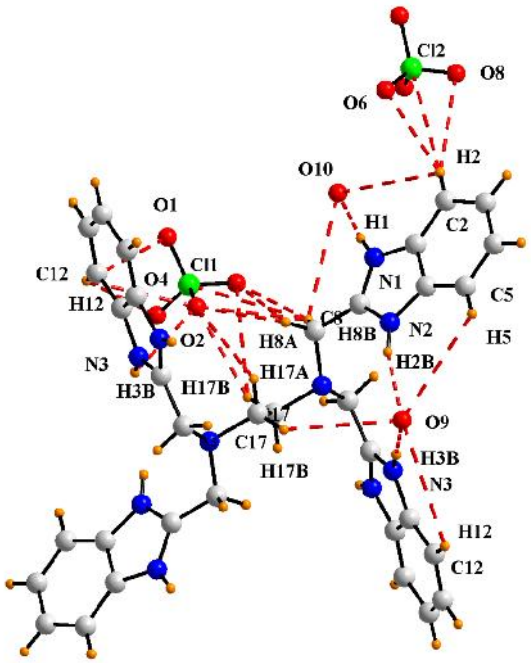


**Fig. 3.34** Different non-covalent interactions in salt **3a**. Color code: C, grey; N, blue; H, orange; O, red; Cl, green

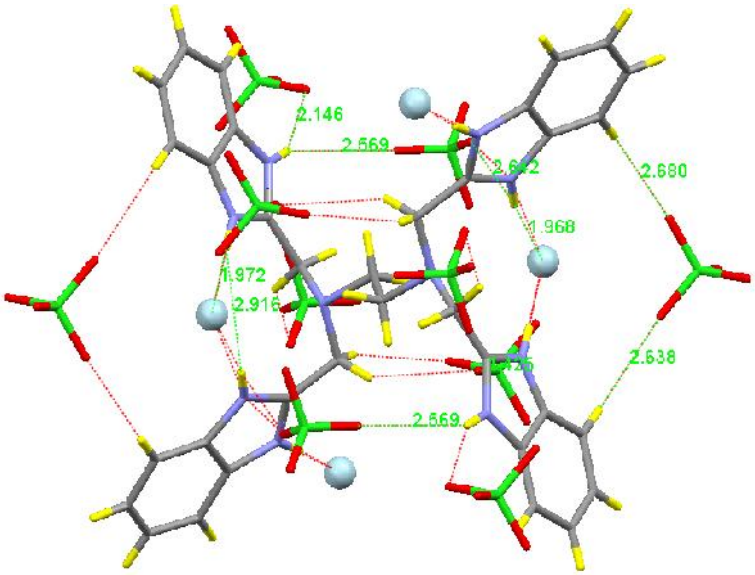


**Fig. 3.35** Two wings of the benzimidazole ring of the ligand, bridged by water and perchlorate molecule through N-H···O and C-H···O interactions on both in salt**3a**. Color code: C, grey; N, blue; H, orange; O, red; Cl, green

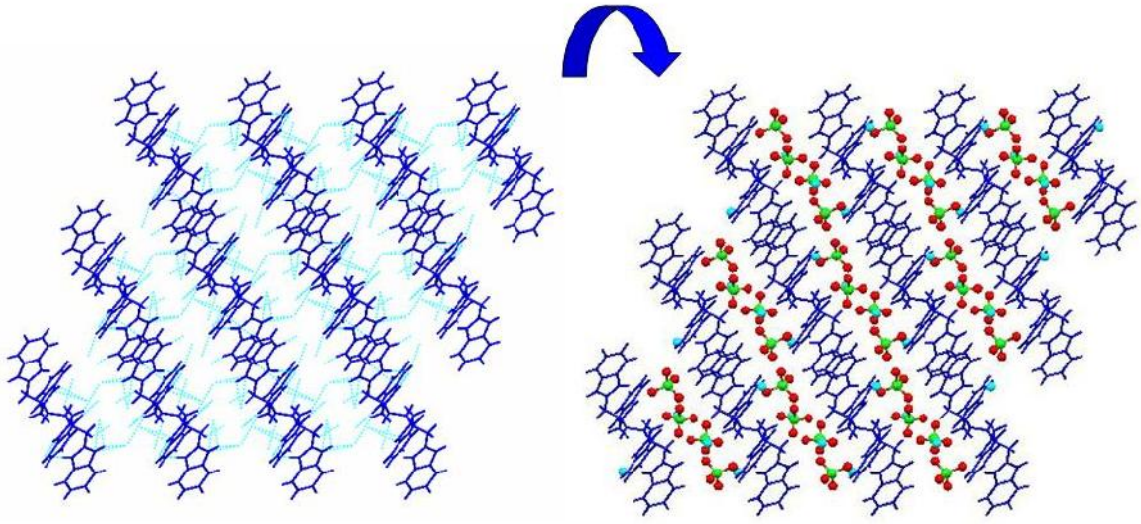

**Fig. 3.36** Alternate channels of host framework formed by the self-assembly of the cationic protonated $H_4$EDTB with guest perchlorate anions and water molecules in salt **3a**.

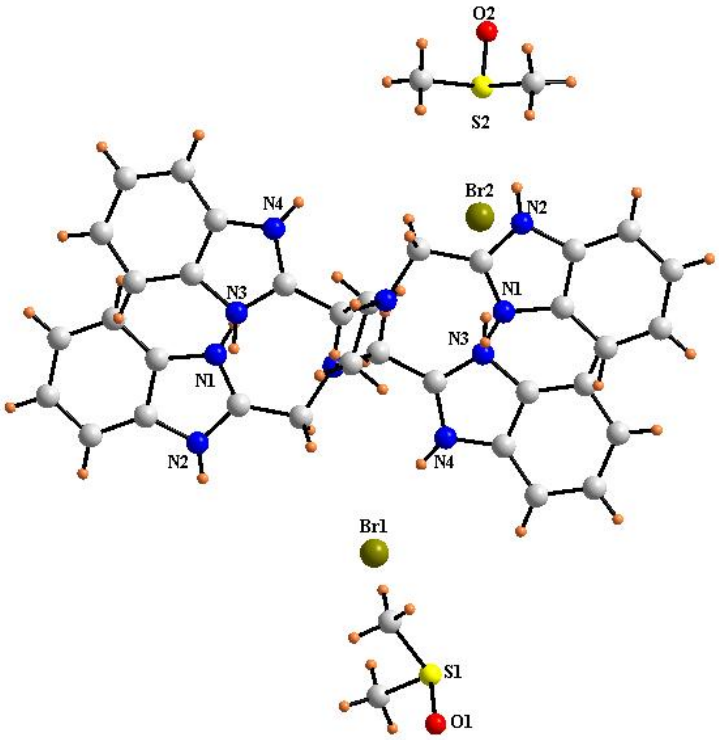


**Fig. 3.37** Crystal structure of salt $[(H_8EDTB)^{4+}.4(Br)^{-}.4DMSO]$ **3b**. Color code: C, grey; N, blue; H, orange; O red

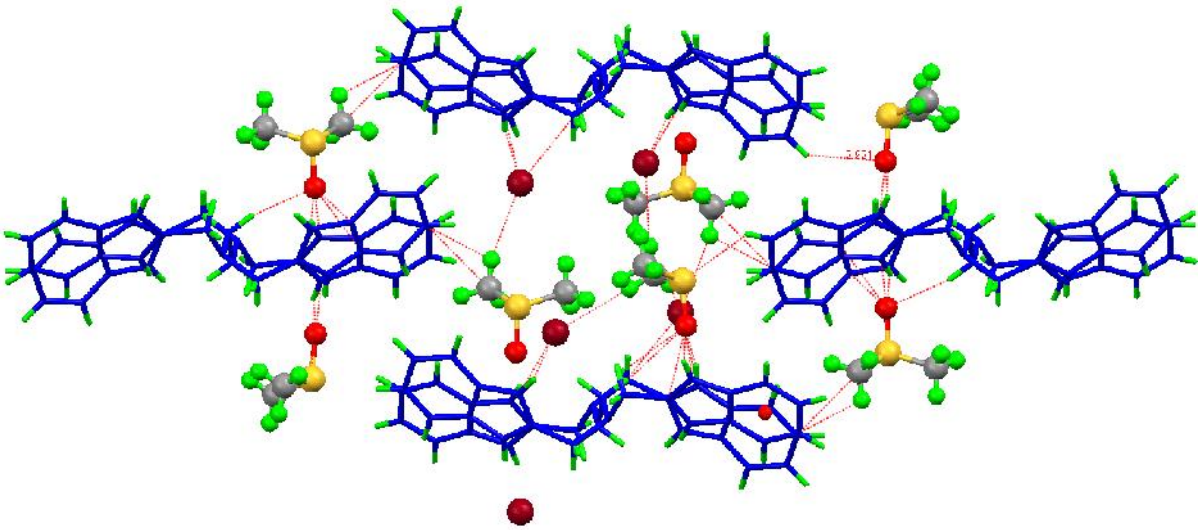

**Fig. 3.38** Different non-covalent interactions in salt **3b.** Proonated ligand, blue; DMSO, green; water, red

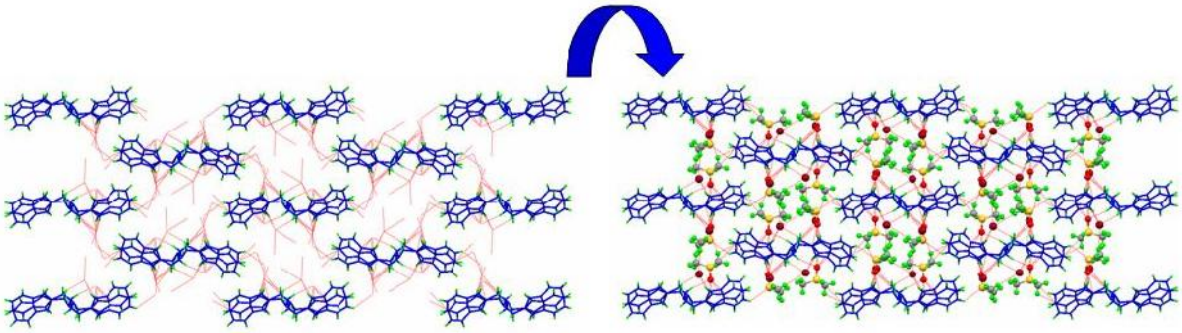

**Fig. 3.39** Host-guest assembly in salt **3b.** Color code: Proonated ligand, blue; DMSO, green; water, red

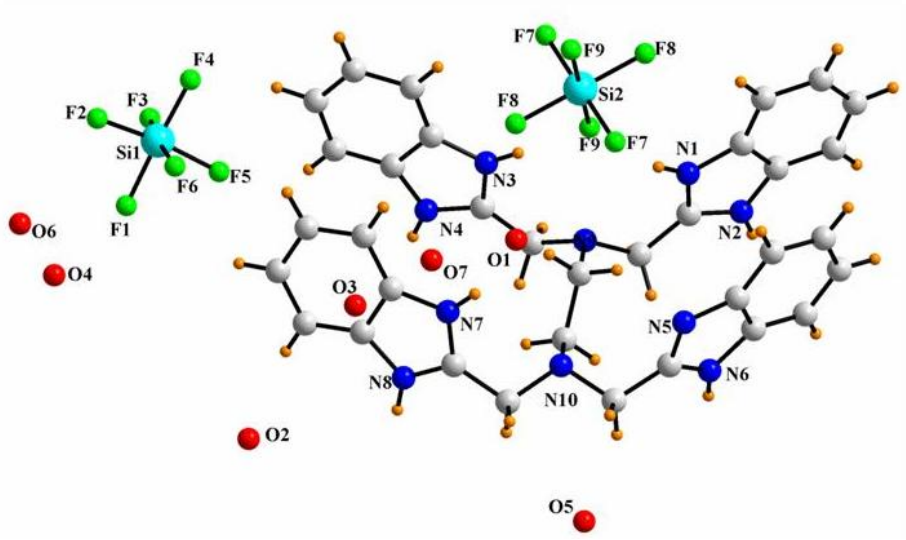


**Fig. 3.40** Crystal structure of salt $[2(H_7EDTB)^{3+}.3(SiF_6)^{2-}.14H_2O]$ **3c**. Color code: C, grey; N, blue; F, green; Si Cyan

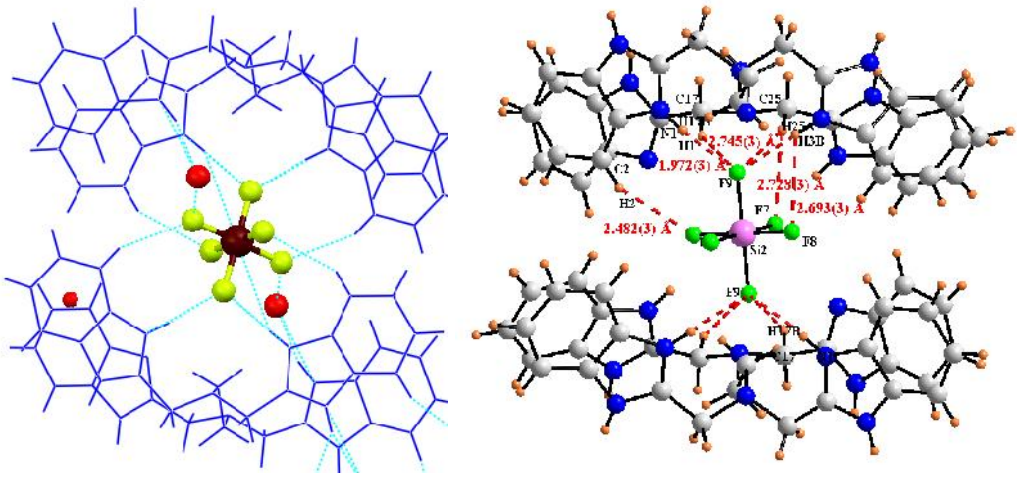


**Fig. 3.41** Pseudo cavity formed by the protonated ligand for trapping $SiF_6^{2-}$ ions in salt **3c**. Color code: C, grey; N, blue; H, orange; F, green; Si Pink

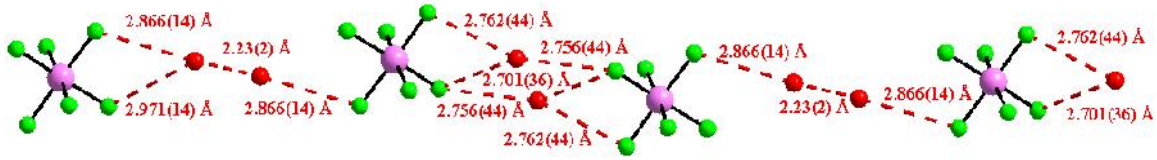


**Fig. 3.42** Continuous chain through F-O interaction among hexaflourosilicate anions and the water molecules in salt **3c**

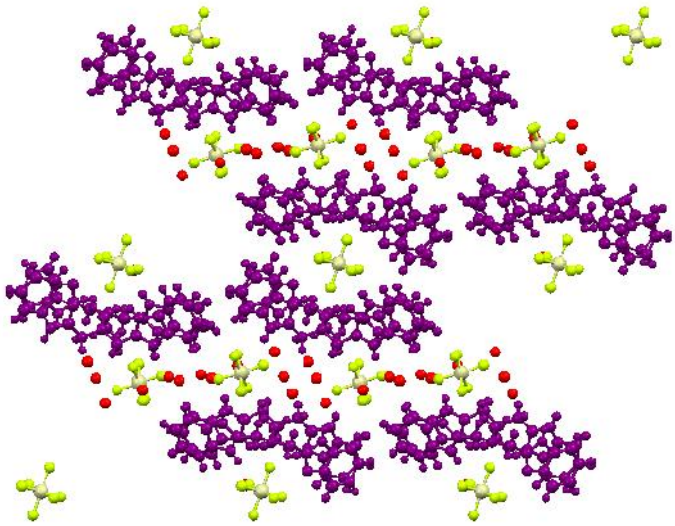

**Fig. 3.43** Host-guest assembly having both pseudo cavity as well as alternate channels in salt **3c**

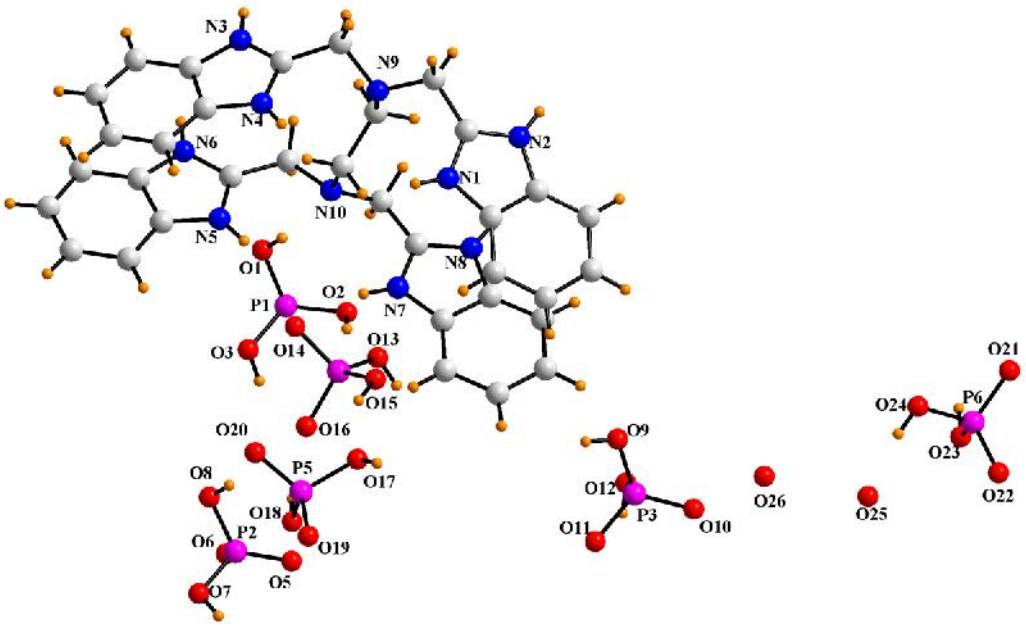


**Fig. 3.44** Crystal structure of salt $[(H_8EDTB)^{4+}.4(H_2PO_4)^{-}.2H_3PO_4]$ **3d.** Color code: C, grey; N, blue; H, orange; P, pink

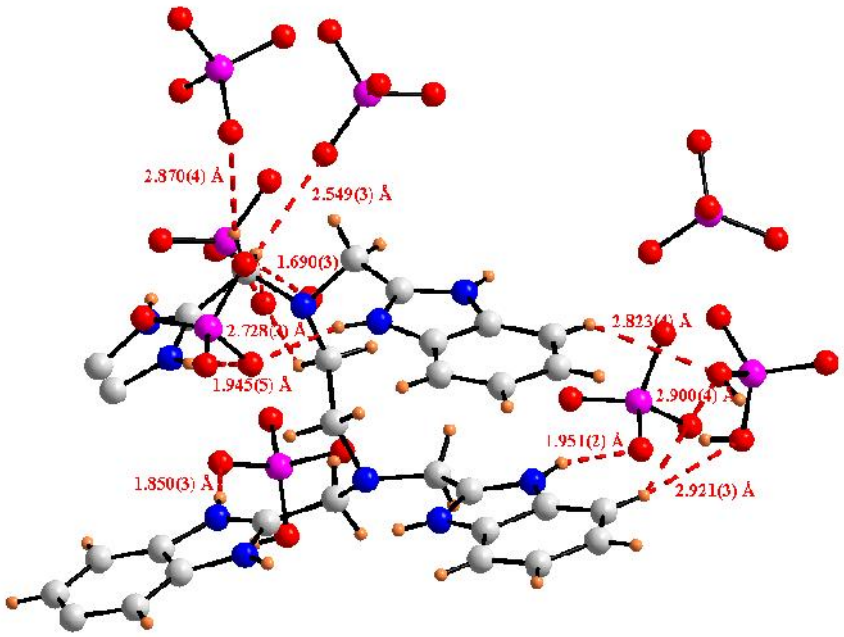


**Fig. 3.45** Different non-covalent interactions in salt **3d.** Color code: C, grey; N, blue; H, orange; O, red; P, pink

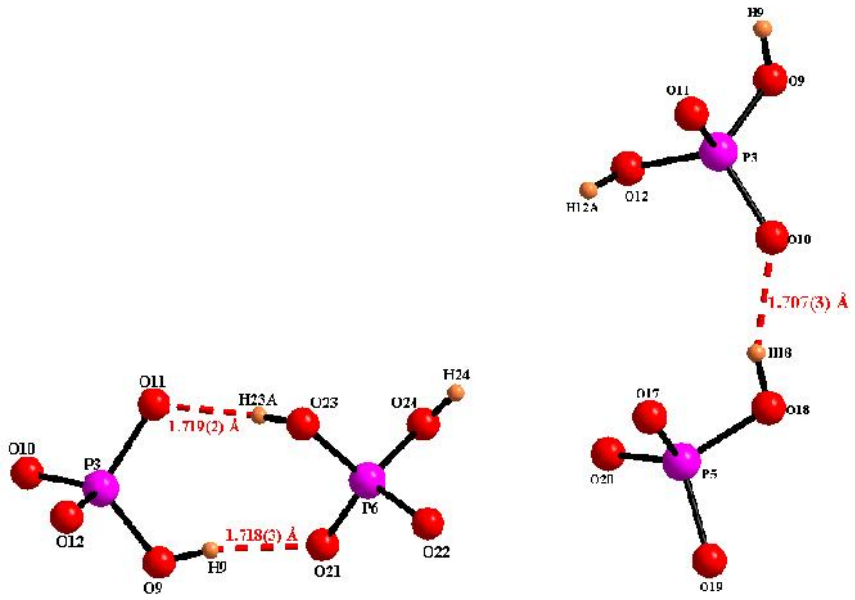


**a** **b**

**Fig. 3.46** Self-dimerization $R_2^2(8)$ and head-to-tail hydrogen bonding in salt **3d**. Color code: H, orange; O, red; P, pink

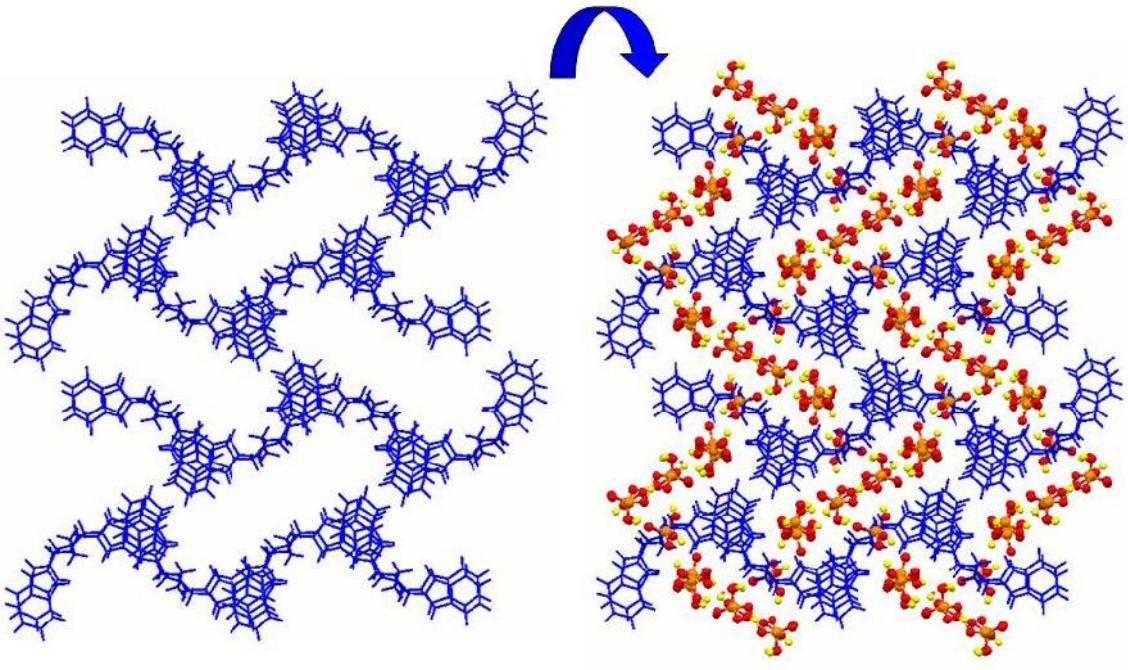

**Fig. 3.47** Three dimensional herring bone type of packing in salt **3d**

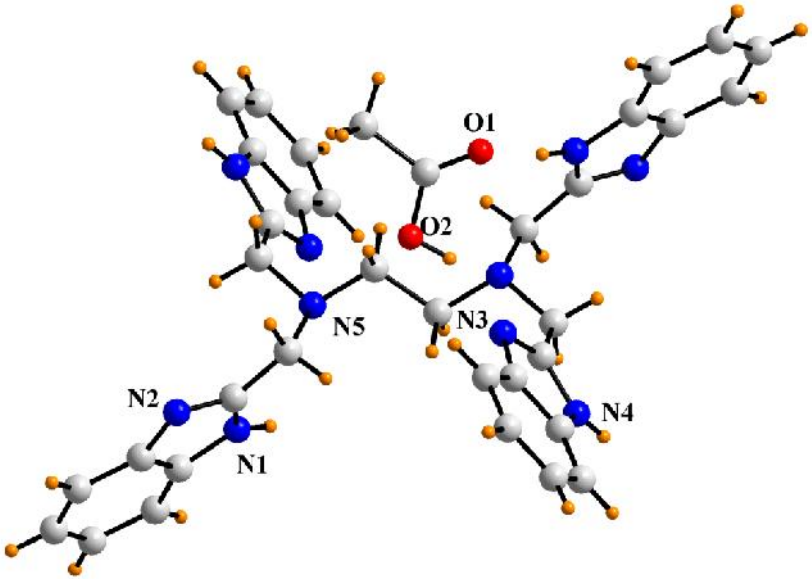


**Fig. 3.48** Crystal structure of co-crystal [$H_4$EDTB.2$CH_3$COOH] **3e.** Color code: C, grey; N, blue; H, orange; O, red

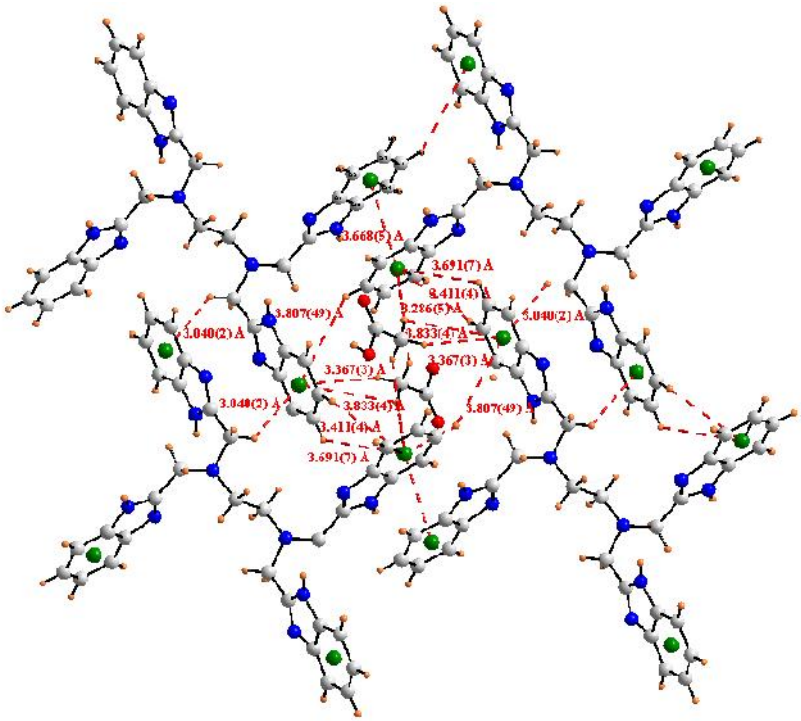


**Fig. 3.49** Different non-covalent interactions in co-crystal **3e**. Color code: C, grey; N, blue; H, orange; O, red; dummy, green

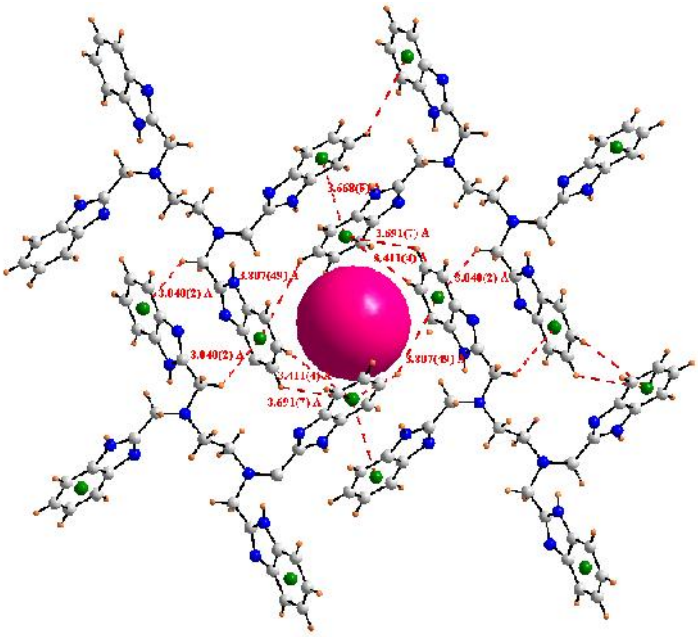

**Fig. 3.50** For the sake of clarity the cavity is shown as pink dummy (*via.*, C-H· · π and π· · π interactions) in co-crystal **3e**. Color code: C, grey; N, blue; H, orange; dummy, green

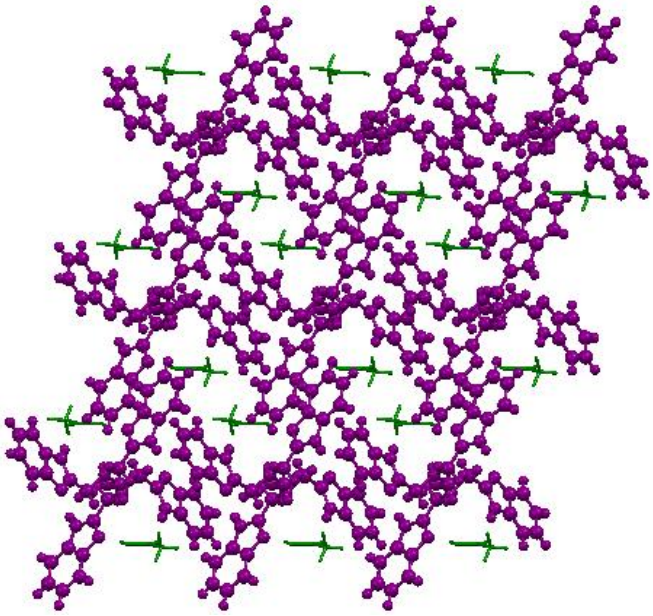

**Fig. 3.51** Three dimensional packing of co-crystal **3e**. Guest acetic acid molecules are entrapped in the cage formed by the host cationic ligand assembly. Color code: Cage; purple; acetic acid, green

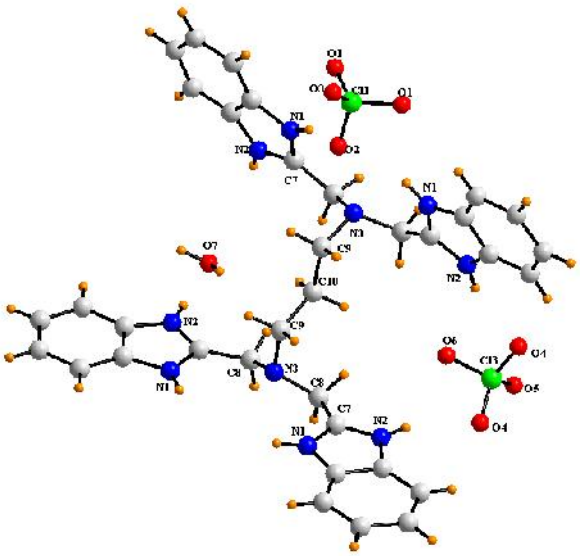

**Fig. 3.52** Crystal structure of salt $[(H_8PDTB)^{4+}.4(ClO_4)^{-}.H_2O]$ **3f.** Color code: C, grey; N, blue; H, orange; O, red; Cl, green

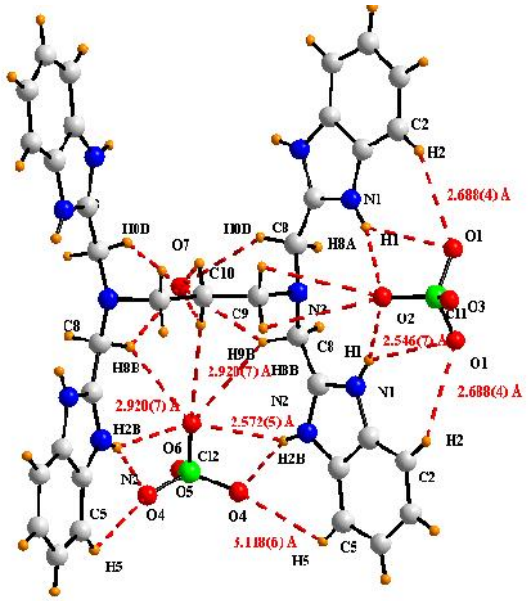


**Fig. 3.53** Different non-covalent interactions in salt **3f.** Color code: C, grey; N, blue; H, orange; O, red; Cl, green

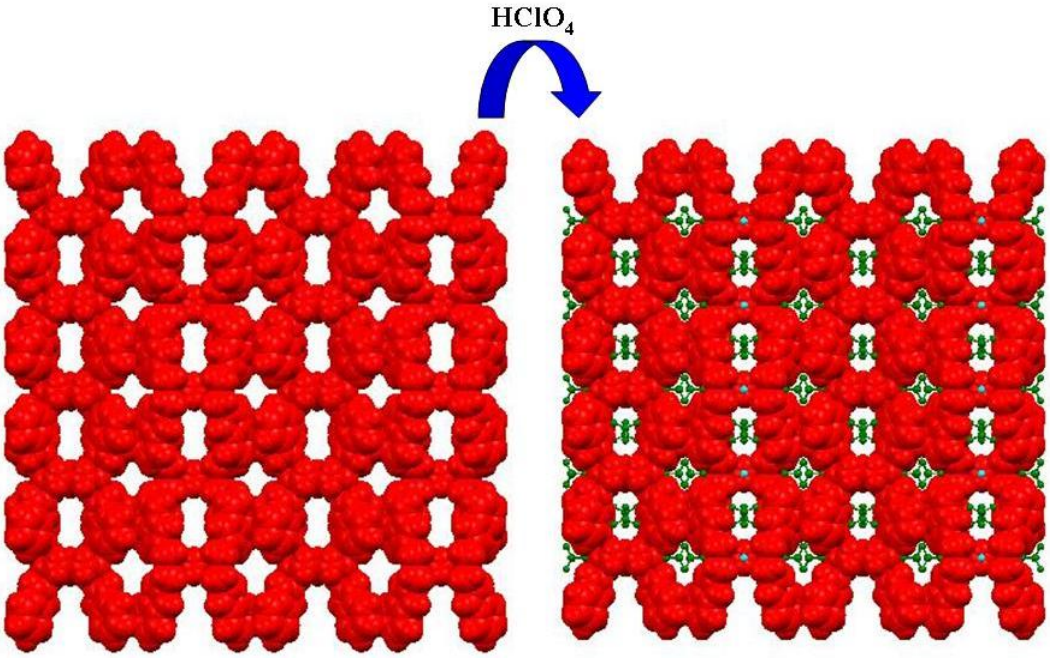


**Fig. 3.54** Mat like packing with three different types of cavity in salt **3f**. Color code: Ligand, red; anion, green

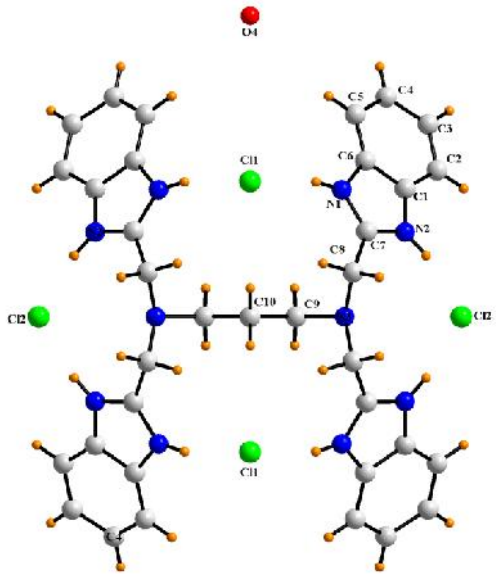


**Fig. 3.55** Crystal structure of salt $[(H_8PDTB)^{4+}.4(Cl)^{-}.2H_2O]$ **3g**. Color code: C, grey; N, blue; H, orange; O, red; Cl, green

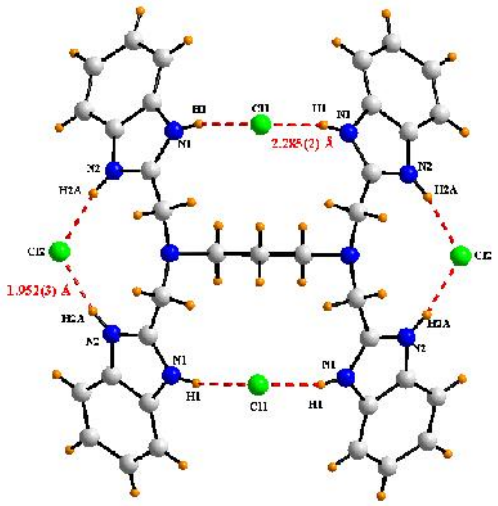


**Fig. 3.56** Different non-covalent interactions in **3g**. Color code: C, grey; N, blue; H, orange; O, red; Cl, green

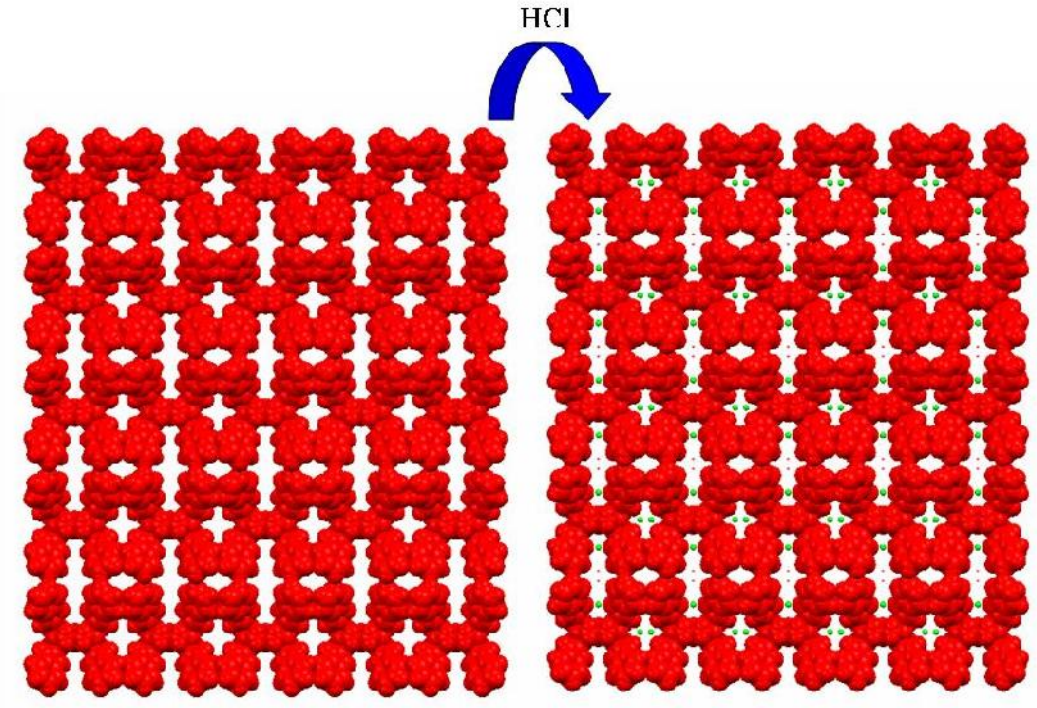


**Fig. 3.57** Three different types of cavity entrapping chloride anion and water molecules in **3g**. Color code: Ligand, red; anion, green

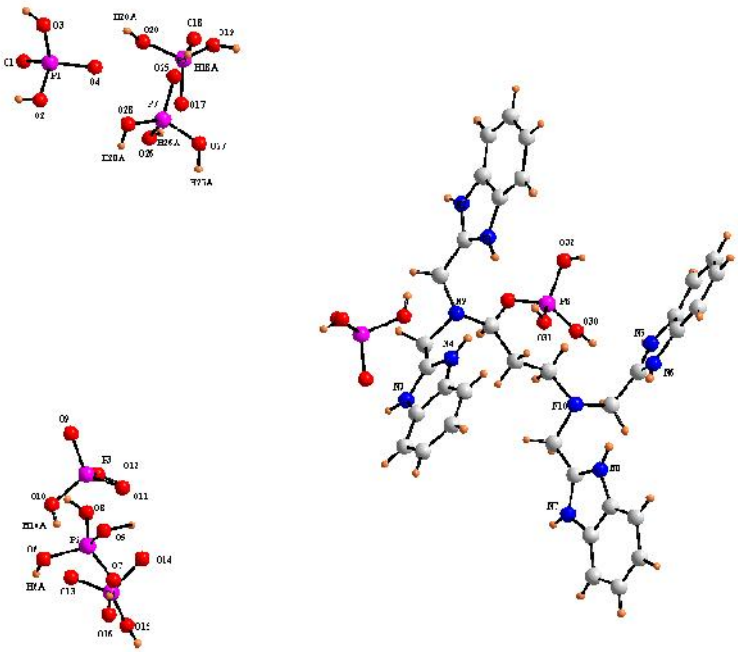

**Fig. 3.58** Crystal structure of salt $[(H_8PDTB)^{4+}.2(H_2PO_4)^{-}.(H_7P_3O_{12})^{2-}.3H_3PO_4]$ **3h**. Color code: C, grey; N, blue; H, orange; O, red; P, pink

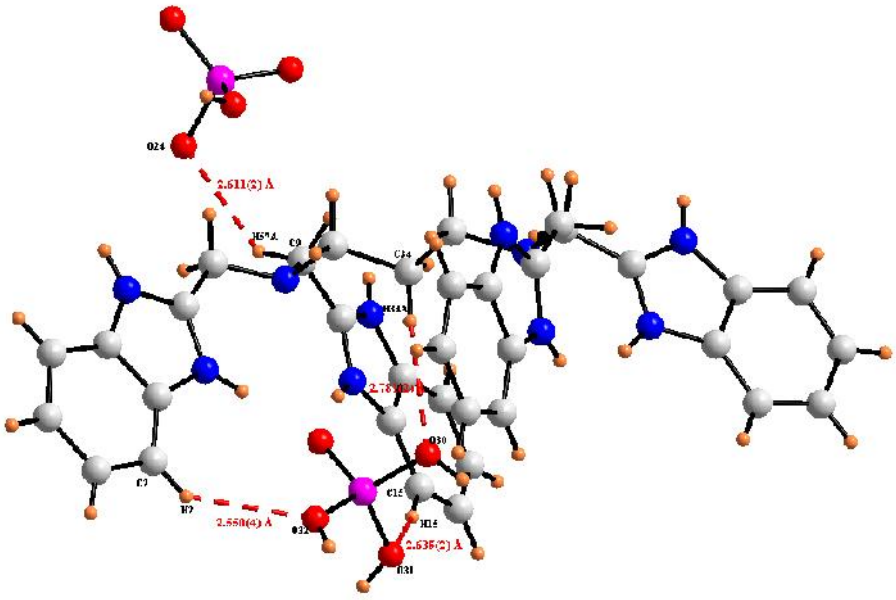

**Fig. 3.59** Different non-covalent interactions in salt **3h**. Color code: C, grey; N, blue; H, orange; O, red; P, pink

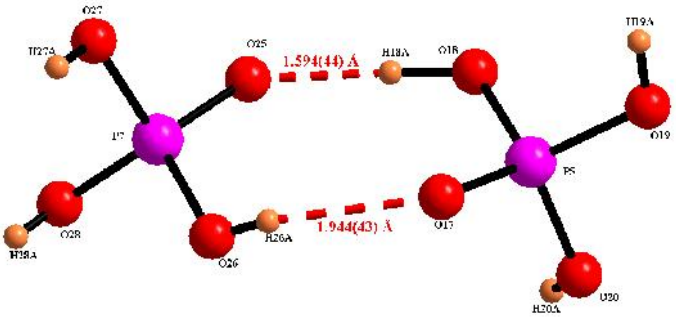


**Fig. 3.60** $R_2^2(8)$ motif through O-H···O interaction in **3h**

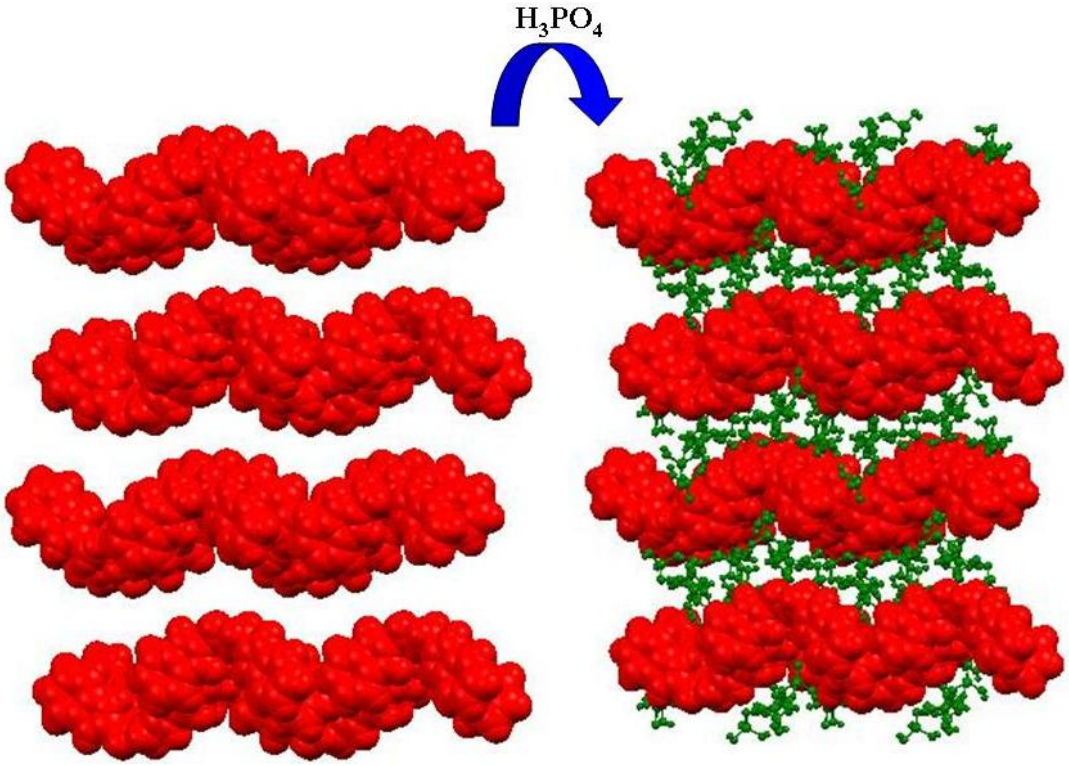


**Fig. 3.61** Alternate channels of host framework formed by the self-assembly of the cationic protonated ligand ($H_4$PDTB) with guest phosphate anions in **3h**

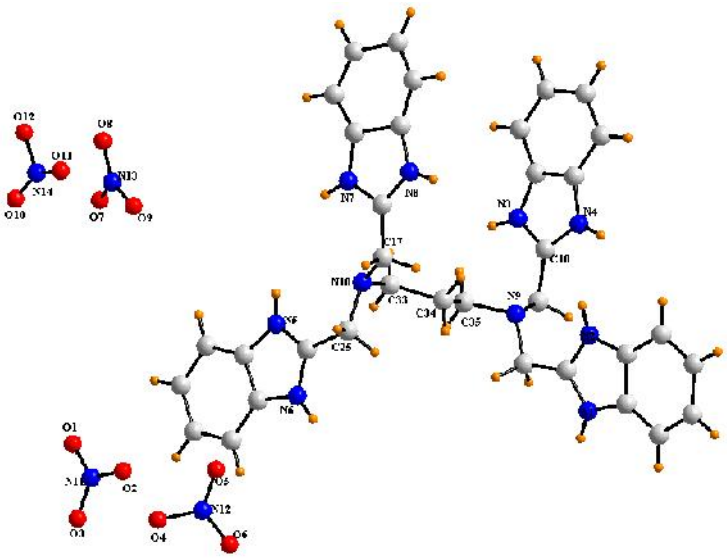

**Fig. 3.62** Crystal structure of salt $[(H_8PDTB)^{4+}.4(NO_3)^-]$ **3i**. Color code: C, grey; N, blue; H, orange; O, red

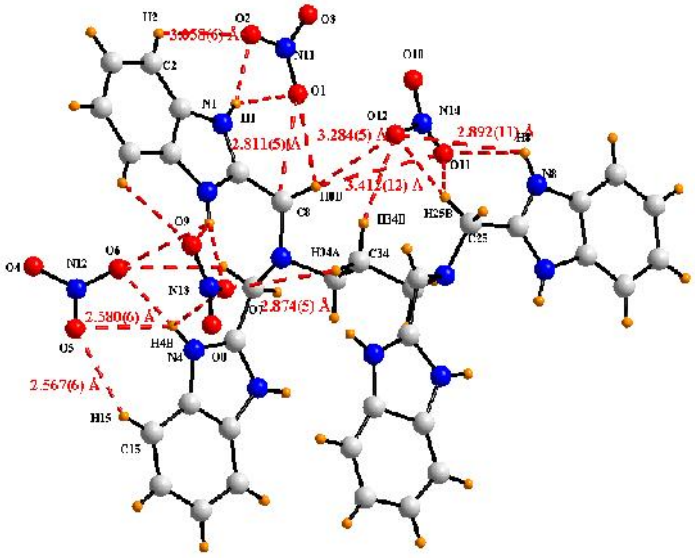


**Fig. 3.63** Different non-covalent interactions in **3i.** Color code: C, grey; N, blue; H, orange; O, red

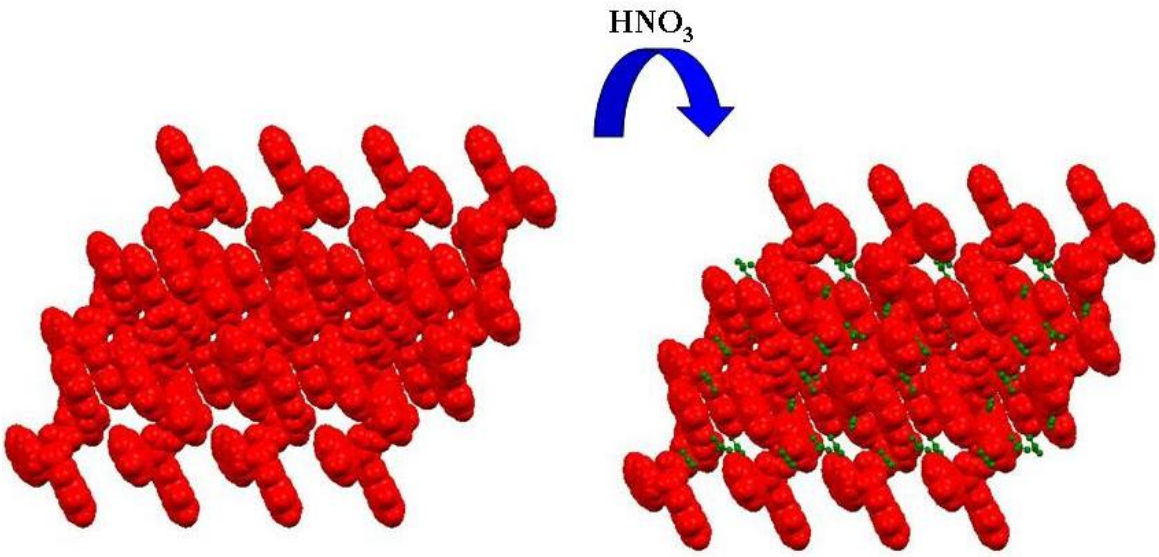


**Fig. 3.64** Three dimensional packing in **3i.** Color code: Ligand, red; anion, green.

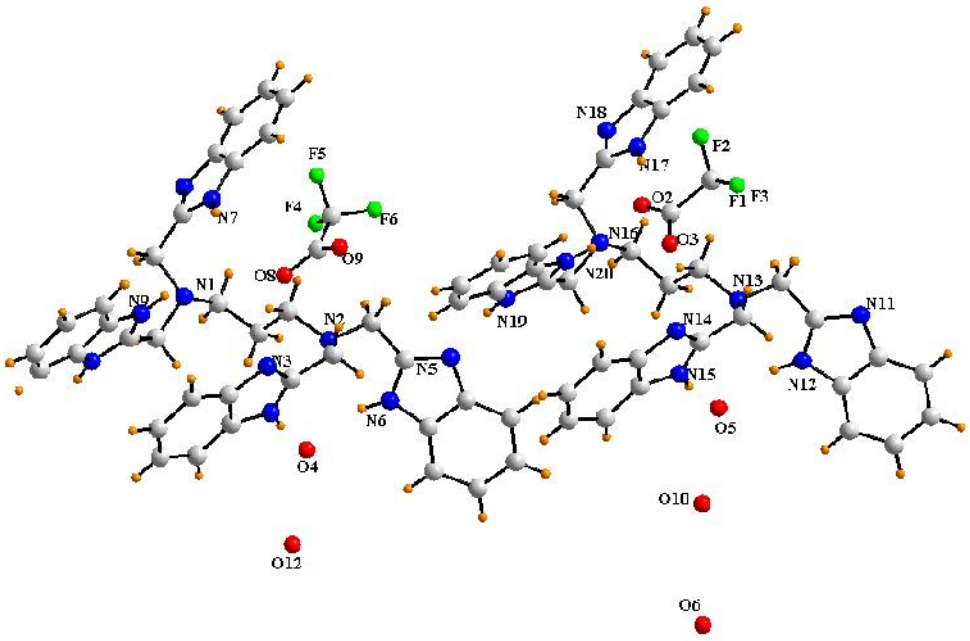


**Fig. 3.65** Crystal structure of salt $[2(H_5PDTB)^{+}.2(CF_3COO)^{-}.5H_2O]$, **3j**. Color code: C, grey; N, blue; H, orange; O, red; F, green.

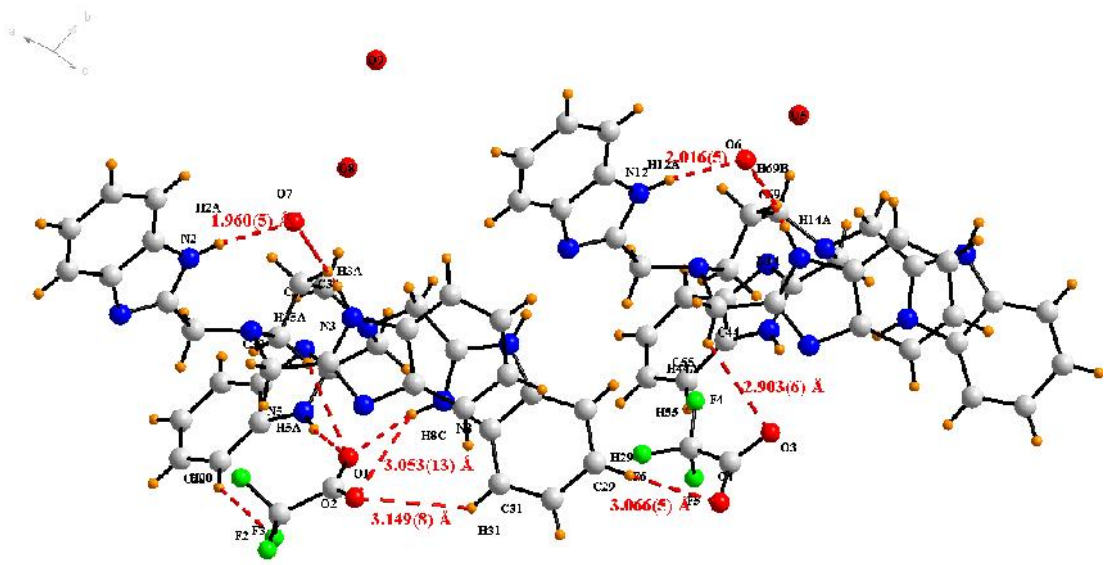


**Fig. 3.66** Different non-covalent interactions in **3j**. Color code: C, grey; N, blue; H, orange; O, red; F, green

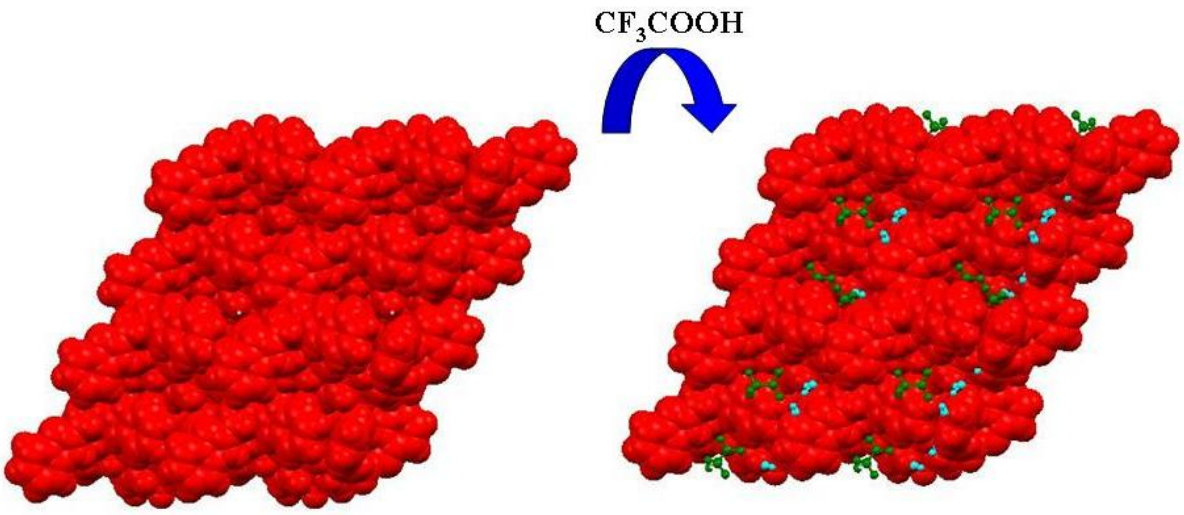


**Fig. 3.67** Three dimensional packing in **3j**

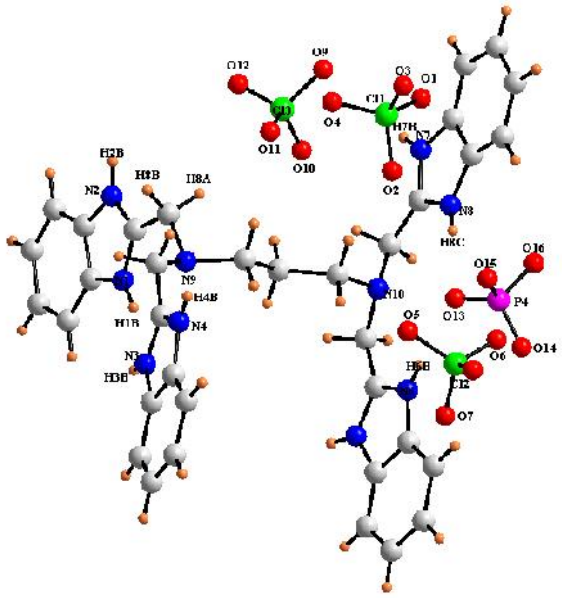

**Fig. 3.68** Crystal structure of salt $[(H_8PDTB)^{4+}.3(ClO_4)^{-}.(H_2PO_4)^{-}]$ **3k**. Color code: C, grey; N, blue; H, orange; O, red; F, green

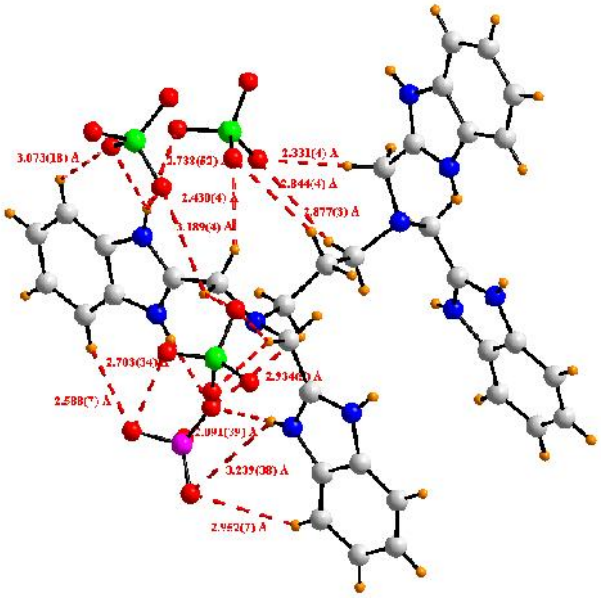

**Fig. 3.69** Different non-covalent interactions in salt **3k**. Color code: C, grey; N, blue; H, orange; O, red; Cl, green

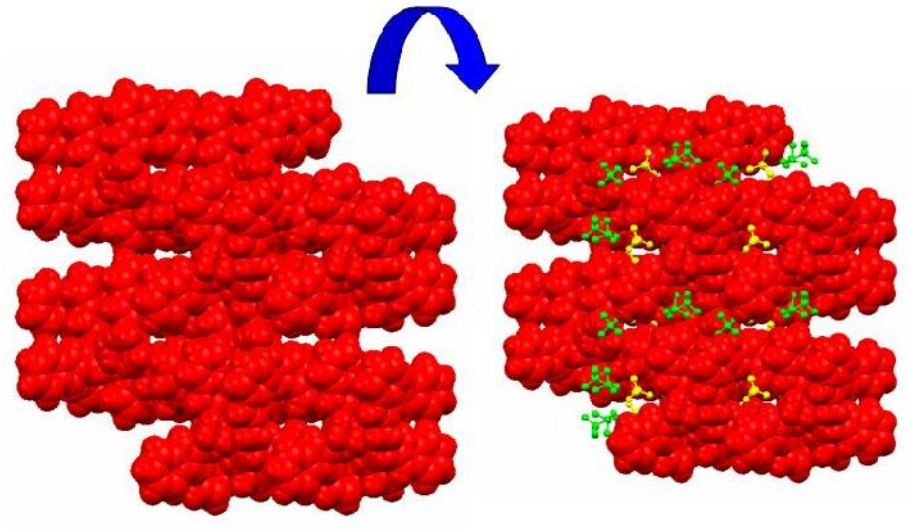

**Fig. 3.70** Three dimensional packing in salt **3k**

**A** **B** **C** **D** **E** **F**

**Fig.3.71** Color change after the addition of different acids in the methanolic solution of ligand **(A)** $H_4$EDTB **(B)** $H_4$EDTB + 0.5 mL $HClO_4$ **(C)** $H_4$EDTB + 0.5 mL HBr **(D)** $H_4$EDTB + 0.5 mL HF **(E)** $H_4$EDTB + 0.5 mL $H_3PO_4$ **(F)** $H_4$EDTB + 0.5 mL $CH_3COOH$

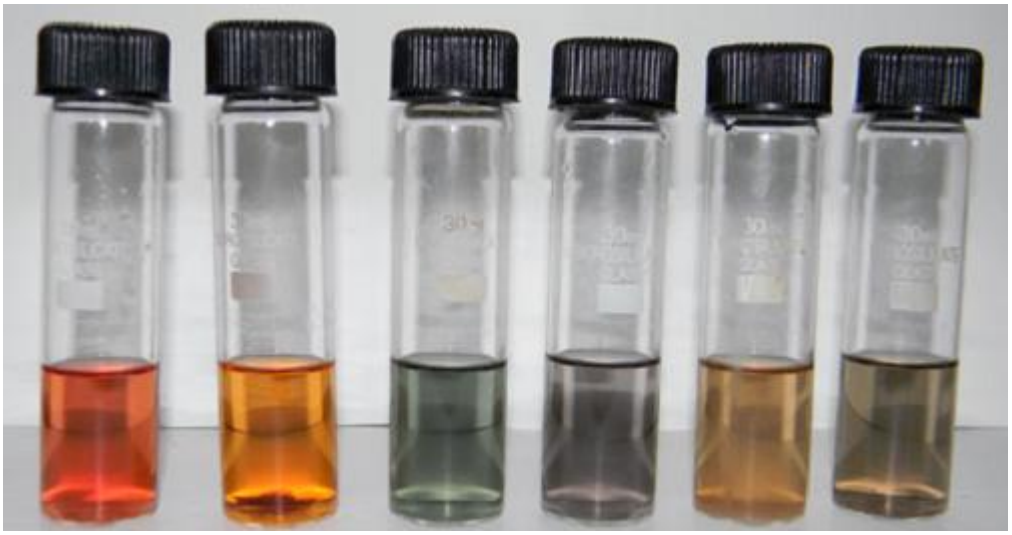

**A** **B** **C** **D** **E** **F**

**Fig.3.72** Color change after the addition of different acids in the methanolic solution of ligand **(A)** Ligand $H_4PDTB$ **(B)** $H_4PDTB$ + 0.5 mL $HClO_4$ **(C)** $H_4PDTB$ + 0.5 mL HCl **(D)** $H_4PDTB$ + 0.5 mL $H_3PO_4$ **(E)** $H_4PDTB$ + 0.5 mL $HNO_3$ **(F)** $H_4PDTB$ + 0.5 mL $CF_3COOH$

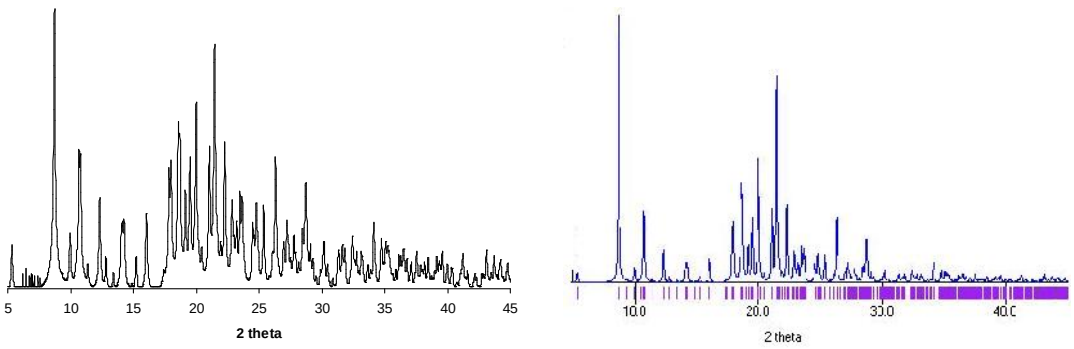


**(a)**

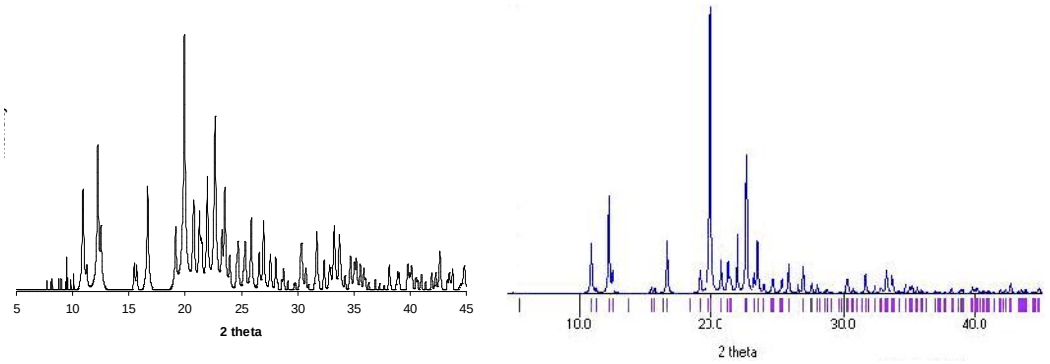


**(b)**

**Fig. 3.73** Representative powder XRD patterns of **(a)** salt **3a** and **(b) 3h**. The left and right patterns in each case correspond to experimental and simulated, respectively

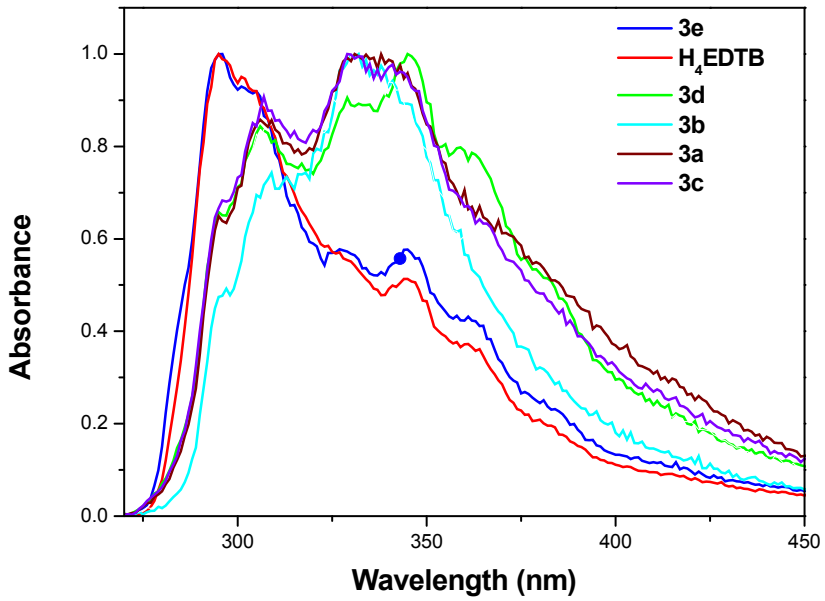


**Fig. 3.74:** Absorption spectra of ligand ($H_4$EDTB), their salts and co-crystal

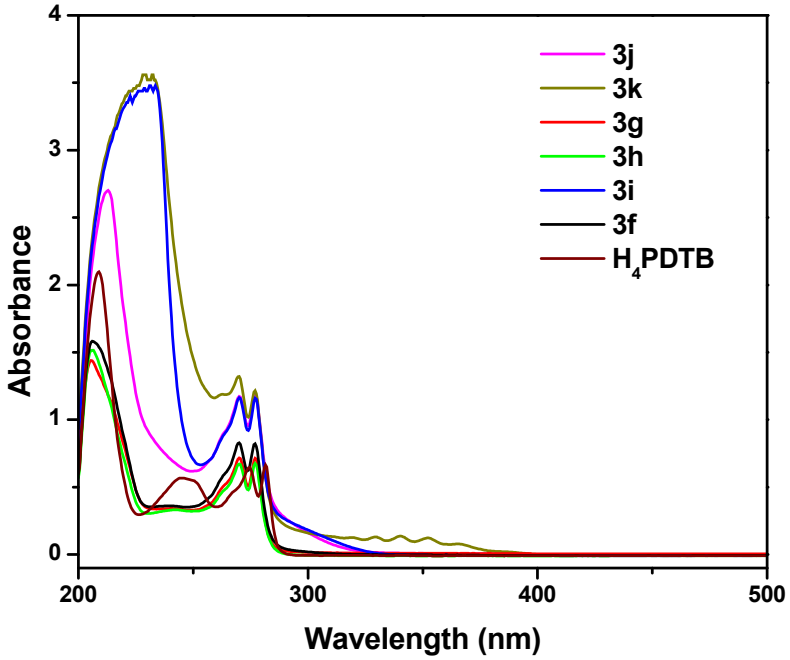


**Fig. 3.75:** Absorption spectra of ligand ($H_4$PDTB), their salts

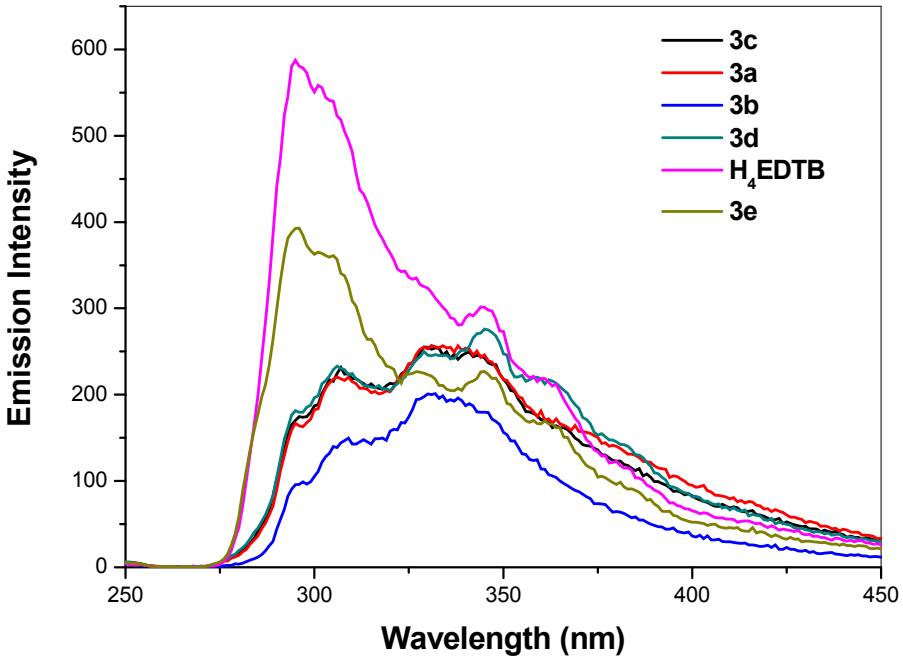


**Fig.3.76** Fluorescence spectra of ligand ($H_4$EDTB) and their salts

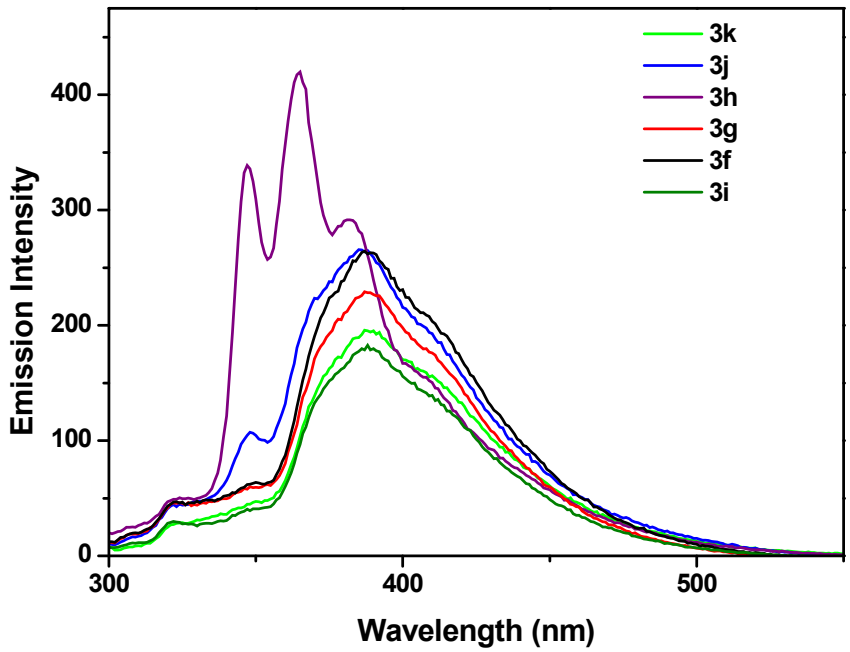


**Fig.3.77** Fluorescence spectra of ligand ($H_4$PDTB) and their salts

**References**


1. Amendola, V., Gòmez, E. D., Fabbrizzi, L. and Licchelli, M. A., "What anions do to N−H-containing receptors", *Chem. Res*, **39**, 343 (2006).
2. Bowman-James, K., "Alfred Werner Revisited: The coordination chemistry of anions", *Acc. Chem. Res.*, **8,** 671 (2005).
3. Gale, P. A., "Anion and ion-pair receptor chemistry: Highlights from 2000 and 2001", *Coord. Chem. Rev*., **240**, 191 (2003).
4. Sessler, J. L., Gale, P. A., Cho, W. S. and Stoddart, J. F., "Eds monographs in supramolecular chemistry royal society of chemistry cambridge U.K, 2006.
5. Gale, P. A., "Preface", *Coord. Chem. Rev*., **250**, 2917 (2006).
6. Kang, S. O., Powell, D., Day, V. W. and Bowman-James, K., "Trapped bifluoride", *Angew. Chem., Int. Ed*., **45**, 1921 (2006).
7. Kang, S. O., Begum, R. A. and BowmanJames, K., "Amide-based ligands for anion coordination", *Angew. Chem., Int. Ed*, **45**, 7882 (2006).
8. Bisson, A. P., Lynch, V. M., Monahan, M. K. C. and Anslyn, E. V., "Recognition of anions through NH···π hydrogen bonds in a bicyclic cyclophane selectivity for nitrate", *Angew. Chem., Int. Ed*., **36**, 2340 (1997).
9. Vance, D. H. and Czarnik, A. W., "Real-time assay of inorganic pyrophosphatase using a high-affinity chelation-enhanced fluorescence chemosensor", *J. Am. Chem. Soc*., **116**, 9397 (1994).
10. Schmuck, C. and Machon, U., "2-(Guanidiniocarbonyl)furans as a new class of potential anion hosts: Synthesis and first binding studies", *Eur. J. Org. Chem*., 4385 (2006).
11. Gale, P. A., "Synthetic indole, carbazole, biindole and indolocarbazole-based receptors: Applications in anion complexation and sensing", *Chem. Commun*., **38**, 4525 (2008).
12. Caltagirone, C., Hiscock, J. R., Hursthouse, M. B., Light, M. E. and Gale, P. A. "1,3-Diindolylureas and 1,3-diindolylthioureas: Anion complexation studies in solution and the solid state", *Chem. Eur. J*., **14,** 10236 (2008).
13. Sessler, J. L., Cho, D. G. and Lynch, V., "Diindolylquinoxalines: Effective indole-based receptors for phosphate anion", *J. Am. Chem. Soc*., **128,** 16518 (2006).
14. Sessler, J. L., Camiolo, S. and Gale, P. A., "Pyrrolic and polypyrrolic anion binding agents", *Coord. Chem. Rev*., **240,** 17 (2003).

15. Sessler, J. L., Kim, S. K., Gross, D. E., Lee, C. H., Kim, J. S. and Lynch, V. M., "Crown-6-calix[4]arene-capped calix[4]pyrrole: An ion-pair receptor for solvent-separated CsF Ions", *J. Am. Chem. Soc.*, **130**, 13162 (2008).
16. Quinlan, E., Matthews, S. E. and Gunnlaugsson, T. J., "Colorimetric recognition of anions using preorganized tetra-amidourea derived calix[4]arene sensors", *J. Org. Chem*., **72,** 7497 (2007).
17. Jose, D. A., Kumar, D. K., Ganguly, B. and Das, A., "Efficient and simple colorimetric fluoride ion sensor based on receptors having urea and thiourea binding sites", *Org. Lett*., **6,** 3445 (2004).
18. Sharma, D., Narasimhan, B., Kumar, P., Judge, V., Narang, R., Clercq, E. D. and Balzarini, J. J., "Synthesis, antimicrobial and antiviral activity of substituted benzimidazoles", *J. Enzym. Inhib. Med. Chem*., **24**, 1161 (2009).
19. Abonia, R., Cortes, E., Insuasty, B., Quiroga, J., Nogueras, M. and Cobo, J., "Synthesis of novel 1,2,5-trisubstituted benzimidazoles as potential antitumor agents", *Eur. J. Med. Chem*., **46,** 4062 (2011).
20. Kumar, D., Kumar, N. M., Chang, K. H. and Shah, K., "Synthesis and anticancer activity of 5-(3-indolyl)-1,3,4-thiadiazoles", *Eur. J. Med. Chem*., **45,** 4664 (2010).
21. Gowda, N. R. T., Kavitha, C. V., Chiruvella, K. K., Joy, O., Rangappa, K. S. and Raghavan, S. C., "Synthesis and biological evaluation of novel 1-(4-methoxyphenethyl)-1H-benzimidazole-5-carboxylic acid derivatives and their precursors as antileukemic agents", *Bioorg. Med. Chem. Lett*., **19,** 4594 (2009).
22. Tonelli, M., Simone, M., Tasso, B., Novelli, F., Boido, V., Sparatore, F., Paglietti, G., Prid, S., Gilliberti, G., Blois, S., Ibba, C., Sanna, G., Loddo, R. and Colla, P. L., "Antiviral activity of benzimidazole derivatives. II. Antiviral activity of 2-phenylbenzimidazole derivatives", *Biorg. Med. Chem*., **18**, 2937 (2010).
23. Chen, G., Liu, Z., Zhang, Y., Shan, X., Jhang, L., Zhao, Y., He, W., Feng, Z. Yang, S. and Liang, G., "Synthesis and anti-inflammatory evaluation of novel benzimidazole and imidazopyridine derivatives", *Med. Chem. Lett*., **4**, 69 (2013).
24. Coon, T., Moore, W. J., Li, B., Yu, J., Zarkani-Kord, S., Malanv, S., Santos, M. A., Hernandez, L. M., Petroshi, K. E., Sun, A., Wen, J., Sullivan, S., Haelewyn, J., Hedrick, M., Hoare, S. J., Bradbury, M. J., Crowe, P. D. and Beaton, G.,

"Brain-penetrating 2-aminobenzimidazole H1-antihistamines for the treatment of insomnia", *Bioorg. Med. Chem. Lett*., **19**, 4380 (2009).

25. Kuo, H. L., Lien, J. C., Chung, C. H., Lo, S. C., Tsai, I. C., Peng, H. C., Luo, S. C. and Huang, T. E., "NP-184[2-(5-methyl-2-furyl) benzimidazole], a novel orally active antithrombotic agent with dual antiplatelet and anticoagulant activities", *Naunyn. Schmiedebergs Arch. Pharmacol*., **381**, 495 (2010).
26. Hossain, M. A., Liljegren, J. A., Powell, D. and Bowman-James, K., "Anion binding with a tripodal amine", *Inorg. Chem*., **43**, 3751 (2004).
27. Kim, H., In, S. and Kang, J., "Anion receptor with two imidazolium rings on the glycoluril", *Supramol. Chem*., **18**, 141 (2006).
28. Amendola, V., Boiocchi, M., Colasson, B., Fabbrizzi, L., Douton, M. J. R. and Ugozzoli, F., "A metal-based trisimidazolium cage that provides six C-H hydrogen-bond-donor fragments and includes anion", *Angew. Chem; Int. Ed*., **45**, 6920 (2006).
29. Dickson, S. J., Wallace, E. V. B., Swinburne, A. N., Paterson, M. J., Lloyd, G. O., Beeby, A., Belcher, W. J. and Steed, J. W., "Intramolecular binding site competition as a means of tuning the response of a colourimetric anion sensor", *New J. Chem*., **32**, 786 (2008).
30. Arunachalam, M., Chakraborty, S., Marivel, S. and Ghosh, P., "Anion-assisted formation of discrete homodimeric and heterotetrameric assemblies by benzene based protonated heteroaryl receptors", *Cryst. Growth Des*., **12**, 2097 (2012).
31. Gogoi, A. and Das, G., "Charge-assisted complexation of anions of different dimensionality by benzimidazole-based receptors bearing -OH functionality", *Cryst. Growth Des*., **12**, 4012 (2012).
32. Singh, N. and Jang, D. O., "Benzimidazole-based tripodal receptor: Highly selective fluorescent chemosensor for iodide in aqueous solution", *Org. Lett*., **9**, 1991 (2007).
33. Lee, D. Y., Singh, N., Kim, M. J. and Jang, D. O., "Chromogenic and fluorescent recognition of iodide with a benzimidazole-based tripodal receptor", *Org. Lett*., **13**, 3024 (2011).
34. Joo, T. Y., Singh, N., Lee, G. W. and Janga, D. O., "Benzimidazole-based ratiometric fluorescent receptor for selective recognition of acetate", *Tetrahedron Lett*., **48,** 8846 (2007).

35. Yu, M., Lin, H., Zhao, G. and Lin, H., "A benzimidazole-based chromogenic anion receptor", *J. Mol. Recognit*., **20**, 69 (2007).
36. Ghosh, K. and Kar, D.,"Fluorometric recognition of both dihydrogen phosphate and iodide by a new flexible anthracene linked benzimidazolium-based receptor", *Beilstein J. Org. Chem*., **7**, 254 (2011).
37. Molina, P., Tárraga, A. and Otón, F., "Imidazole derivatives: A comprehensive survey of their recognition properties", *Org. Biomol. Chem*., **10**, 1711 (2012).
38. Lirag, R. C., Le, H. T. M. and Miljanic, O. S., "L-shaped benzimidazole fluorophores: Synthesis, characterization and optical response to bases, acids and anions", *Chem. Commun*., **49**, 4304 (2013).
39. Gale, P. A., Hiscock, J. R., Lalaoui, N., Light, M. E., Wells, N. J. and Wenzel, M., "Benzimidazole-based anion receptors: Tautomeric switching and selectivity", *Org. Biomol. Chem*., **10**, 5909 (2012).
40. Lee, K. M., Lee, C.-K. and Lin, I. J. B., "N,N′-dihexylbenzimidazolium salts. Anion-controlled bilayer structures via π–π dimer or C–H···π catemer motifs", *Cryst. Eng. Comm*., **12**, 4347 (2010).
41. Matthew, G., Fisher, P. A., Gale, and Mark, E. L., "A simple benzimidazole-based receptor for barbiturate and urea neutral", *New J. Chem*., **31**, 1583 (**2007**).
42. Hiscock, J. R., Gale, P. A., Lalaoui, N., Lighta, M. E. and Wells, N. J., "Benzimidazole-based anion receptors exhibiting selectivity for lactate over pyruvate", *Org. Biomol. Chem*., **10**, 7780 (2012).
43. Yoon, J., Kim, S. K., Singh, N. J. and Kim, K. S., "Imidazolium receptors for the recognition of anions", *Chem. Soc. Rev*., **35**, 355 (2006).
44. Ji, B. M., Deng, D. S., Ma, N., Miao, S. B., Yang, X. G., Ji, L. G. and Du, M., "Multicomponent hydrogen-bonding salts constructed from tris(2-benzimidazylmethyl)amine and various carboxylic acids: Role of benzimidazolium-carboxylate supramolecular heterosynthons on network assembly", *Cryst. Growth Des*., **10**, 3060 (2010).
45. Ghosh, K., Sen, T. and Patra, A., "Binding induced destruction of an excimer in anthracene-linked benzimidazole diamide: A case toward the selective detection of organic sulfonic acids and metal ions", *New J. Chem*., **34**, 1387 (2010).

46. Cui, Y., Mo, H. -J., Chen, J. -C., Niu, Y. -L. Zhong, Y. -R. Zheng, K. -C. Ye, B. -H., "Anion-selective interaction and colorimeter by an optical metalloreceptor based on ruthenium (II) 2,2‘-biimidazole: Hydrogen bonding and proton transfer", *Inorg. Chem*., **46**, 6427 (2007).
47. Saha, D., Das, S., Bhaumik, C., Dutta, S. and Baitalik, S., "Bimetallic reactivity. Synthesis of bimetallic complexes containing a bis(phosphino)pyrazole ligand", *Inorg. Chem*., **49**, 2334 (2010).
48. Matthews, C. J., Broughton, V., Bernardinelli, G., Melich, X., Brand, G., Willis, A. C, and Williams, A. F., "Molecular bricklaying: The protonated benzimidazole moiety as a synthon for crystal engineering molecular bricklaying: The protonated benzimidazole moiety as a synthon for crystal engineering", *New J. Chem*., **27**, 354 (2003).
49. Oki, A. R., Bommarreddy, P. R., Zhang, H. and Hosmane, N., "Manganese (II) complex of the ‘tripod’ ligand tris(2-benzimidazolylmethyl)amine. Five-coordinate and six-coordinate Mn(II) in the crystal structure", *Inorg. Chim. Acta*., **231**, 109 (1995).
50. Hossain, M. A., Morehouse, P., Powell, P. D., and Bowman-James, K., "Tritopic (cascade) and ditopic complexes of halides with an azacryptand", *Inorg. Chem*., **44,** 2143 (2005**).**
51. Singh, U. P., Kashyap, S., Singh, H. J. and Butcher, R. J., "Anion directed supramolecular architecture of pyrazole based ionic salts", *Cryst. Eng. Comm*., **13**, 4110 (2011).
52. Singh, U. P., Kashyap, S., and Singh, H. J., "Effect of electron donating substituents on supramolecular structure of salts having phenylphosphonic acid and pyrazoles", *Struct. Chem*., **22**, 931 (2011).
53. Kang, S. O., Llinares, J. M., Powell, D., VanderVelde, D. and Bowman-James, K., "New polyamide cryptand for anion binding", *J. Am. Chem. Soc*., **125**, 10152 (2003).
54. Ilioudis, C. A., Tocher, D. A. and Steed, J. W, "A highly efficient, preorganized macrobicyclic receptor for halides based on CH⋯ and NH⋯anion interactions", *J. Am. Chem. Soc*., **126**, 12395 (2004).
55. Lakshminarayanan, P. S., Kumar, D. K. and Ghosh, P., "Counteranion-controlled water cluster recognition in a protonated octaamino cryptand", *Inorg. Chem*., **44**, 7540 (2005).

56. Chmielewski, M. J., Charon, M. and Jurczak, J., “1,8-Diamino-3,6-ichlorocarbazole: A promising building block for anion receptors”, *Org. Lett*., **6**, 3501 (2004).
57. Lakshminarayanan, P. S., Ravikumar, I., Suresh, E. and Ghosh, P., “Trapped inorganic phosphate dimer”, *Chem. Comm*., 5214 (2007).
58. Etter, M. C., “Encoding and decoding hydrogen-bond patterns of organic compounds”, *Acc. Chem. Res*., **23**, 120 (1990).
59. Amendola, V., Boiocchi. M., Esteban-Gomez, D., Fabbrizzi, L. and Monzani, E., “Chiral receptors for phosphate ions”, *Org. Biomol. Chem*., **3**, 2632 (2005).
60. Sessler, J. L., Cho, D. G. and Lynch, V., “Diindolylquinoxalines: Effective indole-based receptors for phosphate anion”, *J. Am. Chem. Soc*., **128**, 16518 (2006).
61. Ju, J., Park, M., Suk, J. -M., Lah, M. -S. and Jeong, K. -S., “An anion receptor with NH and OH Groups for hydrogen bonds”, *Chem. Comm*., 3546 (2008).
62. Wu, B., Huang, X., Xia, Y., Yang. -J. and Janiak, C., “Oxo-anion binding by protonated (dimethylphenyl)(pyridyl)ureas”, *Cryst. Eng. Comm*., **9**, 676 (2007).
63. Ali, H. D. P., Kruger, P. E. and Gunnlaugsson, T., “Colorimetric ‘naked-eye’ and fluorescent sensors for anions based on amidourea functionalised 1,8-naphthalimide structures: Anion recognition via either deprotonation or hydrogen bonding in DMSO”, *New J. Chem*., **32,** 1153 (2008).
64. Steed, J. W., “Coordination and organometallic compounds as anion receptors and sensors”, *Chem. Soc. Rev*., **38**, 506 (2009).

# Chapter 4

# Synthesis, Structural and Photoluminescence Studies of Zinc (II) and Cadmium (II) Complexes with Benzimidazole Based Ligands

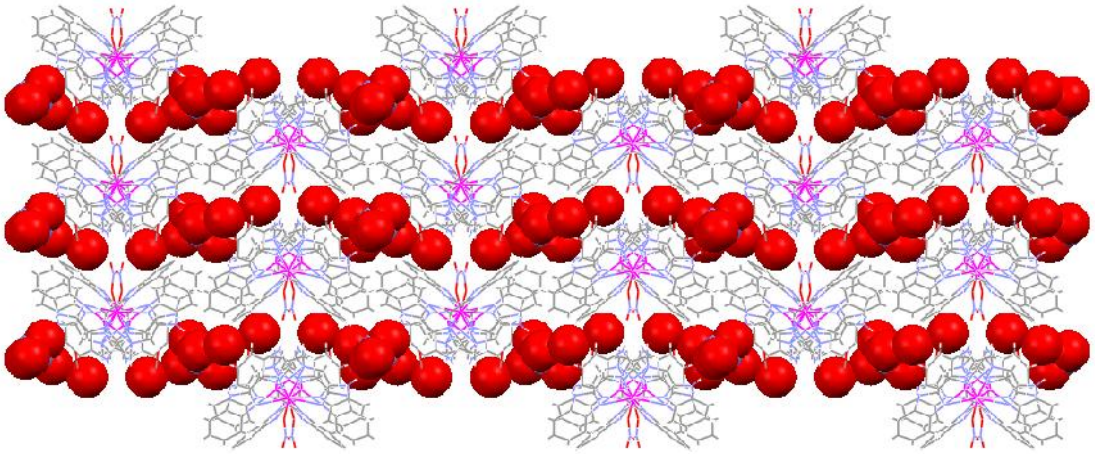

The development of inorganic supramolecular network is an intensive area of chemistry due to fundamental interest in self-assembly processes, supramolecular chemistry and most significantly in crystal engineering [1-8]. The rational design and exploration of new synthetic strategies for novel metal complexes have attracted much attention not only because of their fascinating structural diversities but also for their promising applications in catalysis, separation, gas storage, luminescence, nonlinear optics and many more [9-24]. The structure primarily depends on the coordination nature of the metal, coordination geometries around the metal centers, the metal-ligand ratio and various other experimental conditions. Moreover, literature also reveals that in the design and synthesis of metal complexes, the structural features of the organic ligands play a crucial role due to their diversities in coordination modes and conformations [25]. Along with these, the counter ions also play an important role in governing the network formation [26-27].

Benzimidazole derivatives have been widely used as a versatile ligand in coordination and supramolecular chemistry and have a strong tendency to coordinate with the metal centers, which can lead to materials with potential applications in various fields. It has significant roles in different areas such as in catalysis, pharmacological, antimicrobial, fungicidal, herbicidal and therefore they are extensively used in pharmaceutical and chemical industries [28-31]. The flexible benzimidazole or benzimidazole based ligands are an excellent organic building block for the construction of 1-D, 2-D and 3-D supramolecular networks. It has been used in coordination chemistry with different binding modes e.g., as a bidentate bridging ligand [32], as a terminal ligand [33] or as a host molecule [34] and can exhibits different conformation geometries due to the presence of the flexible methylene group between the benzimidazole rings, which may be further involved in hydrogen bonding and/or π-stacking interactions [35].

Zinc and Cadmium are congeners of mercury and belong to the group 12 of the periodic table. The lightest element zinc of this group occurs as an essential constituent in numerous proteins whereas cadmium is toxic in nature. Cadmium apart from toxicity and carcinogenicity have some positive biological effects (e.g., in the growth of fungal species) [36]. A recent report on first cadmium enzyme ascertained the role of cadmium in biological system [37]. Zinc is the second most abundant transition element in the human organism, following iron and involved in virtually all aspects of metabolism. It is present in a large number of enzymes and proteins where metal is attached to the

protein backbone preferentially by nitrogen (histidine) donors and less prominently by oxygen (aspartate, glutamate) donors. The major role of zinc in the active centre of enzymes is to catalyse the hydrolytic reactions [38-39].

The transition metal complexes derived from imidazole/benzimidazole based ligand possess intriguing structural features and fascinating chemical properties. Recent studies focused to these types of complexes for their applications in material science. The low-cost, commercial availability and excellent emission properties associated with the complexes of these ligands, especially those containing Zn(II) and Cd(II) ions shows potential for the development of light-emitting devices. [40-41].

In the recent years a considerable amount of interest has been emerged in the development of luminescent compounds because of their various applications in chemical sensors, photochemistry and electroluminescent (EL) display. Among them, the majority is constituted by zinc (II) and cadmium (II) complexes due to their unique properties. It has been observed that presence of zinc (II) or cadmium (II) ion coordinated to the ligand results in enhancement in the emission intensity of the ligand molecule which may be due to several facts.

(i) The enhancement of luminescence in metal complexes could be attributed due to the coordination of ligand to the metal center, which improves the "rigidity" of the molecule and thereby reduces the loss of energy through a radiationless pathway.

(ii) Second, the quenching of emission intensity by paramagnetism as observed for several copper (II) complexes is not possible, however this is possible for zinc(II) or cadmium(II) ion due to their diamagnetic nature (close shell configuration, $d^{10}$).

(iii) The presence of zinc (II) or cadmium (II) ion in the ligand solution enhances the observed fluorescence because the coordination makes photoinduced electron transfer (PET) processes thermodynamically inaccessible [42-45].

Lei et al. [46] synthesized various metal-organic coordination architectures with benzimidazole-based rigid ligand, $[CuL_I]_2.2CHCl_3.H_2O$ (**1**), $[CdL_2(NO_3)_2].4C_2H_5OH$ (**2**), $[AgL(BF_4)].3CHCl_3$ (**3**), $[AgL(NO_3)].2CHCl_3$ (**4**) and $[MnL_2Cl_2].2CHCl_3$ (**5**) ( L = 9,10-bis(N-benzimidazolyl)anthracene) and characterized them by elemental analyses, IR spectroscopy and X-ray crystallography. They found that in **1**, the Cu(I) ion takes

tetrahedral coordination geometry and the rigid ligands bridged two dinuclear [$Cu_2I_2$] units to form a two-dimensional (2-D) layer, whereas **2** and **5** shows 2-D network structure with (4,4) topology in which the metal ions have octahedral coordination geometry (Fig. 4.1 a-b). They also noticed that **3** and **4** displayed 1-D chain structures, but show different crystal packing modes due to the effect of anions. Therefore they concluded that the nature of ligand, metal coordination geometry and counter anions have an important effect on the structural topologies of such complexes and found that complexes **1-4** displays a strong blue emissions in the solid state at room temperature (Fig. 4.2).

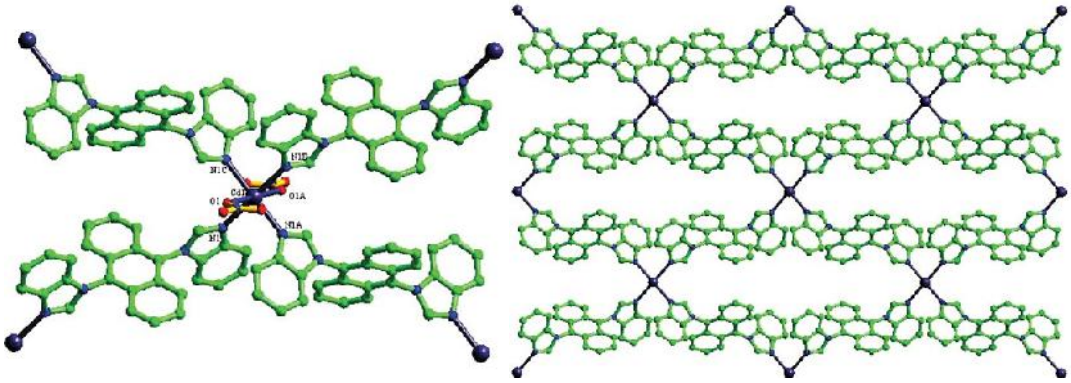

**(a)** **(b)**

**Fig. 4.1 (a)** View of the coordination environments of Cd(II) ions **(b)** 2-D (4,4) network

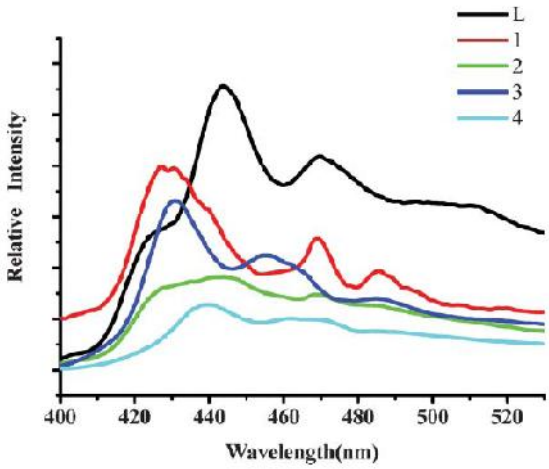


**Fig. 4.2** Fluorescence spectra of L and complexes **1-4** in solid state at room temperature

Yue et al. [47] synthesised a series of luminescent Zn(II) and Cd(II) complexes with three different π-conjugated ligands, 2-(2-pyridyl)-imidazole (HL1), 2-(2-pyridyl)-

benzimidazole (HL2) and 2,6-bis(benzimidazol-2yl)-pyridine ($H_2L3$) viz., . $Zn(L1)_2.H_2O$ (**1**), $Cd(L1)_2.2H_2O$ (**2**), $[Zn(HL1)_2]Cl_2$ (**3**), $[Cd(HL1)_2]Cl_2$ (**4**), $Zn(L2)_2H_2O$ (**5**), $[Cd(L2)_2(H_2O)_2].2DMSO$ (**6**), $[Zn(HL2)_2](ClO_4)_2$ (**7**), $[Cd(HL2)_2](ClO_4)_2$ (**8**), $Zn(HL3)_2$ (**9**), $Cd(HL3)_2$ (**10**) and characterized by X-ray crystallography. They described the structure of **5** as best square pyramid and the coordination geometries of **6**, **9** and **10** as distorted octahedrons (Fig. 4.3a-d). They found that the photo luminescence spectra of the ligands exhibit a bathochromic shift due to the extended π -conjugation of the ligand and the spectra of the complexes with the ligands follow the same. They noticed that these complexes show emission maxima in the blue region in the solid state as well as in DMSO and have a bathochromic shift of the emission energy in contrast to the free ligands and further more they displayed blue luminescence and their high luminescence quantum efficiency (Fig. 4.3e). They established with theoretical study that the emissions are intraligand transitions of the deprotonated L2 and HL3 ligands and the metal ions in the complexes play a key role in stabilizing the ligand and promoting the luminescence.

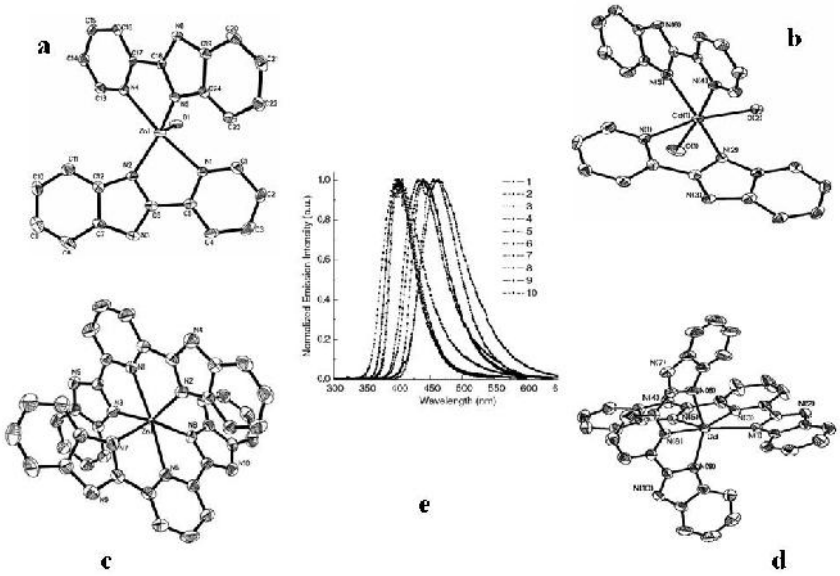


**Fig**. **4.3** (**a-d**) Crystal Structure of $Zn(L2)_2H_2O$ (**5**), $[Cd(L2)_2(H_2O)_2].2DMSO$ (**6**), $Zn(HL3)_2$ (**9**), $Cd(HL3)_2$ (**10**). (**e**) Solid PL spectra of the complexes **1-10**

Feng et al. [48] synthesized three coordination polymers viz., $[Co(HL)(HBDC)]_n$ (**1**), $[Co(HL)(BDC)_{0.5}]_n$ (**2**) and $\{[Zn_2(H_2L)(BTC)_2](H_4L)(H_2O)_2\}_n$ (**3**) (L = 2,2′-(ethanediyl)bis(1H-benzimidazole), $H_2BDC$ = 1,4-benzenedicarboxylic acid, $H_3BTC$ = 1,3,5-benzene-tricarboxylic acid) under hydrothermal condition and

characterized by X-ray single-crystal diffraction (Fig.4.4a-b). They demonstrated that the diverse coordination modes of $H_2L$ ligand and the varying geometries of multi-dentate carboxylate ligands play an important role in the construction of coordination polymers. They showed the room temperature photoluminescence of compound **3**, which have a maximum emission at 463 nm with one shoulder peaks at 488 nm and one sharp peaks at 438 nm ($\lambda_{ex}$=369 nm), whereas free L ligand displayed a maximum emission at 433 nm with a shoulder peak at 457 nm ($\lambda_{ex}$=362 nm) (Fig.4.4 b). Furthermore, they demonstrated a red shift of the emission at 463 nm in the L ligands probably due to the incorporation into Zn(II) and suggest a mechanism of ligand-to-metal charge transfer (LMCT) [49-50].

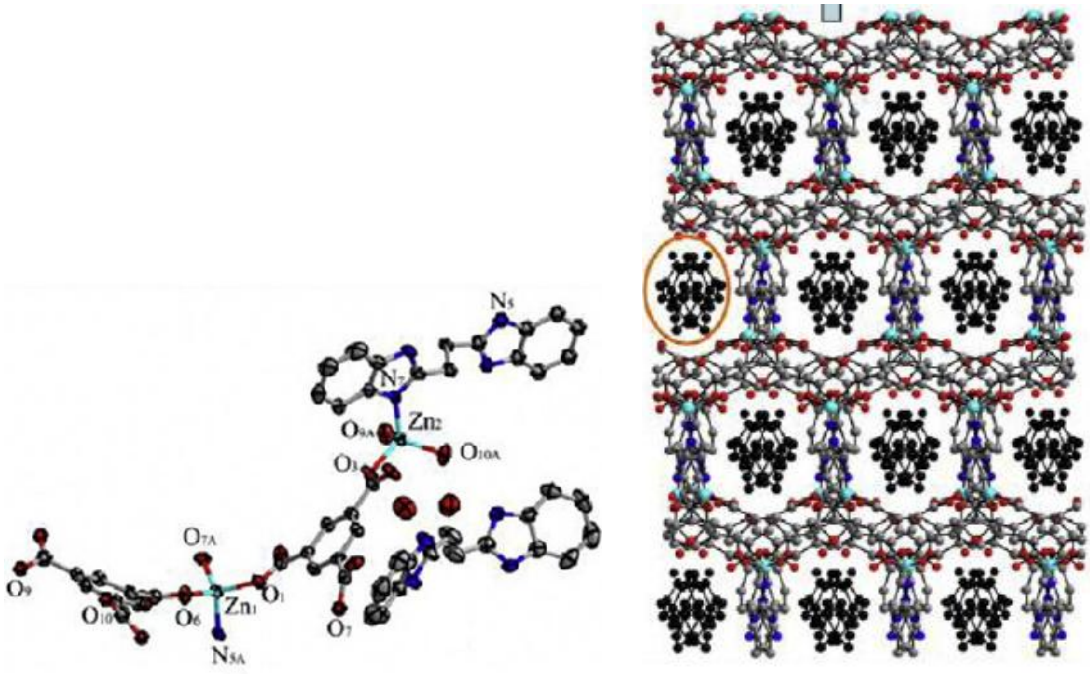


**(a)** **(b)**

**Fig. 4.4 (a)** The coordination environments of zinc atoms in **3**. **(b)** Perspective view of the three-dimensional network along the '*a*' axis

Jiang et al. [51] synthesized hydrothermally two new metal-organic frameworks, $[Cd_2(H_2C_3PIm)(BDC)_4(H_2O)_3]_n$ (**1**) and $[Zn_3(H_2C_3PIm)_3(BTC)_2(H_2O)_2]_n$ (**2**) ($H_2C_3PIm$ = 2,2′-(1,3-propanediyl)bis(1H-benzimidazole), $H_2BDC$ = 1,4-benzenedicarboxylic acid, $H_3BTC$ = 1,3,5-benzene tricarboxylic acid) and characterized by single crystal X-ray diffraction method (Fig. 4.5 a-b). They found that compound **1** presents a 1D columnar structure and compound **2** exhibits a 2D sheet

with novel extra-large rings of 4.82 topology and both the complexes exhibits strong photoluminescence at room temperature. They noticed that the free $H_2C_3PIm$ ligand shows a maximum emission at 423 nm when excited at 349 nm, whereas complex **2** shows a maximum emission at 404 nm when excited at 314 nm and complex **1** exhibits a wide maximum emission at 444 nm when excited at 377 nm (Fig. 4.6). They also supported that the large shift in the emission wavelength of the $H_2C_3PIm$ ligand was due to their incorporation into Cd(II)-containing and Zn(II)-containing polymeric complexes, because of ligand-to-metal charge transfer (LMCT).

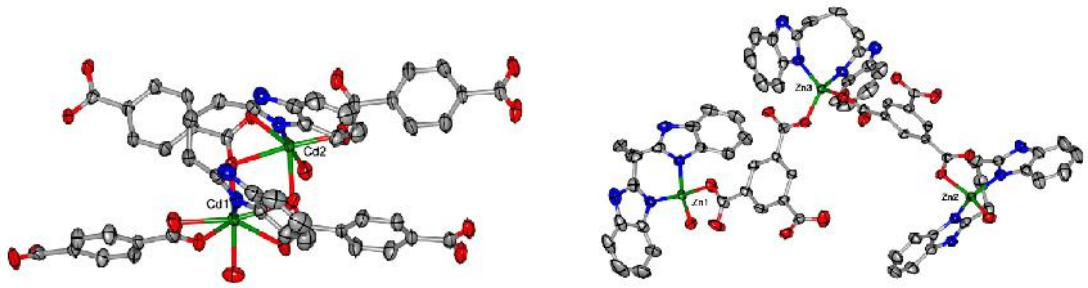


**(a)** **(b)**

**Fig.4.5 (a)** The coordination geometry of Cd(II) atom in complex **1**. **(b)** The coordination geometry of Zn(II) atom in complex **2** (50% thermal ellipsoids)

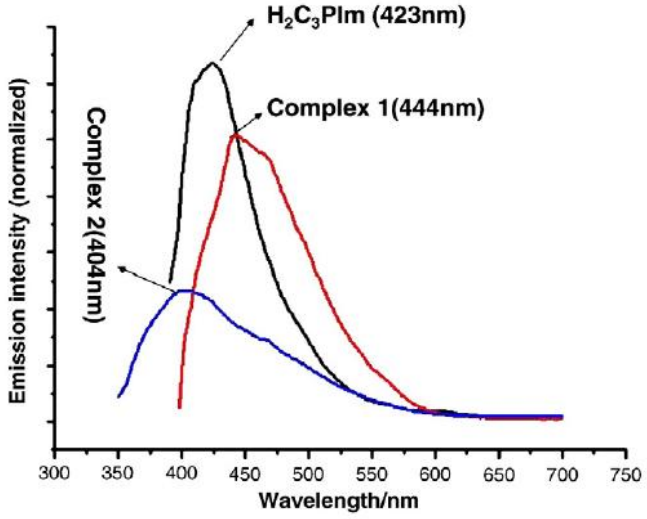


**Fig.4.6** Normalized fluorescence emission spectra of complexes **1**, **2** and the free ligand in the solid state at room temperature

Wang et al. [52] reported 3-D chiral complex $[Zn(adi)_{0.5}(imb)]_n$ (**1**) by the hydrothermal reaction of 2-(1H-imidazolyl-1-methyl)-1H-benzimidazole (Himb), adipic acid ($H_2adi$) with $Zn(NO_3)_2.6H_2O$ in an aqueous solution of DMF and $H_2O$. These complexes were characterized by thermogravimetric analysis (TG), X-ray powder diffraction patterns (XPRD) as well as single-crystal X-ray diffraction methods (Fig. 4.7) and found that the complex **1** showed two types of channels with left-handed helical chains and second one of zig-zag chains. They also measured the excitation and emission spectra of complex in the solid state at room temprture and found an intense emission at 303 nm when excited at 270 nm and compared its emission which attributed to π-π* transitions. (Fig. 4.8).

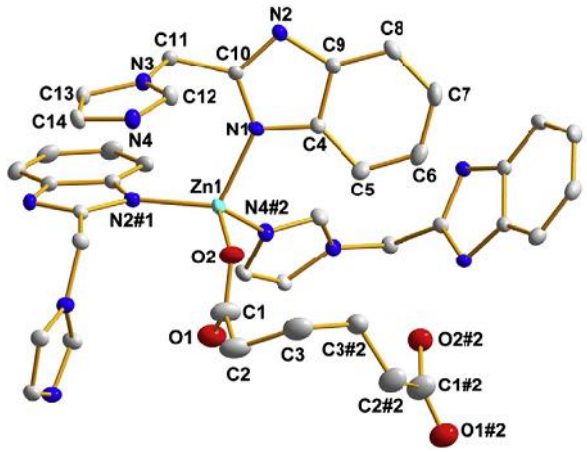


**Fig. 4.7 (a)** Asymmetric crystal structure of complex $[Zn(adi)_{0.5}(imb)]_n$

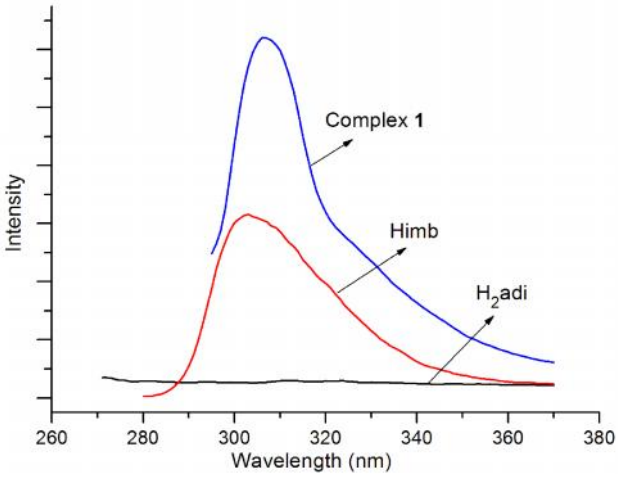


**Fig. 4.8** Fluorescence properties of free Himb, $H_2adi$, and complexes **1**

Wang et al. [53] further synthesized zinc (II) complex with planar tridentate ligand bzimpy (bzimpy = 2,6-bis(benzimidazol-2-yl) pyridine) and characterized by

UV-Vis, NMR, infrared spectroscopy and fluorescence spectra (Fig. 4.9a-b). They exposed that the zinc complex acts as dibasic acids, where N-H protons on benzimidazole moieties were responsible for a deprotonation site and noticed that both the absorption spectra and reduction potentials were strongly dependent on the solution pH, which leads to the basis of a proton-induced molecular switch. They also investigated the binding of this complex with calf thymus DNA through absorption, luminescence titrations and viscosity measurements.

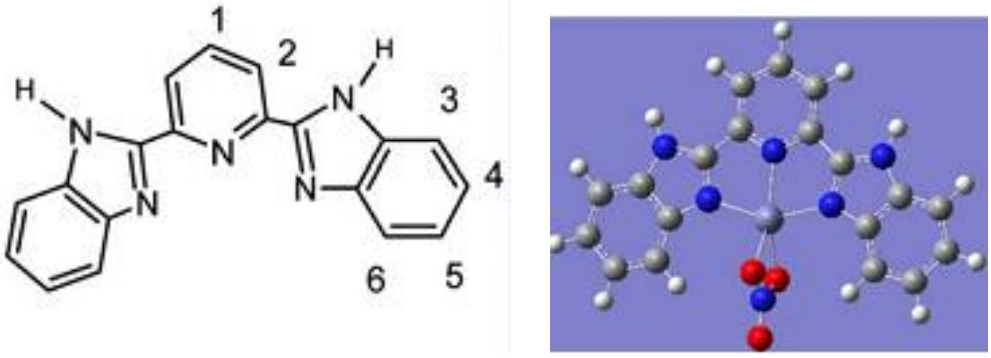


**(a)** **(b)**

**Fig**. **4.9** Molecular structure of **(a)** bzimpy ligand and **(b)** Zn(II) complex

Wu et al. [54] synthesized two novel zinc (II) complexes $[Zn(bbt)_2](pic)_2.DMF.2CH_3OH$ (**1**) and $[Zn(et\text{-}bbt)(acrylate)_2]$ (**2**) (bbt = 1,3-bis(2-benzimidazyl)-2-thiapropane; et-bbt = 1,3-bis(1-ethylbenzimidazol-2-yl)-2-thiapropane; pic = picrate) and characterized by elemental analysis, electrical conductivities, IR, UV-Vis spectral measurements and single crystal X-ray diffraction. On the basis of crystal structures they revealed that both the Zn(II) complexes were four-coordinated forming a distorted tetrahedral geometry with ZnN4 and ZnN2O2 environment respectively (Fig. 4.10-4.11).

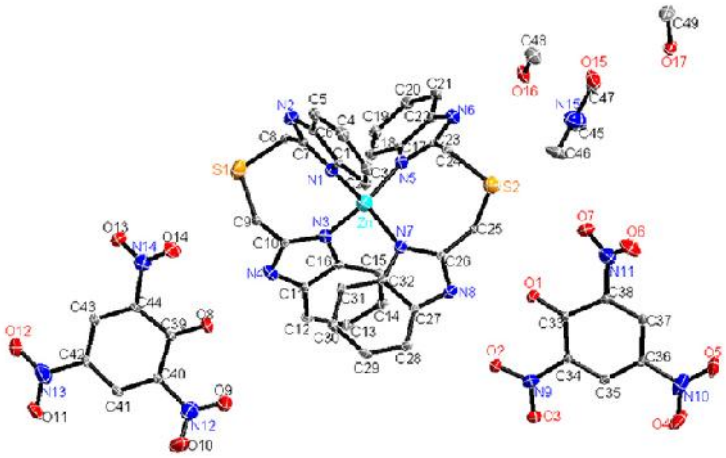

**Fig**. **4.10** Crystal structure of $[Zn(bbt)_2](pic)_2.DMF.2CH_3OH$ (**1**)

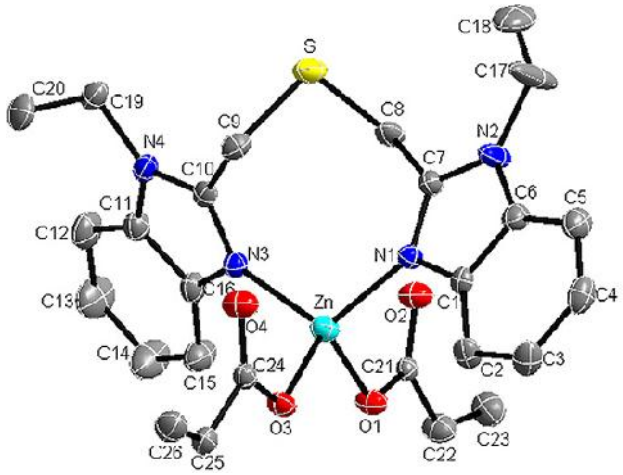

**Fig 4.11** Crystal structure of complex $[Zn(et\text{-}bbt)(acrylate)_2]$ (**2**)

Wu et al. [55] further reported two V-shaped ligands, bis(2-benzimidazol-2-ylmethyl)benzylamine ($L^1$) and bis(N-allylbenzimidazol-2-ylmethyl)benzylamine ($L^2$) and their zinc complexes namely, $[ZnL^1_2](pic)_2.2MeCN.Et_2O$ (**1**) and $[ZnL^2_2](pic)_2$ (**2**) (pic = picrate) and characterized by elemental analysis, UV–Vis, IR spectroscopy. They showed from single crystal X-ray diffraction study that the two Zn(II) complexes have similar distorted octahedral coordination geometry, except with that of the degree of distortion (Fig. 4.12) and investigated their DNA-binding properties by viscosity measurement, electronic absorption and fluorescence titration.

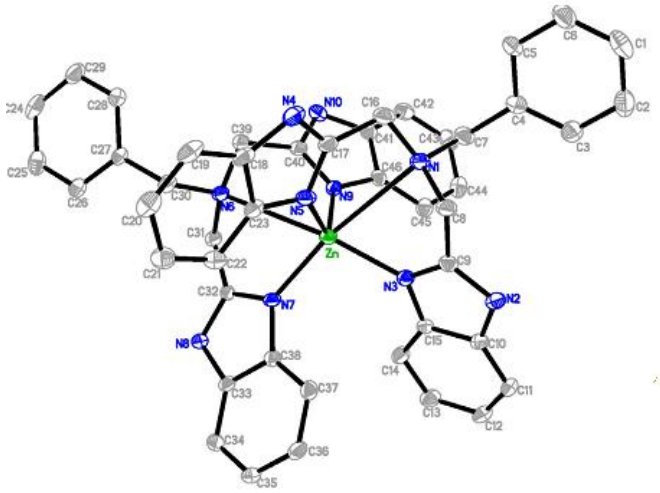


**Fig**. **4.12** Crystal structure of $[ZnL^{1}_{2}]^{2+}$ (**1**)

Liu et al. [56] synthesized six coordination polymers under solvothermal conditions based on three related flexible bis-[(pyridyl)-benzimidazole] ligands (Scheme 4.1) and different carboxylates namely, $[Zn_2(m\text{-BDC})_2(L^1)].2H_2O$ (**1**), $[Zn_2(p\text{-BDC})_2(L^1)(H_2O)_2]$ (**2**), $[Zn_2(m\text{-BDC})_2(L^2)].2.25H_2O$ (**3**), $[Zn_2\text{-}(p\text{-BDC})_2(L^2)].CH_3OH$ (**4**), $[Zn_2(m\text{-BDC})_2(L^3)].2H_2O$ (**5**) and $[Zn_2(p\text{-BDC})_2(L^3)].2CH_3OH$ (**6**) ($L^1$ = 1,10-(1,4-butanediyl)-bis[2-(2-pyridyl)benzimidazole], $L^2$ = 1,10-(1,6-hexanediyl)bis[2-(2-pyridyl)benzimidazole], $L^3$ = 1,10-(1,10-decanediyl)bis-[2-(2-pyridyl)benzimidazole], *m*-BDC = *m*-benzenedicarboxylate anion, and *p*-BDC = *p*-benzenedicarboxylate anion) and determined their structures by single crystal X-ray diffraction analyses (Fig. 4.13). They also studied the luminescent properties of $L^1$-$L^3$ and **1**-**6** in the solid state at room temperature (Fig. 4.14).

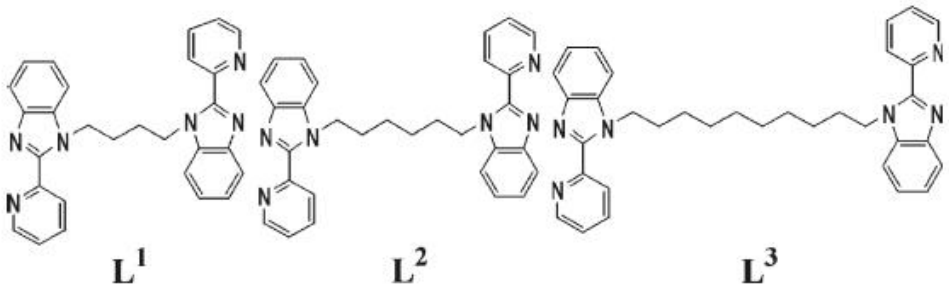


**Scheme 4.1**

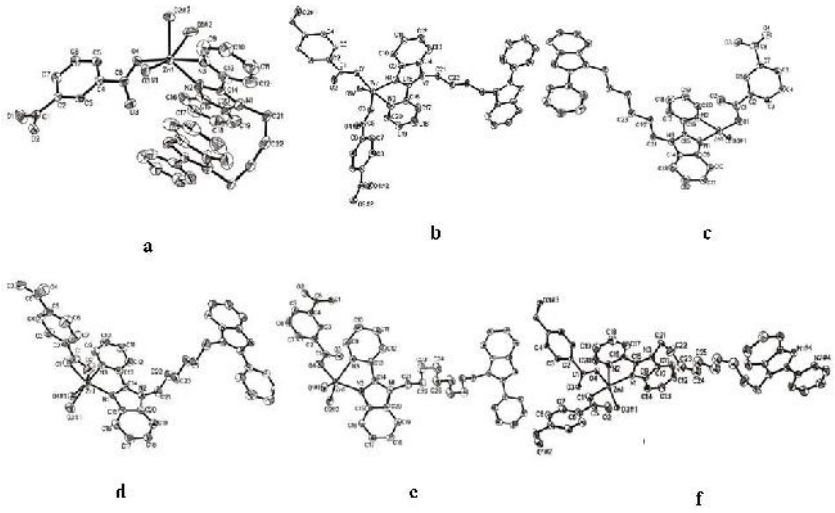


**Fig**. **4.13** Crystal structure of complexes **1-6**

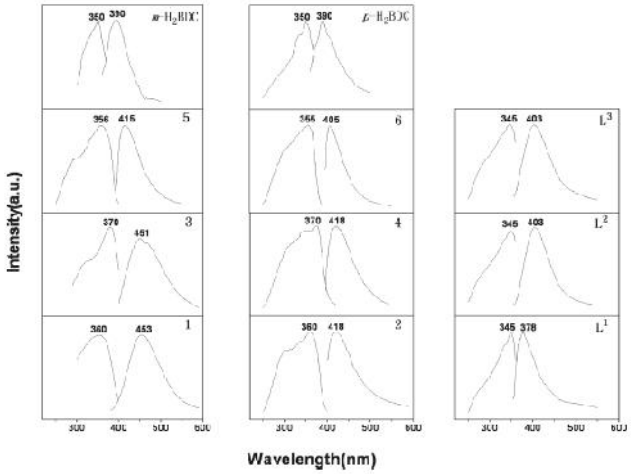


**Fig**. **4.14** The excitation-emission spectra of **1-6**, $L^1$-$L^2$, *m*-$H_2$BDC and *p*-$H_2$BDC

Liu et al. [57] further hydrothermally synthesized zinc and cadmium metal complexes namely, [Zn(*m*-bdc)(L)] (**1**), [Zn($NH_2$–bdc)(L)] (**2**), [$Zn_3$(*p*-bdc)$_3$(L)].2$H_2O$ (**3**), [$Zn_3$(btc)$_2$(L)($H_2O$)].$H_2O$ (**4**), [Cd(*o*-bdc)(L)($H_2O$)] (**5**), [Cd(*m*-bdc)(L)] (6), [Cd(*p*-bdc)(L)($H_2O$)] (**7**) and [$Cd_2$(btda)(L)].$H_2O$ (**8**) (*m*-$H_2$bdc = 1,3-benzenedicarboxylic acid, $NH_2$–$H_2$bdc = 5-$NH_2$–1,3-benzenedicarboxylic acid, *p*-$H_2$bdc = 1,4-benzenedicarboxylic acid, $H_3$btc = 1,3,5-benzenetricarboxylic acid, *o*-$H_2$bdc =1,2-benzenedicarboxylic acid, btda = 3,3´,4,4´-benzophenonetetracarboxylic dianhydride, L = 1,1´-(1,4-butanediyl)-bis[2-(3-pyridyl)benzimidazole]). They characterized them by single-crystal X-ray diffraction and investigated their photoluminescent properties. They further concluded on the basis of the emission peaks and the luminescent

lifetimes, that the N-donor L ligand and O-donor anions might show contributions to the fluorescent emissions of **1**, **2**, **3**, **5** and **6** simultaneously.

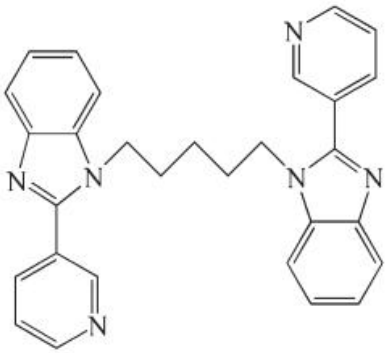

**Fig. 4.15** Structure of the ligand 1,1´-(1,4-butanediyl)-bis[2-(3-pyridyl)benzimidazole])

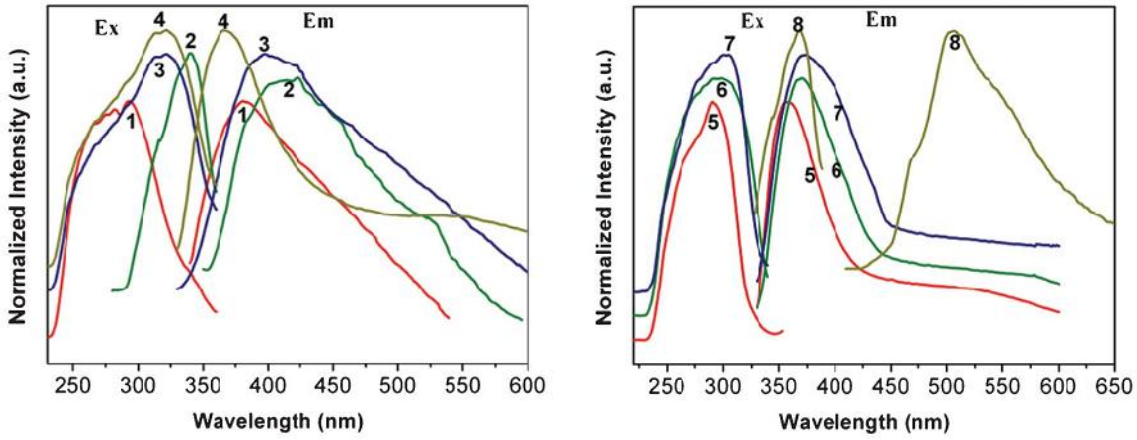


**(a)** **(b)**

**Fig. 4.16 (a)** Photoluminescent emission spectra of Zn(II)(**1, 2, 3** and **4**) and **(b)**Cd(II)(**5**, **6**, **7** and **8**) compounds at room temperature

The zinc (II) and cadmium (II) complexes of the benzimidazole based ligands have different exciting physical and chemical properties. Along with zinc and cadmium, manganese, copper, cobalt and many other different metal ions also been reported in literature for different applications e.g., SOD activity, antioxidant, DNA interaction and nuclease activity, catalytic activity and many more. [58-59].

The present chapter deals with the synthesis of metal complexes with different zinc and cadmium salts and various ligands to know the effect of anions (nitrate and perchlorate) and ligand on structural diversity. The photoluminescence studies of ligands and their respective zinc and cadmium complexes have also been studied.

**Results and discussion**

The reactions of hydrated metal salts viz., $Zn(NO_3)_2.6H_2O$, $Zn(ClO_4)_2.6H_2O$ and $Cd(NO_3)_2.4H_2O$ with N,N,N',N'-tetrakis(1H-benzimidazol-2yl)methyl)ethane-1,2-diamine ($H_4$EDTB) and N,N,N′,N′-tetrakis(1H-benzimidazol-2ylmethyl)propane-1,3-diamine ($H_4$PDTB) resulted in the formation of various types of metal complexes namely, $[Zn(H_4EDTB)](NO_3)_2.CH_3OH$ **(4a)**, $[Cd(H_4EDTB)NO_3]NO_3.CH_3OH.2H_2O$ **(4b)**, $[Zn(H_4EDTB)](ClO_4)_2$ **(4c)**, $[Zn(H_4PDTB)](NO_3)_2.DMF$ **(4d)**, $[Cd_2(H_4PDTB)(\eta^1\text{-}NO_3)_2(\eta^2\text{-}NO_3)_2H_2O].2H_2O$ **(4e)** $[Zn_2(H_4PDTB)(H_2O)_2(DMF)_2](ClO_4)_4.2(H_2O)$ **(4f)** as presented in the scheme 4.2-4.3. The different formulations were confirmed by elemental analysis, infrared spectroscopy and X-ray crystallography.

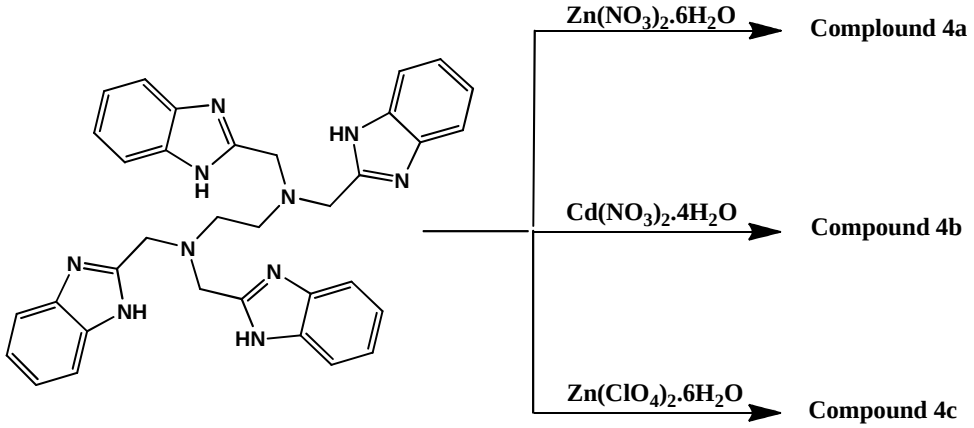


**Scheme 4.2**

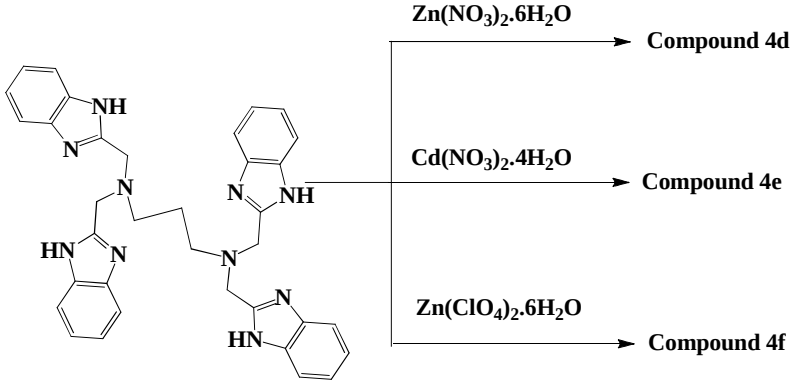


**Scheme 4.3**

The IR spectra of all complexes are very similar showing the characteristic absorption bands of the poly-dentate ligand: 1610-1625 $cm^{-1}$ ($\nu_{as}$ NH), 1305-1315, 1350-1365 ($\nu_s$ NH) and 795-805 (δNH). The peaks at 540 and 490 $cm^{-1}$ are assigned to

$\nu_{M-O}$ and $\nu_{M-N}$. The bands between 3100 and 2800 $cm^{-1}$ and 1675- 400 $cm^{-1}$ are attributed to the C-H, $C_{ar}$-$C_{ar}$, and $C_{ar}$=N stretching frequencies of the aromatic group respectively. In addition, the peaks at 1280, 1277, 1070 and 830 $cm^{-1}$ are assigned to the C-H in-plane or out-of-plane bending of the organic ligands.

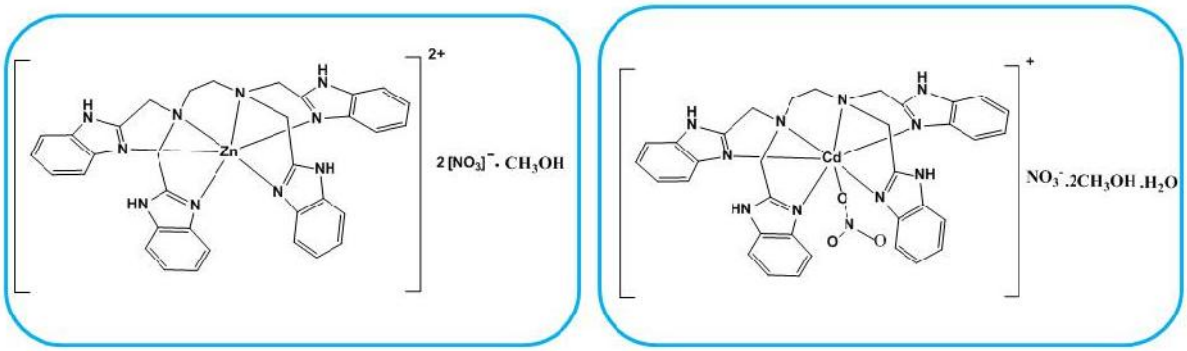


**$[Zn(H_4EDTB)](NO_3)_2.CH_3OH$ (4a)** **$[Cd(H_4EDTB)NO_3]NO_3.CH_3OH.2H_2O$ (4b)**

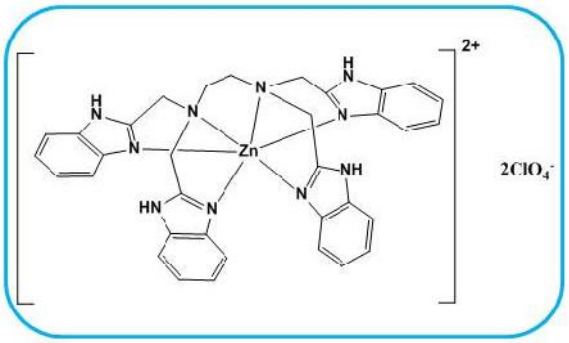


**$[Zn(H_4EDTB)](ClO_4)_2$ (4c)**

**Scheme 4.4**

**Crystal structure of $[Zn(H_4EDTB)](NO_3)_2.CH_3OH$ (4a)**

The single crystals of compound **4a** suitable for X-ray diffraction analysis were obtained by slow evaporation of methanolic solution. Complex **4a** crystallizes in the triclinic system with P-1 space group (Scheme 4.4 and Fig. 4.17). The Crystal data and structure refinement parameters are listed in Table 4.1 and selected bond lengths and bond angles are given in Table 4.2. The asymmetric unit consists of a mononuclear Zn(II) cation, resulting from the coordination of $H_4$EDTB ligand to the metal ion through four benzimidazole nitrogen donors (N2, N3, N6 and N8) and two amine

donors (N9 and N10). The Zn(II) centre in complex **4a** adopted a distorted octahedral geometry and the distortion could be manifested by large deviations in the bond angles (N3-Zn1-N10, (154.64(6); N2-Zn1-N6, 163.58(6)$^{o}$) from the ideal value for a perfect octahedron. All bond distances from the nitrogen donors to the metal centre were found consistence with the literature values [60]. Two nitrate anions were also present in the lattice and provide the charge balance. Along with this, methanol molecule is also present as solvent of crystallization. The crystal structure of compound **4a** exhibits several non-covalent interactions. Weak hydrogen bonding interactions were observed spanning over a wide range of 1.899(3)–2.994(1) Å which have been shown in Fig 4.18 and accounted in detail in Table 4.11. All the four imidazoloyl N-H are extensively involved in N-H···O interactions. Out of four, three imidazoloyl N-H holds nitrate anion (N1-H1···O3, 2.259(2); N5-H5A···O2, 2.529(2); N5-HA···O3, 2.0472(2); N7-H7A···O4, 2.003(3); N7-H7A···O9, 2.356(3) Å) and the rest fourth is engaged with the oxygen of methanol molecule (N4-H4B···O7, 1.899(3) Å). Furthermore, the aryl hydrogen atoms (H4 and H14) of benzimidazole rings in **4a** were also involved in C-H···π interactions with the benzimidazole rings of neighbouring molecules at the distances of 3.143(2) to 3.203(5) Å. These interactions resulted in the three dimensional packing of complex **4a** (Fig. 4.19).

**Crystal structure of [Cd($H_4$EDTB)$NO_3$]$NO_3$.$CH_3OH$.2$H_2O$ (4b)**

The single crystal X-ray diffraction studies confirmed the formulation of complex **4b** as [Cd($H_4$EDTB)$NO_3$]$NO_3$.$CH_3OH$.2$H_2O$. Complex **4b** crystallizes in the monoclinic crystal system with $P2_1/c$ space group (Scheme 4.4 Fig 4.20). The Crystal data and structure refinement parameters are listed in Table 4.3 and selected bond lengths and bond angles are given in Table 4.4. The crystal structure of complex **4b** depicts that the ligand is coordinated with the metal ion in hexadentate fashion via., six nitrogen donors (N1, N3, N5, N8, N9 and N10) similar to the complex **4a**. The Cd(II) centre exhibits a heptacoordinated donor environment and the seventh coordination site was occupied by a nitrate ion binding in a monodentate fashion. The overall coordination geometry around the metal centre was roughly pentagonal bipyramidal. The basal plane comprised of two benzimidazole nitrogen donors (N1 and N8) and two amines nitrogen donors (N9 and N10) from the ligand ($H_4$EDTB) and one oxygen donor (O1) from the monodentate nitrate anion. The axial positions were occupied by two remaining nitrogen donors (N3 and N5) of the benzimidazole rings present in the ligand ($H_4$EDTB). The benzimidazole rings present in the equatorial plane were

roughly parallel to each other with the dihedral angle 7.34°. The axial benzimidazole rings were almost perpendicular to each other having a dihedral angle of 87.64°. The distortion in the geometry could be manifested by the bond angle N3-Cd1-N5 of 164.45° and the sum of angles (379.69°) between the donor atoms forming the equatorial plane. The Cd-N bond distances were within the range of 2.332(14) - 2.575(12) Å which were found consistent with the literature values and the Cd-O bond distance for the nitrate ligand was 2.392(13) Å, which was slightly greater than the reported values [61-62]. A non-coordinating nitrate ion provides the charge balance was also present in the crystal lattice along with two methanol molecules and one water molecule. Several non-covalent interactions were also observed in the crystal structure of **4b** which are shown in Fig. 4.21 and are listed in Table 4.11. Oxygen atoms of both coordinated and uncoordinated nitrate ion were involved in various types of intermolecular interactions. Out of four benzimidazoloyl N-H, two are engaged with the coordinated nitrate (N4-H4B···O2, 2.094(1); N4-H4B···O3, 2.396(2); N6-H6···O2, 2.001(1); N6-H6···O3, 2.6498(8)Å) and rest two are involved with the nitrate ion (N2-H2B···O6, N2-H2B···O4, N7-H7···O5) present in the lattice at their respective sides. In the unit cell the non bonded nitrate ion attracts three complex molecules and one complex attracts three uncoordinated nitrate anions as shown in Fig.4.22. Thus both complex as well as nitrate ions act as a receptors for each other. The three dimensional packing of complex **4b** is represented in Fig 4.23, along '*c*' axis, where the butterfly-shaped molecules are linked with nitrate anion and water molecules.

**Crystal structure of [Zn($H_4$PDTB)]($NO_3$)$_2$.DMF (4d)**

Complex **4d** crystallizes in the triclinic system with space group P-1. The crystal structure of complex **4d** is illustrated in Fig 4.24 (Scheme 4.5). The crystal data and refinement parameters are tabulated in Table 4.5 and selected bond lengths and bond angles are listed in Table 4.6. The asymmetric unit featured a mononuclear cation comprised of Zn(II) coordinated with one molecule of ($H_4$PDTB). The complex exhibited an octahedral geometry around the metal centre where all six coordination sites were satisfied by benzimidazole and amine nitrogen donors of ligand $H_4$PDTB similar to the complex **4a**. The octahedral geometry of the complex was remarkably distorted and the distortion could be explained by the angles N7-Zn1-N1 (118.49(7)°) and N3-Zn1-N5 (160.90(6)°) which differed significantly from the ideal values of 90° and 180° respectively. The Zn(II)-N bond distances for benzimidazole rings were

spanning over a narrow range of 2.095(3)-2.130(5) Å whereas those pertaining to amine nitrogen donors were 2.318(3) and 2.383(5) Å respectively. These bond distances were found consistence with the values reported in the litrature [63]. Moreover, two non-coordinating nitrate anions were providing the charge balance, present in the lattice along with one molecule of dimethylformamide. The imidazole hydrogen atoms of benzimidazole rings contributed to hydrogen bonding network and exhibit interactions with the oxygen atoms of nitrate anions and dimethylformamide ranging from 1.823(5) to 2.280(7) Å (Fig. 4.25). The methyl and formyl hydrogen atoms of DMF molecule also participates in C-H···π interactions with the phenyl rings of adjacent benzimidazole moieties. These non-covalent interactions stabilizes the three dimensional packing of molecules in the crystal structure and a perspective view has been illustrated in Fig. 4.26.

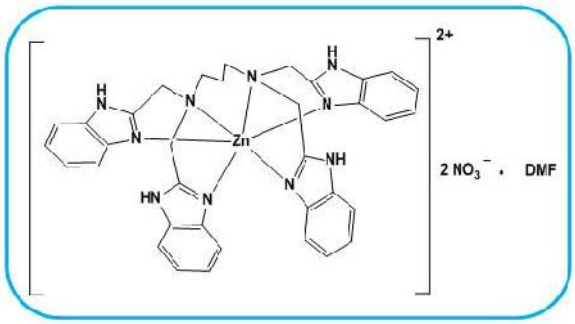


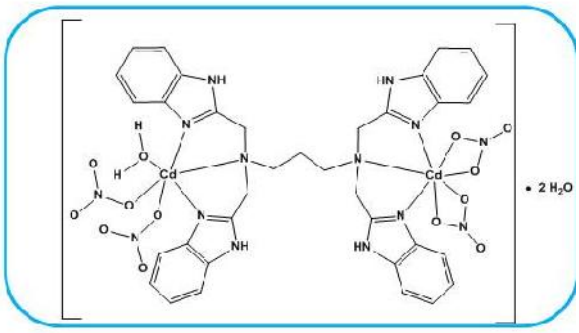


**$[Zn(H_4PDTB)](NO_3)_2.DMF$ (4d)** **$[Cd_2(H_4PDTB)(\mu^1\text{-}NO_3)_2(\mu^2\text{-}NO_3)_2H_2O].2H_2O$ (4e)**

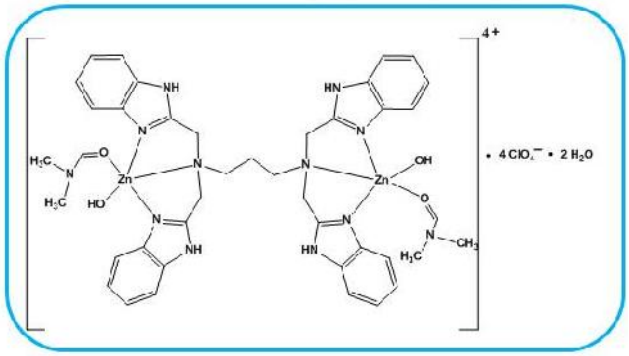


**$[Zn_2(H_4PDTB)(H_2O)_2(DMF)_2](ClO_4)_4.(H_2O)_2$ (4f)**

**Scheme 4.5**

**Crystal structure of $[Cd_2(H_4PDTB)(\mu^1\text{-}NO_3)_2(\mu^2\text{-}NO_3)_2H_2O].2H_2O$ (4e)**

The single crystal X-ray diffraction studies confirmed the formulation of complex **4e** as $[Cd_2(H_4PDTB)(\eta^1\text{-}NO_3)_2(\eta^2\text{-}NO_3)_2H_2O].2H_2O$ and crystallizes in

monoclinic system with $P2_1/c$ space group (Fig. 4.27 and Scheme 4.5). The crystallographic data and experimental details are summarized in Table 4.7 and selected bond lengths and bond angles are listed in Table 4.8. The asymmetric unit consists of a binuclear complex with different co-ordination geometry and the structure of **4e** could be described as two Cd(II) ions held together at a distance of 8.239(5) Ǻ by a single ligand ($H_4$PDTB). The two Cd(II) ions in the site I and site II exhibites quite different coordination geometries, where similar binding site was provided by the ligand comprised of two benzimidazole nitrogen donors and one amine nitrogen donor coordinating facially with each metal ions. The $Cd^1$ (site I) adopted an octahedral coordination geometry where the remaining three coordination site were fulfilled by oxygen donors of two monodentate nitrate anions and one water molecule. The octahedral geometry of $Cd^1$ have significant distortion manifested by angles (O13-Cd1-O1, 68.21(17); O4-Cd1-N1, 118.57(17) and N1-Cd1-O1, 148.62(15)), which deviated markedly from the ideal values. On the other hand $Cd^2$ (site II) adopted a hepta-coordinated geometry where three coordination site were occupied by the ligand ($H_4$PDTB) and remaining four coordination sites were occupied by two nitrate anions ligating in a bidentate fashion. The Cd(II)-N and Cd(II)-O bond distances fall well within the reported range as in case of similar compounds [64]. In addition, the asymmetric unit contained two molecules of water as solvent of crystallization.

Several non-covalent interactions were also visualized in the crystal structure of **4e.** The benzimidazoloyl N-H and various C-H were extensively involved in hydrogen bonding interactions with the oxygen atoms of nitrate anion and water molecules with the distances varying from 1.934(3) to 2.222(4) Å (Fig.4.28). Furthermore, few C-H$\cdots\pi$ interactions between the aryl hydrogen atoms of benzimidazole rings and the phenyl rings of adjacent molecules have also been observed with the distance ranging from 3.156(3) to 3.870(5) Å. These non-covalent interactions resulted in a 2D sheet structure (Fig. 4.29).

**Crystal structure of $[Zn_2(H_4PDTB)(H_2O)_2(DMF)_2](ClO_4)_4.(H_2O)_2$ (4f)**

Complex **4f** crystallizes in the monoclinic crystal system with $P2_1/c$ space group and its crystal structure is depicted in Fig.4.30 (Scheme 4.6). The crystallographic data and experimental details are given in Table 4.9 and selected bond lengths and bond angles are listed in Table 4.10. The asymmetric unit consists of a binuclear complex having same co-ordination geometry at both the metal centre. The X-ray structure demonstrate that each metal center is five coordinated with three nitrogens from the

ligand ($H_4$EDTB) and rest two vacant sites are occupied by the oxygen atom of water and DMF molecule (N3O2 donor atoms) in a distorted square pyramidal arrangement. The four perchlorate anions present in the lattice neutralize the charge over the complex. The aryl as well as methylene C-H and benzimidazoloyl N-H are extensively involved in various type of C-H···O and N-H···O interactions with readily available oxygens of the perchlorate anions (Fig. 4.31).The Zn-Zn separation is 8.988(2) Å in complex **4f**, which is quite larger in complex **4e**. Due to the presence of different intermolecular interactions, the packing of complex **4f** shows a three dimensional structure with star shaped cavities entrapping perchlorate anions (Fig. 4.32).

**Photoluminescence Properties**

The photoluminescence properties of the ligands ($H_4$EDTB and $H_4$PDTB) and their Zn(II) and Cd(II) complexes were investigated at room temperature. The emission spectra of free ligands $H_4$EDTB and $H_4$PDTB along with their metal complexes are represented in Fig. 4.33 and 4.34 respectively. The solutions were excited at 265 nm and the emission spectra were recorded in between 280-520 nm. The ligands $H_4$EDTB and $H_4$PDTB exhibit a weak fluorescence with $\lambda_{max}$ of 295 and 298 nm respectively. The emission spectra of Zn(II) and Cd(II) complexes consists a wide emission bands with $\lambda_{max}$ in between 331-344 nm for **4a-4c** and 384-394 nm for **4d-4f** respectively when excited at 265 nm. A considerable red shifts in the emission spectra were evident after complexation thus precludeing their $\pi \rightarrow \pi^*$ or $n \rightarrow \pi^*$ transition [65] and hence the emission bands could be assigned as originating from the intraligand charge transfer [66] or ligand to metal charge transfer transitions [67]. These studies predict that the ligands $H_4$EDTB and $H_4$PDTB can be used for the detection of Zn(II) and Cd(II) ions in solutions.

A significant enhancement (2 to 2.5 fold) in the emission intensity has been observed with the emission properties of zinc or cadmium complexes of the ligands when compared with those of free ligands (Fig. 4.34-4.35). This behaviour could be rationalised in terms of efficient binding of the ligands with metal ions having $d^{10}$ electronic configuration. The coordination of the ligands with metal ion resulted in the enhancement in the rigidity of the molecular structure thereby reducing the loss of energy via a radiationless pathway and promotes a fine chelation enhanced fluorescence (CHEF) effect [68].

**CONCLUSIONS**

The reaction of $Zn(NO_3)_2.6H_2O$, $Cd(NO_3)_2.4H_2O$ and $Zn(ClO_4)_2.6H_2O$ with N,N,N',N'-tetrakis(1H-benzimidazol-2yl)methyl)ethane-1,2-diamine and N,N,N′,N′-tetrakis(1H-benzimidazol-2ylmethyl)propane-1,3-diamine resulted in the formation of mononuclear and dinuclear metal complexes. These metal complexes showed variation in coordination number due to change in the nature of counter ion as well as the nature of ligand. These complexes were characterized by elemental analysis, infrared spectroscopy and X-ray crystallography. Both the zinc complexes (**4a** and **4d**) are six coordinated derived from zinc nitrate either with $H_4$EDTB or $H_4$PDTB and the two counter nitrate anion are present in the lattice with the difference of solvent. The cadmium nitrate with $H_4$EDTB forms a seven coordinated mononuclear system whereas with $H_4$PDTB form a dinuclear system with different coordination number. The photoluminescence properties of these metal complexes had also been studied with excitation and emission spectra. These complexes showed large luminescence as compared to the free ligands due to their complexation.

**Table 4.1: Crystal data and collection details of $[Zn(H_4EDTB)](NO_3)_2.CH_3OH$ (4a)**

| | |
|---|---|
| Emprical formula | $C_{35}H_{36}N_{12}O_7Zn$ |
| Formula weight | 802.15 |
| Crystal system | Triclinic |
| Space group | P-1 |
| *a*/ Å | 11.8261(3) |
| *b*/ Å | 12.1351(3) |
| *c*/ Å | 14.4785(3) |
| α/ $^o$ | 91.761(1) |
| *β*/ $^o$ | 103.621(1) |
| γ/ $^o$ | 113.678(1) |
| *V* / Å$^3$ | 1830.97(8) |
| *Z* | 2 |
| $D_{calc}$ (g cm$^{-3}$) | 1.455 |
| $\mu$/mm$^{-3}$ | 0.737 |
| $\theta$ range/ $^o$ | 2.19-31.32 |
| Reflections collected | 9131 |
| Independent reflections | 6860 |
| Parameters/ Restraints | 498/0 |
| GOF ($F^2$) | 1.102 |
| $R_1$; w$R_2$ [$I>2\sigma(I)$] | 0.065; 0.230 |
| $R_1$; w$R_2$ (all data) | 0.081; 0.240 |

**Table 4.2: Bond distances and angles for $[Zn(H_4EDTB)](NO_3)_2.CH_3OH$ (4a)**

| Bond Distances (Å) | | Bond Angles ($^o$) | |
|---|---|---|---|
| Zn1-N2 | 2.1585(15) | N2-Zn1-N3 | 92.27(6) |
| Zn1-N3 | 2.0776(16) | N2-Zn1-N6 | 163.58(6) |
| Zn1-N6 | 2.1792(15) | N2-Zn1-N9 | 78.44(6) |
| Zn1-N8 | 2.0400(18) | N2-Zn1-N10 | 88.25(5) |
| Zn1-N9 | 2.2439(19 | N3-Zn1-N6 | 94.06(6) |
| Zn1-N10 | 2.3571(13) | N3-Zn1-N9 | 76.06(7) |
| | | N3-Zn1-N10 | 154.65(6) |
| | | N6-Zn1-N9 | 92.39(6) |
| | | N6-Zn1-N10 | 76.53(6) |
| | | N8-Zn1-N9 | 154.82(7) |
| | | N8-Zn1-N10 | 76.96(6) |
| | | N9-Zn1-N10 | 78.87(5) |

**Table 4.3: Crystal data and collection details of $[Cd(H_4EDTB)NO_3]NO_3.CH_3OH.2H_2O$ (4b)**

| | |
|---|---|
| Emprical formula | $C_{35}H_{31}N_{12}O_7Cd$ |
| Formula weight | 988.54 |
| Crystal system | Monoclinic |
| Space group | $P2_1/c$ |
| *a*/ Å | 9.6180(12) |
| *b*/ Å | 25.156(3) |
| *c*/ Å | 17.251(2) |
| α/ $^o$ | 90.00 |
| *β*/ $^o$ | 104.488(7) |
| γ/ $^o$ | 90.00 |
| *V* / Å$^3$ | 4041.20(8) |
| *Z* | 4 |
| $D_{calc}$ (g cm$^{-3}$) | 1.625 |
| $\mu$/mm$^{-3}$ | 1.119 |
| $\theta$ range/ $^o$ | 1.46-27.16 |
| Reflections collected | 8518 |
| Independent reflections | 4517 |
| Parameters/ Restraints | 523/0 |
| GOF ($F^2$) | 1.198 |
| $R_1$; w$R_2$ [$I>2\sigma(I)$] | 0.072; 0.230 |
| $R_1$; w$R_2$ (all data) | 0.074; 0.280 |

**Table 4.4: Bond distances and angles for $[Cd(H_4EDTB)NO_3]NO_3.CH_3OH.2H_2O$ (4b)**

| Bond Distances (Å) | | Bond Angles ($^o$) | |
|---|---|---|---|
| Cd1-N1 | 2.446(15) | N5-Cd1-N3 | 164.45(40) |
| Cd1-N3 | 2.353(14) | N5-Cd1-O1 | 112.82(33) |
| Cd1-N5 | 2.332(14) | N5-Cd1-N1 | 87.12(36) |
| Cd1-N8 | 2.510(1) | N3-Cd1-N1 | 82.59(35) |
| Cd1-N10 | 2.575(12) | N3-Cd1-O1 | 82.06(36) |
| Cd1-O1 | 2.392(13) | O1-Cd1-N1 | 82.31(47) |
| | | N8-Cd1-N10 | 67.00(4) |
| | | N5-Cd1-N10 | 68.90(4) |
| | | N3-Cd1-N10 | 68.70(4) |
| | | O1-Cd1-N10 | 154.40(7) |
| | | N5-Cd1-N8 | 98.10(4) |
| | | O1-Cd1-N8 | 83.80(3) |
| | | N3-Cd1-N8 | 85.30(4) |

**Table 4.5: Crystal data and collection details of $[Zn(H_4PDTB)](NO_3)_2.DMF$ (4d)**

| | |
|---|---|
| Emprical formula | $C_{38}H_{41}N_{13}O_7Zn$ |
| Formula weight | 857.23 |
| Crystal system | Triclinic |
| Space group | P-1 |
| *a*/ Å | 12.5037(8) |
| *b*/ Å | 12.7701(8) |
| *c*/ Å | 14.4448(2) |
| α/ $^o$ | 88.53(3) |
| *β*/ $^o$ | 75.16(3) |
| γ/ $^o$ | 61.47(3) |
| *V* / Å$^3$ | 1946.00(2) |
| *Z* | 2 |
| $D_{calc}$ (g cm$^{-3}$) | 1.463 |
| $\mu$/mm$^{-3}$ | 0.699 |
| $\theta$ range/ $^o$ | 1.47-28.32 |
| Reflections collected | 9694 |
| Independent reflections | 7559 |
| Parameters/ Restraints | 534/0 |
| GOF ($F^2$) | 1.031 |
| $R_1$; w$R_2$ [$I>2\sigma(I)$] | 0.048; 0.190 |
| $R_1$; w$R_2$ (all data) | 0.062; 0.230 |

**Table 4.6: Bond distances and angles for $[Zn(H_4PDTB)](NO_3)_2.DMF$ (4d)**

| Bond Distances (Å) | | Bond Angles (°) | |
|---|---|---|---|
| Cd1-N1 | 2.446(15) | N5-Cd1-N3 | 164.45(40) |
| Cd1-N3 | 2.353(14) | N5-Cd1-O1 | 112.82(33) |
| Cd1-N5 | 2.332(14) | N5-Cd1-N1 | 87.12(36) |
| Cd1-N8 | 2.510(1) | N3-Cd1-N1 | 82.59(35) |
| Cd1-N10 | 2.575(12) | N3-Cd1-O1 | 82.06(36) |
| Cd1-O1 | 2.392(13) | O1-Cd1-N1 | 82.31(47) |
| | | N8-Cd1-N10 | 67.00(4) |
| | | N5-Cd1-N10 | 68.90(4) |
| | | N3-Cd1-N10 | 68.70(4) |
| | | O1-Cd1-N10 | 154.40(7) |
| | | N5-Cd1-N8 | 98.10(4) |
| | | O1-Cd1-N8 | 83.80(3) |
| | | N3-Cd1-N8 | 85.30(4) |

**Table 4.7: Crystal data and collection details of $[Cd_2(H_4PDTB)(\mu^1\text{-}NO_3)_2(\mu^2\text{-}NO_3)_2.H_2O].2H_2O$ (4e)**

| | |
|---|---|
| Emprical formula | $C_{35}H_{36}Cd_2N_{14}O_{15}$ |
| Formula weight | 1117.60 |
| Crystal system | Monoclinic |
| Space group | $P2_1/c$ |
| *a*/ Å | 18.9971(8) |
| *b*/ Å | 10.6259(4) |
| *c*/ Å | 23.6716(9) |
| α/ $^o$ | 90.00 |
| *β*/ $^o$ | 111.285(2) |
| γ/ $^o$ | 90.00 |
| $V$ / Å$^3$ | 4452.4(3) |
| $Z$ | 4 |
| $D_{calc}$ (g cm$^{-3}$) | 1.667 |
| $\mu$/mm$^{-3}$ | 1.037 |
| $\theta$ range/ $^o$ | 1.15-28.40 |
| Reflections collected | 11187 |
| Independent reflections | 6989 |
| Parameters/ Restraints | 600/0 |
| GOF ($F^2$) | 1.079 |
| $R_1$; w$R_2$ [$I>2\sigma(I)$] | 0.053; 0.210 |
| $R_1$; w$R_2$ (all data) | 0.067; 0.220 |

**Table 4.8 Bond distances and angles for [$Cd_2$($H_4$PDTB)(¦¹-$NO_3$)$_2$(¦²-$NO_3$)$_2$$H_2O$].2$H_2O$(4e)**

| Bond Distances (Å) | | Bond Angles ($^o$) | |
|---|---|---|---|
| Cd1-N1 | 2.446(15) | N5-Cd1-N3 | 164.45(40) |
| Cd1-N3 | 2.353(14) | N5-Cd1-O1 | 112.82(33) |
| Cd1-N5 | 2.332(14) | N5-Cd1-N1 | 87.12(36) |
| Cd1-N8 | 2.510(1) | N3-Cd1-N1 | 82.59(35) |
| Cd1-N10 | 2.575(12) | N3-Cd1-O1 | 82.06(36) |
| Cd1-O1 | 2.392(13) | O1-Cd1-N1 | 82.31(47) |
| | | N8-Cd1-N10 | 67.00(4) |
| | | N5-Cd1-N10 | 68.90(4) |
| | | N3-Cd1-N10 | 68.70(4) |
| | | O1-Cd1-N10 | 154.40(7) |
| | | N5-Cd1-N8 | 98.10(4) |
| | | O1-Cd1-N8 | 83.80(3) |
| | | N3-Cd1-N8 | 85.300(4) |

**Table 4.9: Crystal data and collection details of $[Zn_2(H_4PDTB)(H_2O)_2.(C_3H_7NO)_2](ClO_4)_4.2H_2O$ (4f)**

| | |
|---|---|
| Emprical formula | $C_{43}H_{50}Cl_4N_{12}O_{21}Zn_2$ |
| Formula weight | 1308.08 |
| Crystal system | Monoclinic |
| Space group | $P2_1/c$ |
| *a*/ Å | 14.7964(7) |
| *b*/ Å | 23.9754(11) |
| *c*/ Å | 18.7634(9) |
| α/ $^o$ | 90.00 |
| *β*/ $^o$ | 101.287(3) |
| γ/ $^o$ | 90.00 |
| *V* / Å$^3$ | 6527.6(5) |
| *Z* | 4 |
| $D_{calc}$ (g cm$^{-3}$) | 1.331 |
| $\mu$/mm$^{-3}$ | 0.931 |
| $\theta$ range/ $^o$ | 2.48-29.11 |
| Reflections collected | 13407 |
| Independent reflections | 7145 |
| Parameters/ Restraints | 753/0 |
| GOF ($F^2$) | 1.228 |
| $R_1$; w$R_2$ [$I>2\sigma(I)$] | 0.085; 0.240 |
| $R_1$; w$R_2$ (all data) | 0.091; 0.270 |

**Table 4.10 Bond distances and angles for $Zn_2(H_4PDTB)(H_2O)_2.(C_3H_7NO)_2](ClO_4)_4.2H_2O$ (4f)**

| Bond Distances (Å) | | Bond Angles ($^o$) | |
|---|---|---|---|
| Zn1-O2 | 1.948(6) | O2-Zn1-N6 | 122.84(20) |
| Zn1-N6 | 1.996(5) | O2-Zn1-N10 | 114.34(22) |
| Zn1-N10 | 2.002(6) | O2-Zn1-O1 | 91.34(20) |
| Zn1-O1 | 2.096(5) | O2-Zn1-N10 | 97.14(20) |
| Zn1-N8 | 2.392(5) | N6-Zn1-N10 | 119.47(19) |
| Zn2-O4 | 1.958(6) | N6-Zn1-O1 | 96.48(18) |
| Zn2-N3 | 1.990(6) | N6-Zn1-N8 | 76.98(18) |
| Zn2-N1 | 1.991(5) | N10-Zn1-O1 | 100.56(6) |
| Zn2-O3 | 2.096(5) | N10-Zn1-N8 | 78.06(19) |
| Zn2-N9 | 2.401(5) | O1-Zn1-N8 | 171.21(18) |
| | | O4-Zn2-N3 | 122.05(23) |
| | | O4-Zn2-N1 | 114.04(23) |
| | | O4-Zn2-O3 | 91.78(25) |
| | | O4-Zn2-N9 | 97.35(22) |
| | | N3-Zn2-N1 | 120.18(19) |
| | | N3-Zn2-O3 | 96.80(22) |
| | | N3-Zn2-N9 | 76.73(18) |
| | | N1-Zn2-O3 | 100.74(21) |
| | | N1-Zn2-N9 | 77.30(19) |
| | | O3-Zn2-N9 | 170.67(18) |

**Table 4.11 Non-covalent interactions for Zn(II) and Cd(II) complexes (Å and $^{o}$)**

| S. N | D-H···A | d(D-H) | d(H-A) | d(D-A) | <(DHA)> |
|---|---|---|---|---|---|
| **1.** | **4a** | | | | |
| | N5-H5A···O2 | 0.860(1) | 2.529(2) | 3.240(2) | 140.61 |
| | N5-H5A···O3 | 0.860(1) | 2.047(2) | 2.873(2) | 160.95 |
| | N5-H5A···N11 | 0.860(8) | 2.655(2) | 3.494(23) | 165.25 |
| | C5-H5···N7 | 0.930(2) | 2.994(1) | 3.720(2) | 136.06 |
| | C5-H5···N8 | 0.930(2) | 2.824(2) | 3.479(2) | 128.41 |
| | C8-H8A···O4 | 0.970(2) | 2.491(2) | 3.435(3) | 141.57 |
| | C8-H8A···O8 | 0.970(2) | 2.491(2) | 3.435(3) | 164.42 |
| | C8-H8A ···N12 | 0.970(2) | 2.805(2) | 3.758(3) | 167.53 |
| | C23-H23···N3 | 0.930(2) | 2.787(1) | 3.477(2) | 131.85 |
| | C33-H33B···O4 | 0.970(2) | 2.873(1) | 3.485(3) | 121.98 |
| | C33-H33B···O8 | 0.970(2) | 2.783(2) | 3.680(3) | 122.27 |
| | C34-H34A···O4 | 0.970(2) | 2.833(2) | 3.449(2) | 122.27 |
| | N1-H1···O3 | 0.860(2) | 2.259(2) | 2.971(2) | 140.24 |
| | C2-H2···O3 | 0.930(2) | 2.659(2) | 3.313(3) | 128.18 |
| | C2-H2···O3 | 0.930(2) | 2.659(2) | 3.313(3) | 128.14 |
| | N1-H1···O8 | 0.860(2) | 2.508(2) | 3.152(3) | 132.25 |
| | C8-H8B···O9 | 0.970(2) | 2.300(2) | 3.156(3) | 146.66 |
| | N4-H4B···O7 | 0.860(2) | 1.899(3) | 2.750(4) | 169.84 |
| | C25-H25A ···O1 | 0.970(2) | 2.755(2) | 3.421(3) | 126.47 |
| | O7-H7···O1 | 0.820(2) | 2.305(2) | 3.068(3) | 155.16 |

| | | | | | |
|---|---|---|---|---|---|
| | O7-H7···O2 | 0.820(2) | 2.324(2) | 3.029(2) | 144.39 |
| | O7-H7···O7 | 0.820(2) | 2.648(2) | 3.442(3) | 163.45 |
| | N7-H7A···O4 | 0.860(2) | 2.003(3) | 2.794(3) | 152.37 |
| | N7-H7A···O9 | 0.860(2) | 2.356(3) | 3.039(4) | 136.73 |
| | N7-H7A···N12 | 0.860(2) | 2.527(2) | 3.334(3) | 156.83 |
| | C2-H2···O2 | 0.930(2) | 2.706(2) | 3.473(3) | 140.33 |
| | C9-H9A···N11 | 0.970(3) | 2.921(2) | 3.816(4) | 153.80 |
| | C20-H20···O8 | 0.930(2) | 2.641(2) | 3.385(3) | 137.52 |
| | C13-H13···O9 | 0.930(3) | 2.602(2) | 3.525(4) | 172.22 |
| **2** | **4b** | | | | |
| | C2-H2···O1 | 0.930(2) | 2.632(9) | 3.369(2) | 136.60 |
| | C2-H2···O3 | 0.930(2) | 2.984(1) | 3.881(2) | 162.53 |
| | C2-H2···N11 | 0.930(1) | 2.722(1) | 3.530(3) | 145.81 |
| | C12-H12···N8 | 0.930(2) | 2.951(12) | 3.551(3) | 123.64 |
| | C25-H25B ···O9 | 0.970(2) | 2.918(6) | 3.846(6) | 160.52 |
| | C31-H31···O1 | 0.930(1) | 2.804(1) | 3.490(2) | 131.37 |
| | C31-H31···O2 | 0.930(1) | 2.844(2) | 3.575(2) | 136.35 |
| | C31-H31···O3 | 0.930(5) | 2.747(1) | 3.675(8) | 176.11 |
| | C31-H31···N11 | 0.930(5) | 2.521(9) | 3.373(17) | 152.45 |
| | C33-H33A···O9 | 0.970(19) | 2.507(5) | 3.470(5) | 171.66 |
| | N2-H2B···O4 | 0.860(14) | 2.655(3) | 3.721(4) | 148.96 |
| | N2-H2B···O6 | 0.860(2) | 2.129(3) | 2.902(3) | 149.33 |
| | N2-H2B···N12 | 0.860(1) | 2.604(3) | 3.441(4) | 164.90 |
| | C8-H8A···O4 | 0.970(2) | 3.000(3) | 3.640(3) | 124.69 |
| | N4-H4B···N11 | 0.860(3) | 2.556(14) | 3.385(20) | 162.31 |

| | | | | | |
|---|---|---|---|---|---|
| | N4-H4B···O2 | 0.860(13) | 2.094(14) | 2.927(2) | 163.01 |
| | C15-H15···O3 | 0.930(2) | 2.815(2) | 3.533(2) | 126.72 |
| | N4-H4B···O3 | 0.860(2) | 2.396(2) | 3.096(2) | 138.81 |
| | N6-H6···N11 | 0.860(11) | 2.653(13) | 3.209(2) | 149.49 |
| | N6-H6···O1 | 0.860(11) | 2.001(10) | 2.858(15) | 174.04 |
| | N5-H7···O5 | 0.860(1) | 1.919(22) | 2.741(25) | 159.58 |
| | C25-H25A···O5 | 0.970(2) | 2.722(2) | 3.429(3) | 130.20 |
| | C9-H9A···O10 | 0.970(4) | 2.383(2) | 3.282(3) | 153.76 |
| | C14-H14···O4 | 0.930(2) | 2.609(4) | 3.535(4) | 173.64 |
| | C22-H22···N12 | 0.930(2) | 2.788(4) | 3.577(4) | 143.21 |
| | C22-H22···N12 | 0.930(18) | 2.680(4) | 3.520(4) | 150.52 |
| | C25-H25A···O10 | 0.970(19) | 2.622(5) | 3.554(5) | 161.26 |
| **3.** | **4d** | | | | |
| | N2-H2B···O7 | 0.860(2) | 1.823(3) | 2.643(4) | 158.76 |
| | C12-H12···N7 | 0.930(2) | 2.826(1) | 3.570(2) | 131.76 |
| | C20-H20···N1 | 0.930(2) | 2.793(1) | 3.497(2) | 133.31 |
| | C8-H8B ··O6 | 0.970(3) | 2.817(3) | 3.532(4) | 131.24 |
| | C9-H9B ···O7 | 0.970(2) | 2.499(2) | 3.295(15) | 139.26 |
| | C9-H9B ···O2 | 0.970(2) | 2.631(2) | 3.570(3) | 162.81 |
| | C34-H34A ···O1 | 0.970(2) | 2.607(1) | 3.468(3) | 147.97 |
| | C9-H9B···N11 | 0.970(2) | 2.607(3) | 3.861(3) | 158.56 |
| | C38-H38···O5 | 0.930(3) | 2.867(2) | 3.770(4) | 164.14 |
| | C38-H38···O6 | 0.930(3) | 2.804(2) | 3.605(4) | 144.96 |
| | C9-H9A ···O3 | 0.970(2) | 2.346(3) | 3.265(3) | 157.97 |
| | C9-H9A ···N11 | 0.970(2) | 2.726(2) | 3.483(3) | 135.27 |

| | | | | | |
|---|---|---|---|---|---|
| | C8-H8B ···O3 | 0.970(3) | 2.899(2) | 3.646(3) | 134.55 |
| | N4-H4B···O4 | 0.860(2) | 2.228(2) | 2.977(2) | 145.61 |
| | N6-H6···O4 | 0.860(1) | 2.028(2) | 2.833(2) | 155.52 |
| | N6-H6···O6 | 0.860(1) | 2.481(2) | 3.209(2) | 142.97 |
| | C23-H23···O2 | 0.930(2) | 2.395(2) | 3.289(2) | 161.10 |
| | C23-H23···N11 | 0.930(3) | 2.939(2) | 3.740(3) | 145.16 |
| | N6-H6···N12 | 0.860(1) | 2.600(2) | 3.420(2) | 159.98 |
| | N8-H8···N11 | 0.860(2) | 2.504(3) | 3.324(3) | 159.79 |
| | N8-H8···O1 | 0.860(2) | 2.045(2) | 2.838(3) | 153.04 |
| | C17-H17A ···O5 | 0.970(2) | 2.527(3) | 3.488(4) | 170.62 |
| | C33-H33A ···N6 | 0.970(3) | 2.862(2) | 3.684(3) | 143.08 |
| | C3-H3 ···O3 | 0.930(3) | 2.542(2) | 3.455(3) | 167.12 |
| | C4-H4 ···N4 | 0.930(2) | 2.878(1) | 3.807(3) | 176.97 |
| **4** | **4e** | | | | |
| | N4-H4B···O9 | 0.860(4) | 2.171(5) | 2.972(5) | 154.80 |
| | N4-H4B···N13 | 0.860(4) | 2.884(5) | 3.587(7) | 140.21 |
| | N6-H6 ···O14 | 0.860(6) | 2.935(7) | 2.771(9) | 163.79 |
| | C2-H2 ···O9 | 0.930(7) | 2.717(7) | 3.511(1) | 143.88 |
| | C9-H9A···O9 | 0.970(5) | 2.721(4) | 3.503(6) | 138.06 |
| | C15-H15···O4 | 0.930(5) | 2.971(5) | 3.708(7) | 137.24 |
| | C15-H15···O5 | 0.930(5) | 2.867(5) | 3.743(7) | 157.47 |
| | C15-H15B···N12 | 0.930(5) | 2.798(7) | 3.573(7) | 141.44 |
| | C23-H23···O10 | 0.930(7) | 2.625(7) | 3.388(7) | 139.62 |
| | C23-H23···N14 | 0.930(7) | 2.820(8) | 3.586(1) | 140.41 |
| | C31-H31···O11 | 0.930(6) | 2.544(7) | 3.264(9) | 134.40 |

| | | | | | |
|---|---|---|---|---|---|
| | C33-H33A···O2 | 0.970(5) | 2.492(5) | 3.307(7) | 141.52 |
| | C34-H34A···O7 | 0.970(6) | 2.582(4) | 3.354(7) | 136.52 |
| | C34-H34A···N13 | 0.970(6) | 2.855(5) | 3.792(7) | 162.67 |
| | O13-H12W···O5 | 0.820(5) | 2.223(7) | 2.999(9) | 157.81 |
| | C5-H5···O15 | 0.930(9) | 2.581(2) | 3.480(2) | 162.72 |
| | C8-H8B···O1 | 0.970(7) | 2.498(4) | 3.323(7) | 142.93 |
| | O13-H12W···N12 | 0.820(5) | 2.896(6) | 3.527(8) | 135.38 |
| | C33-H33W···O4 | 0.970(5) | 2.567(5) | 3.476(8) | 156.12 |
| | O13-H13W···O3 | 0.7190(6) | 2.127(5) | 2.825(6) | 164.05 |
| | C34-H34B···O13 | 0.970(5) | 2.802(4) | 3.703(7) | 154.83 |
| | C29-H29···O10 | 0.930(7) | 2.761(6) | 3.672(9) | 166.65 |
| | N2-H2B···O5 | 0.860(5) | 2.537(6) | 3.285(7) | 146.04 |
| | N8-H8···O2 | 0.860(4) | 1.986(5) | 2.817(6) | 162.01 |
| | N8-H8···N11 | 0.860(4) | 2.568(4) | 3.365(6) | 154.67 |
| | C3-H3···O12 | 0.930(8) | 2.948(7) | 3.770(1) | 148.41 |
| | C3-H3···O14 | 0.930(8) | 2.857(9) | 3.660(7) | 145.34 |
| | C12-H12···O6 | 0.930(5) | 2.531(9) | 3.227(9) | 131.96 |
| | C13-H13···O8 | 0.930(6) | 2.475(5) | 3.232(8) | 138.73 |
| | C30-H30···O12 | 0.930(7) | 2.824(5) | 3.636(8) | 146.53 |
| **5.** | **4f** | | | | |
| | C5-H5···O3 | 0.930(7) | 2.662(5) | 3.393(8) | 135.96 |
| | C5-H5···O13 | 0.930(7) | 2.771(2) | 3.408(2) | 126.51 |
| | C13-H13···O1 | 0.930(7) | 2.941(2) | 3.399(4) | 111.87 |
| | C13-H13···O15 | 0.930(7) | 2.805(2) | 3.513(2) | 133.78 |
| | C11-H11···O18 | 0.930(1) | 2.451(1) | 3.337(1) | 159.31 |

| | | | | | |
|---|---|---|---|---|---|
| | C18-H18···O3 | 0.930(8) | 2.726(5) | 3.342(9) | 124.47 |
| | O3-H3A···Cl4 | 0.820(6) | 2.874(4) | 3.614(7) | 151.23 |
| | O3-H3A···O11 | 0.820(6) | 2.016(1) | 3.763(2) | 151.22 |
| | O3-H3A···O13 | 0.820(6) | 2.871(2) | 3.590(2) | 147.53 |
| | C32-H32B···O18 | 0.970(7) | 2.619(2) | 3.510(2) | 152.75 |
| | C16-H16A···O17 | 0.970(7) | 2.408(2) | 3.336(3) | 159.81 |
| | C30-H30···O20 | 0.970(7) | 2.710(3) | 3.600(2) | 152.86 |
| | N2-H2A···O14 | 0.860(6) | 2.159(2) | 3.973(2) | 157.96 |
| | C16-H16A···O20 | 0.970(7) | 2.997(3) | 3.849(3) | 147.27 |
| | C8-H8B···O17 | 0.970(7) | 2.619(2) | 3.510(3) | 152.81 |
| | C2-H2···O9 | 0.930(8) | 2.596(9) | 3.452(1) | 153.25 |
| | C53-H53A···O20 | 0.960(2) | 2.492(3) | 3.370(3) | 152.07 |
| | C3-H3···O20 | 0.930(1) | 2.405(2) | 3.231(2) | 147.93 |
| | N5-H5A···O12 | 0.860(6) | 2.225(2) | 3.005(2) | 150.79 |
| | C10-H10···O11 | 0.930(9) | 2.689(1) | 3.532(2) | 151.01 |
| | C25-H25···O3 | 0.930(8) | 2.910(6) | 3.692(1) | 142.54 |
| | N4-H4A···O56 | 0.860(7) | 2.149(1) | 2.926(2) | 150.00 |
| | C52-H52C···O57 | 0.960(3) | 2.589(2) | 3.506(3) | 159.79 |
| | C5-H5···O3 | 0.930(7) | 2.662(5) | 3.393(8) | 135.96 |
| | C5-H5···O13 | 0.930(7) | 2.771(2) | 3.408(2) | 126.51 |

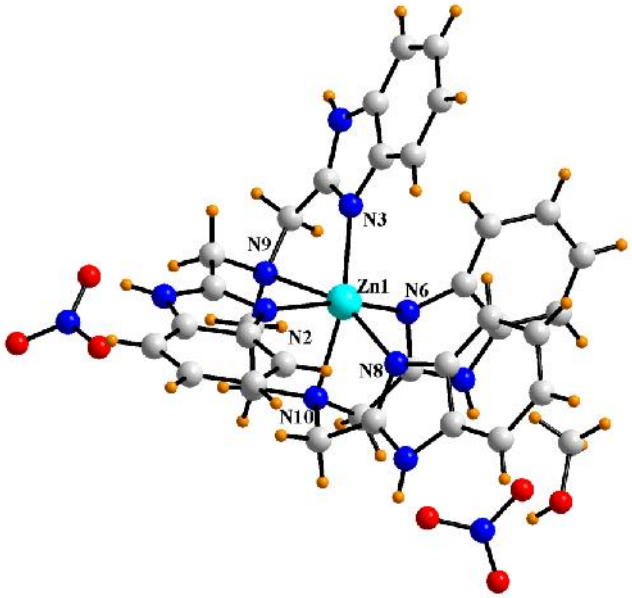


**Fig.4.17** Crystal Structure of $[Zn(H_4EDTB)](NO_3)_2.CH_3OH$ **4a**. Color code: C, grey; N, blue; H, orange; O, red; Zn, cyan

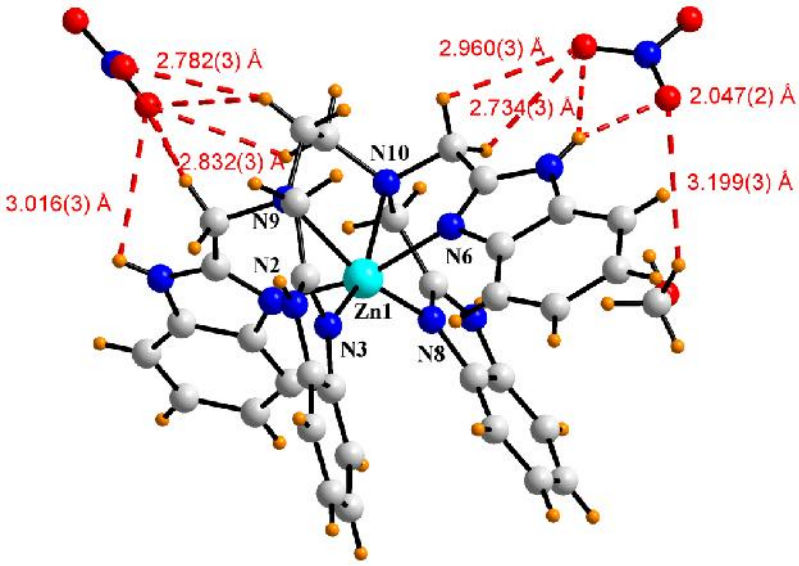


**Fig.4.18** Different non-covalent interaction in **4a**. Color code: C, grey; N, blue; H, orange; O, red; Zn, cyan

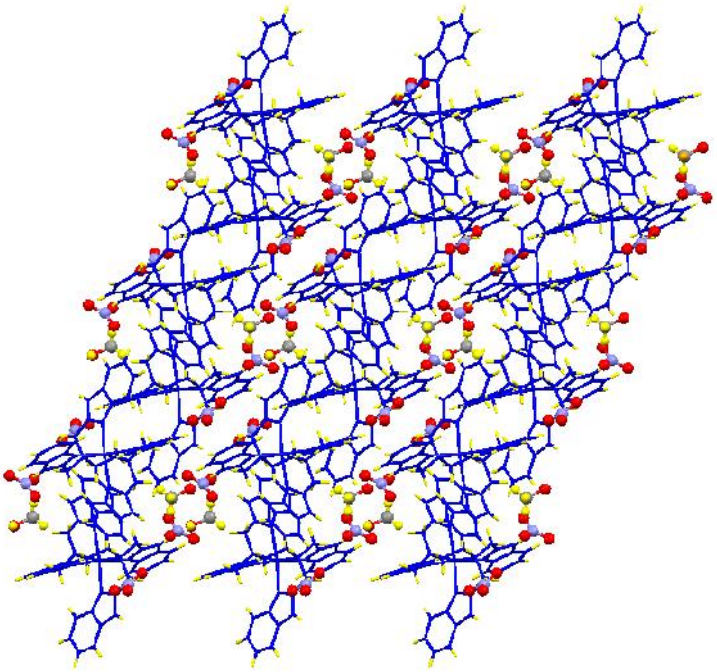

**Fig.4.19** 3D packing in **4a**. Color code: complex, blue; H, orange; O, red

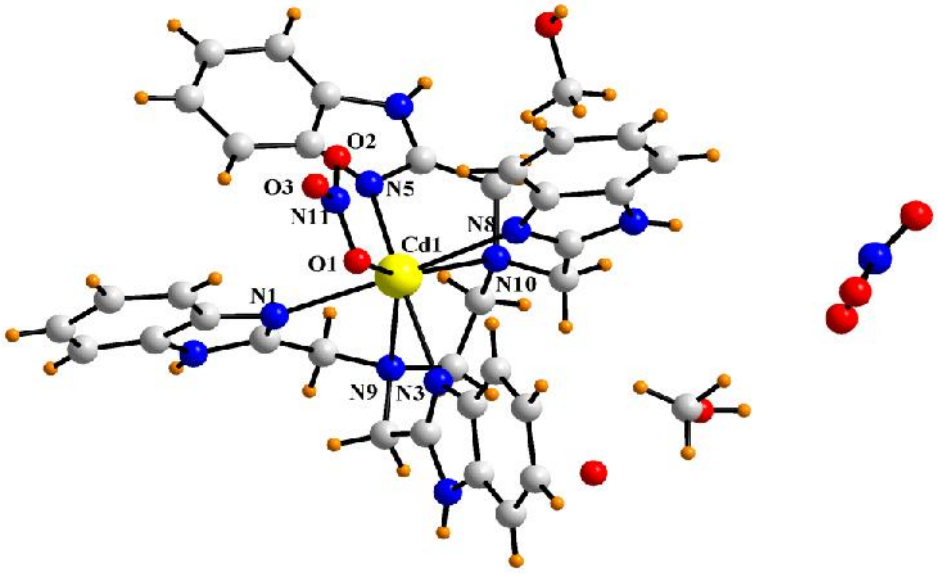


**Fig.4.20** Crystal Structure of $[Cd(H_4EDTB)NO_3]NO_3.CH_3OH.2H_2O$ **4b**. Color code: C, grey; N, blue; H, orange; O, red; Cd, yellow

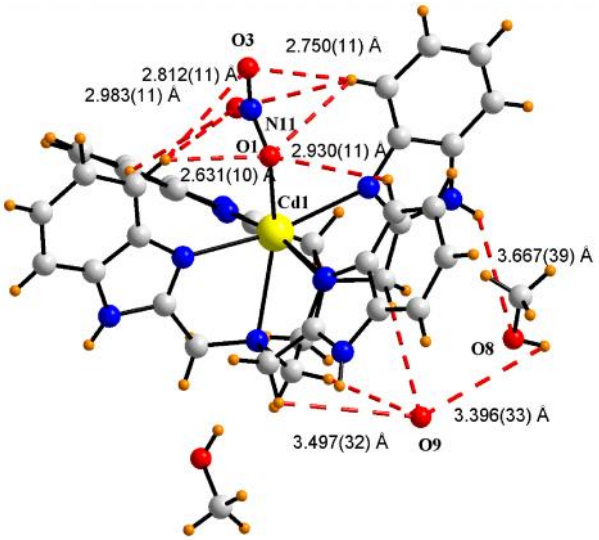


**Fig.4.21** Different non-covalent interaction in **4b**. Color code: C, grey; N, blue; H, orange; O, red; Cd, yellow

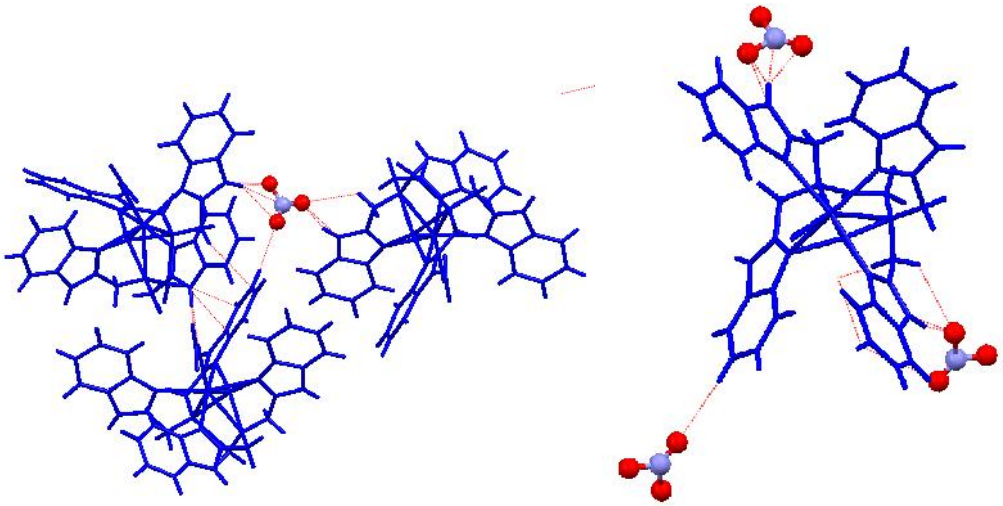

**(a)** **(b)**

**Fig.4.22 (a)** An uncoordinated nitrate anion holding three molecules of **4b. (b)** A cationic complex attracted three uncoordinated nitrate anion present in the lattice. Color code: Complex **4b**, blue; N, light blue; O, red

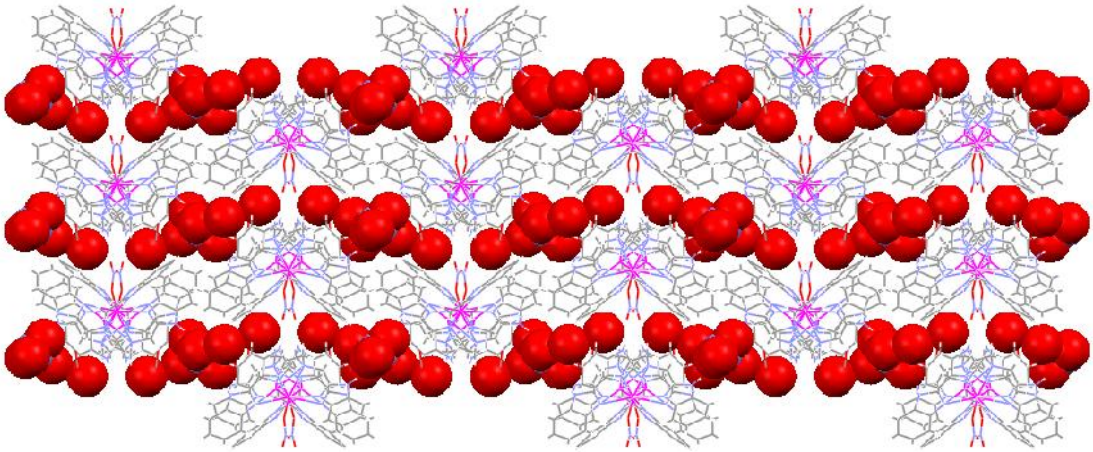

**Fig.4.23** 3D packing in **4b**. Color code: Complex, blue; H, orange; $NO_3^-$, red

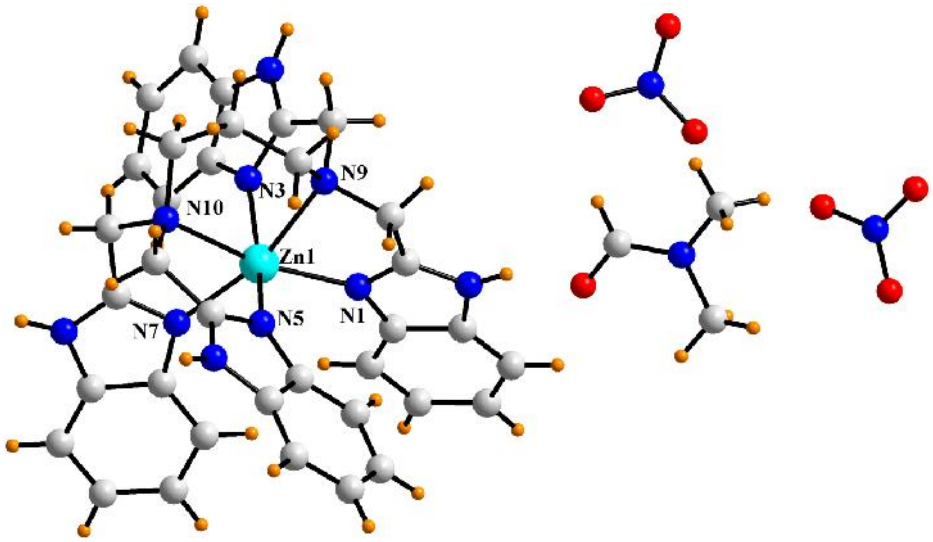


**Fig. 4.24** Crystal structure of $[Zn(H_4PDTB)](NO_3)_2.DMF$ **4d**. Color code: C, grey; N, blue; H, orange; O, red; Zn, cyan

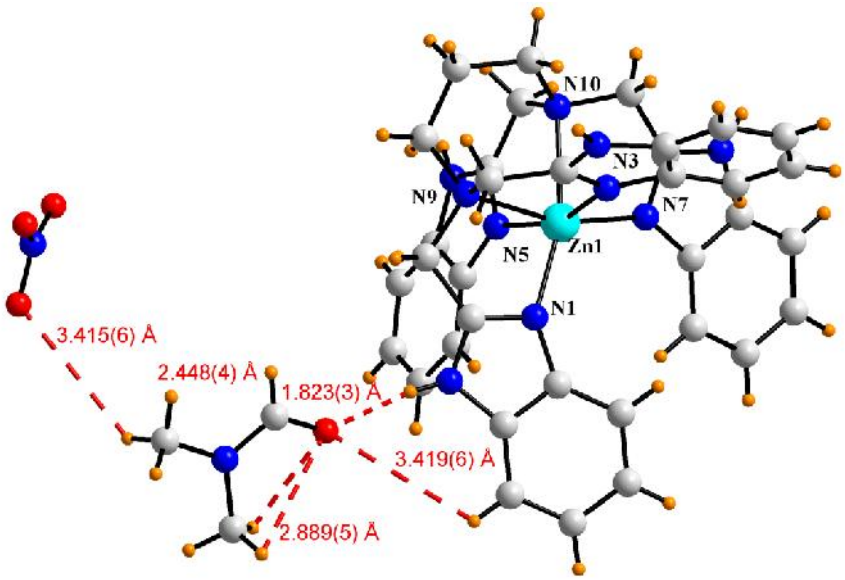


**Fig.4.25** Different non-covalent interaction in **4d.** Color code: C, grey; N, blue; H, orange; O, red; Zn, cyan

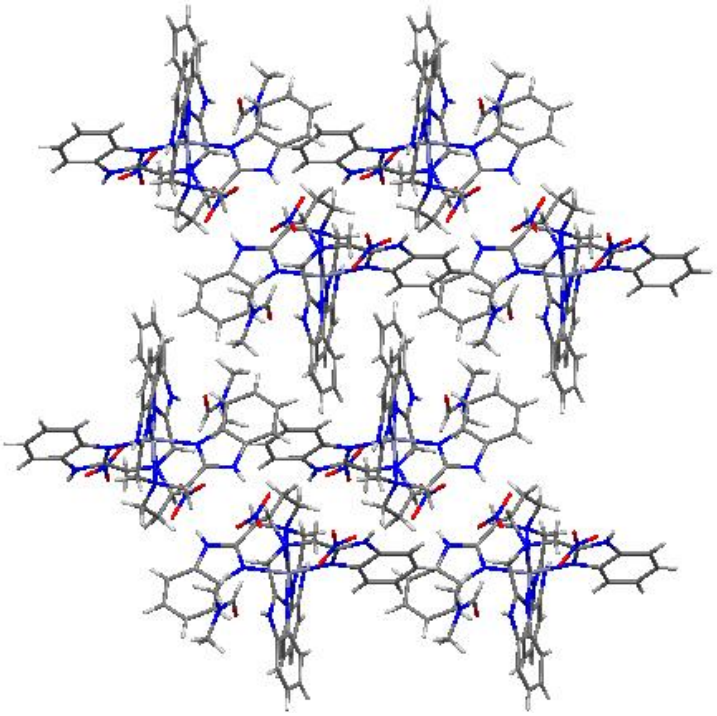

**Fig 4.26** 2D packing diagram of **4d** viewed down along *a*-axis

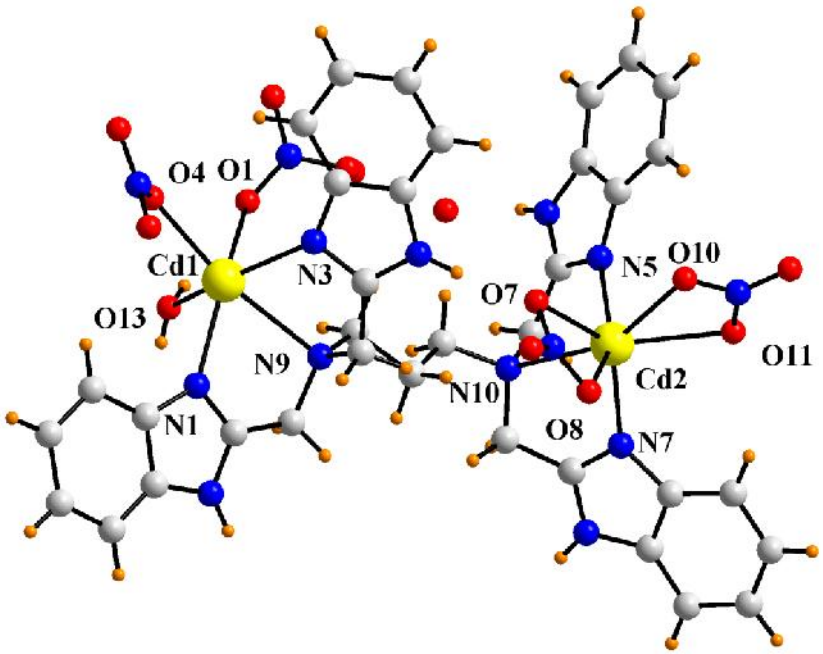


**Fig.4.27** Crystal structure of $[Cd_2(H_4PDTB)(\eta^1\text{-}NO_3)_2(\eta^2\text{-}NO_3)_2H_2O].2H_2O$ **4e.** Color code: C, grey; N, blue; H, orange; O, red; Cd, yellow

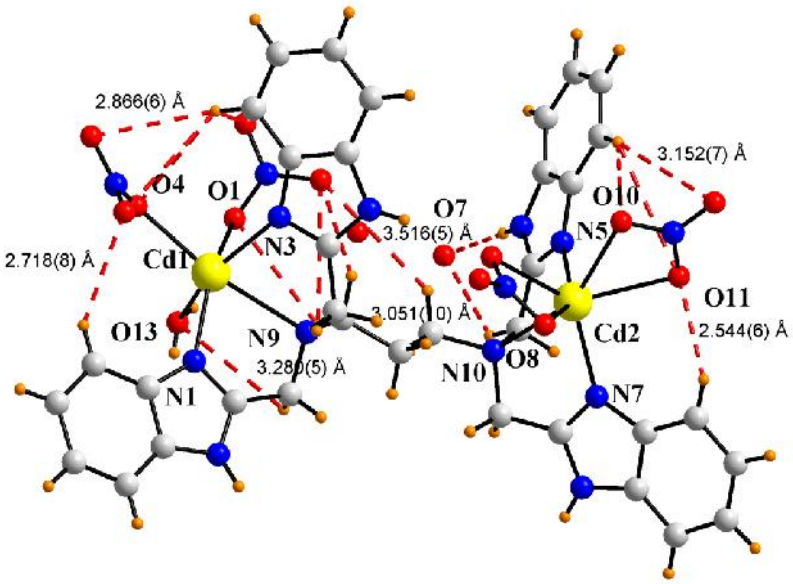


**Fig. 4.28** Different non-covalent interactions in **4e.** Color code: C, grey; N, blue; H, orange; O, red; Cd, yellow

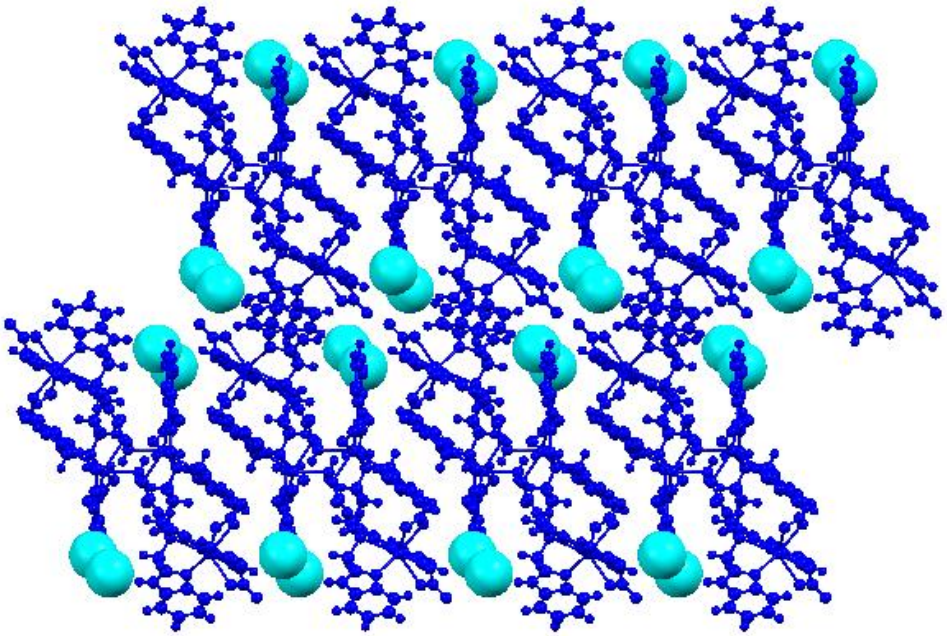

**Fig. 4.29** 2D sheet like structure in **4e**

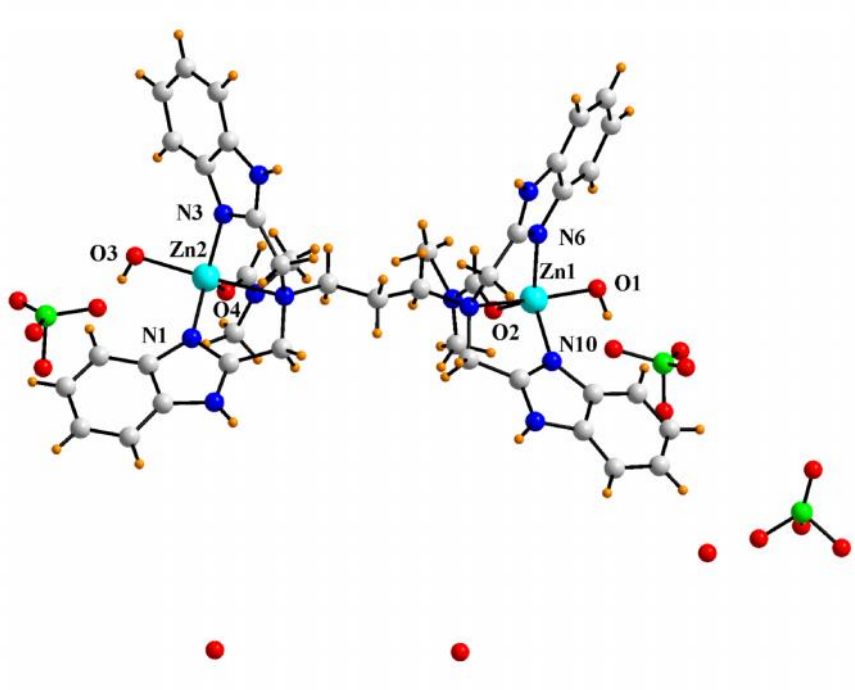


**Fig.4.30** Crystal structure of $[Zn_2(H_4PDTB)(H_2O)_2(DMF)_2](ClO_4)_4.(H_2O)_2$ **4f.** Color code: C, grey; N, blue; H, orange; O, red; Cl, green; Zn, cyan

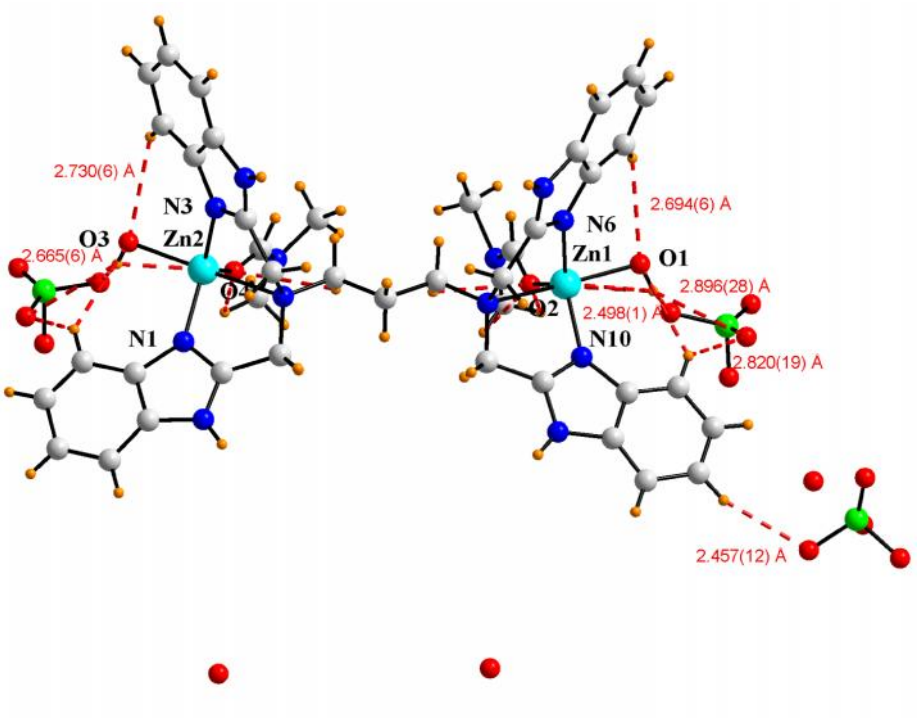


**Fig. 4.31** Different non-covalent interactions in **4f.** Color code: C, grey; N, blue; H, orange; O, red; Zn, cyan

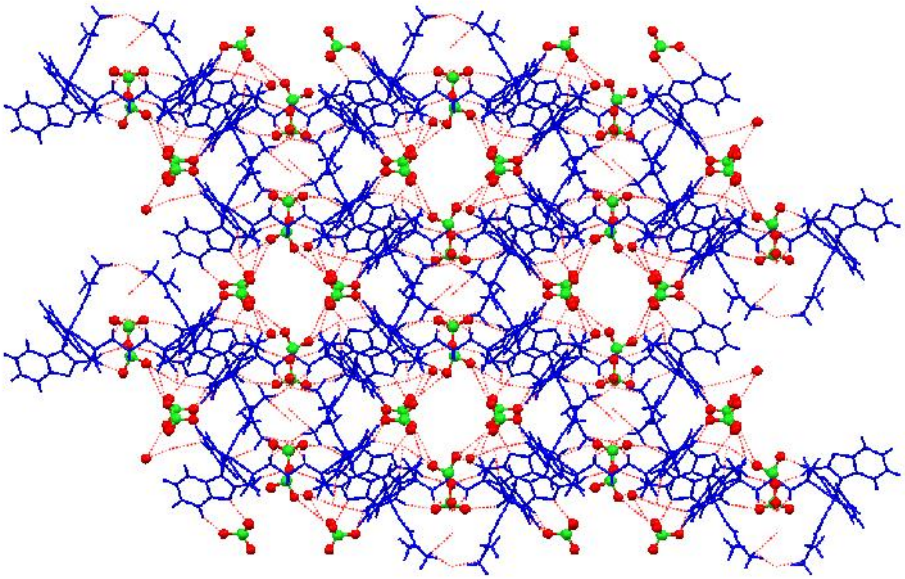

**Fig.4.32** 3D packing in **4f**. Color code: Color code: complex, blue; O, red; chlorine, green

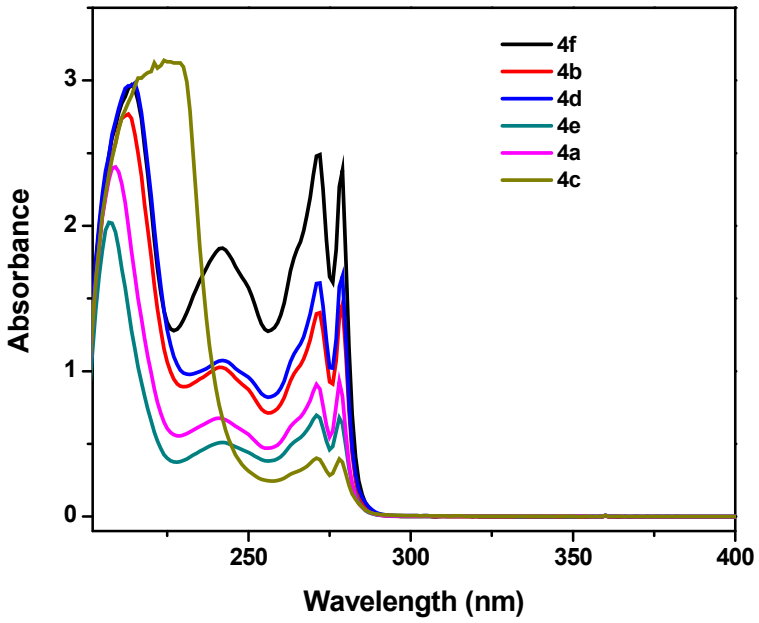


**Fig 4.33** UV spectrum of metal complexes of **4a-4f**

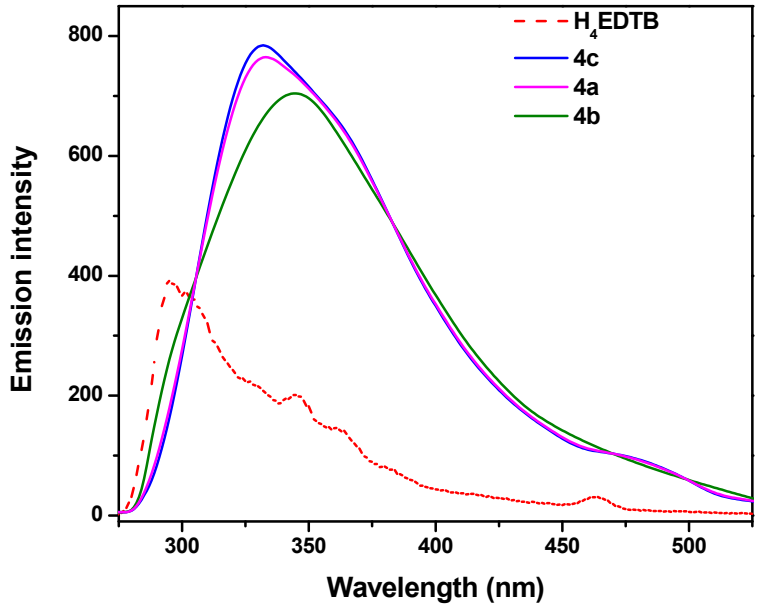


**Fig 4.34** Fluorescence spectrum of ligand, $H_4$EDTB and complexes, **4a-4c**

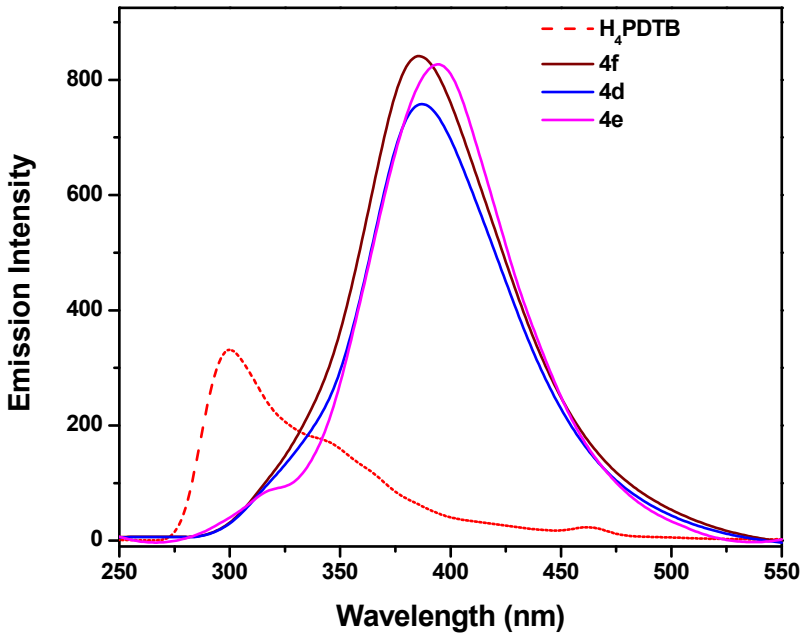


**Fig 4.35** Fluorescence spectrum of ligand, $H_4$PDTB and complexes **4d-4f**

**References**


1. Batten, S. R. and Robson, R., "Interpenetrating nets: Ordered, periodic entanglement", *Angew. Chem. Int. Ed*., **37**, 1460 (1998).
2. Blake, A. J., Champness, N. R., Hubberstey, P., Li, W. -S., Schröder, M. and Withersby, M. A., "Inorganic crystal engineering using self-assembly of tailored building-blocks", *Coord. Chem. Rev*., **183**, 117 (1999).
3. Moulton, B. and Zaworotko, M. J., "From molecules to crystal engineering: Supramolecular isomerism and polymorphism in network solids", *Chem. Rev*., **101**, 1629 (2001).
4. Fujita, M., "Comprehensive supramolecular chemistry", *Pergamon*, Oxford (1995).
5. Lehn, J. -M., "Comprehensive supramolecular chemistry", *Pergamon*, Oxford (1996).
6. Desiraju, G. R., "Perspectives in supramolecular chemistry: The crystal as a supramolecular entity", *Wiley*, Chichester (1996).
7. Desiraju, G. R., "Supramolecular synthons in crystal engineering: A new organic synthesis", *Angew. Chem. Int. Ed. Engl*., **34**, 2311 (1995).
8. Aakeroy, C. B., "Crystal engineering: Strategies and architectures", *Acta. Crystallogr*., B **53**, 569 (1997).
9. Erxleben, A., "Structures and properties of Zn(II) coordination polymers", *Coord. Chem. Rev*., **246**, 203 (2003).
10. Zhao, X., Xiao, B., Fletcher, A. J., Thomas, K. M., Bradshaw, D. and Rosseinsky, M. J., "Hysteretic adsorption and desorption of hydrogen by nanoporous metal-organic frameworks", *Science*, **306**, 1012 (2004).
11. James, S. L., "Metal-organic frameworks", *Chem. Soc. Rev*., **32**, 276 (2003).
12. Seo, J. S., Whang, D., Lee, H., Jun, S. I., Oh, J., Jeon, Y. J. and Kim, K., "A homochiral metal-organic porous material for enantioselective separation and catalysis", *Nature*, **404**, 982 (2000).
13. Eddaoudi, M., Moler, D. B., Li, H., Chen, B., Reineke, T. M., O'Keefee, M. and Yaghi, O. M., "Modular chemistry: Secondary building units as a basis for the design of highly porous and robust metal-organic carboxylate frameworks", *Acc. Chem. Res*., **34**, 319 (2001).

14. Tian, G., Zhu, G. S., Yang, X. Y., Fang, Q. R., Xue, M., Sun, J. Y., Wei, Y. and Qiu, S. L., "A chiral layered Co(II) coordination polymer with helical chains from achiral materials", *Chem. Commun*., 1396 (2005).
15. Pang, J., Marcotte, E. J. P., Seward, C., Brown, R. S. and Wang, S. N., "A blue luminescent star-shaped Zn(II) complex that can detect benzene", *Angew. Chem., Int. Ed*., **40**, 4042 (2001).
16. Lin, W., Evans, O. R., Xiong, R. G. and Wang, Z., "Supramolecular engineering of chiral and acentric 2D networks: Synthesis, structures and second-order nonlinear optical properties of bis(nicotinato)zinc and bis{3-[2-(4-pyridyl)ethenyl]benzoato}cadmium", *J. Am. Chem. Soc*., **120**, 13272 (1998).
17. Shi, X., Zhu, G. S., Qiu, S. L., Huang, K. L., Yu, J. H. and Xu, R. R., "$Zn_2[(S)$-$O_3PCH_2NHC_4H_7CO_2]_2$: A homochiral 3D zinc phosphonate with helical channels", *Angew. Chem*., *Int. Ed*., **43**, 6482 (2004).
18. Barthelet, K., Marrot, J., Riou, D. and Ferey, G., "A breathing hybrid organic-inorganic solid with very large pores and high magnetic characteristics", *Angew. Chem., Int. Ed*., **41**, 281 (2002).
19. Zhao, H., Ye, Q., Qu, Z. R., Fu, D. W., Xiong, R. G., Huang, S. D. and Chan, P. W. H., "Huge deuterated effect on permittivity in a metal–organic framework", *Chem. Eur. J*., **14**, 1164 (2008).
20. Yaghi, O. M., O'Keeffe, M., Ockwig, N. W., Chae, H. K., Eddaoudi, M. and Kim, J., "Reticular synthesis and the design of new materials", *Nature*, **423**, 705 (2003).
21. Xiong, R., You, X., Abrahams, B. F., Xue, Z. and Che, C., "Enantioseparation of racemic organic molecules by a zeolite analogue", *Angew. Chem., Int. Ed*., **40**, 4422 (2001).
22. Cave, D., Gascon, J. M., Bond, A. D., Teat, S. J. and Wood, P. T., "Layered metal organosulfides: Hydrothermal synthesis, structure and magnetic behaviour of the spin-canted magnet $Co(1,2\text{-}(O_2C)(S)C_6H_4)$", *Chem. Commun*., 1050 (2002).
23. Zheng, Y. Z., Tong, M. L., Xue, W., Zhang, W. X., Chen, X. M., Grandjean, F. and Long, G. J., "A "star" antiferromagnet: A polymeric iron (III) acetate that exhibits both spin frustration and long-range magnetic ordering", *Angew. Chem., Int. Ed*., **46**, 6076 (2007).

24. Hagrman, P. J., Hagrman, D. and Zubieta, J., "Organic-inorganic hybrid materials: From "simple" coordination polymers to organodiamine-templated molybdenum oxides", *Angew. Chem., Int. Ed.*, **38**, 2638 (1999).
25. Barnett, S. A. and Champness, N. R., "Structural diversity of building-blocks in coordination framework synthesis-combining $M(NO_3)_2$ junctions and bipyridyl ligands", *Coord. Chem. Rev*., **246**, 145 (2003).
26. Eom, G. H., Park, H. M., Hyun, M. Y., Jang, S. P., Kim, C., Lee, J. H., Lee, S. J., Kim, S. -J. and Kim, Y., "Anion effects on the crystal structures of Zn(II) complexes containing 2,20-bipyridine: Their photoluminescence and catalytic activities" *Polyhedron*, **30**, 1555 (2011).
27. Wang, R., Yuan, D., Jiang, F., Han, L., Gong, Y. and Hong, M., "Anion effect on the structural conformation of tetranuclear cadmium (II) complexes", *Cryst. Growth Des*., **6**, 1351 (2006).
28. Ye, B. H., Ding, B. B., Weng, Y. Q. and Chen, X. M., "Multidimensional networks constructed with isomeric benzenedicarboxylates and 2,2′-biimidazole based on mono-, bi- and tri-nuclear units", *Cryst. Growth Des*., **5**, 801 (2005).
29. Qi, Y., Che, Y. X. and Zheng, J. M., "Self-penetrating and interpenetrating 3D metal-organic frameworks constructed from the rigid 1,4-bis(1-imidazolyl)-benzene ligand and aromatic carboxylate", *Cryst. Growth Des*., **8**, 3602 (2008).
30. Zhu, S. R., Zhang, H., Zhao, Y. M., Shao, M., Wang, Z. X. and Li, M. X., "Synthesis, structures and luminescence of three coordination polymers constructed from rigid 1,3,5-benzenetricarboxylic acid and flexible bis(imidazol-1-ylmethyl)-benzene", *J. Mol. Struct*., **892**, 420 (2008).
31. Su, Z., Xu, J., Fan, J., Liu, D. J., Chu, Q., Chen, M. S., Chen, S. S., Liu, G. X., Wang, X. F. and Sun, W. Y., "Highly connected three-dimensional metal-organic frameworks based on polynuclear secondary building units", *Cryst. Growth Des*., **10**, 3675 (2009).
32. Ma, L. -F., Wang, L. -Y., Wang, Y. -Y., Batten, S. R. and Wang, J. -G., "Self-assembly of a series of cobalt (II) coordination polymers constructed from $H_2$tbip and dipyridyl-based ligands", *Inorg. Chem*., **48**, 915 (2009).
33. Wang, Q. -M. and Mak, T. C. W., "Assembly of discrete, one-, two- and three-dimensional silver (I) supramolecular complexes containing encapsulated acetylide dianion with nitrogen-donor spacers", *Inorg. Chem*., **42**, 1637 (2003).

34. Amiri, M. G., Morsali, A., Hunter, A. D. and Zeller, M., "Spectroscopy, thermal and structural studies of new $Zn^{II}$ coordination polymer, $[Zn_3(m\text{-}bpa)_{4.5}(AcO)_3](ClO_4)_3.4.26H_2O$", *Solid State Sci*., **9**, 1079 (2007).
35. Aslani, A., Morsali, A. and Zeller, M., "Novel homochiral holodirected three-dimensional lead (II) coordination polymer, $[Pb_2(m\text{-}bpa)_3(m\text{-}NO_3)_2(NO_3)_2]_n$: Spectroscopic, thermal, fluorescence and structural studies", *Solid State Sci*., **10**, 854 (2008).
36. Meisch, H. -U., Scholl, A. -R., and Schmitt, "Cadmium as a growth factor for the mushroom agaricus abruptibulbus (Peck) Kauffmann (in German)", *Z. Naturforsch C*, **36**, 765 (1981).
37. Lane, T. W. and Morel, F. M. M., "A biological function for cadmium in marine diatoms", *Proc. Natl. Acad. Sci.* USA, **97,** 4627 (2000).
38. Spiro, T. G., "Zinc enzymes", Ed. Willy, New York (1983).
39. Birtini, I., Luchinat, C., Maret, M. and Zeppezauer, M., "Zinc enzymes", Eds., Birkhauser, Bostan (1986).
40. Hou, T., Yue, S., Yue, X. and Ma, J., "Syntheses, crystal structures, and properties of nickel and cadmium complexes containing imidazole derivatives", *J. Coord. Chem.*, **65**, 3895 (2012).
41. Zhong, C., Guo, R., Wu, Q. And Zhang, H., "Design and syntheses of blue luminescent Cu(II) and Zn(II) polymeric complexes with 2-(2'-pyridyl)benzimidazole derivative ligand", *React. Funct. Polym*., **67**, 408 (2007).
42. Prodi, L., Bolletta, F., Montalti, M. and Zaccheroni, N., "Luminescent chemosensors for transition metal ions", *Coord. Chem. Rev*., **205**, 59 (2000).
43. Li, S. -L., Lan, Y. -Q., Ma, J. –F., Fu, Y. -M., Yang, J., Ping, G. -J., Liu, J. and Su, Z. M., "Structures and luminescent properties of a series of zinc (II) and cadmium (II) 4,4′-oxydiphthalate coordination polymers with various ligands based on bis(pyridyl imidazole) under hydrothermal conditions", *Cryst. Growth Des*., **8**, 1610 (2008).
44. Zheng, S. -L., Yang, J. -H., Yu, X. -L., Chen, X. -M. and Wong, W. -T., "Syntheses, structures, photoluminescence, and theoretical studies of $d^{10}$ metal complexes of 2,2′-dihydroxy-[1,1′]binaphthalenyl-3,3′-dicarboxylate", *Inorg. Chem*., **43**, 830 (2004).

45. Zheng, S. -L., Tong, M. -L., Tan, S. -D., Wang, Y., Shi, J. -X., Tong, Y. -X., Lee, H. -K. and Chen, X. -M., "A novel, highly electrical conducting, single-component molecular material: $[Ag_2(ophen)_2]$ (Hophen = 1H-[1,10]phenanthrolin-2-one)", *Organometallics*, **20**, 5319 (2001).
46. Lei, Li., Tong, -L. H., Jian, -R. L., Duo, -Z. W., Yong, -F, Z. and Xian, -H. B., "Metal–organic coordination architectures of 9,10-bis(N-benzimidazolyl)anthracene: Syntheses, structures and emission properties'', *Cryst. Eng. Comm*., **9,** 412, (2007).
47. Yue, S. -M., Xu, H. -B., Ma, J. -F., Su, Z. -M., Kan, Y. -H. and Zhang, H. -J., "Design and syntheses of blue luminescent zinc (II) and cadmium (II) complexes with bidentate or tridentate pyridyl-imidazole ligands", *Polyhedron*, **25**, 635 (2006).
48. Feng, G. D., Jiang, L., Li, Z. -X., Chen, Q., Wang, X. -L., Shao, K. -Z., Sun, C. -Y., Li, L. -J., Yu, J. -H. and Su, Z. M., "Coordination polymers with bis(2-benzimidazole) ligand as bridging ligand: From 1D chain to 3D microporous structure", *Inorg. Chem. Commun*., **24**, 247 (2012).
49. Song, J. L., Zhao, H. H., Mao, J. G. and Dunbar, K. R., "New types of layered and pillared layered metal carboxylate-phosphonates based on the 4,4′-bipyridine ligand", *Chem. Mater*., **16**, 1884 (2004).
50. Tao, J., Tong, M. L., Shi, J. X., Chen, X. M. and Ng, S. W., "Blue photoluminescent zinc coordination polymers with supertetranuclear cores", *Chem. Commun*., **20**, 2043 (2000).
51. Jiang, L. J., Li, Z. -Y., Wang, Y., Feng, G. -D., Zhao, W. -X., Shao, K. -H., Sun, C. -Y., Li, L. -J. and Su, Z. -M., "Structures and fluorescence properties of two novel metal-organic frameworks based on the bis(2-benzimidazole) and aromatic carboxylate ligands", *Inorg. Chem. Commun..*, **14**, 1077 (2011).
52. Wang, X., Yu, M., Li, T. and Meng, X., "A 3D chiral Zn(II) complex based on achiral ligands 2-(1H-imidazolyl-1-methyl)-1H-benzimidazole and adipate", *Inorg. Chem. Commun*., **40**, 187 (2014).
53. Wang, J., Shuai, L., Xiao, X., Zeng, Y., Li, Z. and -Inoue, T. M., "Synthesis, characterization and DNA binding studies of a zinc complex with 2,6-bis(benzimidazol-2-yl) pyridine", *J. Inorg. Biochem*., **99,** 883 (2005).
54. Wu, H. -L., Wang, K. -T., Liu, B., Kou, F., Jia, F., Yuan, J. -K. and Bai, Y., "Synthesis, characterization, crystal structure and DNA-binding studies of two

zinc (II) complexes with the V-shaped bis(benzimidazole)-thiapropane and its derivative ligand", *Inorg. Chim. Acta*., **384**, 302 (2012).

55. Wu, H., Yuan, J., Zhang, Y., Shi, F., Pan, G., Kong, J. and Fan, X., "Synthesis, crystal structure, DNA-binding properties and antioxidant activity of zinc (II) complexes based on the V-shaped bis(2-benzimidazol-2-ylmethyl)benzylamine ligand and its derivative", *Inorg. Chim. Acta*., **404**, 13 (2013).
56. Liu, Y. -R., Lei, L., Yong, T., Yu, X. -W. and Su, C. -Y., "Dehydration and rehydration behavior of a trinodal topological 3-D framework of Cd(II) benzimidazole-5,6-dicarboxylate'', *Cryst. Eng. Comm*., **11**, 2712 (2009).
57. Liu, H. -Y., Ma, J. -F., Liu, Y. -Y. and Yang, J., "A series of Zn(II) and Cd(II) coordination polymers based on flexible bis-[(pyridyl)-benzimidazole] ligand and different carboxylates: Syntheses, structures, and photoluminescent properties", *Cryst. Eng. Comm*., **15**, 2699 (2013).
58. Liao, Z. -R., Zheng, X. -F., Luo, B. -S., Shen, L. -R., Li, D. -F., Liu, H. -L. and Zhao, W., "Synthesis, characterization and SOD-like activities of manganese-containing complexes with N,N,N',N'-tetrakis(2'-benzimidazolylmethyl)-1,2-ethanediamine (EDTB)", *Polyhedron*, **20,** 2813 (2001).
59. Klinkel, K. L., Kiemele, L. A., Gin, D. L. and Hagadorn, J. R., "Effect of ligand modifications and varying metal-to-ligand ratio on the catalyzed hydrolysis of phosphorus triesters by bimetallic tetrabenzimidazole complexes", *J. Mol. Catal. A: Chem*., **26**7, 173 (2007).
60. Zhu, Y., Xia, C. -K., Meng, S. -C., Chen, J., Chen, J. and Xie, J. -M., "Syntheses, structures, properties and DFT calculations of coordination polymers constructed by 2,6-bis(benzimidazolyl)pyridine", *Polyhydron***, 61**, 181 (2013).
61. Sessler, J. L., Murai, T. and Lynch, V., "Binding of pyridine and benzimidazole to a cadmium "Expanded porphyrin": Solution and X-ray structural studies", *Inorg. Chem.*, **28**, 1333 (1989).
62. Orpen, A. G., Brammer, Lee., Allen, F. H., Kennard, O., Watson, D. G. and Taylor, R., "Tables of bond lengths determined by X-ray and neutron diffraction, part 2 organometallic compounds and co-ordination complexes of the d- and f-block metals", *J. Chem. Soc. Dalton Trans*., S1 (1989).
63. Castro, E. Q., Bernes, S., Behrens, N. B., Benavides, R. T., Contreras, R. and Noth, H., "Structural and spectroscopic characterisation of tris(2-

benzimidazolylmethyl)amine coordination compounds of Zn(II), Cd(II) and Hg(II)", *Polyhedron*, **19**, 1479 (2000).

64. Xiao, S. -L., Du, X., He, C. -H. and Cui, G. -H., "Synthesis, crystal structures and fluorescence properties of two one-dimensional cadmium (II) coordination polymers containing flexible bis(benzimidazole) ligands", *J. Inorg. Organomet. Polym.*, **22,** 1384 (2012).
65. Yu, Q., Zeng, Y. -F., Zhao, J. -P., Yang, Q. and Bu, X. -H., "Zeolite-like metal-organic framework based on a flexible 2-(1H-benzimidazol-2-ylthio)acetic ligand: Synthesis, structures, and properties", *Cryst. Growth Des*., **10**, 1878 (2010).
66. Zhou, Y., Zhong, C., He, Y., Xioa, L., Liu, Y. and Zhang, H., "Novel polymeric metal complexes of 2,7-bis[2-(2'-pyridyl)benzimidazole]-9,9'-dioctylfluorene with Cu(II) and Zn(II): Synthesis and luminescence properties", *J. Inorg. Organomet. Polym*., **19**, 328 (2009).
67. Wang, Z. -W., Ji, C. -C., Li, J., Guo, Z. -J., Li, Y. -Z. and Zheng, H. -G., "Synthesis, X-ray structures, and fluorescent properties of coordination networks constructed from 2-(2-pyridinyl-benzimidazolyl)acetic anion", *Cryst. Growth Des*., **9**, 475 (2009).
68. Majzoub, A, E., Cadiou, C., Déchamps-Olivier, I., Tinant, B. and Chuburu, F., "Cyclam-methylbenzimidazole: A selective OFF-ON fluorescent sensor for zinc", *Inorg. Chem*., **50**, 4029 (2011).

# *Chapter 5*

# *Experimental*

**Materials**

All manipulations were performed in air using commercial grade solvents pre-dried by appropriate drying agents [1]. Pyridine-2,3-dicarboxylic acid, pyridine-2,4-dicarboxylic acid, pyridine-2,5-dicarboxylic acid, pyridine-2,6-dicarboxylic acid, pyridine-3,4-dicarboxylic acid and pyridine-3,5-dicarboxylic acid were purchased from Aldrich Chemical Company, USA. Trifluoroacetic acid (99.5 %) was purchased from Himedia, whereas hydrochloric acid (35 %), hydrobromic acid (40 %), hydrofluoric acid (40 %), nitric acid (65 %), acetic acid (99.8 %), glutaric acid, adipic acid, suberic acid, 2,2',2''-nitrilotriacetic acid, 2,2',2'',2'''-(ethane-1,2-diylbis(azanetriyl))tetraacetic acid, 2,2',2'',2'''-(propane-1,3-diyl bis(azanetriyl))tetraacetic acid, *o*-phenylene diamine and glycol were purchased from Rankem (Laboratory reagent grade). Orthophosphoric acid (85 %), perchloric acid (70 %), $Ni(NO_3)_2.6H_2O$, $Zn(NO_3)_2.6H_2O$, $Zn(ClO_4)_2.6H_2O$ and $Cd(NO_3)_2.4H_2O$ were purchased from s.d. fine-chem Limited.

**Instrumentation**

Crystallized salts, co-crystal and metal complexes were carefully dried under vacuum for several hours prior to elemental analysis on the Elementar Vario EL III analyzer. IR spectra were obtained on Thermo Nikolet Nexus FT-IR spectrometer in KBr. Absorption spectra were recorded on Perkin Elmer UV-Visible spectrophotometer, (Lambda 35). The emission spectra were measured on Perkin-Elmer LS-55 spectrophotometer.

**X-Ray Crystallography**

The X-ray data collection were performed on a Bruker Kappa Apex four circle-CCD diffractometer using graphite monochromated MoKα radiation (λ = 0.71070 Å). In the reduction of data, Lorentz and polarization corrections, empirical absorption corrections were applied [2]. Crystal structures were solved by Direct/Patterson methods. Structure solution, refinement and data output were carried out with the SHELXTL program [3-4]. Non-hydrogen atoms were refined anisotropically. Hydrogen atoms were placed in geometrically calculated positions using a riding model. Images and hydrogen bonding interactions were created in the crystal lattice with DIAMOND and MERCURY softwares [5-6].

**Chapter-2**

1,3-Bis(1H-benzimidazol-2-yl)propane ($H_2$BBPr) [7], 1,4-bis(1H-benzimidazol-2-yl) butane **(**$H_2$BBBu) [8], 1,6-bis(1H-benzimidazol-2-yl)hexane

($H_2$BBHex) [9] and tris(1H-benzimidazol-2-yl)methyl)amine ($H_3$NTB) [10] were synthesized by the literature methods.

**Synthesis of $[(H_4BBBu)^{2+}.(2,3\text{-}PDCA)^{2-}]$ (2a)**

To the 5 mL methanolic solution of 1,4-bis(1H-benzimidazol-2-yl)butane ($H_2$BBBu) (0.29 g, 1.00 mmol), methanolic solution (10 mL) of pyridine-2,3-dicarboxylic acid (2,3-$PDCAH_2$) (0.17 g, 1.00 mmol) was added and the resulting solution was stirred for 8 hrs. Suitable colorless crystals for X-ray data collection were obtained at room temperature in 77 % (0.36 g, 0.77 mmol) yield. Anal. Calcd. (%) for $C_{25}H_{23}N_5O_4$ (457): C, 65.63; H, 5.07; N, 15.31. Found: C, 65.79; H, 5.27; N, 15.57. IR (KBr, $cm^{-1}$): 3422, 3066, 2925, 2626, 1707, 1628, 1461, 1371, 1272, 1182, 868, 751, 650.

**Synthesis of $[(H_4BBBu)^{2+}.(2,4\text{-}PDCA)^{2-}]$ (2b)**

Salt **2b** was prepared and crystallized by the same procedure as outlined above for **2a** using pyridine-2,4-dicarboxylic acid (2,4-$PDCAH_2$) (0.17 g, 1.00 mmol) in 68 % (0.31 g, 0.68 mmol) yield. Anal. Calcd. (%) for $C_{25}H_{23}N_5O_4$ (457): C, 65.63; H, 5.07; N, 15.31. Found: C, 65.52; H, 5.12; N, 15.29. IR (KBr, $cm^{-1}$): 3408, 2925, 2628, 2339, 1719, 1617, 1297, 1177, 1006, 873, 764, 689, 523.

**Synthesis of $[(H_4BBBu)^{2+}.(2,5\text{-}PDCA)^{2-}]$ (2c)**

Salt **2c** was prepared and crystallized by the same procedure as outlined above for **2a** using pyridine-2,5-dicarboxylic acid (2,5-$PDCAH_2$) (0.17 g, 1.00 mmol) in 72 % (0.32 g, 0.72 mmol) yield. Anal. Calcd. (%) for $C_{25}H_{23}N_5O_4$ (457): C, 65.63; H, 5.07; N, 15.31. Found: C, 65.58; H, 5.05; N, 15.98. IR (KBr, $cm^{-1}$): 3406, 3095, 2932, 2860, 1729, 1625, 1544, 1414, 1332, 1009, 742, 547.

**Synthesis of $[(H_4BBBu)^{2+}.(2,6\text{-}PDCA)^{2-}.H_2O]$ (2d)**

Salt **2d** was prepared and crystallized by the same procedure as outlined above for **2a** using pyridine-2,6-dicarboxylic acid (2,6-$PDCAH_2$) (0.17 g, 1.0 mmol) in 62 % (0.29 g, 0.62 mmol) yield. Anal. Calcd. (%) for $C_{25}H_{25}N_5O_5$ (475): C, 63.15; H, 5.30; N, 14.73. Found: C, 63.36; H, 5.17; N, 14.41. IR (KBr, $cm^{-1}$): 3403, 3048, 2746, 1750, 1624, 1458, 1293, 872, 752, 690, 616.

**Synthesis of $[(H_4BBBu)^{2+}.2(3,4\text{-}PDCAH)^{-}.H_2O]$ (2e)**

Salt **2e** was prepared and crystallized by the same procedure as outlined above for **2a** using pyridine-3,4-dicarboxylic acid (3,4-$PDCAH_2$) (0.17 g, 1.0 mmol) in 81 % (0.52 g, 0.81 mmol) yield. Anal. Calcd. (%) for $C_{32}H_{30}N_6O_9$ (642): C, 59.81; H, 4.71;

N, 13.08. Found: C, 59.66; H, 4.31; N, 13.21. IR (KBr, $cm^{-1}$): 3404, 2939, 2484, 1705, 1633, 1584, 1467, 1389, 1217, 1012, 608.

**Synthesis of $[(H_4BBBu)^{2+}.(3,5\text{-}PDCA)^{2-}.3H_2O]$ (2f)**

Salt **2f** was prepared and crystallized by the same procedure as outlined above for **2a** using pyridine-3,5-dicarboxylic acid (3,5-$PDCAH_2$) (0.17 g, 1.00 mmol) in 71 % (0.36 g, 0.71 mmol) yield. Anal. Calcd. (%) for $C_{25}H_{29}N_5O_7$ (511): C, 58.71; H, 5.71; N, 13.69. Found: C, 58.26; H, 5.57; N, 13.25. IR (KBr, $cm^{-1}$): 3411, 2756, 1717, 1630, 1468, 1387, 1262, 974, 756, 692.

**Synthesis of $[H_5NTB^{2+}.2(2,3\text{-}PDCAH)^{-}.DMF]$ (2g)**

To the 10 mL methanol/DMF solution mixture (v/v, 1:4) of tris(1H-benzimidazol-2-yl)methyl)amine ($H_3NTB$) (0.41 g, 1.00 mmol), pyridine-2,3-dicarboxylic acid (2,3-$PDCAH_2$) (0.34 g, 2.00 mmol) was added and the resulting solution was stirred for 6 hrs. Suitable colorless crystals for X-ray data collection were obtained at room temperature in 76 % (0.61 g, 0.76 mmol) yield. Anal. Calcd. (%) for $C_{41}H_{38}N_{10}O_9$ (814): C, 60.46; H, 4.70; N, 17.19. Found: C, 60.13; H, 4.43; N, 17.63. IR (KBr, $cm^{-1}$): 3146, 2947, 1888, 1688, 1222, 1162, 992, 853, 744, 587.

**Synthesis of $[H_4NTB^{+}.(2,4\text{-}PDCAH)^{-}.2CH_3OH\ .H_2O]$ (2h)**

Salt **2h** was prepared and crystallized by the same procedure as outlined above for **2g** using pyridine-2,4-dicarboxylic acid (2,4-$PDCAH_2$) (0.17 g, 1.00 mmol) in 65 % (0.42 g, 0.65 mmol) yield. Anal. Calcd. (%) for $C_{33}H_{36}N_8O_7$ (656): C, 60.36; H, 5.53; N, 17.06. Found: C, 60.83; H, 5.33; N, 17.41. IR (KBr, $cm^{-1}$): 3503, 3407, 2620, 2360, 2205, 1731, 1616, 1234, 1107, 871, 763, 696, 521.

**Synthesis of $[H_5NTB^{2+}.(2,5\text{-}PDCA)^{2-}.DMF]$ (2i)**

Salt **2i** was prepared and crystallized by the same procedure as outlined above for **2g** using pyridine-2,5-dicarboxylic acid (2,5-$PDCAH_2$) (0.17 g, 1.00 mmol) in 69 % (0.44 g, 0.69 mmol) yield. Anal. Calcd. (%) for $C_{34}H_{33}N_9O_5$ (647): C, 63.05; H, 5.14; N, 19.46. Found: C, 63.41; H, 5.03; N, 19.27. IR (KBr, $cm^{-1}$): 3515, 2453, 1736, 1665, 1539, 1447, 1268, 846, 773, 605.

**Synthesis of $[(H_4NTB)^{+}.(2,6\text{-}PDCAH)^{-}.C_2H_5OH.CH_3OH.H_2O]$ (2j)**

Salt **2j** was prepared and crystallized by the same procedure as outlined above for **2g** using $H_3NTB$ (0.41 g, 1.00 mmol) and pyridine-2,6-dicarboxylic acid (2,6-$PDCAH_2$) (0.17 g, 1.00 mmol) in an ethanol–methanol mixture. Suitable colorless crystals for X-ray data collection were obtained at room temperature in 59 % (0.39 g, 0.59 mmol) yield. Anal. Calcd. (%) for $C_{34}H_{38}N_8O_7$ (670): C, 60.88; H, 5.71; N, 16.71.

Found: C, 60.91; H, 5.52; N, 16.28. IR (KBr, $cm^{-1}$): 3001, 2608, 1700, 1628, 1573, 1446, 1290, 1107, 1083, 744, 702, 642.

**Synthesis of $[(H_5NTB)^{2+}.(3,4\text{-}PDCA)^{2-}.DMF]$ (2k)**

Salt **2k** was prepared and crystallized by the same procedure as outlined above for **2g** using pyridine-3,4-dicarboxylic acid (3,4-$PDCAH_2$) (0.17 g, 1.00 mmol) in 73 % (0.47 g, 0.73 mmol) yield. Anal. Calcd. (%) for $C_{34}H_{33}N_9O_5$ (647): C, 63.05; H, 5.14; N, 19.46. Found: C, 63.26; H, 5.32; N, 19.23. IR (KBr, $cm^{-1}$): 3146, 2929, 1682, 1543, 1440, 1277, 1228, 1113, 968, 835, 732, 690.

**Synthesis of $[(H_6NTB)^{3+}.(3,5\text{-}PDCA)^{2-}.(3,5\text{-}PDCAH)^{-}.DMF]$ (2l)**

Salt **2l** was prepared and crystallized by the same procedure as outlined above for **2g** using pyridine-3,5-dicarboxylic acid (3,5-$PDCAH_2$) (0.33 g, 2.00 mmol) in 77 % (0.62 g, 0.77 mmol) yield. Anal. Calcd. (%) for $C_{41}H_{38}N_{10}O_9$ (814): C, 60.44; H, 4.70; N, 17.19. Found: C, 60.13; H, 4.52; N, 17.68. IR (KBr, $cm^{-1}$): 3376, 2511, 1706, 1531, 1434, 1277, 1126, 1023, 835, 750, 678.

**Synthesis of $(H_3BBPr)^{+}[Zn(2,3\text{-}PDCAH)_3]^{-}$ (2m)**

To the 10 mL methanolic solution of $Zn(NO_3).6H_2O$ (0.29 g, 1.00 mmol) and 1,3-bis(1H-benzimidazol-2-yl)propane ($H_2BBPr$) (0.27 g, 1.0 mmol), the methanolic solution (5 mL) of pyridine-2,3-dicarboxylic acid (2,3-$PDCAH_2$) (0.51 g, 3.00 mmol) was added. The resultant mixture was stirred at room temperature for 8 hrs and filtered. The filtrate was dried under vacuum to afford powdered white solid in 74 % (0.62 g, 0.74 mmol) yield. Anal. Calcd. (%) for $C_{38}H_{29}N_7O_{12}Zn$ (839): C, 54.27; H, 3.48; N, 11.66. Found: C, 54.09; H, 3.67; N, 11.71. IR (KBr, $cm^{-1}$): 3427, 2922, 1619, 1581, 1450, 1385, 1280, 1224, 1112, 1044, 841, 750.

**Synthesis of $(H_3BBBu)^{+}Zn(2,3\text{-}PDCAH)_3]^{-}$ (2n)**

Complex **2n** was prepared by the same procedure as outlined above for **2m** using 1,4-bis(1H-benzimidazol-2-yl)butane ($H_4BBBu$) (0.29 g, 1.00 mmol). Suitable colorless crystals for X-ray data collection were obtained at room temperature in 71 % (0.60 g, 0.71 mmol) yield. Anal. Calcd. (%) for $C_{39}H_{31}N_7O_{12}Zn$ (853): C, 54.78; H, 3.65; N, 11.48. Found: C, 54.29; H, 3.47; N, 11.11. IR (KBr, $cm^{-1}$): 3461, 3078, 2931, 1678, 1500, 1353, 1257, 1097, 863, 753, 661.

**Synthesis of $(H_3BBHex)^{+}[Zn(2,3\text{-}PDCAH)_3]^{-}$ (2o)**

Complex **2o** was prepared by the same procedure as outlined above for **2m** using 1,6-bis(1H-benzimidazol-2-yl)hexane ($H_2BBHex$) (0.32 g, 1.00 mmol) in 74 %

(0.65 g, 0.74 mmol) yield. Anal. Calcd. (%) for $C_{41}H_{35}N_7O_{12}Zn$ (881): C, 55.76; H, 3.99; N, 11.10. Found: C, 55.38; H, 3.54; N, 11.27. IR (KBr, $cm^{-1}$): 3448, 2931, 1673, 1495, 1389, 1258, 1097, 862, 826, 756, 694, 664.

**Synthesis of $(H_4BBPr)^{2+}[Ni(2,6\text{-}PDCA)_2]^{2-}.7H_2O$] (2p)**

Complex **2p** was prepared by the same procedure as outlined above for **2m** using of $Ni(NO_3).4H_2O$ (0.29 g, 1.00 mmol), 1,3-bis(1H-benzimidazol-2-yl)propane ($H_2BBPr$) (0.29 g, 1.00 mmol) and pyridine-2,6-dicarboxylic acid (2,6-$PDCAH_2$) (0.33 g, 2.00 mmol). Suitable green crystals for X-ray data collection were obtained at room temperature in 76 % (0.60 g, 0.76 mmol) yield. Anal. Calcd. (%) for $C_{31}H_{38}N_6NiO_{15}$ (792): C, 46.93; H, 4.83; N, 10.59. Found: C, 46.13; H, 4.64; N, 10.19. IR (KBr, $cm^{-1}$): 3390, 2395, 1627, 1388, 1286, 1085, 1002, 944, 891, 823, 764, 695.

**Synthesis of $(H_4BBBu)^{2+}[Ni(2,6\text{-}PDCA)_2]^{2-}$] (2q)**

Complex **2q** was prepared by the same procedure as outlined above for **2m** using $Ni(NO_3).4H_2O$ (0.29 g, 1.00 mmol), 1,4-bis(1H-benzimidazol-2-yl)butane ($H_2BBBu$) (0.29 g, 1.00 mmol) and pyridine-2,6-dicarboxylic acid (2,6-$PDCAH_2$) (0.33 g, 2.00 mmol) in 68 % (0.46 g, 0.68 mmol) yield. Anal. Calcd. (%) for $C_{32}H_{26}N_6NiO_8$ (680): C, 56.41; H, 3.85; N, 12.34. Found: C, 56.68; H, 3.51; N, 12.12. IR (KBr, $cm^{-1}$): 3430, 3096, 2928, 2894, 1590, 1380, 1280, 1194, 1112, 1071, 1015, 979, 873, 835, 732, 608.

**Synthesis of $(H_4BBHex)^{2+}[Ni(2,6\text{-}PDCA)_2]^{2-}.CH_3OH$ (2r)**

Complex **2r** was prepared by the same procedure as outlined for **2m** using pyridine-2,6-dicarboxylic acid (0.33 g, 2.00 mmol), 1,6-bis(1H-benzimidazol-2-yl)hexane ($H_2BBHex$) (0.32 g, 1.0 mmol) and pyridine-2,6-dicarboxylic acid (2,6-$PDCAH_2$) (0.33 g, 2.00 mmol). Green crystals suitable for X-ray crystallography were obtained in 73 % (0.54 g, 0.73 mmol) yield by slow evaporation of the reaction mixture. Anal. Calcd. (%) for $C_{35}H_{34}N_6NiO_9$ (740): C, 56.70; H, 4.62; N, 11.34. Found: C, 56.57; H, 4.28; N, 11.19. IR (KBr, $cm^{-1}$): 3391, 2928, 2645, 1675, 1383, 1082, 1026, 891, 829, 765, 682.

## Chapter-3

N,N,N',N'-tetrakis(1H-benzimidazol-2yl)methyl)ethane-1,2-diamine ($H_4EDTB$) and N,N,N',N'-tetrakis(1H-benzimidazol-2yl)methyl)propane-1,3-diamine ($H_4PDTB$) were synthesized by the literature method [11-12].

**Synthesis of $[(H_8EDTB)^{4+}.4(ClO_4)^{-}.H_2O]$ (3a)**

To the 5 mL methanol/water solution of ligand ($H_4EDTB$) (0.58 g, 1.00 mmol), 0.5 mL of $HClO_4$ (v/v%, 5:1) was added and the resulting solution was stirred for 4 hrs. The colorless crystals of salt **3a** suitable for X-ray data collection were obtained by slow evaporation of solvent at room temperature in 71 % (0.71 g, 0.71 mmol) yield. Anal. Calcd. (%) for $C_{34}H_{38}Cl_4N_{10}O17$ (1000): C, 40.81; H, 3.83; N, 14.00. Found: C, 40.97; H, 3.45; N, 14.17. IR (KBr, $cm^{-1}$): 3237, 2927, 1626, 1573, 1521, 1453, 1389, 1285, 1146, 951, 753, 625, 466.

**Synthesis of $[(H_8EDTB)^{4+}.4(Br)^{-}.4DMSO]$ (3b)**

To the 5 mL methanol/DMSO solution of ligand ($H_4EDTB$) (0.58 g, 1.00 mmol), 0.5 mL of HBr was added and the resulting solution was stirred for 4 hrs. The colorless crystals of salt **3b** suitable for X-ray data collection were obtained by slow evaporation of solvent at room temperature in 73 % (0.88 g, 0.73 mmol) yield. Anal. Calcd. (%) for $C_{42}H_{60}Br_4N_{10}O_4S_4$ (1216): C, 41.45; H, 4.97; N, 11.51; S, 10.54. Found: C, 41.92; H, 4.81; N, 11.21; S, 10.36. IR (KBr, $cm^{-1}$): 3417, 3039, 2868, 2642, 1622, 1452, 1386, 1222, 1097, 893.

**Synthesis of $[2(H_7EDTB)^{3+}.3(SiF_6)^{2-}.14H_2O]$ (3c)**

Salt **3c** was prepared and crystallized by the same procedure as outlined above for **3a** using HF in 49 % (0.90 g, 0.49 mmol) yield. Anal. Calcd. (%) for $C_{68}H_{98}F_{18}N_{20}O_{14}Si_3$ (1844): C, 44.25; H, 5.35; N, 18.53. Found: C, 44.61; H, 5.14; N, 14.81. IR (KBr, $cm^{-1}$): 2857, 1625, 1570, 1456, 1388, 1222, 1120, 1023, 955, 783, 618.

**Synthesis of $[(H_8EDTB)^{4+}.4(H_2PO_4)^{-}.2H_3PO_4]$ (3d)**

Salt **3d** was prepared and crystallized by the same procedure as outlined above for **3a** using $H_3PO_4$ in 67 % (0.78 g, 0.67 mmol) yield. Anal. Calcd. (%) for $C_{34}H_{50}N_{10}O_{24}P_6$ (1168): C, 34.94; H, 4.31; N, 11.99. Found: C, 34.54; H, 4.79; N, 11.66. IR (KBr, $cm^{-1}$): 2927, 1625, 1570, 1460, 1405, 1040, 746, 620, 570, 462.

**Synthesis of $[H_4EDTB.2CH_3COOH]$ (3e)**

Co-crystal **3e** was prepared and crystallized by the same procedure as outlined above for **3a** using $CH_3COOH$ in 71 % (0.49 g, 0.71 mmol) yield. Anal. Calcd. (%) for $C_{38}H_{40}N_{10}O_4$ (700): C, 65.13; H, 5.75; N, 19.99. Found: C, 65.49; H, 5.98; N, 19.71. IR (KBr, $cm^{-1}$): 3173, 3055, 2913, 1942, 1677, 1541, 1442, 1352, 1268, 1117, 1043, 886, 744, 442.

**Synthesis of $[(H_8PDTB)^{4+}.4(ClO_4)^{-}.H_2O]$ (3f)**

To the 5mL methanol/water solution of ligand ($H_4$PDTB**)** (0.59 g, 1.00 mmol), 0.4 mL of $HClO_4$ (v/v%, 5:1) was added and the resulting solution was stirred for 5 hrs. The colorless crystals of salt **3f** suitable for X-ray data collection were obtained by slow evaporation of solvent at room temperature in 43% (0.43 g, 0.43 mmol) yield. Anal. Calcd. (%) for $C_{35}H_{40}Cl_4N_{10}O_{17}$ (1014): C, 41.43; H, 3.97; N, 13.98. Found: C, 41.17; H, 3.52; N, 13.46. IR (KBr, $cm^{-1}$): 3413, 3119, 2741, 1625, 1529, 1449, 1275, 892, 744, 619.

**Synthesis of $[(H_8PDTB)^{4+}.4(Cl)^{-}.2H_2O]$ (3g)**

Salt **3g** was prepared and crystallized by the same procedure as outlined above for **3f** using HCl in 70 % (0.54 g, 0.70 mmol) yield. Anal. Calcd. (%) for $C_{35}H_{42}Cl_4N_{10}O_2$ (776): C, 54.13; H, 5.45; N, 18.04. Found: C, 54.49; H, 5.37; N, 18.41. IR (KBr, $cm^{-1}$): 3417, 3110, 2910, 1623, 1570, 1457, 1221, 853, 755, 619, 549.

**Synthesis of $[(H_8PDTB)^{4+}.2(H_2PO_4)^{-}.(H_7P_3O_{12})^{2-}.3H_3PO_4]$ (3h)**

Salt **3h** was prepared and crystallized by the same procedure as outlined above for **3f** using $H_3PO_4$ in 59 % (0.81 g, 0.59 mmol) yield. Anal. Calcd. (%) for $C_{35}H_{58}N_{10}O_{32}P_8$ (1378): C, 30.49; H, 4.24; N, 10.16. Found: C, 30.73; H, 4.42; N, 10.06. IR (KBr, $cm^{-1}$): 3310, 3104, 2862, 1815, 1631, 1460, 1397, 1059, 758, 619, 495.

**Synthesis of $[(H_8PDTB)^{4+}.4(NO_3)^{-}]$ (3i)**

Salt **3i** was prepared and crystallized by the same procedure as outlined above for **3f** using $HNO_3$ in 82 % (0.69 g, 0.82 mmol) yield. Anal. Calcd. (%) for $C_{35}H_{38}N_{14}O_{12}$ (846): C, 49.64; H, 4.52; N, 23.16. Found: C, 49.82; H, 4.30; N, 23.33. IR (KBr, $cm^{-1}$): 3414, 3185, 2926, 1670, 1625, 1396, 1270, 1195, 1026, 748, 610, 475.

**Synthesis of $[2(H_5PDTB)^{+}.2(CF_3COO)^{-}.5H_2O]$ (3j)**

Salt **3j** was prepared and crystallized by the same procedure as outlined above for **3f** using $CF_3COOH$ in 57 % (0.85 g, 0.57 mmol) yield. Anal. Calcd. (%) for $C_{74}H_{80}F_6N_{20}O_9$ (1506): C, 58.96; H, 5.35; N, 18.58. Found: C, 58.79; H, 5.77; N, 18.81. IR (KBr, $cm^{-1}$): 3414, 3145, 2923, 1625, 1388, 1042, 744, 616, 474.

**Synthesis of $[(H_8PDTB)^{4+}.3(ClO_4)^{-}.(H_2PO_4)^{-}]$ (3k)**

Salt **3k** was prepared and crystallized by the same procedure as outlined above for **3f** using mixture of all acids. The colorless crystals of salt **3k** suitable for X-ray data collection were obtained by slow evaporation of solvent at room temperature in 78 % (0.77 g, 0.78 mmol) yield. Anal. Calcd. (%) for $C_{35}H_{40}Cl_3N_{10}O_{16}P$ (994): C, 42.29; H, 4.06; N, 14.09. Found: C, 42.09; H, 4.27; N, 14.31. IR (KBr, $cm^{-1}$): 3422, 3156, 2929, 1616, 1352, 1079, 994, 755, 625, 498.

**Chapter-4**

**Synthesis of [Zn($H_4$EDTB)]($NO_3$)$_2$.$CH_3OH$ (4a)**

The 5 mL DMF solution of $H_4$EDTB (0.58 g, 1.00 mmol) was added to the equal volume of methanolic solution of $Zn(NO_3)_2.6H_2O$ (0.29 g, 1.00 mmol). The mixture was stirred for 6 hrs., filtered and evaporated to dryness under vacuum to afford powdered white solid in 71 % (0.56 g, 0.71 mmol) yield. Suitable crystals were obtained from methanolic solution at room temperature. Anal. Calcd. (%) for $C_{35}H_{36}N_{12}O_7Zn$ (800): C, 52.41; H, 4.52; N, 20.95. Found: C, 52.67; H, 4.31; N, 20.49. IR (KBr, $cm^{-1}$): 3280, 2918, 1661, 1538, 1388, 1280, 1099, 1034, 996, 943, 837, 749, 650.

**Synthesis of [Cd($H_4$EDTB)$NO_3$]$NO_3$.$CH_3OH$.2$H_2O$ (4b)**

Compound **4b** was synthesized and crystallized by the method described for the preparation of complex **4a** using $Cd(NO_3)_2.4H_2O$ (0.30 g, 1.00 mmol) in 68 % (0.60 g, 0.68 mmol) yield. Anal. Calcd. (%) for $C_{35}H_{40}CdN_{12}O_9$ (886): C, 47.49; H, 4.55; N, 18.99. Found: C, 47.73; H, 4.29; N, 18.61. IR (KBr, $cm^{-1}$): 3410, 3061, 2928, 2791, 2397, 1759, 1622, 1392, 1277, 1115, 1039, 958, 827, 752, 611, 498, 432.

**Synthesis of [Zn($H_4$EDTB)]($ClO_4$)$_2$ (4c)**

Compound **4c** was synthesized and crystallized by the method described for the preparation of complex **4a** using $Zn(ClO_4)_2.6H_2O$ (0.37 g, 1.00 mmol) in 63 % (0.53 g, 0.63 mmol) yield. Anal. Calcd. (%) for $C_{34}H_{32}Cl_2N_{10}O_9Zn$ (842): C, 48.33; H, 3.82; N, 16.58. Found: C, 48.88; H, 4.02; N, 16.25. IR (KBr, $cm^{-1}$): 3449, 3066, 2931, 2866, 2395, 1957, 1653, 1489, 1450, 1389, 1263, 1097, 923, 855, 753, 664, 626.

**Synthesis of [Zn($H_4$PDTB)]($NO_3$)$_2$.DMF (4d)**

Compound **4d** was synthesized and crystallized by the method described for the preparation of complex **4a** using $Zn(NO_3)_2.6H_2O$ (0.29 g, 1.00 mmol) and $H_4$PDTB (0.59 g, 1.00 mmol) in 81 % (0.69 g, 0.81 mmol) yield. Anal. Calcd. (%) for $C_{38}H_{41}N_{13}O_7Zn$ (857): C, 53.24; H, 4.82; N, 21.24. Found: C, 53.66; H, 4.69; N, 21.67. IR (KBr, $cm^{-1}$): 3106, 2919, 1654, 1539, 1446, 1334, 1275, 1079, 926, 903, 838, 748, 676, 508.

**Synthesis of [$Cd_2$($H_4$PDTB)(¦$^1$-$NO_3$)$_2$(¦$^2$-$NO_3$)$_2$ $H_2O$].2$H_2O$ (4e)**

Compound **4e** was synthesized and crystallized by the method described for the preparation of complex **4a** using $Cd(NO_3)_2.4H_2O$ (0.30 g, 1.00 mmol) and $H_4$PDTB (0.29 g, 0.50 mmol) in 65 % (0.73 g, 0.65 mmol) yield. Anal. Calcd. (%) for

$C_{35}H_{40}Cd_2N_{14}O_{15}$ (1124): C, 37.48; H, 3.59; N, 17.48. Found: C, 37.23; H, 3.41; N, 17.19. IR (KBr, $cm^{-1}$): 3336, 2338, 1951, 1625, 1540, 1388, 1159, 1118, 1037, 989, 909, 831, 753, 658.

**Synthesis of $[Zn_2(H_4PDTB)(H_2O)_2.(DMF)_2](ClO_4)_4.2H_2O$ (4f)**

Compound **4f** was synthesized and crystallized by the method described for the preparation of complex **4a** using $Zn(ClO_4)_2.6H_2O$ (0.37 g, 1.00 mmol) and $H_4PDTB$, (0.29 g, 0.50 mmol) in 59 % (0.78 g, 0.59 mmol) yield. Anal. Calcd. (%) for $C_{41}H_{56}Cl_4N_{12}O_{22}Zn_2$ (1336): C, 36.71; H, 4.21; N, 12.53. Found: C, 36.57; H, 4.53; N, 12.17. IR (KBr, $cm^{-1}$): 3371, 2020, 1622, 1543, 1461, 1387, 1397, 1278, 1085, 912, 849, 753, 629.

## References


1. Perrin, D. D., Armarego, W. L. and Perrin, D. R., "Purification of laboratory chemicals", 2nd ed., Pergamon, New York (1980).
2. Sheldrick, G. M., "Phase annealing in SHELX-90: Direct methods for larger structures", *Acta Cryst*., A **46**, 467 (1990).
3. Sheldrick, G. M., "SHELXTL-NT 2000 version 6.12, reference manual", University of Göttingen, Göttingen, Germany.
4. Sheldrick, G. M., "SADABS", University of Göttingen, Germany (1996).
5. Klaus, B., "Diamond: Visual crystal structure information system (Version 2.1d)", Bonn, Germany (2000).
6. Mercury, Cambridge crystallographic data centre, 12 Union Road, Cambridge CB2 1EZ, United Kingdom. Available from: Website: http://www.ccdc.cam.ac.uk/.
7. Siddiqi, Z. A., Shahid, A. M., Khalid, M., Sharma, P. K. and Siddique, A., "Spectroscopic, luminescence, electrochemical and antimicrobial studies of lanthanide complexes of bis-benzimidazole derived ligands", *J. Mol. Struct*., **1037,** 402 (2013).
8. Verdan, S., Melich, X., Bernardinelli, G. and Williams, A. F., "Molecular bricklaying anion and chain length effects in bisbenzimidazolonium salts", *Cryst. Eng. Comm*., **11,** 1416 (2009).
9. Zhang, L -Y., Liu, Y., Li, K., Pan, M., Yan, C., Wei, S. -C., Chena, Y. -X. and Su, C. -Y., "Formation of OD $M_5L_2$ helicate cage and 1D loop-and chain complexes: Stepwise assembly and catalytic activity", *Cryst. Eng. Comm*., **15,** 7106 (2013).
10. Ni, X. -L., Yi, J. -M., Song, S., Zhang, Y. -Q., Xue, S. -F., Zhu, Q. -J. and Tao, Z., "Supramolecular interactions of bisbenzimidazolyl derivatives with cucurbit [7] uril, potential axle molecules bearing a novel fluorescent signal response", *Tetrahedron*, **69**, 6219 (2013).
11. Zhou, Q. and Yang, P., "Crystal structure and DNA-binding studies of a new Cu(II) complex involving benzimidazole", *Inorg. Chim. Acta*., **359,** 1200 (2006).
12. Nakao, Y., Oonishi, M., Uzu, T., Kashihara, H., Suzuki, S., Sakai, M. and Fukuda, Y., "Synthesis and properties of dinuclear copper (II) complexes

containing dinucleating ligands with imidazole nitrogen and two exogenous bridging ligands", *Bull. Chem. Soc. Jap*., **67**, 2586 (1994).